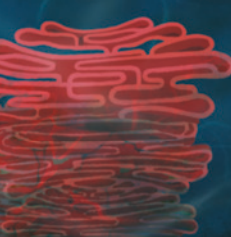


# THE DESTINY OF ANTI-CANCER DRUGS

THE IMPACT OF DRUG TRANSPORTERS AND  
DRUG-METABOLIZING ENZYMES ON THE  
PHARMACOKINETICS OF ANTI-CANCER THERAPIES

Stéphanie Sigrid van Hoppe





## **The destiny of anti-cancer drugs:**

The impact of drug transporters and drug-metabolizing enzymes on the pharmacokinetics of anti-cancer therapies

© Stéphanie Sigrid van Hoppe, Amsterdam, 2019. All rights reserved.

ISBN 978-94-6375-554-2

Cover by Gülsüm Yalcin

Layout by Jos Hendrix

Printed by Ridderprint BV, [www.ridderprint.nl](http://www.ridderprint.nl)

The research described in this thesis was performed at the Divisions of Molecular Oncology and Pharmacology of the Netherlands Cancer Institute, Amsterdam, The Netherlands.

Printing of this thesis was financially supported by the Onderzoeksschool Oncologie Amsterdam.

# **The destiny of anti-cancer drugs:**

The impact of drug transporters and drug-metabolizing enzymes on the pharmacokinetics of anti-cancer therapies

Het lot van anti-kanker middelen:

De impact van drug transporteurs en drug metaboliserende enzymen op de farmacokinetiek van anti-kanker therapieën.  
(met een samenvatting in het Nederlands)

Le destin des médicaments anticancéreux:

L'impact des transporteurs de médicaments et des enzymes qui métabolisent les médicaments sur la pharmacocinétique des traitements anticancéreux.  
(avec un résumé en français)

## **Proefschrift**

ter verkrijging van de graad van doctor aan de  
Universiteit Utrecht  
op gezag van de  
rector magnificus, prof.dr. H.R.B.M. Kummeling,  
ingevolge het besluit van het college voor promoties  
in het openbaar te verdedigen op

woensdag 25 september 2019 des middags te 2.30 uur

door

**Stéphanie Sigrid van Hoppe**  
geboren op 7 april 1986

te Bonaire, Nederlandse Antillen

**Promotor:**

Prof. dr. J.H. Beijnen

**Copromotor:**

Dr. A.H. Schinkel

## TABLE OF CONTENTS

<b>Preface</b>		<b>7</b>
<b>Chapter 1</b>	Introduction	<b>9</b>
<b>Chapter 2</b>	Breast cancer resistance protein (BCRP/ABCG2) and P-glycoprotein (P-gp/ABCB1) transport afatinib and restrict its oral availability and brain accumulation	<b>21</b>
<b>Chapter 3</b>	Brain accumulation of osimertinib and its active metabolite AZ5104 is restricted by ABCB1 (P-glycoprotein) and ABCG2 (Breast Cancer Resistance Protein)	<b>43</b>
<b>Chapter 4</b>	P-glycoprotein (MDR1/ABCB1) restricts brain penetration of the Bruton's tyrosine kinase inhibitor ibrutinib while Cytochrome P450-3A (CYP3A) limits its oral bioavailability	<b>69</b>
<b>Chapter 5</b>	Brain accumulation of ponatinib and its active metabolite N-desmethyl ponatinib is limited by P-glycoprotein (P-GP/ABCB1) and breast cancer resistance protein (BCRP/ABCG2)	<b>99</b>
<b>Chapter 6</b>	The impact of Organic Anion-Transporting Polypeptides (OATPs) on disposition and toxicity of antitumor drugs; insights from knockout and humanized mice	<b>125</b>
<b>Chapter 7</b>	Conclusions and future perspectives	<b>167</b>
<b>Chapter 8</b>	Summary	<b>173</b>
<b>Appendices</b>	Nederlandse samenvatting	181
	Résumé en français	183
	Curriculum vitae	185
	List of publications	186
	Acknowledgements	188



## PREFACE

Membrane transporters are key players in the regulation of homeostasis, cell integrity and metabolism in organisms. The ATP-binding cassette (ABC) efflux transporters and Organic Anion-transporting Polypeptide (OATP) influx transporters are two main superfamilies that are expressed in pharmacologically important organs such as the liver, small intestine, kidney and the blood-brain barrier (BBB). These transporters can transport endogenous and exogenous molecules and thereby are important in the absorption, disposition, elimination and toxicity of many drugs.

This thesis mainly addresses the pharmacokinetic impact of ABCB1 and ABCG2 efflux transporters and the Cytochrome P450 metabolizing enzymes on a subset of anti-cancer drugs, and we conclude with a review on the OATP1A/1B family.

**Chapter 1** introduces the ABC transporters and their tissue localization and their pharmacologic role in the distribution of their substrates. This chapter also introduces the Cytochrome P450 enzymes and the tyrosine kinase inhibitors (TKIs).

**Chapter 2** presents the role of ABCB1 and ABCG2 in the distribution of the irreversible TKI afatinib.

In **chapter 3** we demonstrate the importance of these ABC transporters, especially ABCB1, for brain accumulation of the irreversible TKI osimertinib and its main active metabolite AZ5104.

In **chapter 4** we investigate the roles ABCB1 and ABCG2, as well as CYP3A, play in the disposition of the irreversible TKI ibrutinib and its main metabolite, ibrutinib-DiOH.

**Chapter 5** describes the effects of the ABC transporters and CYP3A on the distribution of ponatinib and its main metabolite, DMP.

**Chapter 6** reviews the impact of the OATP1A/1B family on the disposition and toxicity of anti-cancer drugs and how the recent use of knockout and humanized OATP1A/1B mouse models has helped us gain insight into the *in vivo* role of these OATP1A/1B transporters. We especially focused on their functional role in drug pharmacokinetics and their implications for therapeutic efficacy and toxic side effects of anti-cancer and other drug treatments.



# 1

---

## Introduction

---

**Stéphanie van Hoppe, Alfred H. Schinkel**

Division of Pharmacology, The Netherlands Cancer Institute, Amsterdam

Adapted in part from 'What next? Preferably development of drugs that are no longer transported by the ABCB1 and ABCG2 efflux transporters.'

*Pharmacol Res.* 2017 Sep;123:144.



## ABC TRANSPORTERS

Transport proteins play a central role in this thesis. Especially the ATP-binding cassette (ABC) transporters, which form a superfamily of active multi-spanning transmembrane efflux proteins. They make up one of the largest protein families and are highly preserved across living organisms of all kingdoms, from bacteria to humans, indicating their essential functions.

ABC transporters utilize energy derived from ATP hydrolysis in order to translocate specific substrates or regulate the activity of membrane channels. ATP hydrolysis is mediated in the majority of ABC transporters by two nucleotide-binding domains (NBDs), which interact with two transmembrane domains (TMDs). The NBDs bind and hydrolyze ATP, while the TMDs recognize and bind a specific substrate to translocate it across the membrane, driven by conformational changes in the NBDs upon ATP binding and hydrolysis (1). This process is rendered schematically and simplified in Figure 1.

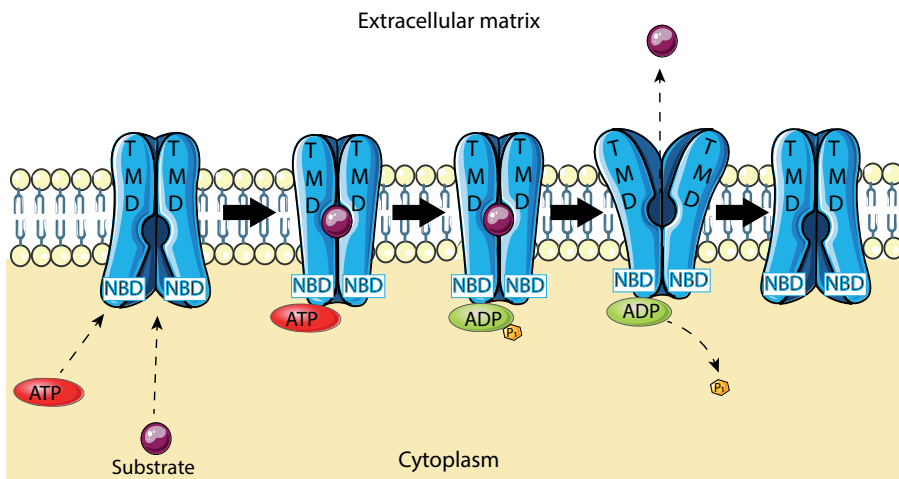


**Figure 1** - Schematic and simplified representation of the transport mechanism of ABC efflux proteins. NBDs bind ATP, while TMDs recognize and bind the transport substrate. ATP is hydrolyzed to ADP and a phosphate group, whereby the conformation of the protein changes and the substrate is transported across the cell membrane to the extracellular matrix.

There are 48 known human ABC transporters, which are classified into 6 subfamilies (ABCA, ABCB, ABCC, ABCD, ABCE/ABCF and ABCG). They transport endogenous and exogenous molecules and regulate cell integrity, metabolism and homeostasis, and are involved in a large number of processes that play a role in various human diseases, such

as cardiovascular disease, ulcerative colitis, Alzheimer or cancer (2-6).

In this thesis we have studied two members in particular, ABCB1 (MDR1, P-glycoprotein or P-gp) and ABCG2 (Breast Cancer Resistance Protein, BCRP), which are especially important in pharmacokinetics (7, 8). They both influence the disposition of a wide variety of endogenous and exogenous compounds, including many anticancer drugs, and can thus affect their efficacy and toxicity. For this reason, changes in the level of expression and functionality of these transporters can influence the efficacy and safety of transported drugs. ABCB1 and ABCG2 are expressed at pharmacologically important sites such as the apical membranes of enterocytes, hepatocytes and renal tubular epithelial cells, as depicted in Figure 2, where they can limit gastrointestinal absorption or mediate direct intestinal, hepatic, or renal excretion of their substrates (7, 8). Furthermore, they are both expressed in apical membranes of barriers protecting sanctuary tissues such as the blood-brain, blood-placenta and blood-testis barriers, where substrates are pumped directly out of the epithelial or endothelial cells into the blood. Consequently, many chemotherapeutic and other anticancer agents that are ABCB1 and/or ABCG2 substrates have restricted brain accumulation (7-10).

**Figure 2:** Schematic representation of the expression sites of ABCB1 and ABCG2 and their transport direction in pharmacologically important organs. Shown is the transport direction of the ABCB1 and ABCG2 substrates in the kidney from the proximal tubular cells into the tubular lumen (i.e., towards the urine). In the intestines ABCB1 and ABCG2 transport their substrates from the enterocytes into the intestinal lumen (i.e., towards the feces), while in the brain these efflux transporters transport their substrates from the endothelial cells into the blood. In the liver ABCB1 and ABCG2 transport their substrates from the hepatocytes into the bile, i.e., towards the intestinal lumen.

## CYTOCHROME P450

The human cytochrome P450s are a family of monooxygenases, comprising 57 genes, that catalyze the metabolism of a wide variety of endogenous and exogenous compounds including xenobiotics, drugs, environmental toxins, steroids and fatty acids. These enzymes are responsible for metabolism of approximately 60% of prescribed drugs and they are essential to maintain homeostasis (11, 12). The basic catalytic mechanism appears to be common to all CYPs and involves a two-electron reduction of molecular oxygen to form a reactive oxygen species and water. Of the human CYP enzymes, CYP1A2, 2B6, 2C9, 2C19, 2D6, and 3A4 have been described to contribute to the Phase I metabolism of the vast majority of drugs compared with other Phase I oxidative enzymes. The human CYP3A subfamily includes CYP3A4, 3A5, 3A7 and

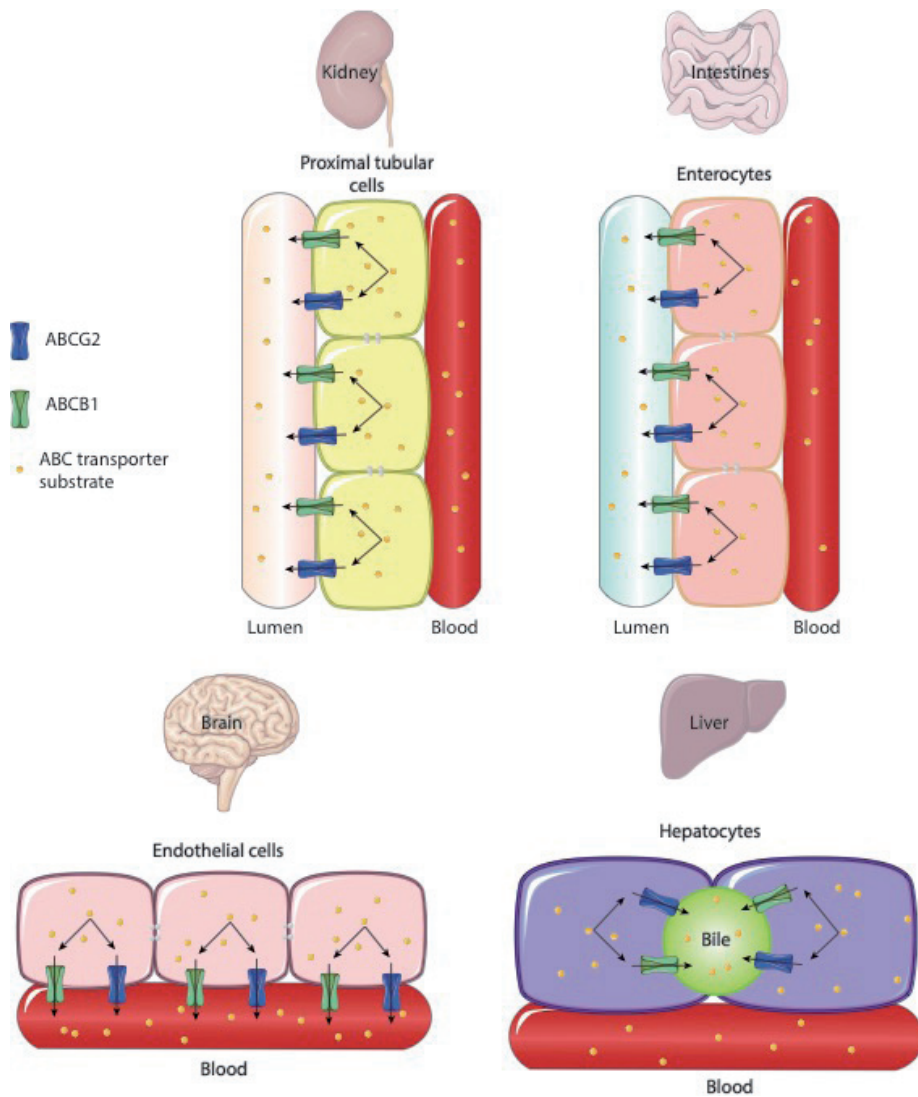


**Figure 2** - Schematic representation of the expression sites of ABCB1 and ABCG2 and their transport direction in pharmacologically important organs. Shown is the transport direction of the ABCB1 and ABCG2 substrates in the kidney from the proximal tubular cells into the tubular lumen (i.e., towards the urine). In the intestines ABCB1 and ABCG2 transport their substrates from the enterocytes into the intestinal lumen (i.e., towards the feces), while in the brain these efflux transporters transport their substrates from the endothelial cells into the blood. In the liver ABCB1 and ABCG2 transport their substrates from the hepatocytes into the bile, i.e., towards the intestinal lumen.

3A43, with CYP3A4 having the highest abundance in the liver, comprising between 30 and 50% of the total hepatic CYP content (13, 14). CYP3A and CYP2C represent the major intestinal CYPs, accounting for approximately 80% and 18% of the intestinal CYP content, respectively (15). CYP3A4 is therefore one of the main drug-metabolizing enzymes. It has a large and flexible active site that enables its interaction with a wide range of structurally diverse compounds and permits metabolism of (and/or inhibition by) such diverse molecules and drugs as hormones (testosterone, estrogen), anti-cancer drugs (docetaxel, tamoxifen), and anti-fungal agents (ketoconazole), amongst others (12, 16). It has been shown that inhibition of CYPs may achieve rapid increases in the blood concentration and bioavailability of drugs, but inhibition of CYPs may also lead to the toxicity or lack of efficacy of a drug (17, 18).

## **TYROSINE KINASE INHIBITORS**

Conventional chemotherapy typically does not discriminate effectively between rapidly dividing normal cells (e.g., bone marrow and gastrointestinal tract) and tumor cells, thereby often leading to severe toxic side effects. Tumor responses from these kinds of cytotoxic chemotherapy are usually unpredictable. In contrast, targeted therapies interfere with defined molecular targets that have a demonstrated role in tumor growth or progression, and are often specifically located in tumor cells. Therefore, targeted therapies have a generally higher specificity towards tumor cells and thereby provide a broader therapeutic window with less toxicity (19). One of the most prominent types of targeted therapies are formed by the tyrosine kinase inhibitors (TKIs).

Tyrosine kinases play a critical role in the modulation of growth factor signaling, and thus activated forms of these enzymes can cause an increase in tumor cell proliferation and growth, induce anti-apoptotic effects and promote angiogenesis and metastasis. In addition to activation by growth factors, protein kinase activation or alteration by somatic mutation is a common mechanism of tumorigenesis (20). Because all these effects are mediated by the activation of tyrosine kinase receptors, it makes these targets key for the development of their inhibitors. In this thesis we have studied the pharmacokinetics of the following TKIs: afatinib, osimertinib, ibrutinib and ponatinib.

## **USES AND LIMITATIONS OF MOUSE STUDIES**

Mouse studies are useful to establish basic principles governing pharmacokinetic behavior, and studies often make use of single and/or combination knockout mouse

models as well as humanized transgenic mouse models in order to unravel interactions between the ABC transporters, CYP enzymes and many drugs. In this thesis we made use of previously generated single and combination knockout mouse models of the ABCB1 and ABCG2 transporters as well as the Cyp3a knockout mouse model along with the humanized transgenic CYP3A4 mouse models to study their interactions with the tyrosine kinase inhibitors afatinib, osimertinib, ibrutinib and ponatinib.

For all of these drugs we found that they are transported to a greater or lesser extent by ABCB1 and/or ABCG2. In the mouse models this transport sometimes modestly restricted the oral availability, but it always resulted in pronounced decreases in brain penetration of the drugs. Implications of the latter findings are that brain tumors or (micro)metastases that are positioned behind a functional blood-brain barrier may not be readily accessible to these drugs, and therefore respond very poorly to the therapy. The same might apply to tumors that themselves substantially express one or both of these transporters. For this reason it may be considered to try and combine therapy with these TKIs with coadministration of efficient ABCB1 and/or ABCG2 inhibitors, such as elacridar in mice. In the past we and other groups have shown that this principle works well in improving brain penetration of substrate drugs in preclinical (mouse) studies.

However, mouse models should not be used in a simplistic one-to-one way to predict what is going to happen in humans. Ultimately, this can only be done in trials in humans, optimally designed with a basic understanding of the underlying principles in mind. Many of the targeted anticancer drugs that we (and various other groups) have tested so far are strongly affected by both ABC transporters, albeit to variable relative extents (21, 22). From this perspective, perhaps the use of primarily ABCB1 inhibitors in the past instead of highly effective dual inhibitors of both ABCB1 and ABCG2 may also have contributed to failure of some clinical inhibitor trials. However, the real-life clinical treatment of tumors is complicated, and there can be many additional reasons why application of ABCB1 inhibitors has so far failed to substantially improve therapy response.

## WHAT NEXT?

Improving brain accumulation of drugs is of high interest in the clinic due to the fact that current therapies are often inefficient in eradicating brain tumors or brain metastases situated in whole or in part behind an intact blood-brain barrier (BBB) (9, 10). However, it appears to be a challenge for pharmaceutical companies to develop drugs that are not transported by these ABC transporters. The promise of improved brain penetration for scores of drugs using potent 3rd generation ABCB1 and/or ABCG2 inhibitors has

been as yet elusive, not only for cancer therapy, but also for other drugs targeting CNS diseases (23-25).

It is fair to say that we don't think there is a longer-term future for chronic clinical administration of strong ABCB1 and ABCG2 inhibitors together with targeted anticancer drugs, especially when it concerns improving brain (tumor) access. It is risky to completely inhibit ABCB1 and ABCG2 in the blood-brain barrier of patients in a chronic setting, as would be required for clinical treatment with most targeted anticancer drugs. Unpredictable (CNS) toxicity of drugs, pesticides and even some food components, to which such patients will inevitably be exposed, might emerge. Indeed, we have observed severe and sometimes lethal toxicity of otherwise well tolerated drugs, pesticides, and even food components in ABCB1 and/or ABCG2 knockout mouse strains due to highly increased availability of these compounds (26-28).

In our view, the future lies in the development of effective targeted anticancer drugs that are no longer transported substrates of ABCB1 and ABCG2. This appears to be difficult to achieve, likely related to the many other constraints of developing efficacious new drugs: we estimate that at least 90% of targeted anticancer drugs that have been registered over the past 10 years are significantly transported by either or both of these ABC transporters. However, it does appear to be feasible if a dedicated effort is made [e.g.,(29)]. Such "untransported" drugs would combine the advantages of being no longer susceptible to multidrug resistance mediated by ABCB1 and ABCG2 present in tumor cells, and of having relatively enhanced access to brain (tumor) tissue. Obtaining such compounds should therefore be a main goal for pharmaceutical companies developing new anticancer drugs, especially those targeting tumors or metastases positioned in whole or in part behind the blood-brain barrier.

## REFERENCES

1. Dean M, Hamon Y, Chimini G. The human ATP-binding cassette (ABC) transporter superfamily, *J Lipid Res*, 7 (2001) 1007-1017.
2. Aikawa T, Holm ML, Kanekiyo T. ABCA7 and Pathogenic Pathways of Alzheimer's Disease, *Brain Sci*, 2 (2018) 10.3390/brainsci8020027
3. Mijac D, Vukovic-Petrovic I, Mijac V, et al. MDR1 gene polymorphisms are associated with ulcerative colitis in a cohort of Serbian patients with inflammatory bowel disease, *PLoS One*, 3 (2018) e0194536. 10.1371/journal.pone.0194536
4. Schumacher T, Benndorf RA. ABC Transport Proteins in Cardiovascular Disease-A Brief Summary, *Molecules*, 4 (2017) 10.3390/molecules22040589
5. Zaiou M, Bakillah A. Epigenetic Regulation of ATP-Binding Cassette Protein A1 (ABCA1) Gene Expression: A New Era to Alleviate Atherosclerotic Cardiovascular Disease, *Diseases*, 2 (2018) 10.3390/diseases6020034
6. Dean M, Rzhetsky A, Allikmets R. The human ATP-binding cassette (ABC) transporter superfamily, *Genome Res*, 7 (2001) 1156-1166. 10.1101/gr.184901
7. Schinkel AH, Wagenaar E, Mol CA, et al. P-glycoprotein in the blood-brain barrier of mice influences the brain penetration and pharmacological activity of many drugs, *J Clin Invest*, 11 (1996) 2517-2524. 10.1172/JCI118699
8. Vlaming ML, Lagas JS, Schinkel AH. Physiological and pharmacological roles of ABCG2 (BCRP): recent findings in *Abcg2* knockout mice, *Adv Drug Deliv Rev*, 1 (2009) 14-25. 10.1016/j.addr.2008.08.007
9. Lockman PR, Mittapalli RK, Taskar KS, et al. Heterogeneous blood-tumor barrier permeability determines drug efficacy in experimental brain metastases of breast cancer, *Clin Cancer Res*, 23 (2010) 5664-5678. 10.1158/1078-0432.CCR-10-1564
10. Taskar KS, Rudraraju V, Mittapalli RK, et al. Lapatinib distribution in HER2 overexpressing experimental brain metastases of breast cancer, *Pharm Res*, 3 (2012) 770-781. 10.1007/s11095-011-0601-8
11. Plant N. The human cytochrome P450 sub-family: transcriptional regulation, inter-individual variation and interaction networks, *Biochim Biophys Acta*, 3 (2007) 478-488. 10.1016/j.bbagen.2006.09.024
12. Zanger UM, Schwab M. Cytochrome P450 enzymes in drug metabolism: regulation of gene expression, enzyme activities, and impact of genetic variation, *Pharmacol Ther*, 1 (2013) 103-141. 10.1016/j.pharmthera.2012.12.007
13. Westlind-Johnsson A, Malmebo S, Johansson A, et al. Comparative analysis of CYP3A expression in human liver suggests only a minor role for CYP3A5 in drug metabolism, *Drug Metab Dispos*, 6 (2003) 755-761.
14. Lin YS, Dowling AL, Quigley SD, et al. Co-regulation of CYP3A4 and CYP3A5 and contribution to hepatic and intestinal midazolam metabolism, *Mol Pharmacol*, 1 (2002) 162-172.
15. Thelen K, Dressman JB. Cytochrome P450-mediated metabolism in the human gut wall, *J Pharm Pharmacol*, 5 (2009) 541-558. 10.1211/jpp/61.05.0002
16. Flockhart DA, Rae JM. Cytochrome P450 3A pharmacogenetics: the road that needs traveled, *Pharmacogenomics J*, 1 (2003) 3-5. 10.1038/sj.tpj.6500144
17. Pelkonen O, Turpeinen M, Hakkola J, et al. Inhibition and induction of human cytochrome P450 enzymes: current status, *Arch Toxicol*, 10 (2008) 667-715. 10.1007/s00204-008-0332-8
18. Athukuri BL, Neerati P. Enhanced Oral Bioavailability of Domperidone with Piperine in Male Wistar Rats: Involvement of CYP3A1 and P-gp Inhibition, *J Pharm Pharm Sci*, (2017) 28-37. 10.18433/J3MK72
19. Tsimberidou AM, Eggermont AM, Schilsky RL. Precision cancer medicine: the future is now, only better, *Am Soc Clin Oncol Educ Book*, (2014) 61-69. 10.14694/EdBook\_AM.2014.34.61
20. Blume-Jensen P, Hunter T. Oncogenic kinase signalling, *Nature*, 6835 (2001) 355-365. 10.1038/35077225
21. Durmus S, Sparidans RW, Wagenaar E, et al. Oral availability and brain penetration of the B-RAFV600E inhibitor vemurafenib can be enhanced by the P-GLYCOPROTEIN (ABCB1) and breast cancer resistance protein (ABCG2) inhibitor elacridar, *Mol Pharm*, 11 (2012) 3236-3245. 10.1021/mp3003144

22. Tang SC, Nguyen LN, Sparidans RW, et al. Increased oral availability and brain accumulation of the ALK inhibitor crizotinib by coadministration of the P-glycoprotein (ABCB1) and breast cancer resistance protein (ABCG2) inhibitor elacridar, *Int J Cancer*, 6 (2014) 1484-1494. 10.1002/ijc.28475
23. Cripe LD, Uno H, Paietta EM, et al. Zosuquidar, a novel modulator of P-glycoprotein, does not improve the outcome of older patients with newly diagnosed acute myeloid leukemia: a randomized, placebo-controlled trial of the Eastern Cooperative Oncology Group 3999, *Blood*, 20 (2010) 4077-4085. 10.1182/blood-2010-04-277269
24. Dash RP, Jayachandra Babu R, Srinivas NR. Therapeutic Potential and Utility of Elacridar with Respect to P-glycoprotein Inhibition: An Insight from the Published In Vitro, Preclinical and Clinical Studies, *Eur J Drug Metab Pharmacokinet*, 6 (2017) 915-933. 10.1007/s13318-017-0411-4
25. O'Brien FE, Dinan TG, Griffin BT, et al. Interactions between antidepressants and P-glycoprotein at the blood-brain barrier: clinical significance of in vitro and in vivo findings, *Br J Pharmacol*, 2 (2012) 289-312. 10.1111/j.1476-5381.2011.01557.x
26. Jonker JW, Buitelaar M, Wagenaar E, et al. The breast cancer resistance protein protects against a major chlorophyll-derived dietary phototoxin and protoporphyria, *Proc Natl Acad Sci U S A*, 24 (2002) 15649-15654. 10.1073/pnas.202607599
27. Schinkel AH, Smit JJ, van Tellingen O, et al. Disruption of the mouse *mdr1a* P-glycoprotein gene leads to a deficiency in the blood-brain barrier and to increased sensitivity to drugs, *Cell*, 4 (1994) 491-502.
28. Li W, Sparidans RW, Wang Y, et al. P-glycoprotein and breast cancer resistance protein restrict brigatinib brain accumulation and toxicity, and, alongside CYP3A, limit its oral availability, *Pharmacol Res*, (2018) 47-55. 10.1016/j.phrs.2018.09.020
29. Salphati L, Heffron TP, Aliche B, et al. Targeting the PI3K pathway in the brain--efficacy of a PI3K inhibitor optimized to cross the blood-brain barrier, *Clin Cancer Res*, 22 (2012) 6239-6248. 10.1158/1078-0432.CCR-12-0720





# 2

---

## Breast cancer resistance protein (BCRP/ABCG2) and P-glycoprotein (P-gp/ABCB1) transport afatinib and restrict its oral availability and brain accumulation

---

**Stéphanie van Hoppe<sup>1</sup>, Rolf W. Sparidans<sup>2</sup>, Els Wagenaar<sup>1</sup>,  
Jos H. Beijnen<sup>2</sup> and Alfred H. Schinkel<sup>1</sup>**

<sup>1</sup>Division of Molecular Oncology, The Netherlands Cancer Institute, Amsterdam

<sup>2</sup>Section of Pharmacoepidemiology & Clinical Pharmacology, Department of Pharmaceutical Sciences, Faculty of Science, Utrecht University, Utrecht

*Pharmacol Res.* 2017 Jun;120:43-50.

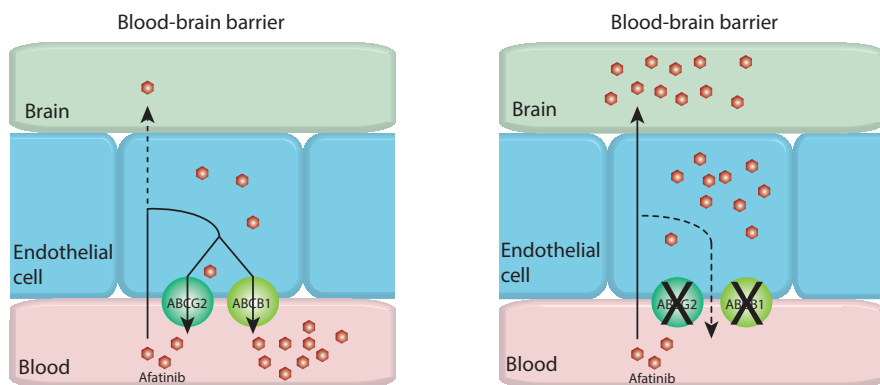
## ABSTRACT

Afatinib is a highly selective, irreversible inhibitor of EGFR and (HER)-2. It is orally administered for the treatment of patients with EGFR mutation-positive types of metastatic NSCLC. We investigated whether afatinib is a substrate for the multidrug efflux transporters ABCB1 and ABCG2 and whether these transporters influence oral availability and brain and other tissue accumulation of afatinib.

We used *in vitro* transport assays to assess human (h)ABCB1-, hABCG2- or murine (m) Abcg2-mediated transport of afatinib. To study the single and combined roles of Abcg2 and Abcb1a/1b in oral afatinib disposition, we used appropriate knockout mouse strains.

Afatinib was transported well by hABCB1, hABCG2 and mAbcg2 *in vitro*. Upon oral administration of afatinib, Abcg2<sup>-/-</sup>, Abcb1a/1b<sup>-/-</sup> and Abcb1a/1b<sup>-/-</sup>;Abcg2<sup>-/-</sup> mice displayed a 4.2-, 2.4- and 7-fold increased afatinib plasma AUC<sub>0-24</sub> compared with wild-type mice. Abcg2-deficient strains also displayed decreased afatinib plasma clearance. At 2 h, relative brain accumulation of afatinib was not significantly altered in the single knockout strains, but 23.8-fold increased in Abcb1a/1b<sup>-/-</sup>;Abcg2<sup>-/-</sup> mice compared to wild-type mice.

Abcg2 and Abcb1a/1b restrict oral availability and brain accumulation of afatinib. Inhibition of these transporters may therefore be of clinical importance for patients with brain (micro)metastases positioned behind an intact blood-brain barrier.



## INTRODUCTION

ATP-binding cassette (ABC) transporters form a superfamily of transmembrane transport proteins. Two members, ABCB1 (MDR1, P-glycoprotein or P-gp) and ABCG2 (Breast Cancer Resistance Protein, BCRP), are especially important in pharmacokinetics [1, 2]. Both affect the disposition of a wide variety of endogenous and exogenous compounds, including many anticancer drugs. They are expressed at pharmacologically important sites such as the apical membranes of enterocytes, hepatocytes and renal tubular epithelial cells, where they can limit gastrointestinal absorption or mediate direct intestinal, hepatic, or renal excretion of their substrates [1, 2]. Furthermore, ABCB1 and ABCG2 are expressed on apical membranes of barriers protecting sanctuary tissues such as the blood-brain, blood-placenta and blood-testis barriers, where substrates are pumped directly out of the epithelial or endothelial cells into the blood. Consequently, several chemotherapeutic agents that are ABCB1 and/or ABCG2 substrates have restricted brain accumulation [1-4]. Improving brain accumulation of drugs is of high interest in the clinic due to the fact that current therapies are often inefficient in eradicating brain tumors or brain metastases situated in whole or in part behind an intact blood-brain barrier (BBB) [3, 4].

Afatinib (Gilotrif/Giotrif, BIBW 2992) is an orally administered tyrosine kinase inhibitor (TKI) for the treatment of patients with distinct types of metastatic non-small cell lung carcinoma (NSCLC), whose tumor genes have epidermal growth factor receptor (EGFR) exon 19 deletions or exon 21 (L858R) substitution mutations [5]. Approved by the FDA in July 2013, afatinib is a highly selective, irreversible inhibitor of the EGFR and of the human epidermal growth-factor receptor (HER)-2 [6]. It is barely metabolized, with a total recovery percentage of 89.5% of unchanged drug in the urine and feces over 72 h after dosing in humans [7]. Both EGFR and HER-2 are members of the receptor tyrosine kinase (RTK) superfamily [8] and overexpression of both receptors is often found in human cancers such as gliomas, carcinomas of the breast, ovaries, bladder, and lung, including NSCLC. The overexpression, due to gene amplification, is often associated with higher EGFR pathway signaling activity, increased proliferation of cancer cells and reduced apoptosis [9]. It has further been shown preliminarily in cell lines, that afatinib appears effective against a subset of these various cancers overexpressing EGFR and HER-2 [10-12], making it an attractive candidate for further clinical research.

Several published studies indicate that afatinib can interact with ABCB1 and ABCG2 [13-15]. It has for instance been shown that afatinib affects ABCB1 and ABCG2 in several cancer cell lines by blocking substrate transport and/or down-regulating mRNA and protein expression of the transporters [13, 15]. However, these same studies reported conflicting data on the ability of afatinib to inhibit ABCB1. FDA and EMA registration

information mentions that afatinib is a transported substrate and inhibitor of ABCB1 and ABCG2 [5, 16, 17], but the limited documentation provided does not allow an assessment of the extent of these processes. In case these efflux transporters can efficiently transport afatinib, this might potentially lead to a decreased accumulation of this drug in target tumors expressing these transporters. Moreover, brain metastases are likely to occur with a subset of cancers, the frequency being highest in lung cancer relative to other common epithelial malignancies [18]. Given the high ABCB1 and ABCG2 expression in the BBB, these transporters could potentially limit afatinib brain accumulation, which might lead to reduced therapeutic efficiency against NSCLC brain metastases. We therefore aimed in this study to investigate whether and to what extent afatinib is transported by one or both of these transporters, and how this might affect oral plasma pharmacokinetics and brain penetration of the drug in *Abcb1a/1b* and *Abcg2* mouse models.

## MATERIALS AND METHODS

### Chemicals

Afatinib (>99%) was obtained from Alsachim (Illkirch, France). Zosuquidar was purchased from Sequoia Research Products (Pangbourne, UK) and Ko143 was obtained from Tocris Bioscience (Bristol, UK). All chemicals used in the chromatographic afatinib assay were described before [19].

### Transport assays

Polarized Madin-Darby Canine Kidney (MDCKII) cell lines and subclones transduced with either human (h)ABCB1, (h)ABCG2 [20], or mouse (m)Abcg2 cDNA were cultured and used in the transepithelial transport assays as described previously [21]. Transport assays were performed using 12-well Transwell® 3402 plates, 3.0 µm pore size (Corning Inc., USA) in DMEM with 10% fetal bovine serum (FBS). The parental cells and subclones were seeded at a density of  $2.5 \times 10^5$  cells per well and cultured for 3 days to allow formation of an intact monolayer. Membrane tightness was assessed by measurement of transepithelial electrical resistance (TEER) using reference values that were previously established and well correlated to <1% transepithelial [<sup>14</sup>C]-inulin leakage per hour [21]. The transepithelial transport experiment was started by pre-incubating the cells with or without the relevant inhibitors during 1 h, thereafter (t = 0) medium in the donor compartments was replaced with complete medium containing 2 µM afatinib alone or in combination with the appropriate inhibitors. In the inhibition experiments, 5 µM zosuquidar (ABCB1 inhibitor) and/or 5 µM Ko143 (ABCG2/Abcg2 inhibitor) were added

to both apical and basolateral compartments. Plates were kept at 37°C in 5% CO<sub>2</sub> during the experiment, and 50-µl aliquots were taken from the acceptor compartment at 2, 4 and 8 h for measurement of afatinib concentrations. Samples were stored at -30°C for later LC-MS/MS measurement. Total amount of drug transported to the acceptor compartment was calculated after correction for volume loss for each sampling time point. Active transport was expressed by the transport ratio (*r*), which is defined as the amount of apically directed transport divided by the amount of basolaterally directed transport at a defined time point.

## Animals

Female wild-type, *Abcb1a/1b*<sup>-/-</sup> [22], *Abcg2*<sup>-/-</sup> [23] and *Abcg2;Abcb1a/1b*<sup>-/-</sup> mice [24], all of a >99% FVB genetic background, were used. Mice between 9 and 14 weeks of age were used in groups of five mice per strain. The mice were kept in a temperature-controlled environment with a 12 h light/12 h dark cycle and received a standard diet (Transbreed, SDS Diets, Technilab - BMI) and acidified water *ad libitum*. Animals were housed and handled according to institutional guidelines in compliance with Dutch and EU legislation.

## Drug solutions and pharmacokinetic experiments

Afatinib was dissolved at a concentration of 20 mg/ml in 50% (v/v) polysorbate 80, 50% (v/v) ethanol. It was then further diluted with 5% (w/v) glucose in water, to obtain a 1 mg/ml afatinib solution in water containing 2.5% (v/v) polysorbate 80, 2.5% (v/v) ethanol, and 4.75% (w/v) glucose. Afatinib was administered orally at a dose of 10 mg/kg (10 µl/g). All working solutions were prepared freshly on the day of the experiment. To minimize variation in absorption, mice were fasted for 3 h prior to oral administration of afatinib using a blunt-ended needle. For the pharmacokinetic experiment, 50-µl blood samples were drawn from the tail vein using heparin-coated capillaries (Sarstedt, Germany) at 0.5, 1, 2, 4 and 8 h or 0.25, 0.5 and 1 h. At 24 h or 2 h, mice were anesthetized using isoflurane and blood was collected via cardiac puncture. Immediately thereafter, mice were sacrificed by cervical dislocation and brain, spleen, liver and kidney were rapidly removed, weighed and subsequently frozen as whole organ at -30°C. Prior to analysis, organs were allowed to thaw and then homogenized in appropriate volumes (1 to 3 ml) of 4% (w/v) bovine serum albumin (BSA) in water using a FastPrep®-24 homogenizer (MP-Biomedicals, NY, USA). Homogenates were stored at -30°C. Blood samples were centrifuged immediately after collection at 9000 × *g* for 6 min at 4°C, and plasma was collected and stored at -30°C until analysis.

## Drug analysis

Afatinib concentrations in culture medium, plasma and tissues were determined with a previously reported liquid chromatography-tandem mass spectrometric (LC-MS/MS) assay for afatinib, with a calibration curve ranging from 0.5 to 500 ng/ml for plasma [19] and tissue homogenates and from 1.5 to 1500 ng/ml for culture medium. Tissue concentrations were calculated correcting for the individual tissue weights, resulting in ng afatinib per gram tissue.

## Statistical analysis and pharmacokinetic calculations

The unpaired two-tailed Student's *t*-test was used to determine statistical significance for transepithelial transport. In pharmacokinetic experiments, the area under the curve (AUC) of the plasma concentration-time plot was calculated using the trapezoidal rule, without extrapolating to infinity. The maximum drug concentration in plasma ( $C_{max}$ ) and the time to reach maximum drug concentration in plasma ( $T_{max}$ ) were determined directly from individual concentration-time data. The elimination rate constant was calculated with the Microsoft Excel plug in PKsolver [25] with the following formula:  $(\ln(y_1) - \ln(y_2)) / (t_2 - t_1)$ . Relative organ accumulation ( $P_{organ}$ ) was calculated by dividing organ concentrations ( $C_{organ}$ ) at either  $t = 2$  h or  $t = 24$  h by the area under the plasma concentration-time curve from 0–2 h ( $AUC_{0-2h}$ ) or 0–24 h ( $AUC_{0-24h}$ ), respectively. One-way analysis of variance (ANOVA) was used to determine significance of differences between groups, after which post-hoc tests with Tukey correction were performed for comparison between individual groups. When variances were not homogeneous, data were log-transformed before statistical tests were applied. Differences were considered statistically significant when  $P < 0.05$ . Data are presented as means  $\pm$  SD.

## RESULTS

### Afatinib is transported by hABC1, hABCG2 and mAbcg2

We first studied the transport of afatinib *in vitro* by measuring afatinib (2  $\mu$ M) translocation through polarized monolayers of MDCKII cell lines transduced with human (h)ABC1, hABCG2 or mouse (m)Abcg2 cDNA. As shown in Fig. 1A, we observed low apically directed afatinib transport in the parental cell line (transport ratio  $r = 1.3$ ). This was somewhat decreased (to an  $r$  of 0.8) when adding the ABCB1 inhibitor zosuquidar (Fig. 1B), suggesting that this background transport could be mediated by the low amount of endogenous canine ABCB1 present in the MDCKII cells [26]. In MDCKII cells transduced with hABC1, we observed extensive apically directed transport with  $r = 7.6$ , which was completely blocked by zosuquidar ( $r = 0.9$ , Fig. 1C, D). To suppress any endogenous

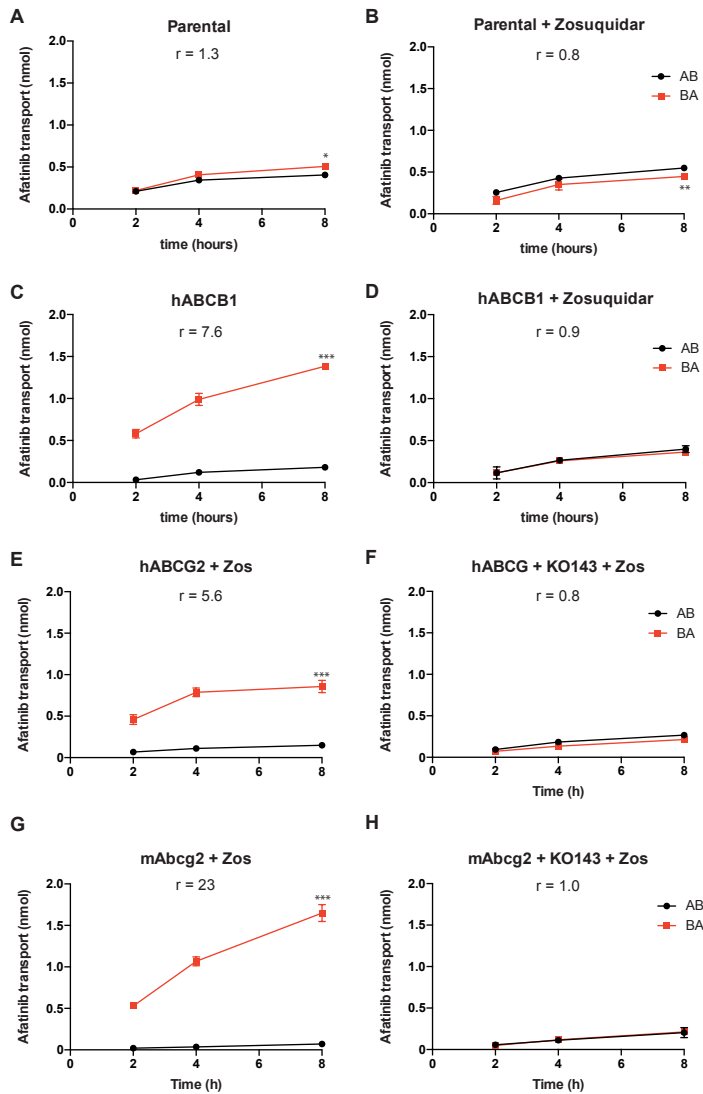


**Figure 1** - *In vitro* transport of afatinib. Transepithelial transport of afatinib (2  $\mu$ M) was assessed in MDCK-II cells either non-transduced (**A**, **B**) or transduced with hABCB1 (**C**, **D**), hABCG2 (**E**, **F**), or mAbcg2 (**G**, **H**) cDNA. At T = 0 h afatinib was added to the donor compartment; thereafter at t = 2, 4 and 8 h the concentrations were measured and plotted as total amount (nmol) of transport (n = 3). **B**, **D**-**H**: Zosuquidar (5  $\mu$ M) and/or Ko143 (5  $\mu$ M) were added as indicated to inhibit hABCB1 and hABCG2 or mAbcg2, respectively. *r*, relative transport ratio. BA (red squares) translocation from the basolateral to the apical compartment; AB (black circles), translocation from the apical to the basolateral compartment. Data are presented as the mean  $\pm$  SD. Owing to high experimental reproducibility, in many cases the error bars are smaller than the symbols used to denote a data point. \*, P < 0.05; \*\*, P < 0.01; \*\*\*, P < 0.001 compared with AB translocation.

canine ABCB1 activity, subsequent experiments on ABCG2-mediated transport were done in the presence of zosuquidar. Both hABCG2 and mAbcg2 efficiently transported afatinib in the apical direction ( $r = 5.6$  and  $r = 23$ , respectively) (Fig. 1E, G). This transport was completely abrogated ( $r = 0.8$  and  $r = 1.0$ , respectively) by treatment with the ABCG2 inhibitor Ko143 (Fig. 1F, H). Overall, afatinib appears to be well transported by hABCB1, hABCG2 and mAbcg2.

### Abcg2 and Abcb1 each restrict the oral availability of afatinib in mice

Afatinib is given orally to patients. We therefore started with a pilot experiment with oral afatinib (10 mg/kg) in WT and *Abcb1a/1b;Abcg2*<sup>-/-</sup> mice, analyzing plasma concentrations and tissue accumulation after 8 h. The results indicated a substantial impact of this combined transporter deficiency on oral availability and brain accumulation of afatinib, with highly increased exposure levels in the knockout strain (Supplemental Figures 1-3). We therefore studied in more detail the single and combined effects of *Abcb1* and *Abcg2* deficiencies on afatinib plasma pharmacokinetics and organ accumulation using WT, *Abcg2*<sup>-/-</sup>, *Abcb1a/1b*<sup>-/-</sup>, and *Abcb1a/1b;Abcg2*<sup>-/-</sup> mice. Plasma exposure of afatinib over 24 h ( $AUC_{0-24}$ ) was increased by the absence of *Abcg2* by 4.2-fold ( $P < 0.001$ ), by the absence of *Abcb1a/1b* by 2.4-fold ( $P < 0.01$ ), and by the absence of both *Abcg2* and *Abcb1a/1b* by 7-fold ( $P < 0.001$ ) compared to WT mice (Fig. 2A; Table I, 24 h data). These results indicate that each of these transporters can substantially affect the intestinal uptake and/or the systemic elimination of afatinib, thus restricting its oral availability. The marked contribution of each of the individual transporters was further supported by comparison of the plasma  $AUC_{0-24}$  values of the single knockout strains with the combination knockout strain (Table I, 24 h data).

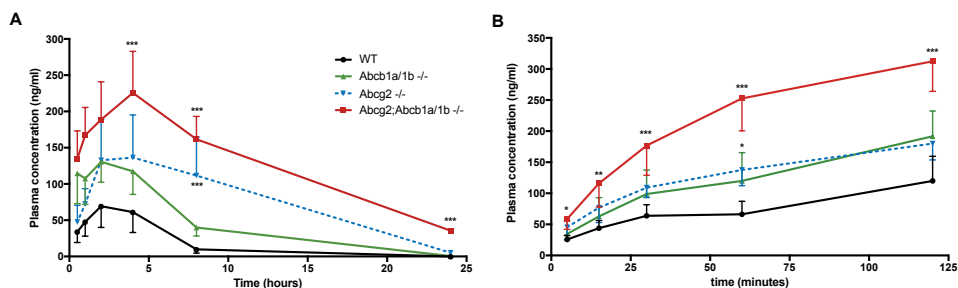


**Figure 2** - Plasma concentration-time curves of afatinib in female WT (black squares), *Abcg2*<sup>-/-</sup> (blue triangles), *Abcb1a/1b*<sup>-/-</sup> (green triangles), and *Abcg2;Abcb1a/1b*<sup>-/-</sup> mice (red squares) over 24 hours (A) and 120 minutes (B) after oral administration of 10 mg/kg afatinib. Data are given as mean  $\pm$  SD (SD rendered one-sided for improved clarity). \*,  $P < 0.05$ ; \*\*,  $P < 0.01$ ; \*\*\*,  $P < 0.001$  compared to WT mice. Statistical analysis for the 24 h graph (A) for the time points up to 4 h yields  $P < 0.001$  at 30 min and 1 h, at 2 h  $P < 0.01$  for *Abcg2;Abcb1a/1b*<sup>-/-</sup> compared to WT mice.

**Table I** - Pharmacokinetic parameters of afatinib after oral administration of 10 mg/kg to female wild-type, *Abcg2*<sup>-/-</sup>, *Abcb1a/1b*<sup>-/-</sup>, and *Abcb1a/1b;Abcg2*<sup>-/-</sup> mice (n = 5 - 6).

Parameter	Time (h)	Genotype			
		WT	<i>Abcg2</i> <sup>-/-</sup>	<i>Abcb1a/1b</i> <sup>-/-</sup>	<i>Abcb1a/1b;Abcg2</i> <sup>-/-</sup>
AUC <sub>0-2</sub> (ng·h/ml)	2	145 ± 33	254 ± 30 <sup>**,+</sup>	239 ± 70 <sup>*,**</sup>	441 ± 86 <sup>***</sup>
C <sub>plasma</sub> (ng/ml)		120 ± 40	180 ± 26 <sup>***</sup>	192 ± 41 <sup>*,***</sup>	312 ± 48 <sup>***</sup>
C <sub>brain</sub> (ng/g)		51 ± 12	65 ± 16 <sup>***</sup>	130 ± 66 <sup>***</sup>	3658 ± 689 <sup>***</sup>
P <sub>brain</sub> (h <sup>-1</sup> )		0.35 ± 0.06	0.25 ± 0.04 <sup>***</sup>	0.51 ± 0.15 <sup>***</sup>	8.34 ± 0.99 <sup>***</sup>
Fold change		1	0.72	1.5	23.8
C <sub>liver</sub> (µg/g)		10.0 ± 2.9	19.6 ± 4.1 <sup>*</sup>	15.0 ± 6.1 <sup>+</sup>	28.7 ± 10.5 <sup>***</sup>
P <sub>liver</sub> (h <sup>-1</sup> )		70.7 ± 19	76.7 ± 8.8	63.3 ± 17.2	64.9 ± 20.9
Fold change		1	1.1	0.9	0.9
AUC <sub>0-24</sub> (ng·h/ml)	24	434 ± 184	1831 ± 651 <sup>***</sup>	1061 ± 253 <sup>**,++</sup>	3020 ± 590 <sup>***</sup>
C <sub>max</sub> (ng/ml)		73.2 ± 31.5	167 ± 39.4 <sup>*</sup>	131 ± 28.3 <sup>+</sup>	227 ± 57.3 <sup>***</sup>
T <sub>max</sub> (h)		2.8 ± 1.1	4.5 ± 2.5	2	4
C <sub>brain</sub> (ng/g)		1.7 ± 0.2	7.8 ± 3.7 <sup>***,+++</sup>	5.5 ± 1.0 <sup>***,+++</sup>	2054 ± 299 <sup>***</sup>
P <sub>brain</sub> (h <sup>-1</sup> )		4.3 ± 2.4	4.1 ± 0.9 <sup>***</sup>	5.4 ± 1.6 <sup>***</sup>	688 ± 80.1 <sup>***</sup>
Fold change		1	0.95	1.2	160
C <sub>liver</sub> (ng/g)		12.6 ± 4.8	371 ± 176 <sup>***,+++</sup>	22.5 ± 5.1 <sup>***</sup>	3598 ± 1192 <sup>***</sup>
P <sub>liver</sub> (*10 <sup>-3</sup> h <sup>-1</sup> )		31.9 ± 15.6	207 ± 110 <sup>***,+++,#</sup>	21.4 ± 3.6 <sup>***</sup>	1214 ± 429 <sup>***</sup>
Fold change		1	6.5	0.67	38

AUC, area under the plasma concentration-time curve; C<sub>max</sub>, maximum drug concentration in plasma; T<sub>max</sub>, the time after drug administration needed to reach maximum plasma concentration; C<sub>brain</sub>, brain concentration; P<sub>brain</sub>, brain accumulation (C<sub>brain</sub> divided by plasma AUC); C<sub>liver</sub>, liver concentration; P<sub>liver</sub>, liver accumulation (C<sub>liver</sub> divided by plasma AUC). Note: C<sub>liver</sub> at 2 hours is shown in µg/g and P<sub>liver</sub> at 24 hours is shown in \*10<sup>-3</sup> h<sup>-1</sup>. \*, P < 0.05; \*\*, P < 0.01; \*\*\*, P < 0.001 compared to WT mice and +, P < 0.05; ++, P < 0.01, +++, P < 0.001 compared to *Abcb1a/1b*<sup>-/-</sup>; *Abcg2*<sup>-/-</sup> mice and ###, P < 0.001 compared to *Abcb1a/b*<sup>-/-</sup> mice. Data are given as mean ± SD.

Similar results were obtained when measuring the afatinib plasma AUC<sub>0-2</sub> in an independent 2-hour experiment, with 1.6- and 1.8-fold increased values in *Abcg2*<sup>-/-</sup> mice and *Abcb1a/1b*<sup>-/-</sup> mice, respectively (P < 0.01 and P < 0.05), and a 3-fold increase in the combination knockout strain (P < 0.001) compared to the WT mice (Table I). Like for the 24-h experiment, the contribution of each of the individual transporters yielded significant differences in the AUC<sub>0-2</sub> with the combination knockout strain, further supporting that *Abcb1* and *Abcg2* can each restrict the oral availability of afatinib.

Interestingly, a semi-log plot of the plasma concentrations in the 24-hour experiment indicated that, from 8 h on, the plasma clearance in *Abcg2*<sup>-/-</sup> mice, but especially also in the combination knockout mice, was substantially reduced compared to that in WT and

Abcb1a/1b<sup>-/-</sup> mice (Supplemental Fig. 4). This indicates that especially Abcg2 but also Abcb1a/1b can contribute to the plasma clearance of afatinib in mice.

### **Abcg2 and Abcb1 each strongly limit afatinib brain accumulation**

Tissue concentrations were measured at the last time point of the above-mentioned pharmacokinetic experiments. At 24 h, brain concentrations in Abcb1a/1b;Abcg2<sup>-/-</sup> mice showed highly significant increases of 1208-fold ( $P < 0.001$ ) compared to WT mice (Fig. 3A; Table I). The Abcg2<sup>-/-</sup> and Abcb1a/1b<sup>-/-</sup> separate knockout strains also showed a significant increase compared to wild type mice, although far lower, with increases of 4.6- and 3.2-fold, respectively ( $P < 0.001$ ). However, as the afatinib plasma concentrations at 24 h were also very different between the strains, this required appropriate correction. Unfortunately, plasma concentrations at 24 h in the WT mice were undetectable, precluding a direct comparison with afatinib brain-to-plasma ratios in the WT mice (Fig. 3B). Correcting the afatinib brain concentrations for the corresponding plasma AUCs resulted in no significant differences in afatinib accumulation in the brains of Abcg2<sup>-/-</sup> and Abcb1a/1b<sup>-/-</sup> mice compared to WT mice (Fig. 3C). However, for Abcb1a/1b;Abcg2<sup>-/-</sup> mice the brain accumulation was 175-fold increased ( $P < 0.001$ ) compared to that in WT mice, with similar differences observed when compared with Abcg2<sup>-/-</sup> and Abcb1a/1b<sup>-/-</sup> mice (Fig. 3C; Table I). This indicates that Abcg2 and Abcb1a/1b each by themselves can drastically restrict the brain accumulation of afatinib, and that a combined deficiency of these transporters is needed for a pronounced increase of the brain accumulation of afatinib.

The liver often equilibrates quickly with plasma levels of a drug, which makes it complicated to assess differences between strains when plasma levels are widely divergent (and undetectable in the WT strain), as is the case at 24 h. As shown in Table I and Fig. 3D, after oral administration, Abcg2<sup>-/-</sup> mice showed a 29-fold increase ( $P < 0.001$ ) in liver afatinib concentrations compared to WT mice, whereas Abcb1a/1b<sup>-/-</sup> mice did not show a significant difference compared to the WT mice. With both Abcb1a/1b and Abcg2 knocked out, we observed a more pronounced increase in liver concentration of afatinib compared to WT mice (286-fold, Table I, Fig. 3D). However, these pronounced differences may well mainly reflect the large differences in plasma afatinib concentration at this time point, as is suggested by the much smaller differences in liver-to-plasma ratios between the strains as far as these could be assessed (Fig. 3E). Rapid equilibration of liver afatinib with plasma afatinib concentrations renders interpretation of a correction for the plasma AUCs (Fig. 3F) problematic, as the strain differences in plasma concentration at 24 h were far greater than the strain differences in plasma AUCs. Similar complications preclude a straightforward interpretation of kidney and spleen parameters at 24 h (Supplemental Figure 5). Such complications can be circumvented

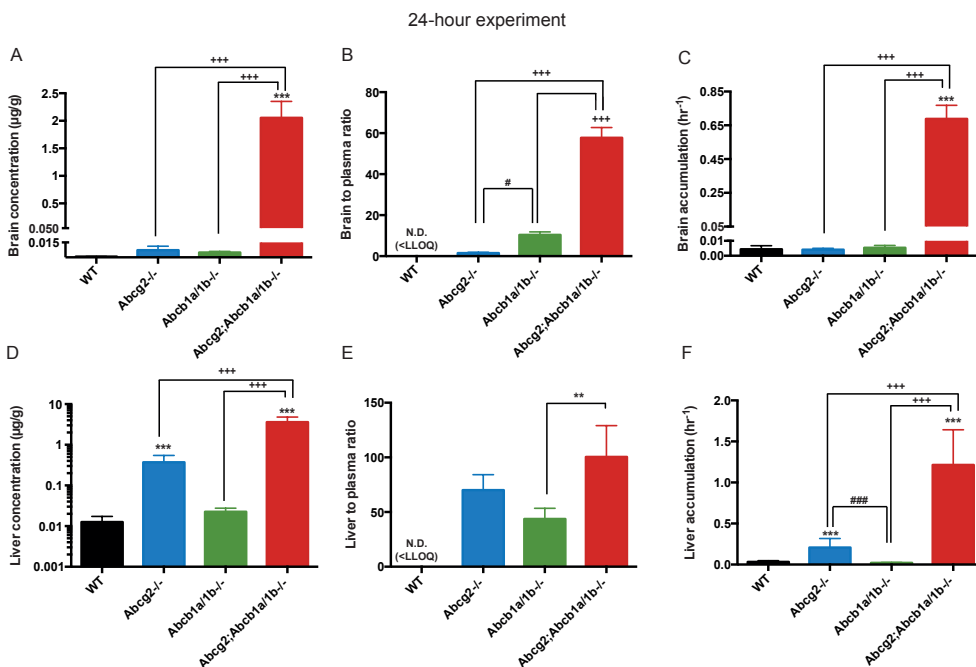


**Figure 3** - Brain and liver concentration (A, D), tissue-to-plasma ratio (B, E) and relative tissue accumulation (C, F) of afatinib in female WT, *Abcg2*<sup>-/-</sup>, *Abcb1a/1b*<sup>-/-</sup> and *Abcg2;Abcb1a/1b*<sup>-/-</sup> mice 24 h after oral administration of 10 mg/kg afatinib. Note the log scale used for the liver concentration in panel D. \*, P < 0.05; \*\*, P < 0.01; \*\*\*, P < 0.001 compared to WT mice, +, P < 0.05, ++, P < 0.01, +++, P < 0.001 compared to *Abcg2;Abcb1a/1b*<sup>-/-</sup> mice; and #, P < 0.05, ##, P < 0.01, ###, P < 0.001 compared to *Abcb1a/1b*<sup>-/-</sup> mice. N.D., not detectable; LLOQ, lower limit of quantification 0.5 ng/ml. Data are presented as the mean ± SD.

by assessing an earlier time point (e.g., 2 h), where plasma concentration differences are much smaller (see below).

The impact of transporter proteins on tissue accumulation of drugs is especially relevant around the time of maximum plasma concentrations. Mice were therefore sacrificed 2 h after oral administration of 10 mg/kg afatinib. Relative plasma concentrations between the strains up to 2 h were very similar to those seen during the 24 h experiment (Compare Figure 2A and B). Similar to the results at 24 h after administration, the brain concentration of afatinib in *Abcb1a/1b;Abcg2*<sup>-/-</sup> mice showed a highly significant 72.4-fold increase (P < 0.001) compared to WT mice. In contrast, no significant differences were found for the single knockout strains compared to WT mice (Fig. 4A, Table 1). Correcting the afatinib brain concentrations for the corresponding plasma concentrations (Fig. 4B) or AUCs (Fig. 4C) yielded similar results. The brain accumulation showed a highly significant, 23.8-fold increase (P < 0.001) for *Abcb1a/1b*<sup>-/-</sup>

$^{-/-};Abcg2^{-/-}$  mice compared to WT mice, whereas brain accumulations in the single knockout strains were not significantly different from those in WT (Fig. 4C; Table 1). Thus, also at 2 h, either *Abcg2* or *Abcb1a/1b* alone could profoundly restrict the brain accumulation of afatinib, and only a combined deficiency for both transporters resulted in a drastically increased brain penetration of afatinib.

As explained above, the liver concentration of drugs often equilibrates relatively quickly with the plasma concentration. The data in Fig. 4D-F and Table 1 support that notion for afatinib. Whereas the liver concentration of afatinib was moderately different between the four strains (Fig. 4D), these differences appeared to entirely reflect the plasma concentrations, as both the liver-to-plasma ratios (Fig. 4E) and liver accumulation data (Fig. 4F) showed virtually equal levels between the four strains. Also measurements of these parameters for kidney and spleen (Supplemental Fig. 6) revealed at most modest differences between the strains. Collectively, these data indicate that the profound difference in brain accumulation of afatinib between the strains, especially at 2 h, is a direct consequence of localized activity of *Abcg2* and *Abcb1a/1b* in the blood-brain barrier.

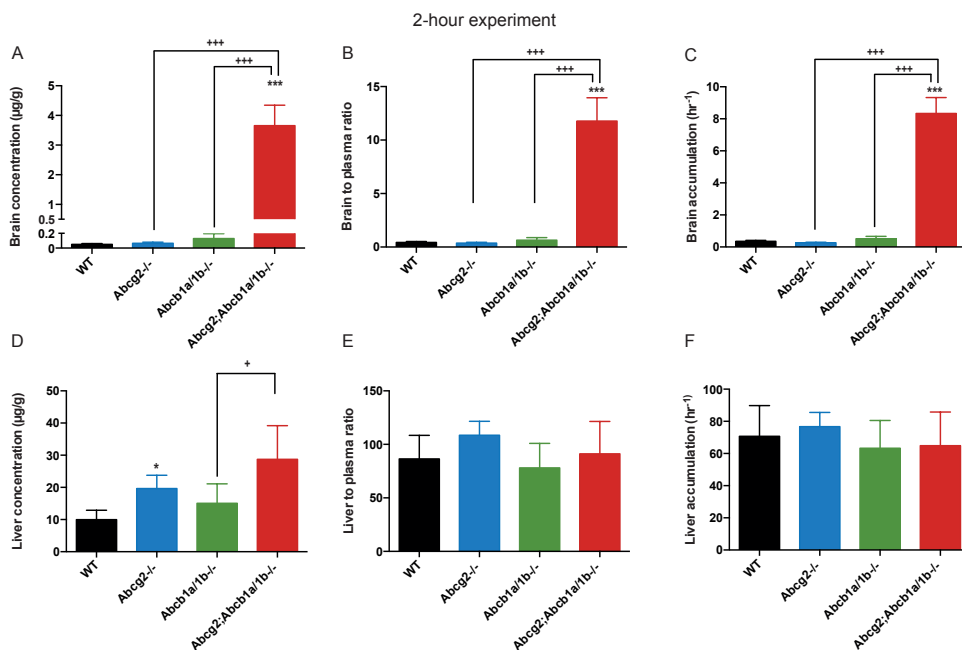


**Figure 4** - Brain and liver concentration (A, D), tissue-to-plasma ratio (B, E) and relative tissue accumulation (C, F) of afatinib in female WT, *Abcg2*<sup>-/-</sup>, *Abcb1a/1b*<sup>-/-</sup> and *Abcg2;Abcb1a/1b*<sup>-/-</sup> mice 2 h after oral administration of 10 mg/kg afatinib. \*,  $P < 0.05$ , \*\*,  $P < 0.01$ , \*\*\*,  $P < 0.001$  compared to WT mice; +,  $P < 0.05$ , ++,  $P < 0.01$ , +++,  $P < 0.001$  compared to *Abcg2;Abcb1a/1b*<sup>-/-</sup> mice. Data are presented as the mean  $\pm$  SD.

## DISCUSSION

A number of ABC transporters, including ABCB1 and ABCG2, cause resistance to a wide range of drugs. Expression of some ABC transporters, especially ABCB1 and ABCG2, was found to be associated with resistance to chemotherapy in several cancers, including NSCLC [27, 28]. This would suggest the possible importance of inhibiting these transporters when treating patients with chemotherapy to reverse such tumor resistance. Furthermore, NSCLC readily metastasizes to the brain [29], where ABCB1 and ABCG2 are expressed at the blood-brain barrier. Inhibiting both these transporters during chemotherapy could therefore possibly also improve treatment of metastases positioned in part or in whole behind the blood-brain barrier. Afatinib has been approved for the first-line treatment of patients with metastatic NSCLC whose tumors have epidermal growth factor receptor (EGFR) mutations [5, 17]. Because the ABC efflux transporters could affect the biological availability of afatinib at several levels, we wanted to investigate the possible effects these transporter proteins might have on afatinib disposition.

We here show that both the ABC efflux transporters ABCG2 and ABCB1 are important factors that can limit uptake of afatinib. We demonstrated that afatinib is efficiently transported by hABCB1, hABCG2 and mAbcg2 *in vitro* (Fig. 1). Similar *in vitro* data were acquired in the past with sunitinib, ceritinib, topotecan and sorafenib [30-32]. The plasma afatinib concentrations in the Abcb1a/1b<sup>-/-</sup>;Abcg2<sup>-/-</sup> mice were highly increased relative to the WT levels. Single Abcg2 or Abcb1a/1b knockout mice also showed a marked increase in afatinib plasma concentrations, albeit not as high as seen in the combination knockout (Fig. 1). This effect was seen for all the experimental studies at the various end-points of 2, 8 and 24 hours after oral administration. These results indicate that the oral availability of afatinib is markedly restricted by both Abcg2 and Abcb1a/1b, which might result from decreased intestinal uptake and/or increased hepatic excretion mediated by these transporters. The results for the single and combination knockout strains suggested roughly additive effects of each transporter in limiting afatinib oral availability. Additionally we found that the plasma clearance was slower in the Abcb1a/1b<sup>-/-</sup>;Abcg2<sup>-/-</sup> mice as well as in the Abcg2<sup>-/-</sup> mice, but perhaps less so for Abcb1a/1b<sup>-/-</sup> mice, compared to WT mice (Supplementary Fig. 4). Their mean elimination rate constants were 0.09 h<sup>-1</sup> (t<sub>1/2</sub> = 7.6 h), 0.18 h<sup>-1</sup> (t<sub>1/2</sub> = 3.8 h), 0.26 h<sup>-1</sup> (t<sub>1/2</sub> = 2.7 h) and 0.36 h<sup>-1</sup> (t<sub>1/2</sub> = 2.0 h) respectively. However, note that the elimination rate constant for the WT mice was calculated only until 8 h because the 24 h time point was below the quantification limit. Our data indicate that especially Abcg2, but also Abcb1a/1b, directly contribute to the plasma clearance of afatinib in mice.

The accumulation of afatinib was highly increased in the brains of the Abcb1a/1b<sup>-/-</sup>

;Abcg2<sup>-/-</sup> mice compared to WT mice (Table I, Fig. 3C, Fig. 4C). However, this was not the case for the two single knockout strains. This suggests that in each case the remaining efflux transporter still present at the BBB could virtually completely take over the role of the knocked out transporter. This disproportionate increase in brain accumulation of afatinib observed in the Abcg2;Abcb1a/1b<sup>-/-</sup> mice compared to the single knockout strains was similar to that found for other TKIs (*e.g.* axitinib, vemurafenib, lapatinib, gefitinib, erlotinib, sunitinib, dasatinib and imatinib [21, 30, 31, 33-37]), and can be explained by relatively straightforward pharmacokinetic models [35, 38]. These indicate that, if the two transporters each have a high contribution of efflux transport relative to the background efflux at the BBB in the absence of both transporters, the effect of single transporter ablation on brain accumulation will be far less than the effect of combined ablation. An interesting implication of these models is that, next to Abcg2 and Abcb1a/1b, there can be no other efflux transporters in the BBB that are remotely as efficient in keeping afatinib out of the brain, at least under the conditions we applied.

The liver is pharmacologically a highly important organ; therefore we have also analyzed the accumulation of afatinib in the liver *in vivo*. We show that when the ABCB1 and ABCG2 efflux transporters are knocked out, there is a significant increase in the accumulation of afatinib in the liver (Fig. 3, 4). However, these changes appear to be driven mainly by the alterations in plasma concentrations between the strains, as suggested by the liver-to-plasma ratios (Fig. 4E; note that the liver-to-plasma ratio in the WT mice at 24 h could not be established because of undetectable plasma levels of afatinib, Fig. 3E).

In previous studies we have found that for some anticancer drugs (everolimus, cabazitaxel) the upregulation of plasma carboxylesterase Ces1c in the ABC transporter knockout strains can affect the pharmacokinetics of these drugs [39, 40]. This can occur by strong binding of some drugs to this protein, resulting in pronounced retention of drug in plasma. If this were the case for afatinib, one would expect a substantially decreased liver-to-plasma ratio in the knockout strains, as previously observed for everolimus and cabazitaxel. As there is no indication whatsoever of such a decrease (Fig. 4E), it appears that afatinib is not substantially affected by such a potentially confounding process.

Clinical trials of afatinib up till now have shown positive results in tumor regression in NSCLC patients with EGFR-mutation positive tumors. Progression-free survival in these patients is enhanced in patients without, as well as with brain metastases [41-43]. A phase III trial in patients with second-line recurrent and/or metastatic head and neck squamous cell carcinoma comparing efficacy of afatinib versus methotrexate has shown favorable results for treatment with afatinib, with a higher progression-free survival rate [44]. Thus, although afatinib has been approved for treatment of NSCLC [5, 17], it may be beneficial for other tumor types containing the relevant EGFR-mutations as well.

Based on our findings, it is likely that tumors expressing ABCB1 and/or ABCG2 will also demonstrate resistance to afatinib-based chemotherapy. Inhibiting these transporters during afatinib therapy might therefore be beneficial for the response of these tumors. It may further be possible to increase afatinib levels in the brain of patients with CNS involvement for better treatment efficacy when afatinib is coadministered with an efficacious dual inhibitor of ABCB1 and ABCG2 such as elacridar. From our study it appears that this sort of coadministration might perhaps also increase the oral availability and consequently overall tissue levels of afatinib, which should be taken into account for possible dose adjustment, to avoid increased toxicity.

## **CONCLUSION**

Our study shows that ABCG2 and ABCB1 by themselves and together markedly restrict oral availability and brain disposition of afatinib, and mediate its elimination. These results indicate that coadministration of efficacious ABCG2 and ABCB1 inhibitors may increase exposure of afatinib in patients, in transporter-expressing tumors, but especially also in the brain, thus providing an option to better treat NSCLC and its metastases positioned in part or in whole behind a functionally intact blood-brain barrier.

## **ACKNOWLEDGEMENTS**

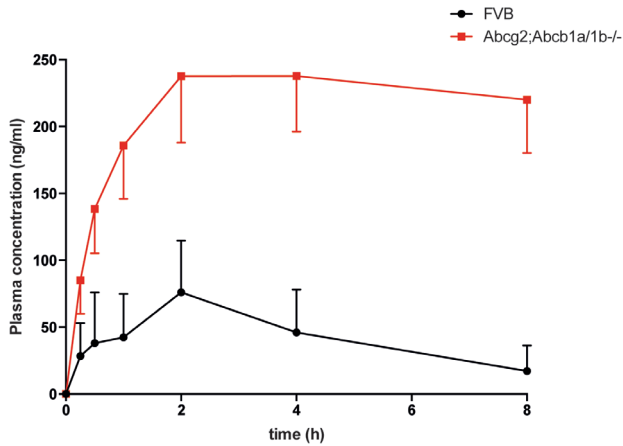
We gratefully acknowledge the technical assistance of Levi Buil during the experimental phase, and Cristina Lebre, Changpei Gan, Diana Martinez, Jing Wang, Xiaozhe Qi and Yaogeng Wang for critical reading of this manuscript.

## REFERENCES

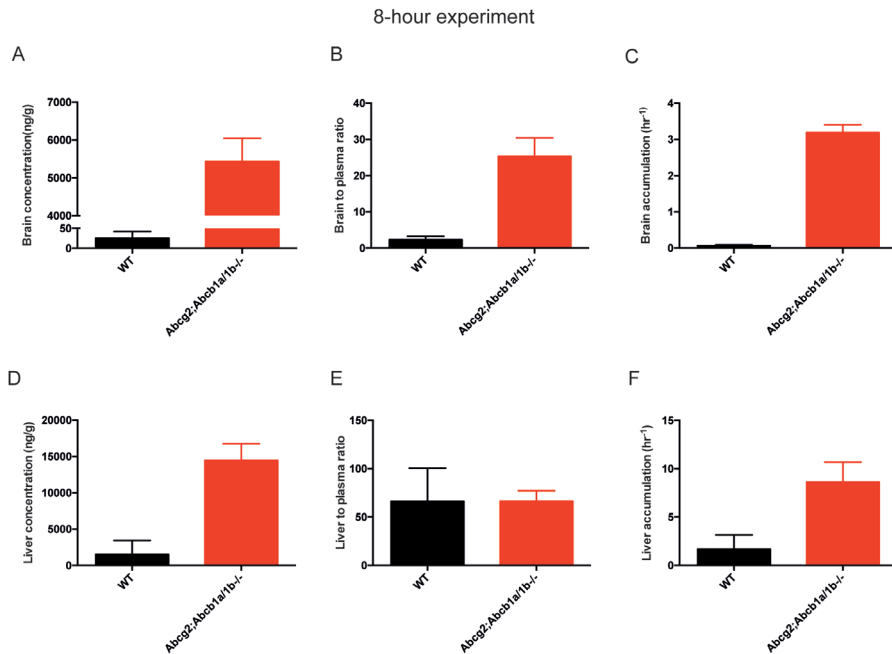
1. Schinkel, A.H., et al., *P-glycoprotein in the blood-brain barrier of mice influences the brain penetration and pharmacological activity of many drugs*. J Clin Invest, 1996. 97(11): p. 2517-24.
2. Vlaming, M.L., J.S. Lagas, and A.H. Schinkel, *Physiological and pharmacological roles of ABCG2 (BCRP): recent findings in Abcg2 knockout mice*. Adv Drug Deliv Rev, 2009. 61(1): p. 14-25.
3. Lockman, P.R., et al., *Heterogeneous blood-tumor barrier permeability determines drug efficacy in experimental brain metastases of breast cancer*. Clin Cancer Res, 2010. 16(23): p. 5664-78.
4. Taskar, K.S., et al., *Lapatinib distribution in HER2 overexpressing experimental brain metastases of breast cancer*. Pharm Res, 2012. 29(3): p. 770-81.
5. *U.S. Food and Drug Administration, Approved Drugs: Afatinib*. 2013; Available from: <http://www.fda.gov/Drugs/InformationOnDrugs/ApprovedDrugs/ucm360574.htm>.
6. Li, D., et al., *BIBW2992, an irreversible EGFR/HER2 inhibitor highly effective in preclinical lung cancer models*. Oncogene, 2008. 27(34): p. 4702-11.
7. Stopfer, P., et al., *Afatinib pharmacokinetics and metabolism after oral administration to healthy male volunteers*. Cancer Chemother Pharmacol, 2012. 69(4): p. 1051-61.
8. Hynes, N.E. and H.A. Lane, *ERBB receptors and cancer: the complexity of targeted inhibitors*. Nat Rev Cancer, 2005. 5(5): p. 341-54.
9. Yarden, Y. and M.X. Sliwkowski, *Untangling the ErbB signalling network*. Nat Rev Mol Cell Biol, 2001. 2(2): p. 127-37.
10. Di Luca, A., et al., *Label-free LC-MS analysis of HER2+ breast cancer cell line response to HER2 inhibitor treatment*. Daru, 2015. 23: p. 40.
11. Tang, Y., et al., *Afatinib inhibits proliferation and invasion and promotes apoptosis of the T24 bladder cancer cell line*. Exp Ther Med, 2015. 9(5): p. 1851-1856.
12. Harbeck, N., F. Solca, and T.C. Gauler, *Preclinical and clinical development of afatinib: a focus on breast cancer and squamous cell carcinoma of the head and neck*. Future Oncol, 2014. 10(1): p. 21-40.
13. Wang, S.Q., et al., *Afatinib reverses multidrug resistance in ovarian cancer via dually inhibiting ATP binding cassette subfamily B member 1*. Oncotarget, 2015. 6(28): p. 26142-60.
14. Chung, C.H., et al., *A phase I study afatinib/carboplatin/paclitaxel induction chemotherapy followed by standard chemoradiation in HPV-negative or high-risk HPV-positive locally advanced stage III/IVa/IVb head and neck squamous cell carcinoma*. Oral Oncol, 2016. 53: p. 54-9.
15. Wang, X.K., et al., *Afatinib circumvents multidrug resistance via dually inhibiting ATP binding cassette subfamily G member 2 in vitro and in vivo*. Oncotarget, 2014. 5(23): p. 11971-85.
16. Wind, S., et al., *Clinical Pharmacokinetics and Pharmacodynamics of Afatinib*. Clin Pharmacokinet, 2016.
17. *CHMP assessment report: Giotrif*. 2013; Available from: [http://www.ema.europa.eu/docs/en\\_GB/document\\_library/EPAR\\_-\\_Public\\_assessment\\_report/human/002280/WC500152394.pdf](http://www.ema.europa.eu/docs/en_GB/document_library/EPAR_-_Public_assessment_report/human/002280/WC500152394.pdf).
18. Schouten, L.J., et al., *Incidence of brain metastases in a cohort of patients with carcinoma of the breast, colon, kidney, and lung and melanoma*. Cancer, 2002. 94(10): p. 2698-705.
19. Sparidans, R.W., et al., *Liquid chromatography-tandem mass spectrometric assay for the tyrosine kinase inhibitor afatinib in mouse plasma using salting-out liquid-liquid extraction*. J Chromatogr B Analyt Technol Biomed Life Sci, 2016. 1012-1013: p. 118-23.
20. Poller, B., et al., *Double-transduced MDCKII cells to study human P-glycoprotein (ABCB1) and breast cancer resistance protein (ABCG2) interplay in drug transport across the blood-brain barrier*. Mol Pharm, 2011. 8(2): p. 571-82.
21. Durmus, S., et al., *Oral availability and brain penetration of the B-RAFV600E inhibitor vemurafenib can be enhanced by the P-GLYCOPROTEIN (ABCB1) and breast cancer resistance protein (ABCG2) inhibitor elacridar*. Mol Pharm, 2012. 9(11): p. 3236-45.
22. Schinkel, A.H., et al., *Normal viability and altered pharmacokinetics in mice lacking mdr1-type (drug-transporting) P-glycoproteins*. Proc Natl Acad Sci U S A, 1997. 94(8): p. 4028-33.
23. Jonker, J.W., et al., *The breast cancer resistance protein protects against a major chlorophyll-derived dietary phototoxin and protoporphyria*. Proc Natl Acad Sci U S A, 2002. 99(24): p. 15649-54.

24. Jonker, J.W., et al., *The breast cancer resistance protein BCRP (ABCG2) concentrates drugs and carcinogenic xenotoxins into milk*. Nat Med, 2005. 11(2): p. 127-9.
25. Zhang, Y., et al., *PKSolver: An add-in program for pharmacokinetic and pharmacodynamic data analysis in Microsoft Excel*. Comput Methods Programs Biomed, 2010. 99(3): p. 306-14.
26. Goh, L.B., et al., *Endogenous drug transporters in in vitro and in vivo models for the prediction of drug disposition in man*. Biochem Pharmacol, 2002. 64(11): p. 1569-78.
27. Yabuki, N., et al., *Gene amplification and expression in lung cancer cells with acquired paclitaxel resistance*. Cancer Genet Cytogenet, 2007. 173(1): p. 1-9.
28. Pesic, M., et al., *Induced resistance in the human non small cell lung carcinoma (NCI-H460) cell line in vitro by anticancer drugs*. J Chemother, 2006. 18(1): p. 66-73.
29. Khalifa, J., et al., *Brain metastases from non-small cell lung cancer: radiation therapy in the era of targeted therapies*. J Thorac Oncol, 2016.
30. Poller, B., et al., *Differential impact of P-glycoprotein (ABCB1) and breast cancer resistance protein (ABCG2) on axitinib brain accumulation and oral plasma pharmacokinetics*. Drug Metab Dispos, 2011. 39(5): p. 729-35.
31. Tang, S.C., et al., *Brain accumulation of sunitinib is restricted by P-glycoprotein (ABCB1) and breast cancer resistance protein (ABCG2) and can be enhanced by oral elacridar and sunitinib coadministration*. Int J Cancer, 2012. 130(1): p. 223-33.
32. Kort, A., et al., *Brain accumulation of the EML4-ALK inhibitor ceritinib is restricted by P-glycoprotein (P-GP/ ABCB1) and breast cancer resistance protein (BCRP/ABCG2)*. Pharmacol Res, 2015. 102: p. 200-7.
33. Polli, J.W., et al., *An unexpected synergist role of P-glycoprotein and breast cancer resistance protein on the central nervous system penetration of the tyrosine kinase inhibitor lapatinib (N-{3-chloro-4-[(3-fluorobenzyl)oxy]phenyl}-6-[5-{{[2-(methylsulfonyl)ethyl]amino }methyl}-2-furyl]-4-quinazolinamine; GW572016)*. Drug Metab Dispos, 2009. 37(2): p. 439-42.
34. Agarwal, S., et al., *Distribution of gefitinib to the brain is limited by P-glycoprotein (ABCB1) and breast cancer resistance protein (ABCG2)-mediated active efflux*. J Pharmacol Exp Ther, 2010. 334(1): p. 147-55.
35. Kodaira, H., et al., *Kinetic analysis of the cooperation of P-glycoprotein (P-gp/Abcb1) and breast cancer resistance protein (Bcrp/Abcg2) in limiting the brain and testis penetration of erlotinib, flavopiridol, and mitoxantrone*. J Pharmacol Exp Ther, 2010. 333(3): p. 788-96.
36. Lagas, J.S., et al., *Brain accumulation of dasatinib is restricted by P-glycoprotein (ABCB1) and breast cancer resistance protein (ABCG2) and can be enhanced by elacridar treatment*. Clin Cancer Res, 2009. 15(7): p. 2344-51.
37. Oostendorp, R.L., et al., *The effect of P-gp (Mdr1a/1b), BCRP (Bcrp1) and P-gp/BCRP inhibitors on the in vivo absorption, distribution, metabolism and excretion of imatinib*. Invest New Drugs, 2009. 27(1): p. 31-40.
38. Kalvass, J.C. and G.M. Pollack, *Kinetic considerations for the quantitative assessment of efflux activity and inhibition: implications for understanding and predicting the effects of efflux inhibition*. Pharm Res, 2007. 24(2): p. 265-76.
39. Tang, S.C., et al., *P-glycoprotein, CYP3A, and plasma carboxylesterase determine brain and blood disposition of the mTOR Inhibitor everolimus (Afinitor) in mice*. Clin Cancer Res, 2014. 20(12): p. 3133-45.
40. Tang, S.C., et al., *P-glycoprotein, CYP3A, and Plasma Carboxylesterase Determine Brain Disposition and Oral Availability of the Novel Taxane Cabazitaxel (Jevtana) in Mice*. Mol Pharm, 2015. 12(10): p. 3714-23.
41. Schuler, M., et al., *Afatinib beyond progression in patients with non-small-cell lung cancer following chemotherapy, erlotinib/gefitinib and afatinib: phase III randomized LUX-Lung 5 trial*. Ann Oncol, 2016. 27(3): p. 417-23.
42. Hochmair, M., S. Holzer, and O.C. Burghuber, *Complete remissions in afatinib-treated non-small-cell lung cancer patients with symptomatic brain metastases*. Anticancer Drugs, 2016.
43. Hoffknecht, P., et al., *Efficacy of the irreversible ErbB family blocker afatinib in epidermal growth factor receptor (EGFR) tyrosine kinase inhibitor (TKI)-pretreated non-small-cell lung cancer patients with brain metastases or leptomeningeal disease*. J Thorac Oncol, 2015. 10(1): p. 156-63.
44. Clement, P.M., et al., *Afatinib versus methotrexate in older patients with second-line recurrent and/or metastatic head and neck squamous cell carcinoma: subgroup analysis of the LUX-Head & Neck 1 trial*. Ann Oncol, 2016. 27(8): p. 1585-93.

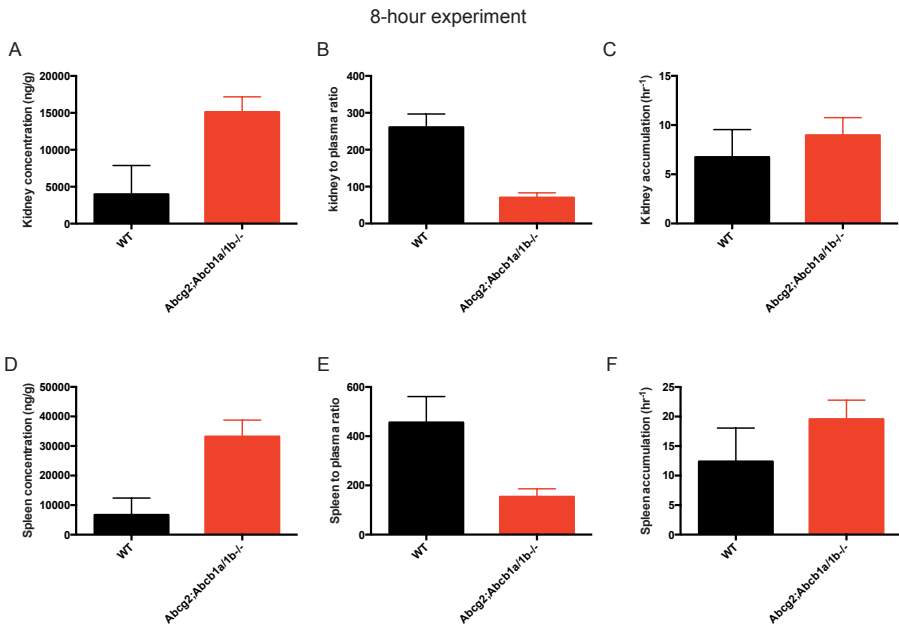
## SUPPLEMENTAL MATERIAL



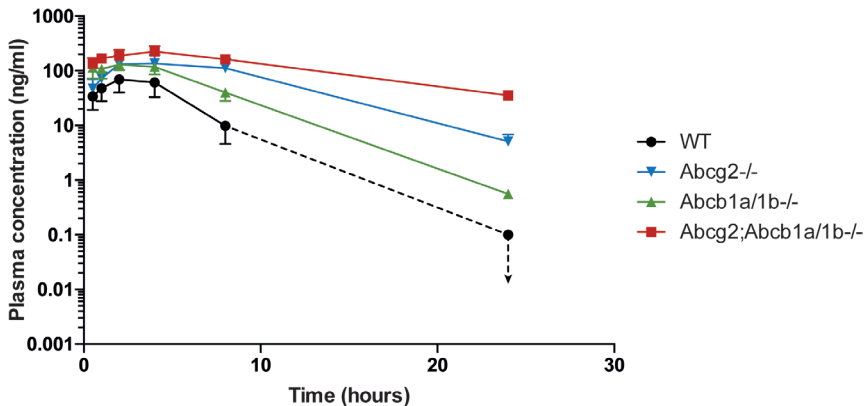
**Supplementary Figure 1** - Plasma concentration-time curves in female WT (black circles) and Abcg2;Abcb1a/1b<sup>-/-</sup> (red squares) over 8 hours after oral administration of 10 mg/kg afatinib. Data are given as mean  $\pm$  SD.



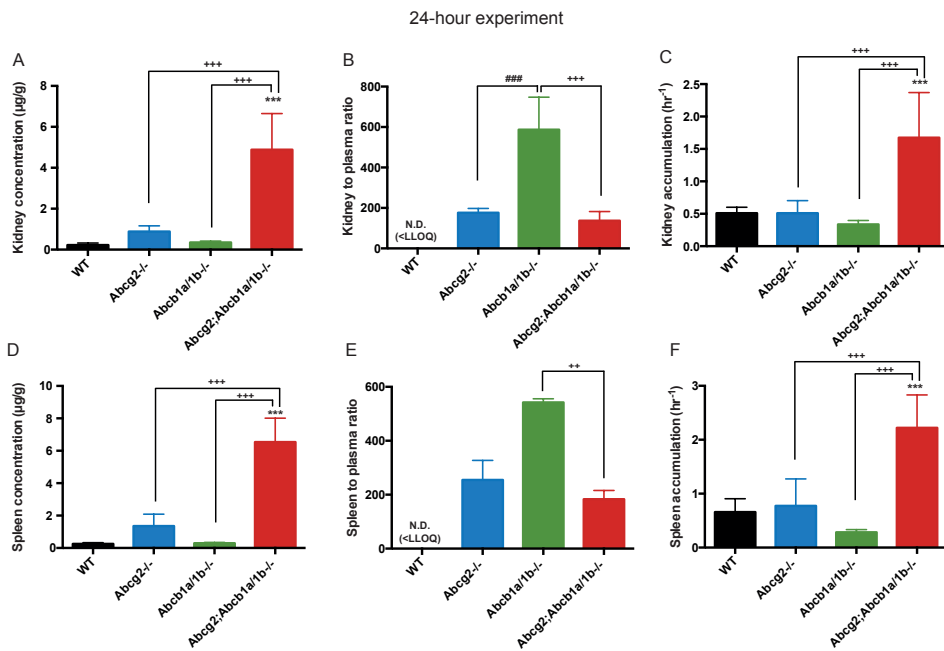
**Supplementary Figure 2** - Brain and liver concentration (A, D), tissue-to-plasma ratio (B, E) and relative accumulation (C, F) of afatinib in female WT and Abcg2;Abcb1a/1b<sup>-/-</sup> mice 8 h after oral administration of 10 mg/kg afatinib. Data are given as mean  $\pm$  SD.



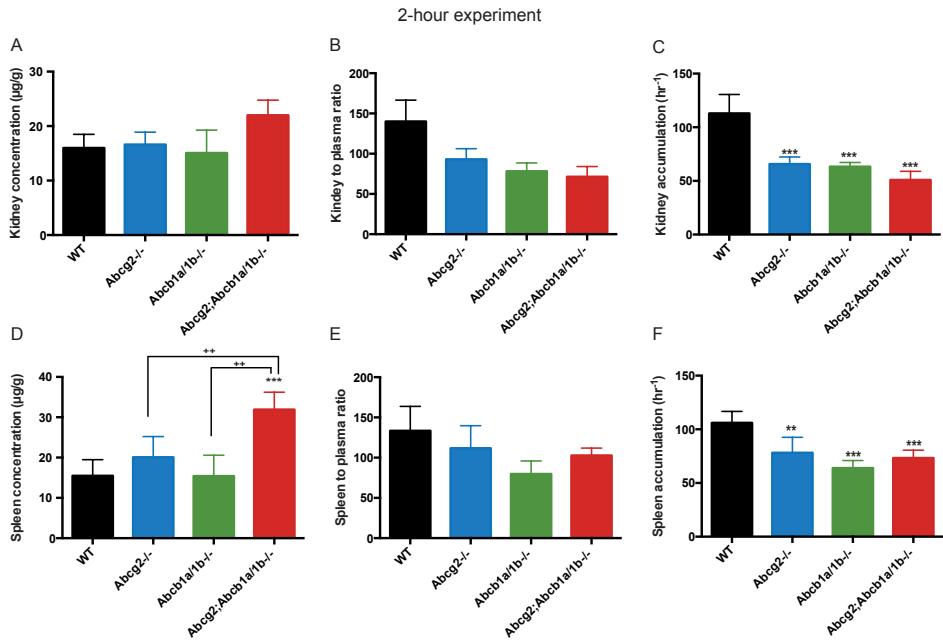
**Supplementary Figure 3** - Kidney and spleen concentration (A, D), tissue-to-plasma ratio (B, E) and relative accumulation (C, F) of afatinib in female WT and *Abcg2;Abcb1a/1b<sup>-/-</sup>* mice 8 h after oral administration of 10 mg/kg afatinib. Data are given as mean  $\pm$  SD.



**Supplementary Figure 4** - Plasma concentration-time curves of afatinib in female WT (black squares), *Abcg2<sup>-/-</sup>* (blue triangles), *Abcb1a/1b<sup>-/-</sup>* (green triangles), and *Abcg2;Abcb1a/1b<sup>-/-</sup>* (red squares) over 24 hours after oral administration of 10 mg/kg afatinib. Data are given as mean  $\pm$  SD and shown in a semi-log plot to illustrate clearance differences at 4-8 h. Note that the WT 24-h time point shows a maximum estimate of the plasma concentration, given that this value was below the quantification limit. The actual concentration may therefore well have been considerably lower (dotted arrow), for this reason this part of the graph is depicted as a dotted line.



**Supplementary Figure 5** - Kidney and spleen concentration (A, D), tissue-to-plasma ratio (B, E) and relative accumulation (C, F) of afatinib in female WT, Abcg2<sup>-/-</sup>, Abcb1a/1b<sup>-/-</sup> and Abcg2;Abcb1a/1b<sup>-/-</sup> mice 24 h after oral administration of 10 mg/kg afatinib. \*, P < 0.05; \*\*, P < 0.01; \*\*\*, P < 0.001 compared to WT mice; +, P < 0.05, ++, P < 0.01, +++, P < 0.001 compared to Abcg2;Abcb1a/1b<sup>-/-</sup> and ### P < 0.001. Data are given as mean  $\pm$  SD.



**Supplementary Figure 6** - Kidney and spleen concentration (A, D), tissue-to-plasma ratio (B, E) and relative accumulation (C, F) of afatinib in female WT, *Abcg2*<sup>-/-</sup>, *Abcb1a/1b*<sup>-/-</sup> and *Abcg2;Abcb1a/1b*<sup>-/-</sup> mice 2 h after oral administration of 10 mg/kg afatinib. \*,  $P < 0.05$ , \*\*,  $P < 0.01$ , \*\*\*,  $P < 0.001$  compared to WT mice; +,  $P < 0.05$ , ++,  $P < 0.01$ , +++,  $P < 0.001$  compared to *Abcg2;Abcb1a/1b*<sup>-/-</sup> mice. Data are given as mean  $\pm$  SD.



# 3

---

## Brain accumulation of osimertinib and its active metabolite AZ5104 is restricted by ABCB1 (P-glycoprotein) and ABCG2 (Breast Cancer Resistance Protein)

---

**Stéphanie van Hoppe<sup>1</sup>, Amer Jamalpoor<sup>1</sup>, Gert-Jan Rood<sup>2</sup>,  
Els Wagenaar<sup>1</sup>, Rolf W. Sparidans<sup>2</sup>, Jos H. Beijnen<sup>1,2</sup>, Alfred H. Schinkel<sup>1</sup>**

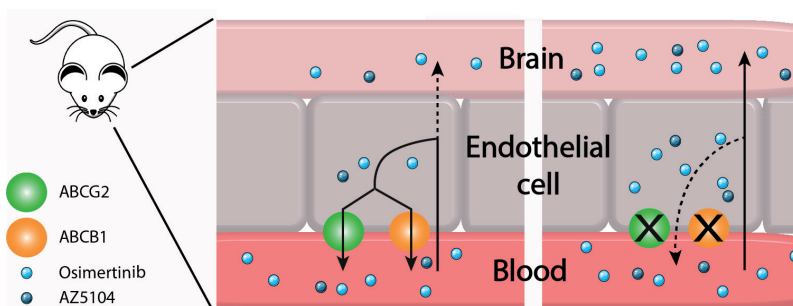
<sup>1</sup>Division of Molecular Pharmacology, The Netherlands Cancer Institute, Amsterdam

<sup>2</sup>Section of Pharmacoepidemiology & Clinical Pharmacology, Department of  
Pharmaceutical Sciences, Faculty of Science, Utrecht University, Utrecht,

*Pharmacol Res.* 2019 Aug;146:104297.

## ABSTRACT

Osimertinib is an irreversible EGFR inhibitor registered for advanced NSCLC patients whose tumors harbor recurrent somatic activating mutations in EGFR (EGFR<sup>m+</sup>) or the frequently occurring EGFR-T790M resistance mutation. Using *in vitro* transport assays and appropriate knockout and transgenic mouse models, we investigated whether the multidrug efflux transporters ABCB1 and ABCG2 transport osimertinib and whether they influence the oral availability and brain accumulation of osimertinib and its most active metabolite, AZ5104. *In vitro*, human ABCB1 and mouse Abcg2 modestly transported osimertinib. In mice, Abcb1a/1b, with a minor contribution of Abcg2, markedly limited the brain accumulation of both osimertinib and AZ5104. However, no effect of the ABC transporters was seen on osimertinib oral availability. In spite of up to 6-fold higher brain accumulation, we observed no acute toxicity signs of oral osimertinib in Abcb1a/1b;Abcg2 knockout mice. Interestingly, even in wild-type mice the intrinsic brain penetration of osimertinib was already high, which may help to explain the documented partial efficacy of this drug against brain metastases. No substantial effects of mouse Cyp3a knockout or transgenic human CYP3A4 overexpression on oral osimertinib pharmacokinetics were observed, presumably due to a dominant role of mouse Cyp2d enzymes in osimertinib metabolism. Our results suggest that pharmacological inhibition of ABCB1 and ABCG2 during osimertinib therapy might potentially be considered to further benefit patients with brain (micro-)metastases positioned behind an intact blood-brain barrier, or with substantial expression of these transporters in the tumor cells, without invoking a high toxicity risk.



## INTRODUCTION

Non-small cell lung cancer (NSCLC) is one of the leading causes of cancer death in the world, and it accounts for approximately 85% of all lung cancer diagnoses [1]. Advanced stage (IV) NSCLC is known to metastasize to a number of organs including the brain [2-6]. The identification of epidermal growth factor receptor (EGFR) mutations as one of the driving factors in NSCLC allowed the development of targeted therapy for NSCLC patients. EGFRtargeting tyrosine kinase inhibitors (TKIs) like gefitinib, erlotinib and several others display promising clinical activity in advanced NSCLC patients whose tumors harbor recurrent somatic activating mutations in EGFR (EGFR<sup>m+</sup>) [7-12]. Unfortunately, although most of the EGFR<sup>m+</sup> NSCLC patients initially respond to these TKIs, there also is a high frequency of acquired resistance. The mechanism of acquired resistance for more than 50% of the patients is the acquisition of an additional EGFR mutation, EGFR-T790M [13-15].

The search for novel therapeutic strategies targeted against this mutation has yielded a potent TKI, osimertinib (AZD9291, Tagrisso). Osimertinib covalently and irreversibly binds to cysteine 797 in the ATP binding site of EGFR, exhibiting 200 times greater potency toward both EGFR<sup>m+</sup> and T790M variants compared to the wild-type EGFR (16). Osimertinib has been approved by the US FDA in April 2018 for the first-line treatment of metastatic NSCLC patients with epidermal growth factor (EGFR) exon 19 deletions or exon 21 L858R mutations in their tumors (17). In clinical trials (phase II AURA), osimertinib has demonstrated an overall objective response rate (ORR) of 62% and median progression-free survival (PFS) greater than 12 months with manageable toxicity. In patients with central nervous system (CNS) metastases the ORR for osimertinib was still 64%, but a shorter median PFS of 7 months was observed compared to patients without CNS metastases [18]. The absolute oral bioavailability of osimertinib is 69.8%, suggesting that it is well absorbed [19]. Additionally, previous reports have shown that osimertinib undergoes minimal first-pass metabolism with low clearance and is highly distributed to organs [19-21]. However, osimertinib is metabolized, mainly by cytochrome-P450 (CYP) 3A, into the active metabolites AZ5104 and AZ7550 (Supplemental Figure 1), each amounting to ~10% of the overall systemic exposure. Interestingly, whereas AZ7550 showed a similar potency to osimertinib, AZ5104 showed greater potency than osimertinib against exon 19 deletion and T790M mutants (~8-fold) and wild-type (~15-fold) EGFR [20, 22].

Multidrug efflux transporters of the ATP-binding cassette (ABC) protein family can influence the disposition of a wide variety of endogenous and exogenous compounds, including many anti-cancer drugs. ABCB1 (P-glycoprotein) and ABCG2 (BCRP) occur

in the apical membrane of epithelia in organs that are central to the absorption and elimination of drugs like kidney, liver, and small intestine. They are also found in blood-facing luminal membranes of barrier tissues protecting pharmacological sanctuary compartments like the blood-placenta, blood-testis, and blood-brain barriers (BBB). At these barriers ABCB1 and ABCG2 pump their substrates immediately out of the epithelial or endothelial cells back into the blood. Consequently, only limited amounts of drug can accumulate in, for instance, the brain to treat (micro) metastases that are located behind a functional BBB (23-25). Many anticancer drugs including TKIs are transported by ABCB1, ABCG2, or both. These transporters can therefore significantly modulate the pharmacokinetics of these drugs, and hence their therapeutic efficacy and toxicity profile (26). Several studies have shown that the oral availability of TKIs and their tissue (especially brain) penetration can be restricted due to interaction with ABCB1 and ABCG2 transporters (27-31). Moreover, pharmacological inhibition of these ABC transporters can markedly enhance the brain accumulation of these drugs (e.g., (27-31)).

Some studies as well as the FDA documentation indicate that osimertinib can inhibit ABCB1 and ABCG2, and may possibly be transported by them (32-34). If these transporters can also efficiently transport osimertinib *in vivo*, this might lead to decreased accumulation of osimertinib in transporter-expressing cancer cells, and thus tumor pharmacokinetic resistance. A recent study using an ABCB1-overexpressing multidrug-resistant KBv200 cell xenograft model in nude mice suggested that osimertinib-mediated inhibition of ABCB1 could enhance the tumor response against other ABCB1-transported drugs (34). Moreover, NSCLC can metastasize to other parts of the body, including the brain. Upon initial diagnosis of NSCLC, brain metastases are observed in 20% of patients, with numbers increasing to 40–50% in those with stage III lung adenocarcinoma (4, 6). The brain is also a common site for disease relapse in patients previously treated with TKIs in about 30–60% of EGFR-mutated NSCLCs (5). Osimertinib could potentially be a more successful candidate drug for these patients, as it is better targeted against these mutations. However, given the high ABCB1 and ABCG2 expression in the BBB, these transporters could potentially limit brain accumulation of osimertinib, which might reduce therapeutic efficiency against NSCLC CNS metastases.

In this study we therefore investigated whether osimertinib and AZ5104 are transported by ABCB1 and ABCG2 *in vitro* or in mouse models, and how this might affect their oral plasma pharmacokinetics and brain penetration. Furthermore, since osimertinib appears to be predominantly metabolized by human CYP3A4 [35, 36], we also studied the influence of CYP3A on the oral systemic availability and tissue exposure of osimertinib.

## MATERIALS AND METHODS

### Chemicals

Osimertinib and zosuquidar were purchased from Sequoia Research Products (Pangbourne, U.K.), and Ko143 was obtained from Tocris Bioscience (Bristol, U.K.). GlutaMAX™ Dulbecco's Modified Eagle Medium (DMEM) and Dulbecco's phosphate buffered saline (PBS) were purchased from Gibco® by Life Technologies™ (The Netherlands). Glucose water 5% w/v was acquired from B. Braun Medical Supplies, Inc. (Melsungen, Germany). Bovine serum albumin (BSA) Fraction V was obtained from Roche Diagnostics GmbH (Mannheim, Germany). Isoflurane was purchased from Pharmachemie (Haarlem, The Netherlands), heparin (5000 IU ml<sup>-1</sup>) was from Leo Pharma (Breda, The Netherlands). All other chemicals were acquired from Sigma-Aldrich (Steinheim, Germany) unless stated otherwise. All chemicals used in the chromatographic osimertinib assay were described before [37].

### Transport assays

Polarized Madin-Darby canine kidney (MDCK-II) cell lines transduced with either human (h)ABCB1, hABCG2 or murine (m)Abcg2 cDNA were used and cultured as described previously [38]. Transepithelial transport assays were performed in triplicate on 12-well microporous polycarbonate membrane filters (3.0 µm pore size, Transwell 3402, Corning Inc., Lowell, MA), as described [38]. In brief, cells were allowed to grow to an intact monolayer over 3 days, which was monitored with transepithelial electrical resistance (TEER; Millipore Corporation, USA) measurements. For all cell lines TEERs had to be above 80 Ohm.cm<sup>2</sup> before the start of the transport experiment, and should not have decreased when re-measured after 8 h at the end of the experiment. On the third day, cells were washed with phosphate-buffered saline and pre-incubated with fresh DMEM medium including 10% fetal bovine serum and the relevant transport inhibitors for 1 h, where 5 µM zosuquidar (ABCB1 inhibitor) and/or 5 µM Ko143 (ABCG2/Abcg2 inhibitor) were added to both apical and basolateral compartments. To inhibit endogenous canine ABCB1 when testing the MDCK-II-mAbcg2 and MDCK-II-hABCG2 cell lines, we added 5 µM zosuquidar (ABCB1 inhibitor) to the culture medium throughout the experiment. The transport experiment was initiated by replacing the pre-incubation medium from the donor compartment (either basolateral or apical) with freshly prepared medium containing 2 µM osimertinib alone or in combination with the appropriate inhibitors. Plates were kept at 37°C in 5% CO<sub>2</sub> and 50 µl aliquots were taken from the acceptor compartment at 1, 2, 4 and 8 h and stored at -30°C until analysis. The total amount of drug transported to the acceptor compartment was calculated after correction for volume loss due to sampling at each time point. Active transport was expressed by the relative transport ratio (r), defined as the amount of apically directed transport divided

by the amount of basolaterally directed transport at the 8 h time point.

### Animals

Male wild-type (WT) FVB, *Abcb1a/1b*<sup>-/-</sup> [39], *Abcg2*<sup>-/-</sup> [40], *Abcb1a/1b;Abcg2*<sup>-/-</sup> [41], *Cyp3a*<sup>-/-</sup> and *Cyp3aXAV* [42] mice of identical genetic background (>99% FVB) were used. Groups of 5-6 mice per strain, aged between 9 to 14 weeks, were used. Animals were kept in a temperature-controlled environment with a 12 h light/dark cycle and received a standard diet (Transbreed, SDS Diets, Technilab-BMI, Someren, The Netherlands) and acidified water *ad libitum*. Mice were housed and handled according to institutional guidelines in compliance with Dutch and EU legislation.

### Drug solutions

Osimertinib was first dissolved in dimethyl sulfoxide (DMSO) at a concentration of 25 mg/mL and further diluted with a mixture of polysorbate 80: ethanol (1:1 v/v), and 5 % w/v glucose water to yield a 1 mg/mL working solution. Final concentrations (v/v) of DMSO, polysorbate 80, ethanol, and glucose water were therefore 4%, 2.5%, 2.5% and 91%, respectively. Osimertinib was administered orally at a dose of 10 mg/kg body weight (10 µL/g).

### Plasma and tissue pharmacokinetics of osimertinib

To minimize variation in absorption, mice were fasted for about 3 h prior to the oral administration of osimertinib using a blunt-ended needle. Fifty µL blood samples were drawn from the tail vein using heparin-coated capillaries (Sarstedt, Germany). At the last time point, mice were anesthetized using isoflurane inhalation, and blood was collected via cardiac puncture. For the 24 h experiment, tail vein sampling took place at 0.5, 1, 2, 4 and 8 h after oral administration; for the 1.5 h experiment, tail vein sampling took place at 5, 10, 15, 30 and 60 min after oral administration. At the end point, mice were sacrificed by cervical dislocation and a set of organs was rapidly removed, weighed, and subsequently frozen as whole organs at -30 °C. Organs were allowed to thaw on ice and homogenized in appropriate volumes of 4% (w/v) BSA in water using a FastPrep-24 device (MP Biomedicals, SA, California, USA). Homogenates were stored at -30 °C until analysis. Blood samples were immediately centrifuged at 9000 × *g* for 6 min at 4 °C, and plasma was collected and stored at -30 °C until analysis.

### Drug analysis

Osimertinib concentrations in culture medium, plasma, and tissue homogenates were analyzed with a previously reported liquid-chromatography tandem mass spectrometric (LC-MS/MS) [37].

## Statistical and pharmacokinetic calculations

The area under the curve (AUC) of the plasma concentration-time data was calculated using the trapezoidal rule, without extrapolating to infinity using GraphPad Prism software 7.0e (GraphPad Software Inc., La Jolla, CA, USA). The maximum drug concentration in plasma (C<sub>max</sub>) and the time to reach maximum drug concentration in plasma (T<sub>max</sub>) were determined directly from individual concentration-time data. Tissue accumulation of osimertinib was calculated by determining the osimertinib tissue concentration relative to its plasma AUC from 0 - 24 h or 0 - 1.5 h. Average tissue to plasma ratios were calculated from individual mouse data. Statistical differences between individual groups were assessed using one-way analysis of variance (ANOVA) followed by Tukey's post-hoc multiple comparisons using GraphPad Prism. When variances were not homogeneously distributed, data were log-transformed before statistical tests were applied. A P value of < 0.05 was considered statistically significant. Data are presented as mean ± SD, with each experimental group containing 5-6 mice.

## RESULTS

### Osimertinib is modestly transported by hABCB1 and mAbcg2 *in vitro*

We first studied the transport of osimertinib (2 μM) *in vitro* by measuring translocation through polarized monolayers of MDCK-II cell lines transduced with human (h)ABCB1, hABCG2 or mouse (m)Abcg2 cDNA. As shown in Figure 1A, in the parental line, both apically and basolaterally directed translocation of osimertinib were identical (efflux transport ratio  $r = 1.0$ ). This  $r$  was somewhat, but not significantly, decreased when adding the ABCB1 inhibitor zosuquidar (Figure 1B). In hABCB1-overexpressing MDCK-II cells, osimertinib was modestly transported in the apical direction ( $r = 1.8$ , Figure 1C), and this transport was completely blocked by zosuquidar ( $r = 1.0$ , Figure 1D). To suppress any possible endogenous canine ABCB1 transport activity, zosuquidar was added in subsequent experiments with MDCK-II cells overexpressing hABCG2 and mAbcg2. No significant active transport of osimertinib by hABCG2 was observed, and accordingly, addition of the hABCG2/mAbcg2 inhibitor Ko143 had little effect on overall translocation (Figure 1E and 1F). In contrast, in mAbcg2-overexpressing cells, clear apically directed transport of osimertinib was observed ( $r = 2.3$ ), and this transport was completely abrogated by the addition of Ko143 (Figure 1G and 1H). Osimertinib thus appears to be modestly transported by hABCB1 and more efficiently by mAbcg2, but not detectably by hABCG2 *in vitro*. It is worth noting, however, that the effective dimeric transporter level per cell is about 5.5-fold lower in MDCKII-hABCG2 cells than in MDCKII-hABCB1 cells [43]. This comparatively low expression level might render a low level of osimertinib transport by hABCG2 undetectable.

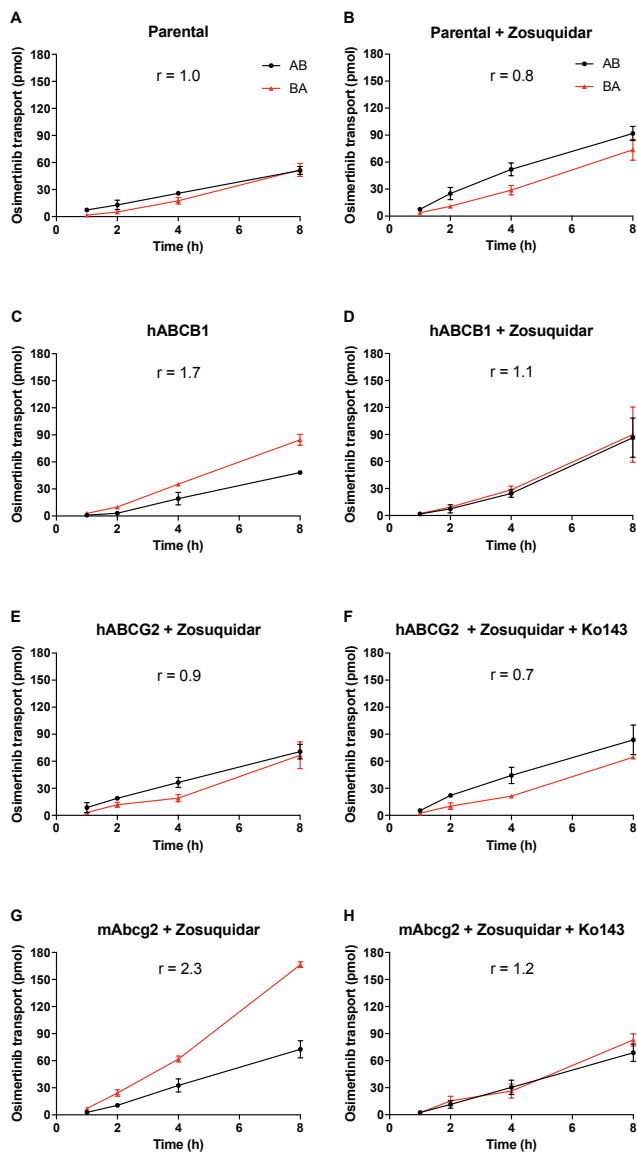


**Figure 1** - *In vitro* transport of osimertinib. Transepithelial transport of osimertinib (2  $\mu\text{M}$ ) was assessed in MDCK-II cells either non-transduced (A, B) or transduced with hABC1 (C, D), hABC2 (E, F), or mAbcg2 (G, H) cDNA. At  $t = 0$  h osimertinib was added to the donor compartment; thereafter at  $t = 1, 2, 4$  and 8 h osimertinib concentrations were measured and plotted as total amount (pmol) of translocated drug ( $n = 3$ ). (B, D–H) Zosuquidar (5  $\mu\text{M}$ ) and/or Ko143 (5  $\mu\text{M}$ ) were added as indicated to inhibit hABC1 or hABC2 and mAbcg2, respectively.  $r$ , relative transport ratio at 8 h. BA (red triangles), translocation from the basolateral to the apical compartment; AB (black circles), translocation from the apical to the basolateral compartment. Data are presented as mean  $\pm$  SD.

### **No substantial effect of Abcb1 and Abcg2, or Cyp3a on plasma pharmacokinetics of oral osimertinib**

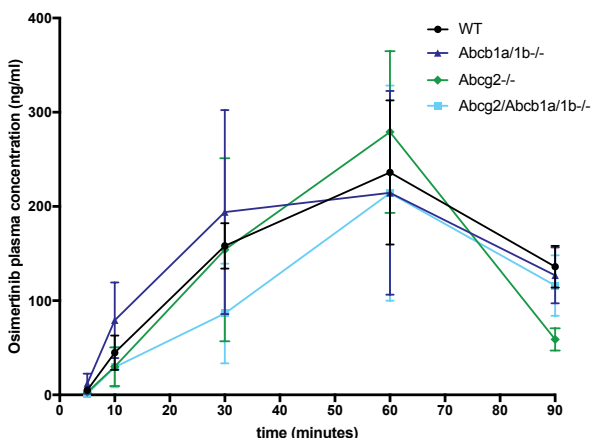
In view of the *in vitro* transport results, we studied the impact of Abcb1 and Abcg2 on the plasma and tissue pharmacokinetics of osimertinib in a pilot experiment in male wild-type (WT) and Abcb1a/1b;Abcg2<sup>-/-</sup> mice. In addition, although metabolism of osimertinib in mice appears to be primarily mediated by mouse Cyp2d proteins and not by Cyp3a as in humans [44], we included Cyp3a<sup>-/-</sup> mice in this pilot. We orally administered osimertinib to the mice at a dosage of 10 mg/kg, physiologically roughly equivalent to the recommended human dose (80 mg oral, once daily). We analyzed the plasma concentrations of osimertinib over 24 h. As shown in Supplemental Figure 2 and Table 1, we found a 1.4-fold higher plasma AUC<sub>0-24h</sub> in Abcb1a/1b;Abcg2<sup>-/-</sup> mice than in WT mice, but this was not statistically significant. Also the absence of Cyp3a enzymes did not cause a statistically significant shift compared to the WT mice in the plasma exposure between 0 and 24 h (Supplemental Figure 2, Table 1).

We next assessed the tissue distribution of osimertinib at 24 h. As the plasma level of osimertinib at this time point was below the lower limit of detection in all strains, we could not directly calculate tissue-to-plasma ratios, but we could calculate the relative tissue accumulation (P) by correcting for the plasma AUC<sub>0-24h</sub>. Interestingly, the tissue concentrations in brain but also liver of Abcb1a/1b;Abcg2<sup>-/-</sup> mice were markedly higher than those in WT or Cyp3a<sup>-/-</sup> mice, and this also applied when assessing the tissue accumulations (Table 1). By far the strongest effect was seen in brain. Although brain concentrations in WT mice were below the detection limit, and experimental variation was high, for instance the average brain concentration of osimertinib compared to that in liver was nearly 10-fold higher in Abcb1a/1b;Abcg2<sup>-/-</sup> mice (0.82) than in Cyp3a<sup>-/-</sup> mice (0.083). This parameter for other tissues such as spleen and kidney was much less affected (Supplemental Figure 3). These data suggest that, at this late distribution phase, Abcb1a/1b and/or Abcg2 play a major role in limiting osimertinib concentrations in the brain, and a smaller role in limiting the concentrations in liver and spleen, in the latter cases perhaps by mediating late elimination from these organs (Table 1 and Supplemental Figure 3). As for Cyp3a<sup>-/-</sup> mice, there were no tissue parameters significantly different from WT values at 24 h, but the C<sub>brain</sub> and P<sub>brain</sub> were markedly lower than in the Abcb1a/1b;Abcg2<sup>-/-</sup> mice (Table 1, Supplemental Figure 3).

**Table 1** - Pharmacokinetic parameters of osimertinib over 24 h after oral administration of 10 mg/kg osimertinib to male WT, Abcb1a/1b;Abcg2<sup>-/-</sup> and Cyp3a<sup>-/-</sup> mice.

Parameter	Genotype		
	Wild-type	Abcb1a/1b;Abcg2 <sup>-/-</sup>	Cyp3a <sup>-/-</sup>
Plasma AUC <sub>0-24</sub> (h*ng/ml)	1833 ± 343	2639 ± 842	1418 ± 290
fold change	1.0	1.4	0.8
C <sub>max</sub> (ng/ml)	272 ± 21	418 ± 167	341 ± 74
T <sub>max</sub> (h)	1	1	1
C <sub>brain</sub> (ng/g)	< 1	183 ± 145***	1.8 ± 1.0*/###
P <sub>brain</sub> (*10 <sup>-3</sup> h <sup>-1</sup> )	< 1	70.8 ± 59.8***	1.4 ± 0.9*/###
C <sub>liver</sub> (ng/g)	9.1 ± 8.4	223 ± 48***	21.6 ± 39.8###
fold change	1	24.4	2.4
P <sub>liver</sub> (*10 <sup>-3</sup> h <sup>-1</sup> )	4.9 ± 5.1	87.0 ± 28.1***	3.0 ± 1.4###
fold change	1	17.7	0.6

AUC, area under the plasma concentration-time curve; C<sub>max</sub>, maximum drug concentration in plasma; T<sub>max</sub>, time (h) to reach maximum drug concentration in plasma; C<sub>tissue</sub>, tissue concentration; P<sub>tissue</sub>, tissue accumulation. The lower limit of quantification (LLOQ) value for osimertinib was set at 1 ng/ml. Osimertinib plasma concentrations in all the groups and brain concentrations in WT mice at 24 h were below the LLOQ. These values resulted occasionally in negative figures and were hence assumed to be zero for calculations. For statistical comparison the C<sub>brain</sub> and P<sub>brain</sub> values for WT mice (< 1) were assumed to be 1.0 ± 1.0. Statistical differences were assessed using one-way analysis of variance (ANOVA) followed by Tukey's post-hoc multiple comparisons. \*, P < 0.05; \*\*, P < 0.01; \*\*\*, P < 0.001 compared to WT mice. #, P < 0.05; ###, P < 0.001 compared to Abcb1a/1b;Abcg2<sup>-/-</sup> mice. Data are expressed as the mean ± SD. (n = 5-6).

**Figure 2** - Plasma concentration-time curves of osimertinib in male wild-type (WT) (black circles), Abcb1a/1b<sup>-/-</sup> (dark blue triangles), Abcg2<sup>-/-</sup> (green diamonds) and Abcb1a/1b;Abcg2<sup>-/-</sup> (light-blue squares) mice, over 90 minutes after oral administration of 10 mg/kg osimertinib. Data are given as mean ± SD. N = 5-6 mice per group.

### **Abcb1 and Abcg2 limit the brain accumulation of osimertinib**

In all three tested mouse strains osimertinib reached its maximum plasma concentration approximately 1 h after oral administration (Supplemental Figure 2). To better assess the separate and combined impact of Abcb1a/1b and Abcg2 on tissue distribution of osimertinib at, or shortly after, peak plasma exposure, we performed a 1.5 hour pharmacokinetic experiment with oral administration of osimertinib (10 mg/kg) to male WT, Abcb1a/1b<sup>-/-</sup>, Abcg2<sup>-/-</sup>, and Abcb1a/1b;Abcg2<sup>-/-</sup> mice. Although, not unexpectedly, the interindividual variation this shortly after oral administration of osimertinib was high, the plasma AUCs of the four strains were very similar, with a C<sub>max</sub> again occurring around 1 h (Figure 2, Table 2). Only at the 90 min time point the Abcg2<sup>-/-</sup> plasma concentrations were significantly lower than those in the other strains, but this was probably related to the substantial experimental variation (Figure 2). These results were generally in line with the 24 h data and suggest that the absence of Abcb1 and Abcg2, alone or combined, has no substantial effect on the plasma exposure of osimertinib in mice during the first hours after administration.

Similar to the results at 24 h after administration, the brain concentration of osimertinib in Abcb1a/1b;Abcg2<sup>-/-</sup> mice showed a highly significant, 5.1-fold increase ( $P < 0.001$ ) compared to WT mice (Figure 3A). Additionally, single Abcb1a/1b<sup>-/-</sup> mice displayed a statistically significant 3.5-fold increase ( $P < 0.01$ ) compared to WT mice. In contrast, no significant difference was found between the single Abcg2<sup>-/-</sup> and WT mice. Correcting the osimertinib brain concentrations for the corresponding plasma concentrations (Figure 3B) or plasma AUCs (Figure 3C) yielded similar results. The brain-to-plasma ratios showed a highly significant, 6.4-fold increase ( $P < 0.001$ ) for Abcb1a/1b;Abcg2<sup>-/-</sup> mice compared to WT mice, and a 4.1-fold increase for Abcb1a/1b<sup>-/-</sup> mice ( $P < 0.05$ ), whereas values in the Abcg2<sup>-/-</sup> mice were not significantly different from those in the WT mice (Figure 3B; Table 2). Analyzing the same parameters for the liver did not show significant differences between the strains (Figure 3 D-F) except for the Abcg2<sup>-/-</sup> liver-to-plasma ratio, which was, however, determined only by the unexpectedly low plasma concentration in this strain at the single 1.5 h time point (Figure 2). Thus, also at 1.5 h, especially Abcb1a/1b could profoundly restrict the brain accumulation of osimertinib, and the combined deficiency for both transporters resulted in a further increased brain penetration of osimertinib. Strikingly, in the absence of Abcb1a/1b and/or Abcg2, the brain-to-plasma ratios of osimertinib (60 to 90) were even higher than the liver-to-plasma ratios (30 to 70), suggesting a high intrinsic capacity of osimertinib to accumulate in the brain as well as the liver (Figure 3B and E). Indeed, even in WT mice the brain-to-plasma ratio of osimertinib was still relatively high (14.5, Figure 3B, Table 2), illustrating the propensity of this drug to accumulate into the brain.

**Table 2** - Pharmacokinetic parameters of osimertinib over 1.5 h after oral administration of 10 mg/kg osimertinib to male WT, Abcb1a/1b<sup>-/-</sup>, Abcg2<sup>-/-</sup>, and Abcb1a/1b;Abcg2<sup>-/-</sup> mice.

Parameter	Genotype			
	Wild-type	Abcb1a/1b <sup>-/-</sup>	Abcg2 <sup>-/-</sup>	Abcb1a/1b;Abcg2 <sup>-/-</sup>
Plasma AUC <sub>0-1.5</sub> (h*ng/ml)	227 ± 50	236 ± 77	225 ± 71	178 ± 78
fold change	1	1	1	0.8
C <sub>max</sub> (ng/ml)	236 ± 77	215 ± 108	279 ± 86	214 ± 114
T <sub>max</sub> (h)	1	1	1	1
C <sub>brain</sub> (ng/g)	2003 ± 1026	6929 ± 3161**	1350 ± 271	10135 ± 1942***
fold change	1	3.5	0.7	5.1
Brain to plasma ratio	14.5 ± 6.4	60.5 ± 36.7*	23.1 ± 3.7	93.0 ± 18.3***
fold change	1	4.1	1.6	6.4
P <sub>brain</sub> (h <sup>-1</sup> )	8.6 ± 3.6	32.8 ± 20.6	6.5 ± 2.3	64.3 ± 22.8***
fold change	1	3.8	0.8	7.5
C <sub>liver</sub> (ng/g)	3912 ± 1180	3934 ± 1842	3917 ± 362	2472 ± 494
fold change	1	1	1	0.6
Liver to plasma ratio	29.0 ± 9.2	33.4 ± 19.8	68.9 ± 16.8**	28.4 ± 14.2
fold change	1	1.2	2.4	1
P <sub>liver</sub> (h <sup>-1</sup> )	17.3 ± 4.6	17.6 ± 9.4	18.6 ± 5.5	15.7 ± 5.7
fold change	1	1	1	0.9
Brain to liver ratio	0.6 ± 0.3	2.1 ± 1.5	0.3 ± 0.1	3.6 ± 1.1***
fold change	1	3.5	0.5	6

AUC, area under the plasma concentration-time curve; C<sub>max</sub>, maximum drug concentration in plasma; T<sub>max</sub>, time (h) to reach maximum drug concentration in plasma; C<sub>tissue</sub>, tissue concentration; P<sub>tissue</sub>, tissue accumulation. Statistical differences were assessed using one-way analysis of variance (ANOVA) followed by Tukey's post-hoc multiple comparisons. \*, P < 0.05; \*\*, P < 0.01; \*\*\*, P < 0.001 compared to WT mice. Data are expressed as the mean ± SD. (n = 5-6).

For some TKIs, such as brigatinib, we have previously observed that increased brain penetration of the drug due to the absence of Abcb1a/1b and Abcg2 activity at the BBB in mice was associated with acute lethal toxicity, whereas WT mice were completely unaffected by the same dose of brigatinib [45]. In contrast, in our current study for osimertinib we did not observe any indication for spontaneous toxicity in the Abcb1a/1b;Abcg2<sup>-/-</sup> mice in either the 24-h or the 1.5-h experiments after a single 10 mg/kg oral dose.

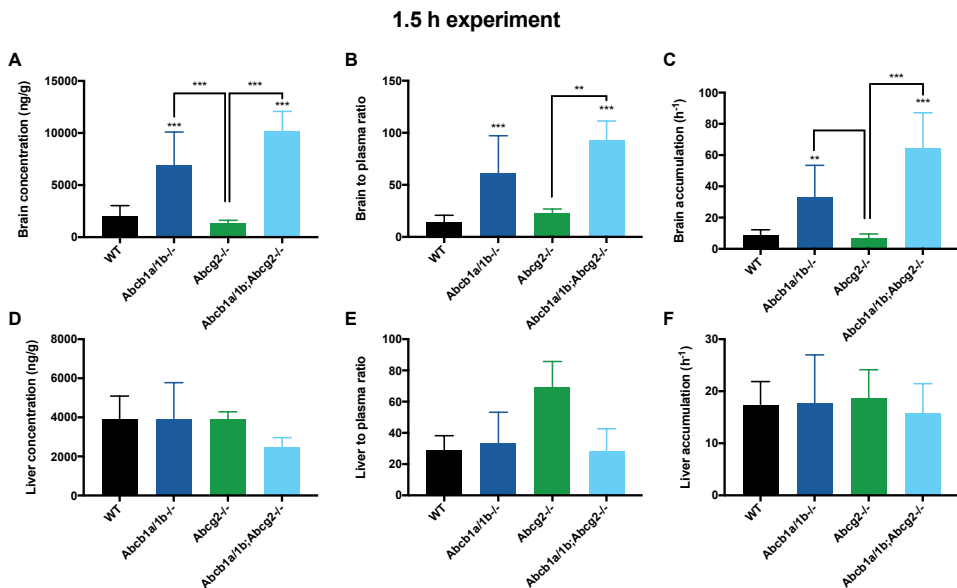


**Figure 3.** Brain and liver concentration (A, D), tissue-to-plasma ratio (B, E) and relative tissue accumulation (C, F) of osimertinib in male WT, *Abcb1a/1b*<sup>-/-</sup>, *Abcg2*<sup>-/-</sup>, and *Abcb1a/1b;Abcg2*<sup>-/-</sup> mice 1.5 h after oral administration of 10 mg/kg osimertinib. \*,  $P < 0.05$ ; \*\*,  $P < 0.01$ ; \*\*\*,  $P < 0.001$  compared to WT mice. Data are presented as the mean  $\pm$  SD.  $N = 5$  mice per group.

### Limited impact of mouse *Cyp3a* and human CYP3A4 on osimertinib pharmacokinetics in mice

Although the 24 h experiment did not suggest a clear impact of mouse *Cyp3a* on osimertinib plasma pharmacokinetics, we did assess a possible impact of *Cyp3a* deficiency, and/or the transgenic overexpression of human CYP3A4 in liver and intestine, on the plasma kinetics and tissue distribution of osimertinib 1.5 h after oral administration at 10 mg/kg to male mice. Figure 4 and Supplemental Table 1 show that, unexpectedly, and in spite of the high interindividual variation, the plasma  $AUC_{0-1.5h}$  was significantly lower in both the *Cyp3a*<sup>-/-</sup> and CYP3A4-transgenic mice compared to the WT strain. For the *Cyp3a*<sup>-/-</sup> mice this contrasts with the 24 h plasma data, and it may be that the high interindividual variation played a role in this result. A possible lowering of the plasma  $AUC$  in *Cyp3a*<sup>-/-</sup> mice might in theory be caused by compensatory upregulation of other osimertinib-clearing proteins. A possible slight (but significant,  $P < 0.05$ ) further decrease in the plasma  $AUC_{0-1.5h}$  in the CYP3A4-transgenic mice compared to the *Cyp3a*<sup>-/-</sup> mice (Supplemental Table 1) might suggest a comparatively small impact of the human CYP3A4 expression in clearing osimertinib. However, all these effects are very modest. Also, when considering the various tissue concentrations of osimertinib, values

for the three strains for brain, liver, kidney, spleen, and testis were all relatively close and not significantly different (Supplemental Table 1 and data not shown). Overall, there is therefore no indication that Cyp3a or CYP3A4 activity has a major impact on the plasma exposure and tissue distribution of osimertinib in mice.

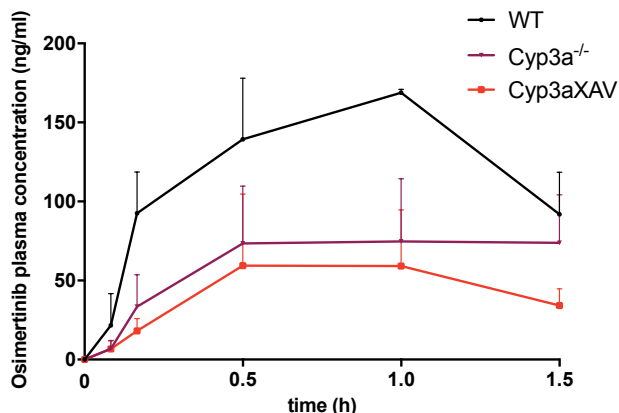


**Figure 4** - Plasma concentration-time curves of osimertinib in male wild-type (WT) (black), Cyp3a<sup>-/-</sup> (purple triangles), Cyp3aXAV (red squares) mice, over 90 minutes after oral administration of 10 mg/kg osimertinib. Data are given as mean  $\pm$  SD. N = 5-6 mice per group.

### Brain accumulation of the active metabolite AZ5104 is restricted by Abcb1a/1b and Abcg2

In the final phase of this study an LC-MS/MS assay became available for the pharmacodynamically most active metabolite of osimertinib, AZ5104 (Supplemental Figure 1). Samples still available from the 1.5 h study with ABC transporter knockout strains could then be re-measured for the presence of this compound after oral administration of osimertinib. As shown in Supplemental Figure 4, the plasma concentrations of AZ5104 and the AZ5104-to-osimertinib ratios gradually rose between 0.5 and 1.5 h, with no significant differences between the four tested strains (WT, Abcb1a/1b<sup>-/-</sup>, Abcg2<sup>-/-</sup>, and Abcb1a/1b;Abcg2<sup>-/-</sup>). The metabolite-to-osimertinib ratio was about 20-25% at 1.5 h. Whereas the plasma levels of AZ5104 were thus hardly affected by the ABC transporters, its brain concentration, brain-to-plasma ratio, and brain accumulation were dramatically increased in the Abcb1a/1b<sup>-/-</sup> mice, but especially in the Abcb1a/1b;Abcg2<sup>-/-</sup> mice (Figure 5A-C). Abcg2 deficiency did not show a significant difference compared to WT mice, however due to the significant difference between Abcb1a/1b and Abcb1a/1b;Abcg2<sup>-/-</sup> mice in the brain ( $P < 0.001$ ), it does suggest that

Abcg2 plays an important role in AZ5104 transport across the BBB. At the same time, the equivalent parameters for AZ5104 in the liver were not significantly altered between the strains (Figure 5D-F). It thus appears that Abcb1a/1b and to a lesser extent also Abcg2 at the BBB can strongly restrict the brain accumulation of AZ5104.

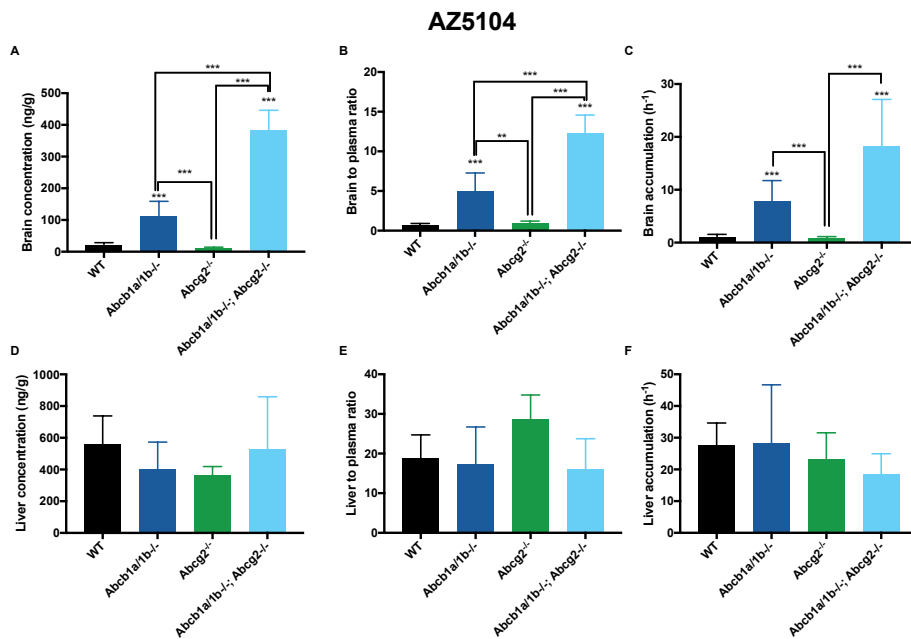


**Figure 5** - Brain and liver concentration (A, D), tissue-to-plasma ratio (B, E) and relative tissue accumulation (C, F) of AZ5104 in male WT, Abcb1a/1b<sup>-/-</sup>, Abcg2<sup>-/-</sup>, and Abcb1a/1b<sup>-/-</sup>; Abcg2<sup>-/-</sup> mice 1.5 h after oral administration of 10 mg/kg osimertinib. \*, P < 0.05; \*\*, P < 0.01; \*\*\*, P < 0.001 compared to WT mice. Data are presented as the mean ± SD. N = 5 mice per group.

## DISCUSSION

ABC efflux transporters, especially ABCB1 and ABCG2, have been shown to be associated with resistance to chemotherapy in several cancer cell lines, including NSCLC [25, 46]. Furthermore, brain metastases are a common occurrence in patients suffering from NSCLC [4-6, 47]. Because ABCB1 and ABCG2 are expressed at the BBB, these transporter proteins may play a significant role in limiting the pharmacotherapeutic treatment of cancer metastases in the brain. Given the recent therapeutic success of osimertinib in NSCLC patients, we wanted to investigate the possible effects of these transporters on osimertinib disposition.

Our results show that osimertinib is transported by hABCB1 and efficiently by mAbcg2, but not detectably by hABCG2 *in vitro*, and that this transport can be inhibited with specific inhibitors. A previous report demonstrated that osimertinib at low concentration (0.4  $\mu\text{M}$ ) can also significantly reverse hABCB1 and hABCG2 mediated multidrug resistance (MDR) via inhibiting their efflux activity *in vitro* [48], illustrating the various interactions of osimertinib with these transporters.

In spite of the clear transport *in vitro*, *in vivo* we did not observe an obvious limiting effect of Abcb1a/1b or Abcg2 on the oral availability of osimertinib in mice. However, the accumulation of osimertinib in the brain was markedly restricted by Abcb1a/1b and Abcg2. The brain distribution of osimertinib was clearly increased by absence of the combination of Abcb1a/1b and Abcg2 in the BBB (6.4-fold compared to WT), but not substantially by absence of Abcg2 alone. This is in contrast to Abcb1a/1b, which by itself showed a clear limiting effect (by 4.1-fold) on osimertinib accumulation in the brain (Figure 3, Table 2). These data suggest that the brain penetration of osimertinib could be further enhanced by effectively inhibiting ABCB1 and ABCG2 activity in the BBB, for instance by coadministration of the dual ABCB1 and ABCG2 inhibitor elacridar with osimertinib.

In this context it is worth noting that we did not observe any indication that the increased brain penetration of osimertinib in Abcb1a/1b;Abcg2<sup>-/-</sup> mice resulted in noticeable toxicity. This is in contrast to the TKI brigatinib, which caused lethal toxicity in Abcb1a/1b;Abcg2<sup>-/-</sup> mice, whereas WT mice were completely unaffected by the same oral dose of brigatinib [45]. This suggests that it may potentially be safe enough to boost osimertinib brain accumulation using ABCB1 and ABCG2 inhibitors, although obviously this will always first need to be carefully tested in appropriately designed clinical trials.

The brain penetration of the most active metabolite of osimertinib, AZ5104, was also strongly limited by Abcb1a/1b activity in the BBB, and more notably so when Abcg2 was additionally deficient (Figure 5). This suggests that AZ5104 is similarly affected by the ABC transporters at the BBB as its parental compound. In contrast, the distribution of osimertinib and AZ5104 to the liver was not markedly affected by these efflux transporters (Figures 3 and 5).

The difference we observed between a high impact on brain accumulation versus no significant impact on oral availability of osimertinib is a common observation for various other shared Abcb1a/1b and Abcg2 substrates such as sunitinib, sorafenib, imatinib, and gefitinib (27, 48-50). We have observed that when a drug is only modestly transported by ABCB1 and/or ABCG2 *in vitro*, we generally see a much more outspoken effect of these transporters in limiting the brain accumulation of this drug, than in reducing its oral availability (51, 52). Only drugs that are very efficiently transported *in vitro*, like afatinib, tend to show a clear role of the transporters in restricting their oral

availability (53). We suspect that this could be due to a much more abundant presence of various other drug uptake systems as well as an overall higher influx capacity in the intestine as compared to the BBB. Thus, when removing or inhibiting ABCB1 and/or ABCG2, the oral availability of a substrate drug will generally be less enhanced than its brain penetration.

In humans, osimertinib is thought to be predominantly metabolized by the CYP3A4/5 enzymes, while in mice this appears to be primarily mediated by mouse Cyp2d proteins [44]. We observed no significant impact of Cyp3a deficiency on the osimertinib systemic availability and its tissue exposure. This is consistent with a study showing that codosing mice with osimertinib and the CYP450 inhibitor benzotriazole-1-amine did not have a significant effect on osimertinib metabolism [55]. Also, we observed only a borderline significant difference in AUC between the Cyp3aXAV and Cyp3a<sup>-/-</sup> mice. These findings can probably be explained by a dominant function of the murine Cyp2d proteins in these mice [44].

Various clinical trials have assessed the therapeutic efficacy of osimertinib for NSCLC and metastatic NSCLC patients. A recent study demonstrated that patients treated with osimertinib developed CNS metastases to a lesser extent compared to the standard EGFR-TKIs treatment. In addition, another study showed that osimertinib had a reasonably high ORR in CNS metastases of 64% [18, 56]. These findings clearly suggest the promising therapeutic efficiency osimertinib could offer for NSCLC patients both with and without CNS involvement. One factor as to why osimertinib seems to be partially effective against brain metastases could be its intrinsically high brain penetration. In fact, the brain-to-plasma ratio in WT mice (14.5, Figure 3, Table 2) was only slightly lower than the liver-to-plasma ratio (29), and in *Abcb1a/1b;Abcg2<sup>-/-</sup>* mice it was even considerably higher (93.0 in brain vs 28.4 in liver). This already favorable behavior of osimertinib with respect to brain metastases might therefore possibly be even further boosted by coadministration of efficient ABCB1 and ABCG2 inhibitors.

Based on our findings, it is further likely that tumors substantially expressing ABCB1 and/or ABCG2 will also display some resistance to osimertinib-based chemotherapy. Thus, inhibiting these transporters with effective dual ABCB1 and ABCG2 inhibitors such as elacridar during osimertinib therapy could potentially further improve the tumor response. However, caution should always be exercised to prevent unexpected toxicities, and these possible approaches will first need to be carefully examined in clinical trials, as would also apply to efforts to increase osimertinib levels in the brain of patients with CNS tumors or metastases.

## **CONCLUSION**

Our study shows that ABCB1 and ABCG2 do not restrict the oral availability of osimertinib, but that they do markedly restrict the brain disposition of both osimertinib and AZ5104. These results suggest that coadministration of ABCB1 and ABCG2 inhibitors may be an option to enhance osimertinib exposure in patients, especially in the brain. This could provide a better option to treat NSCLC and its metastases located in part or in whole behind a functional blood-brain barrier.

## REFERENCES

1. Bareschino MA, Schettino C, Rossi A, et al. Treatment of advanced non small cell lung cancer, *J Thorac Dis*, 2 (2011) 122-133. 10.3978/j.issn.2072-1439.2010.12.08
2. Thippeswamy R, Noronha V, Krishna V, et al. Stage IV lung cancer: Is cure possible?, *Indian journal of medical and paediatric oncology : official journal of Indian Society of Medical & Paediatric Oncology*, 2 (2013) 121-125. 10.4103/0971-5851.116207
3. Quint LE, Tummala S, Brisson LJ, et al. Distribution of distant metastases from newly diagnosed non-small cell lung cancer, *Ann Thorac Surg*, 1 (1996) 246-250.
4. Mamon HJ, Yeap BY, Janne PA, et al. High risk of brain metastases in surgically staged IIIA non-small-cell lung cancer patients treated with surgery, chemotherapy, and radiation, *J Clin Oncol*, 7 (2005) 1530-1537. 10.1200/JCO.2005.04.123
5. Heon S, Yeap BY, Britt GJ, et al. Development of central nervous system metastases in patients with advanced non-small cell lung cancer and somatic EGFR mutations treated with gefitinib or erlotinib, *Clin Cancer Res*, 23 (2010) 5873-5882. 10.1158/1078-0432.CCR-10-1588
6. Barnholtz-Sloan JS, Sloan AE, Davis FG, et al. Incidence proportions of brain metastases in patients diagnosed (1973 to 2001) in the Metropolitan Detroit Cancer Surveillance System, *J Clin Oncol*, 14 (2004) 2865-2872. 10.1200/JCO.2004.12.149
7. Maemondo M, Inoue A, Kobayashi K, et al. Gefitinib or chemotherapy for non-small-cell lung cancer with mutated EGFR, *N Engl J Med*, 25 (2010) 2380-2388. 10.1056/NEJMoa0909530
8. Rosell R, Carcereny E, Gervais R, et al. Erlotinib versus standard chemotherapy as first-line treatment for European patients with advanced EGFR mutation-positive non-small-cell lung cancer (EURTAC): a multicentre, open-label, randomised phase 3 trial, *Lancet Oncol*, 3 (2012) 239-246. 10.1016/S1470-2045(11)70393-X
9. Sequist LV, Yang JC, Yamamoto N, et al. Phase III study of afatinib or cisplatin plus pemetrexed in patients with metastatic lung adenocarcinoma with EGFR mutations, *J Clin Oncol*, 27 (2013) 3327-3334. 10.1200/JCO.2012.44.2806
10. Ramalingam SS, O'Byrne K, Boyer M, et al. Dacomitinib versus erlotinib in patients with EGFR-mutated advanced nonsmall-cell lung cancer (NSCLC): pooled subset analyses from two randomized trials, *Annals of oncology : official journal of the European Society for Medical Oncology / ESMO*, 3 (2016) 423-429. 10.1093/annonc/mdv593
11. Rossi S, Toschi L, Finocchiaro G, et al. Impact of Exon 19 Deletion Subtypes in EGFR-Mutant Metastatic Non-Small-Cell Lung Cancer Treated With First-Line Tyrosine Kinase Inhibitors, *Clin Lung Cancer*, (2018) 82-87. 10.1016/j.clc.2018.10.009
12. Cai Y, Wang X, Guo Y, et al. Successful treatment of a lung adenocarcinoma patient with a novel EGFR exon 20-ins mutation with afatinib: A case report, *Medicine (Baltimore)*, 1 (2019) e13890. 10.1097/MD.00000000000013890
13. Pao W, Miller VA, Politi KA, et al. Acquired resistance of lung adenocarcinomas to gefitinib or erlotinib is associated with a second mutation in the EGFR kinase domain, *PLoS Med*, 3 (2005) e73. 10.1371/journal.pmed.0020073
14. Planchard D, Loriot Y, Andre F, et al. EGFR-independent mechanisms of acquired resistance to AZD9291 in EGFR T790M-positive NSCLC patients, *Ann Oncol*, 10 (2015) 2073-2078. 10.1093/annonc/mdv319
15. Kobayashi S, Boggon TJ, Dayaram T, et al. EGFR mutation and resistance of non-small-cell lung cancer to gefitinib, *N Engl J Med*, 8 (2005) 786-792. 10.1056/NEJMoa044238
16. Cross DA, Ashton SE, Ghiorghiu S, et al. AZD9291, an irreversible EGFR TKI, overcomes T790M-mediated resistance to EGFR inhibitors in lung cancer, *Cancer Discov*, 9 (2014) 1046-1061. 10.1158/2159-8290.CD-14-0337
17. Center for Drug valuation and Research of the U.S., Department of Health and Human Services Food and Drug Administration, <https://www.fda.gov/Drugs/InformationOnDrugs/ApprovedDrugs/ucm605113.htm>, (2018)

18. Yang JC, Ahn MJ, Kim DW, et al. Osimertinib in Pretreated T790M-Positive Advanced Non-Small-Cell Lung Cancer: AURA Study Phase II Extension Component, *J Clin Oncol*, 12 (2017) 1288-1296. 10.1200/JCO.2016.70.3223
19. Vishwanathan K, So K, Thomas K, et al. Absolute Bioavailability of Osimertinib in Healthy Adults, *Clin Pharmacol Drug Dev*, 2 (2019) 198-207. 10.1002/cpdd.467
20. Dickinson PA, Cantarini MV, Collier J, et al. Metabolic Disposition of Osimertinib in Rats, Dogs, and Humans: Insights into a Drug Designed to Bind Covalently to a Cysteine Residue of Epidermal Growth Factor Receptor, *Drug Metab Dispos*, 8 (2016) 1201-1212. 10.1124/dmd.115.069203
21. Planchard D, Brown KH, Kim DW, et al. Osimertinib Western and Asian clinical pharmacokinetics in patients and healthy volunteers: implications for formulation, dose, and dosing frequency in pivotal clinical studies, *Cancer Chemother Pharmacol*, 4 (2016) 767-776. 10.1007/s00280-016-2992-z
22. Center for Drug valuation and Research of the U.S., Department of Health and Human Services Food and Drug Administration., HIGHLIGHTS OF PRESCRIBING INFORMATION, (2017)
23. Schinkel AH, Wagenaar E, Mol CA, et al. P-glycoprotein in the blood-brain barrier of mice influences the brain penetration and pharmacological activity of many drugs, *J Clin Invest*, 11 (1996) 2517-2524. 10.1172/JCI118699
24. Vlaming ML, Lagas JS, Schinkel AH. Physiological and pharmacological roles of ABCG2 (BCRP): recent findings in Abcg2 knockout mice, *Adv Drug Deliv Rev*, 1 (2009) 14-25. 10.1016/j.addr.2008.08.007
25. Yabuki N, Sakata K, Yamasaki T, et al. Gene amplification and expression in lung cancer cells with acquired paclitaxel resistance, *Cancer Genet Cytogenet*, 1 (2007) 1-9. 10.1016/j.cancergencyto.2006.07.020
26. Stuurman FE, Nuijen B, Beijnen JH, et al. Oral anticancer drugs: mechanisms of low bioavailability and strategies for improvement, *Clin Pharmacokinet*, 6 (2013) 399-414. 10.1007/s40262-013-0040-2
27. Tang SC, Lagas JS, Lankheet NA, et al. Brain accumulation of sunitinib is restricted by P-glycoprotein (ABCB1) and breast cancer resistance protein (ABCG2) and can be enhanced by oral elacridar and sunitinib coadministration, *International journal of cancer*, 1 (2012) 223-233. 10.1002/ijc.26000
28. Tang SC, Nguyen LN, Sparidans RW, et al. Increased oral availability and brain accumulation of the ALK inhibitor crizotinib by coadministration of the P-glycoprotein (ABCB1) and breast cancer resistance protein (ABCG2) inhibitor elacridar, *International journal of cancer*, 6 (2014) 1484-1494. 10.1002/ijc.28475
29. Kodaira H, Kusuhara H, Ushiki J, et al. Kinetic analysis of the cooperation of P-glycoprotein (P-gp/Abcb1) and breast cancer resistance protein (Bcrp/Abcg2) in limiting the brain and testis penetration of erlotinib, flavopiridol, and mitoxantrone, *The Journal of pharmacology and experimental therapeutics*, 3 (2010) 788-796. 10.1124/jpet.109.162321
30. Shukla S, Chen ZS, Ambudkar SV. Tyrosine kinase inhibitors as modulators of ABC transporter-mediated drug resistance, *Drug resistance updates : reviews and commentaries in antimicrobial and anticancer chemotherapy*, 1-2 (2012) 70-80. 10.1016/j.drug.2012.01.005
31. Lagas JS, van Waterschoot RA, van Tilburg VA, et al. Brain accumulation of dasatinib is restricted by P-glycoprotein (ABCB1) and breast cancer resistance protein (ABCG2) and can be enhanced by elacridar treatment, *Clinical cancer research : an official journal of the American Association for Cancer Research*, 7 (2009) 2344-2351. 10.1158/1078-0432.ccr-08-2253
32. Hsiao SH, Lu YJ, Li YQ, et al. Osimertinib (AZD9291) Attenuates the Function of Multidrug Resistance-Linked ATP-Binding Cassette Transporter ABCB1 in Vitro, *Mol Pharm*, 6 (2016) 2117-2125. 10.1021/acs.molpharmaceut.6b00249
33. Zhang XY, Zhang YK, Wang YJ, et al. Osimertinib (AZD9291), a Mutant-Selective EGFR Inhibitor, Reverses ABCB1-Mediated Drug Resistance in Cancer Cells, *Molecules*, 9 (2016) 10.3390/molecules21091236
34. Chen Z, Chen Y, Xu M, et al. Osimertinib (AZD9291) Enhanced the Efficacy of Chemotherapeutic Agents in ABCB1- and ABCG2-Overexpressing Cells In Vitro, In Vivo, and Ex Vivo, *Mol Cancer Ther*, 8 (2016) 1845-1858. 10.1158/1535-7163.MCT-15-0939
35. Peters S, Zimmermann S, Adjei AA. Oral epidermal growth factor receptor tyrosine kinase inhibitors for the treatment of non-small cell lung cancer: comparative pharmacokinetics and drug-drug interactions, *Cancer treatment reviews*, 8 (2014) 917-926. 10.1016/j.ctrv.2014.06.010
36. Visentin M, Biason P, Toffoli G. Drug interactions among the epidermal growth factor receptor inhibitors, other biologics and cytotoxic agents, *Pharmacology & therapeutics*, 1 (2010) 82-90. 10.1016/j.pharmthera.2010.05.005

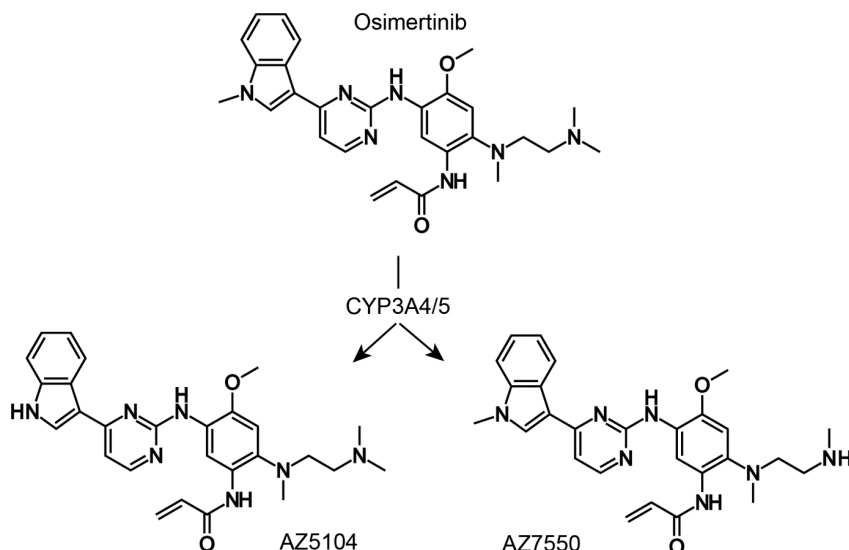
37. Durmus S, Sparidans RW, Wagenaar E, et al. Oral availability and brain penetration of the B-RAFV600E inhibitor vemurafenib can be enhanced by the P-GLYCOprotein (ABCB1) and breast cancer resistance protein (ABCG2) inhibitor elacridar, *Mol Pharm*, 11 (2012) 3236-3245. 10.1021/mp3003144
38. Schinkel AH, Mayer U, Wagenaar E, et al. Normal viability and altered pharmacokinetics in mice lacking *mdr1*-type (drug-transporting) P-glycoproteins, *Proc Natl Acad Sci U S A*, 8 (1997) 4028-4033.
39. Jonker JW, Merino G, Musters S, et al. The breast cancer resistance protein BCRP (ABCG2) concentrates drugs and carcinogenic xenotoxins into milk, *Nat Med*, 2 (2005) 127-129. 10.1038/nm1186
40. Jonker JW, Buitelaar M, Wagenaar E, et al. The breast cancer resistance protein protects against a major chlorophyll-derived dietary phototoxin and protoporphyria, *Proc Natl Acad Sci U S A*, 24 (2002) 15649-15654. 10.1073/pnas.202607599
41. van Waterschoot RA, Lagas JS, Wagenaar E, et al. Absence of both cytochrome P450 3A and P-glycoprotein dramatically increases docetaxel oral bioavailability and risk of intestinal toxicity, *Cancer Res*, 23 (2009) 8996-9002. 10.1158/0008-5472.CAN-09-2915
42. Rood JJM, van Bussel MTJ, Schellens JHM, et al. Liquid chromatography-tandem mass spectrometric assay for the T790M mutant EGFR inhibitor osimertinib (AZD9291) in human plasma, *J Chromatogr B Analyt Technol Biomed Life Sci*, (2016) 80-85. 10.1016/j.jchromb.2016.07.037
43. van Groen BD, van de Steeg E, Mooij MG, et al. Proteomics of human liver membrane transporters: a focus on fetuses and newborn infants, *Eur J Pharm Sci*, (2018) 217-227. 10.1016/j.ejps.2018.08.042
44. MacLeod AK, Lin, Huang JT, et al. Identification of Novel Pathways of Osimertinib Disposition and Potential Implications for the Outcome of Lung Cancer Therapy, *Clin Cancer Res*, 9 (2018) 2138-2147. 10.1158/1078-0432.CCR-17-3555
45. Li W, Sparidans RW, Wang Y, et al. P-glycoprotein and breast cancer resistance protein restrict brigatinib brain accumulation and toxicity, and, alongside CYP3A, limit its oral availability, *Pharmacol Res*, (2018) 47-55. 10.1016/j.phrs.2018.09.020
46. Pesic M, Markovic JZ, Jankovic D, et al. Induced resistance in the human non small cell lung carcinoma (NCI-H460) cell line in vitro by anticancer drugs, *J Chemother*, 1 (2006) 66-73. 10.1179/joc.2006.18.1.66
47. Khalifa J, Amini A, Popat S, et al. Brain Metastases from NSCLC: Radiation Therapy in the Era of Targeted Therapies, *J Thorac Oncol*, 10 (2016) 1627-1643. 10.1016/j.jtho.2016.06.002
48. Lagas JS, van Waterschoot RA, Sparidans RW, et al. Breast cancer resistance protein and P-glycoprotein limit sorafenib brain accumulation, *Molecular cancer therapeutics*, 2 (2010) 319-326. 10.1158/1535-7163.mct-09-0663
49. Oostendorp RL, Buckle T, Beijnen JH, et al. The effect of P-gp (Mdr1a/1b), BCRP (Bcrp1) and P-gp/BCRP inhibitors on the in vivo absorption, distribution, metabolism and excretion of imatinib, *Investigational new drugs*, 1 (2009) 31-40. 10.1007/s10637-008-9138-z
50. Agarwal S, Sane R, Gallardo JL, et al. Distribution of gefitinib to the brain is limited by P-glycoprotein (ABCB1) and breast cancer resistance protein (ABCG2)-mediated active efflux, *The Journal of pharmacology and experimental therapeutics*, 1 (2010) 147-155. 10.1124/jpet.110.167601
51. Kort A, Durmus S, Sparidans RW, et al. Brain and Testis Accumulation of Regorafenib is Restricted by Breast Cancer Resistance Protein (BCRP/ABCG2) and P-glycoprotein (P-GP/ABCB1), *Pharm Res*, 7 (2015) 2205-2216. 10.1007/s11095-014-1609-7
52. Kort A, van Hoppe S, Sparidans RW, et al. Brain Accumulation of Ponatinib and Its Active Metabolite, N-Desmethyl Ponatinib, Is Limited by P-Glycoprotein (P-GP/ABCB1) and Breast Cancer Resistance Protein (BCRP/ABCG2), *Mol Pharm*, 10 (2017) 3258-3268. 10.1021/acs.molpharmaceut.7b00257
53. van Hoppe S, Sparidans RW, Wagenaar E, et al. Breast cancer resistance protein (BCRP/ABCG2) and P-glycoprotein (P-gp/ABCB1) transport afatinib and restrict its oral availability and brain accumulation, *Pharmacol Res*, (2017) 43-50. 10.1016/j.phrs.2017.01.035
54. Finlay MR, Anderton M, Ashton S, et al. Discovery of a potent and selective EGFR inhibitor (AZD9291) of both sensitizing and T790M resistance mutations that spares the wild type form of the receptor, *Journal of medicinal chemistry*, 20 (2014) 8249-8267. 10.1021/jm500973a
55. Reungwetwattana T, Nakagawa K, Cho BC, et al. CNS Response to Osimertinib Versus Standard Epidermal Growth Factor Receptor Tyrosine Kinase Inhibitors in Patients With Untreated EGFR-Mutated Advanced Non-Small-Cell Lung Cancer, *J Clin Oncol*, (2018) JCO2018783118. 10.1200/JCO.2018.78.3118

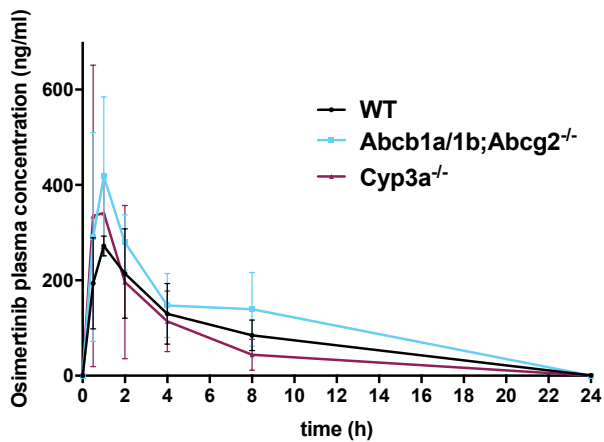
## SUPPLEMENTAL MATERIAL

**Supplemental Table 1** - Pharmacokinetic parameters of osimertinib over 1.5 h after oral administration of 10 mg/kg osimertinib to male WT, Cyp3a<sup>-/-</sup> and Cyp3aXAV mice.

Parameter	Genotype		
	Wild-type	Cyp3a <sup>-/-</sup>	Cyp3aXAV
Plasma AUC <sub>0-1.5</sub> (h*ng/ml)	186 ± 14	94 ± 20***	67 ± 19***/#
fold change	1	0.5	0.4
C <sub>max</sub> (ng/ml)	169 ± 2	74.7 ± 39.5	59.3 ± 45.4*
T <sub>max</sub> (h)	1	1	0.5 - 1
C <sub>brain</sub> (ng/g)	723 ± 84	983 ± 283	942 ± 187
fold change	1	1.4	1.3
C <sub>liver</sub> (ng /g)	6755 ± 3068	4694 ± 2595	7886 ± 972
fold change	1	0.7	1.2

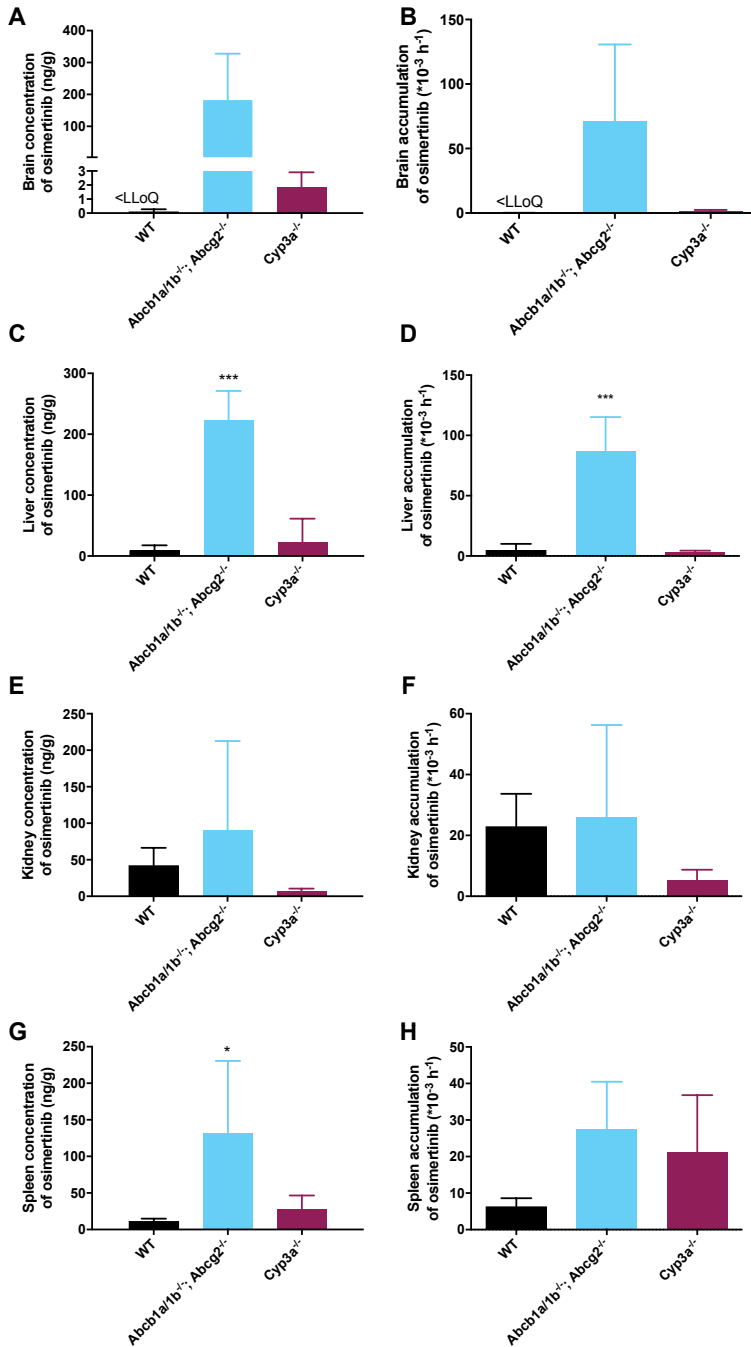
AUC, area under the plasma concentration-time curve; C<sub>max</sub>, maximum drug concentration in plasma; T<sub>max</sub>, time (h) to reach maximum drug concentration in plasma; C<sub>tissue</sub>, tissue concentration; P<sub>tissue</sub>, tissue accumulation; ND, not determined. Statistical differences were assessed using one-way analysis of variance (ANOVA) followed by Tukey's post-hoc multiple comparisons. \*, P < 0.05; \*\*\*, P < 0.001 compared to WT mice, #, P < 0.05 compared to Cyp3a<sup>-/-</sup> mice. Data are expressed as the mean ± SD. (n = 5-6).

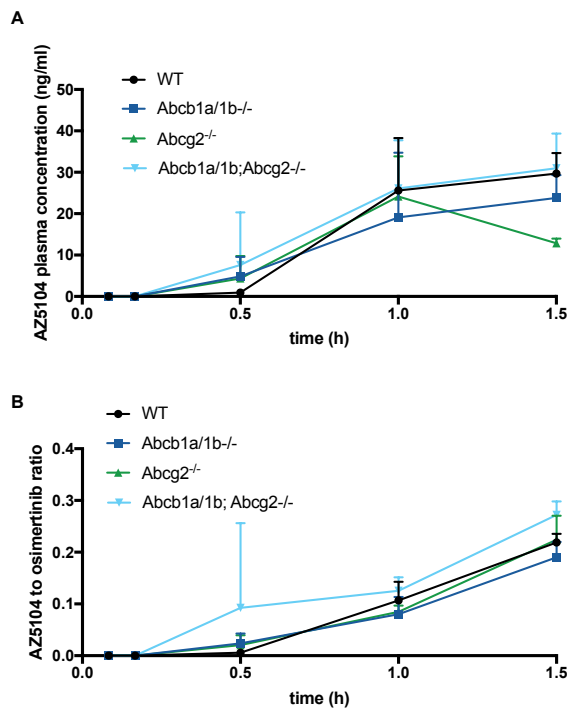
**Supplemental Figure 1** - Schematic representation of the metabolism of osimertinib to AZ5104 and AZ7550 by Cytochrome P450 (mainly CYP3A4).



**Supplemental Figure 2** - Plasma concentration-time curves of osimertinib in male wild-type (WT) (black circles), *Abcb1a/1b;Abcg2<sup>-/-</sup>* (light-blue squares) and *Cyp3a<sup>-/-</sup>* (maroon triangles) mice, over 24 h after oral administration of 10 mg/kg osimertinib. Data are given as mean  $\pm$  SD. N = 4-5 mice per group.

## 24 hours experiment





**Supplemental Figure 4** - Plasma-time curve of AZ5104 (A) and AZ5104 to osimertinib concentration ratio (B) in male wild-type (WT) (black circles), *Abcb1a/1b*<sup>-/-</sup> (dark blue squares), *Abcg2*<sup>-/-</sup> (green triangles) and *Abcb1a/1b;Abcg2*<sup>-/-</sup> (sky-blue triangles) mice, over 90 minutes after oral administration of 10 mg/kg osimertinib. Data are given as mean ± SD. N = 5-6 mice per group.



**Supplemental Figure 3** - Tissue concentration (A, C, E & G) and tissue accumulation (B, D, F & H) of osimertinib at 24 h in male WT, *Abcb1a/1b;Abcg2*<sup>-/-</sup>, and *Cyp3a*<sup>-/-</sup> mice following a single oral dose of 10 mg/kg osimertinib. Statistical differences were assessed using one-way analysis of variance (ANOVA) followed by Tukey's post-hoc multiple comparisons. Statistically significant differences were: \*,  $P < 0.05$ ; \*\*,  $P < 0.01$ ; \*\*\*,  $P < 0.001$  compared with WT mice. Tissue accumulation of osimertinib was calculated by determining the osimertinib tissue concentration relative to its plasma AUC<sub>0-24h</sub>. Note that at 24 h, brain concentrations of osimertinib in WT mice were below the limit of quantification (1 ng/ml). These values resulted occasionally in negative figures and were hence assumed to be zero for calculations. Values are shown as mean ± SD. N = 5 mice per group.



# 4

---

## P-glycoprotein (MDR1/ABCB1) restricts brain penetration of the Bruton's tyrosine kinase inhibitor ibrutinib while Cytochrome P450-3A (CYP3A) limits its oral bioavailability

---

**Stéphanie van Hoppe<sup>1</sup>, Johannes J.M. Rood<sup>2</sup>, Levi Buil<sup>1</sup>, Els Wagenaar<sup>1</sup>, Rolf W. Sparidans<sup>2</sup>, Jos H. Beijnen<sup>1,2</sup>, Alfred H. Schinkel<sup>1</sup>**

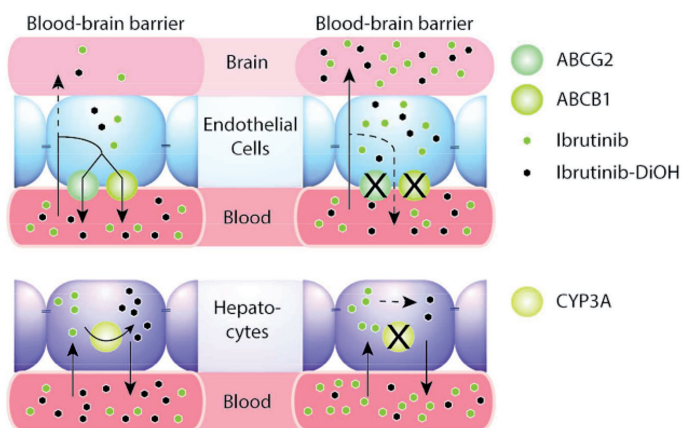
<sup>1</sup>Division of Pharmacology, The Netherlands Cancer Institute, Amsterdam

<sup>2</sup>Section of Pharmacoepidemiology & Clinical Pharmacology, Department of Pharmaceutical Sciences, Faculty of Science, Utrecht University, Utrecht

*Mol Pharm.* 2018 Nov 5;15(11):5124-5134.

## ABSTRACT

Ibrutinib (Imbruvica), an oral tyrosine kinase inhibitor (TKI) approved for treatment of B-cell malignancies, irreversibly inhibits the Bruton's tyrosine kinase (BTK). Its abundant metabolite, dihydrodiol-ibrutinib (ibrutinib-DiOH), which is primarily formed by CYP3A, has a ~10-fold reduced BTK inhibitory activity. Using *in vitro* transport assays and genetically modified mouse models, we investigated whether the multidrug efflux transporters ABCB1 and ABCG2 and the multidrug-metabolizing CYP3A enzyme family can affect the oral bioavailability and tissue disposition of ibrutinib and ibrutinib-DiOH. *In vitro*, ibrutinib was transported moderately by human ABCB1 and mouse Abcg2, but not detectably by human ABCG2. In mice, Abcb1 markedly restricted the brain penetration of ibrutinib and ibrutinib-DiOH, either alone or in combination with Abcg2, resulting in 4.5- and 5.9-fold increases in ibrutinib brain-to-plasma ratios in Abcb1a/1b<sup>-/-</sup> and Abcb1a/1b;Abcg2<sup>-/-</sup> mice relative to wild-type mice. Abcb1 and/or Abcg2 did not obviously restrict ibrutinib oral bioavailability, but Cyp3a deficiency increased the ibrutinib plasma AUC by 9.7-fold compared to wild-type mice. This increase was mostly reversed (5.1-fold reduction) by transgenic human CYP3A4 overexpression, with roughly equal contributions of intestinal and hepatic CYP3A4 metabolism. Our results suggest that pharmacological inhibition of ABCB1 during ibrutinib therapy might benefit patients with malignancies or (micro-)metastases positioned behind an intact blood-brain barrier, or with substantial expression of this transporter in the malignant cells. Moreover, given the strong *in vivo* impact of CYP3A, inhibitors or inducers of this enzyme family will likely strongly affect ibrutinib oral bioavailability, and thus its therapeutic efficacy, as well as its toxicity risks.



## INTRODUCTION

Multidrug efflux transporters of the ATP-binding cassette (ABC) protein family affect the disposition of a wide variety of endogenous and exogenous compounds, including numerous anticancer drugs. ABCB1 (P-glycoprotein) and ABCG2 (BCRP) are expressed in the apical membrane of epithelia in a number of organs that are essential for absorption and elimination of drugs like small intestine, liver, and kidney [1-4]. They are also abundant in luminal membranes of physiological barriers protecting various sanctuary tissues such as the blood-brain (BBB), blood-testis, and blood-placenta barriers. At these barriers, penetrating ABCB1 and ABCG2 substrates are immediately pumped out of the epithelial or endothelial cells back into the blood. As a consequence, only small amounts of drug can accumulate in, for instance, the brain. For anticancer drugs this can compromise treatment of primary brain tumors or (micro-)metastases that are present behind a functionally intact BBB [1-3]. Many anticancer drugs, including tyrosine kinase inhibitors (TKIs), are transported substrates of ABCB1, ABCG2, or both. As a result, these transporters can significantly modulate the pharmacokinetic behavior, including plasma levels and tissue distribution, and hence the therapeutic efficacy and toxicity profiles of these drugs [5]. Moreover, when functionally expressed in tumor cells themselves, the transporters can directly contribute to multidrug resistance of the malignancy.

Ibrutinib (Imbruvica, PCI-32765, Supplemental Figure 1) is an important orally administered TKI currently approved by the FDA and EMA for a number of diseases, including chronic lymphocytic leukemia, small lymphocytic lymphoma, Waldenström's macroglobulinemia, previously-treated mantle cell lymphoma, relapsed/refractory marginal zone lymphoma and chronic graft versus host disease (cGVHD). The latter application represents the first FDA-approved therapy for this disease [6]. Ibrutinib is an irreversible, covalently binding inhibitor of Bruton's tyrosine kinase (BTK), with promising clinical activity and tolerability in B-cell malignancies and other diseases. Although ibrutinib was initially developed for treatment of B-cell malignancies, recent publications suggest that ibrutinib could additionally be used for treatment of a range of other malignancies, resulting in an intense interest in this drug [6-9]. Several clinical trials are currently evaluating the efficacy of ibrutinib in metastatic pancreatic adenocarcinoma (NCT02436668), smoldering myeloma (NCT02943473), non-small cell lung cancer with an epidermal growth factor receptor (EGFR) mutation (NCT02321540), and refractory/recurrent primary or secondary central nervous system lymphoma (NCT02315326). A number of these malignancies obviously encompass central nervous system (CNS) lesions, including brain metastases. This broader application spectrum is likely in part due to ibrutinib specifically inhibiting not only BTK, but also a subset of other kinases such as GPIb and GPVI, ErbB4/HER4, Blk, Bmx/Etk, Txk, TEC, EGFR, ErbB2/

HER2, JAK3, HCK and ITK [8, 10-13].

Given the high ABCB1 and ABCG2 expression in the BBB, these transporters could potentially limit brain accumulation of ibrutinib, which might reduce the therapeutic efficacy against CNS lesions including brain (micro-)metastases. However, the current FDA and EMA documentation for this drug states that *in vitro* studies suggest that ABCB1 and ABCG2 do not transport ibrutinib, although they might be inhibited by ibrutinib at clinical doses [6]. A recent study further reported that ibrutinib can stimulate hABCB1-mediated ATPase activity [14]. It was therefore of interest to study these interactions in more detail.

The absolute oral bioavailability of ibrutinib in patients is low (around 3-8%), and this is likely due in part to extensive first-pass metabolism, primarily by cytochrome-P450 (CYP) 3A. Its main metabolite, dihydrodiol-ibrutinib (DiOH, PCI-45227, Supplemental Figure 1), has an inhibitory activity towards BTK approximately 10-15 times lower than that of the parent compound [6]. Ibrutinib-DiOH, which is thus modestly pharmacodynamically active, is formed through epoxidation and subsequent oxidation of the reactive acrylamide group [15]. Ibrutinib is mainly excreted via feces after phase I and II biotransformation. In humans, CYP3A4 is also the predominant CYP isoenzyme involved in the biotransformation of a range of other TKIs such as imatinib, nilotinib, bosutinib, dasatinib and ponatinib [16-20].

In the present study we investigated whether ibrutinib is a transported substrate of ABCB1 and ABCG2 *in vitro* and *in vivo*, and how this might affect the oral plasma pharmacokinetics and tissue distribution, including brain penetration, of ibrutinib and ibrutinib-DiOH in appropriate knockout mouse models. Furthermore, the substantial metabolism of ibrutinib by CYP3A [6] means that induction or inhibition of this enzyme complex may dramatically influence ibrutinib exposure. We therefore also studied the *in vivo* tissue-specific influence of CYP3A on the oral systemic availability and tissue exposure of ibrutinib and ibrutinib-DiOH in Cyp3a knockout and humanized transgenic mouse models.

## MATERIALS AND METHODS

### Chemicals

Ibrutinib (>99%) was purchased from Alsachim (Illkirch Graffenstaden, France), zosuquidar was obtained from Sequoia Research Products (Pangbourne, UK) and Ko143 was from Tocris Bioscience (Bristol, UK). Isoflurane was purchased from Pharmachemie (Haarlem, The Netherlands), heparin (5000 IU ml<sup>-1</sup>) was from Leo Pharma (Breda, The Netherlands), and Bovine Serum Albumin (BSA) Fraction V from Roche (Mannheim,

Germany). All chemicals used in the chromatographic ibrutinib assay were described before [21].

### Transport assays

Polarized Madin-Darby Canine Kidney (MDCK-II) cell lines transduced with either human (h)ABCB1, murine (m)Abcg2 or hABCG2 cDNA were cultured and used as described previously [22]. Transepithelial transport assays were performed in triplicate on 12-well microporous polycarbonate membrane filters (3.0- $\mu$ m pore size, Transwell 3402, Corning Inc., Lowell, MA) as described [22]. In short, cells were allowed to grow to an intact monolayer in 3 days, which was monitored with transepithelial electrical resistance (TEER) measurements. On the third day, cells were pre-incubated with the relevant inhibitors for 1 hour, where 5  $\mu$ M zosuquidar (ABCB1 inhibitor) and/or 5  $\mu$ M Ko143 (ABCG2/Abcg2 inhibitor) were added to both apical and basolateral compartments. To inhibit endogenous canine ABCB1 when testing the MDCK-II Abcg2 and MDCK-II ABCG2 cell lines, we added 5  $\mu$ M zosuquidar (ABCB1 inhibitor) to the culture medium throughout the experiment. The experiment was initiated by replacing the incubation medium from the donor compartment with freshly prepared medium containing 2  $\mu$ M ibrutinib alone or in combination with the appropriate inhibitors. At 1, 2, 4 and 8 h, 50- $\mu$ l samples were collected from the acceptor compartment and stored at -30°C until analysis. The amount of transported drug was calculated after correction for volume loss due to sampling at each time point. Active transport was expressed by the transport ratio ( $r$ ), which is defined as the amount of apically directed transport divided by the amount of basolaterally directed translocation at a defined time point.

### Animals

Female wild-type (WT), *Abcb1a/1b*<sup>-/-</sup> [23], *Abcg2*<sup>-/-</sup> [24], *Abcb1a/1b;Abcg2*<sup>-/-</sup> [25], and *Cyp3a*<sup>-/-</sup>, *hCyp3aXA*, *hCyp3aXV* and *hCyp3aXAV* mice [26], all of a >99% FVB strain background, were used. Mice between 9 and 14 weeks of age were used in groups of 5-6 mice per strain. The mice were kept in a temperature-controlled environment with a 12 h light/dark cycle and received a standard diet (AM-II, Hope Farms, Woerden, The Netherlands) and acidified water *ad libitum*. Animals were housed and handled according to institutional guidelines in compliance with Dutch and EU legislation.

### Drug solutions

Ibrutinib was dissolved at a concentration of 24.4 mg/ml in DMSO, polysorbate 80 and ethanol (final solvent ratios 1:20:20 (v/v/v)). It was then further diluted with 5% (w/v) glucose in water, to obtain a 1 mg/ml ibrutinib solution in water containing 0.1% DMSO, 2% (v/v) polysorbate 80, 2% (v/v) ethanol, and 4.795% (w/v) glucose. Ibrutinib was

administered orally at a dose of 10 mg/kg (10  $\mu$ l/g).

### **Plasma and tissue pharmacokinetics of ibrutinib**

To minimize variation in absorption, mice were fasted for 3 h prior to oral administration of ibrutinib, using a blunt-ended needle. 50- $\mu$ l blood samples were drawn from the tail vein using heparin-coated capillaries (Sarstedt, Germany). At the last time point mice were anesthetized using isoflurane inhalation and blood was collected via cardiac puncture. For the 8-h experiment, tail vein sampling took place at 0.25, 0.5, 1, 2, and 4 h after oral administration; for the 1-h experiment tail vein sampling took place at 5, 10, 15, and 30 min after oral administration, and finally for the 20-min experiment, tail vein sampling took place at 5, 10, and 15 min after oral administration. At the end point mice were sacrificed by cervical dislocation and a set of organs was rapidly removed, weighed and subsequently frozen as whole organs at  $-30^{\circ}\text{C}$ . Organs were allowed to thaw on ice and homogenized in appropriate volumes of 4% (w/v) BSA in water using a FastPrep<sup>®</sup>-24 device (MP Biomedicals, SA, California, USA). Homogenates were stored at  $-30^{\circ}\text{C}$  until analysis. Blood samples were immediately centrifuged at  $9000 \times g$  for 6 min at  $4^{\circ}\text{C}$ , and plasma was collected and stored at  $-30^{\circ}\text{C}$  until analysis. Ibrutinib concentrations in brain tissue were corrected for the amount of plasma present in the vascular space ( $\sim 1.4\%$ ) [27].

### **Drug analysis**

Ibrutinib and ibrutinib-DiOH concentrations in culture medium, plasma and tissue homogenates were analyzed with a previously reported liquid-chromatography tandem mass spectrometric (LC-MS/MS) assay, using deuterated internal standards [21].

### **Statistics and pharmacokinetic calculations**

The unpaired two-tailed Student's t-test was used to determine the significance of differences in the transepithelial transport assays. The area under the curve (AUC) of the plasma concentration-time curve was calculated using the trapezoidal rule, without extrapolating to infinity. Individual concentration-time data were used to determine the peak plasma concentration ( $C_{\text{max}}$ ) and the time to reach  $C_{\text{max}}$  ( $T_{\text{max}}$ ). Ordinary one-way analysis of variance (ANOVA) was used to determine significant differences between groups. Post-hoc Tukey's multiple comparisons were used to compare significant differences between individual groups. When variances were not homogeneously distributed, data were log-transformed before applying statistical tests. Differences were considered statistically significant when  $P < 0.05$ . Data are presented as mean  $\pm$  SD with each experimental group containing 5-6 mice.

## RESULTS

We first studied the interaction between ibrutinib and ABCB1 and ABCG2 *in vitro* by measuring ibrutinib (2  $\mu$ M) translocation through polarized monolayers of the MDCKII parental cell line and subclones transduced with human (h)ABCB1, hABCG2 or mouse (m)Abcg2 cDNA. As shown in Figure 1A, we observed no net apically directed ibrutinib transport in the parental cell line (transport ratio  $r = 0.88$ ). This was not significantly altered when the cells were treated with the ABCB1 inhibitor zosuquidar ( $r = 0.84$ , Figure 1B), suggesting that there is virtually no background transport mediated by the endogenous canine ABCB1 present in the MDCKII cells [28]. In MDCKII cells transduced with human ABCB1, we observed active apically directed transport with  $r = 2.33$ , which was almost completely blocked by zosuquidar, indicating that ibrutinib is a transport substrate for hABCB1 (Figure 1C and D). In subsequent transport experiments using MDCKII cells expressing human or mouse ABCG2, zosuquidar was included to block any background transport mediated by endogenous canine ABCB1. We observed substantial apically directed transport by mAbcg2 ( $r = 1.93$ ), whereas no transport was detected for hABCG2 ( $r = 0.94$ ) as shown in Figure 1E-H. Ibrutinib transport by mAbcg2 was efficiently blocked by the ABCG2 inhibitor Ko143. Ibrutinib thus appears to be transported by hABCB1 and mAbcg2, but, at this concentration, not noticeably by hABCG2.

Based on these transport data, we studied the single and combined effects of Abcb1 and Abcg2 on the plasma and tissue pharmacokinetics of ibrutinib and its pharmacodynamically active metabolite, ibrutinib-DiOH, using WT, Abcb1a/1b<sup>-/-</sup>, Abcg2<sup>-/-</sup>, and Abcb1a/1b;Abcg2<sup>-/-</sup> mice. Because ibrutinib is taken orally by patients, we administered ibrutinib orally at a dose of 10 mg/kg, roughly physiologically equivalent to the lower end of the human recommended dosages (140 mg/day). In a pilot experiment we analyzed the plasma concentrations of ibrutinib and ibrutinib-DiOH over 8 h in WT and Abcb1a/1b;Abcg2<sup>-/-</sup> mice. In this experiment, performed in our old mouse facility, we found no significant differences in the AUC<sub>0-8h</sub> values between the WT and knockout mice (Supplemental Figure 2A, B; Table 1). Ibrutinib was very rapidly absorbed, with a T<sub>max</sub> occurring before 5 min, and also quite rapidly cleared. Within 15 min, ibrutinib-DiOH concentrations were substantially higher than those of the parent drug, reaching a T<sub>max</sub> around 15-30 min, and with ibrutinib-DiOH/ibrutinib ratios staying well over a factor of 5 from 30 min on to at least 3 h after administration (Supplemental Figure 3, Supplemental Table 1). A subsequent 1-h experiment including all four ABC transporter mouse strains was performed more than a year later, after transfer of these strains to our new mouse facility. This transfer included a full clean-up by hysterectomy and a complete change-over in the microflora to that of another commercial animal supplier.

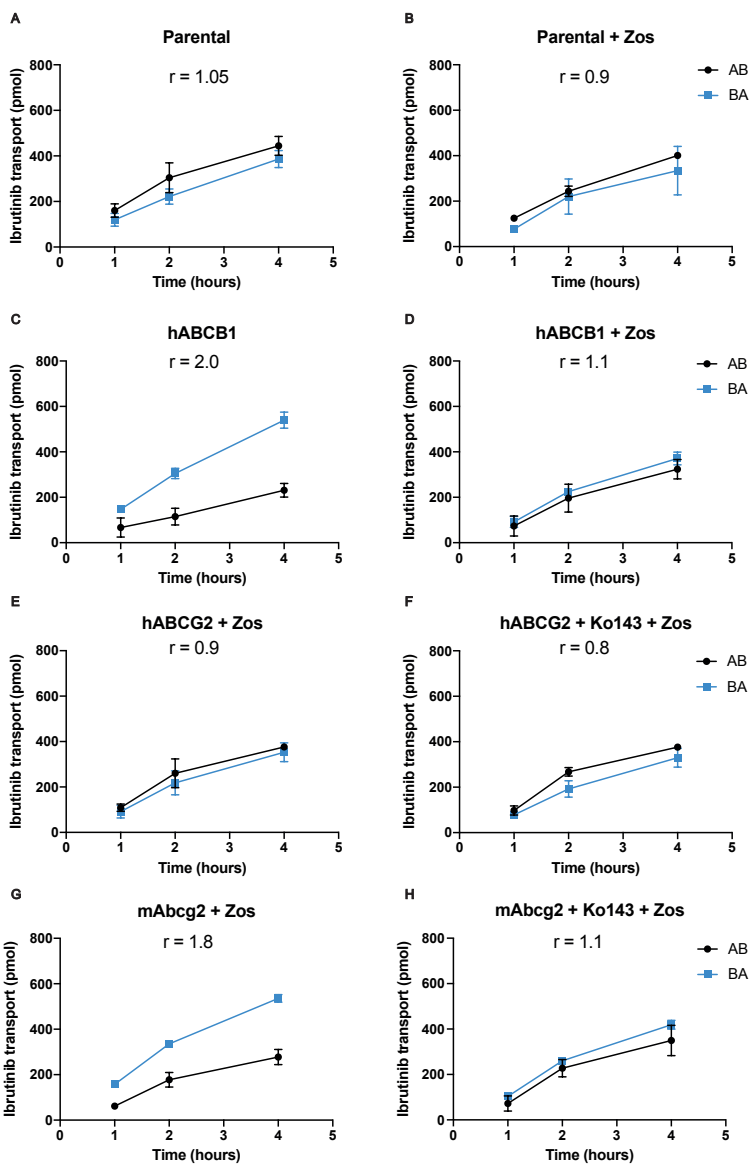


**Figure 1** - In vitro transport of ibrutinib. Transepithelial transport of ibrutinib (2  $\mu$ M) was assessed in MDCK-II cells either nontransduced (A, B) or transduced with hABCB1 (C, D), mAbcg2 (E, F), or hABCG2 (G, H) cDNA. At  $t = 0$  h ibrutinib was added to the donor compartment; thereafter at  $t = 1, 2$  and  $4$  h the concentrations were measured and plotted as total amount (pmol) of translocated drug ( $n = 3$ ). (B, D–H) Zosuquidar (Zos, 5  $\mu$ M) or Ko143 (5  $\mu$ M) were added as indicated to inhibit hABCB1 or hABCG2 and mAbcg2, respectively.  $r$ , relative transport ratio at 4 h. BA (blue squares) translocation from the basolateral to the apical compartment; AB (black circles), translocation from the apical to the basolateral compartment. Data are presented as mean  $\pm$  SD.

Possibly related to this change-over, we observed that under these circumstances the plasma AUC of ibrutinib in Abcb1a/1b;Abcg2<sup>-/-</sup> as well as Abcb1a/1b<sup>-/-</sup> mice was almost 2-fold lower than that in WT mice, whereas Abcg2<sup>-/-</sup> mice behaved more or less like WT mice (Figure 2A, Table 1). In other respects, however, the plasma pharmacokinetics in WT mice of both ibrutinib and ibrutinib-DiOH were very similar to those seen in the pilot experiment, with rapid absorption of ibrutinib ( $T_{max}$  before 5 min), a  $T_{max}$  of ibrutinib-DiOH around 15 min (Figure 2B, Supplemental Table 1), and a ibrutinib-DiOH/ibrutinib ratio rising above a factor of 5 well within 1 hr (Supplemental Figure 4). The  $AUC_{0-1h}$  for ibrutinib in WT mice was also very similar for both experiments (274 and 340 h.ng/ml, respectively). Although there was a tendency for the ibrutinib-DiOH/ibrutinib ratio to be higher in the Abcb1a/1b;Abcg2<sup>-/-</sup> as well as the Abcb1a/1b<sup>-/-</sup> mice compared to the WT mice, this did not reach statistical significance (Supplemental Figure 4). Abcg2<sup>-/-</sup> mice behaved generally similar to WT mice in this respect. Thus, apart from the impact of Abcb1 deficiency, which resulted in ~2-fold lower plasma levels of ibrutinib in the second, but not the first, experiment, there does not seem to be a major impact of Abcb1 and/or Abcg2 on ibrutinib to ibrutinib-DiOH conversion.

**Table 1** - Pharmacokinetic parameters of ibrutinib at 8 and 1 h after oral administration of 10 mg/kg ibrutinib to female WT, Abcb1a/1b<sup>-/-</sup>, Abcg2<sup>-/-</sup> and Abcb1a/1b;Abcg2<sup>-/-</sup> mice.

Parameter	Time	Genotype			
		WT	Abcb1a/1b <sup>-/-</sup>	Abcg2 <sup>-/-</sup>	Abcb1a/1b;Abcg2 <sup>-/-</sup>
$AUC_{0-8}$ (ng/ml.h)	8 h	431 ± 97			404 ± 78
$C_{max}$ (ng/ml)		609 ± 276			837 ± 131
$T_{max}$ (minutes)		7 ± 4			5 ± 0
$AUC_{0-1}$ (ng/ml.h)	1 h	340 ± 59	190 ± 69 ***	350 ± 34 ###	169 ± 31 ***
$C_{max}$ (ng/ml)		748 ± 93	455 ± 164	751 ± 95	372 ± 107
$T_{max}$ (minutes)		£ 5	£ 5	7 ± 3	6 ± 2
$C_{brain}$ (ng/g)		8.93 ± 4.58	18.3 ± 9.86	9.41 ± 1.86 ##	25.9 ± 10.4 **
Brain to plasma ratio		0.081 ± 0.015	0.366 ± 0.086 ***	0.084 ± 0.007 ####	0.481 ± 0.074 ****
Fold change		1	4.5	1	5.9
$C_{liver}$ (ng/g)		162 ± 76	54.3 ± 23	152 ± 37	77 ± 24
Liver:plasma ratio		1.49 ± 0.10	1.39 ± 0.25	1.36 ± 0.19	1.50 ± 0.21
Fold change		1	0.9	0.9	1
Brain to liver ratio		0.05 ± 0.01	0.31 ± 0.05 **** / #	0.06 ± 0.01 ####	0.33 ± 0.08 ****
Fold change		1	5.7	1.2	6.1

AUC, area under the plasma concentration-time curve;  $C_{max}$ , maximum ibrutinib concentration in plasma;  $T_{max}$ , the time (h) after drug administration needed to reach maximum plasma concentration;  $C_{brain}$ , brain concentration;  $P_{brain}$ , brain accumulation ( $C_{brain}$  divided by AUC);  $C_{liver}$ , liver concentration;  $P_{liver}$ , liver accumulation ( $C_{liver}$  divided by AUC). \*, P < 0.05; \*\*, P < 0.01; \*\*\*, P < 0.001; \*\*\*\*, P < 0.0001 compared to WT mice and #, P < 0.05; ##, P < 0.01; ###, P < 0.001; ####, P < 0.0001 compared to Abcb1a/1b;Abcg2<sup>-/-</sup> mice. Data are given as mean ± SD.

To investigate the impact of single and combined knockout of Abcb1a/1b and Abcg2 on ibrutinib brain distribution, we isolated mouse tissues (brain, liver, kidneys, spleen) at the end of the 1 h pharmacokinetic experiment. Figure 3A shows that ibrutinib accumulated to a low extent in the brain of WT and Abcg2<sup>-/-</sup> mice, but more highly in Abcb1a/1b<sup>-/-</sup> and Abcb1a/1b;Abcg2<sup>-/-</sup> mice. Correction for the substantial differences in plasma concentration at 1 h and the plasma AUCs showed that brain-to-plasma ratios and brain accumulation of ibrutinib were markedly (and highly significantly) increased in both the Abcb1-deficient strains, but not in the single Abcg2-deficient strain (Figure 3B and C). In contrast, analysis of the liver, which often equilibrates rapidly with drug levels in plasma, yielded no significant differences in liver-to-plasma ratio or liver accumulation

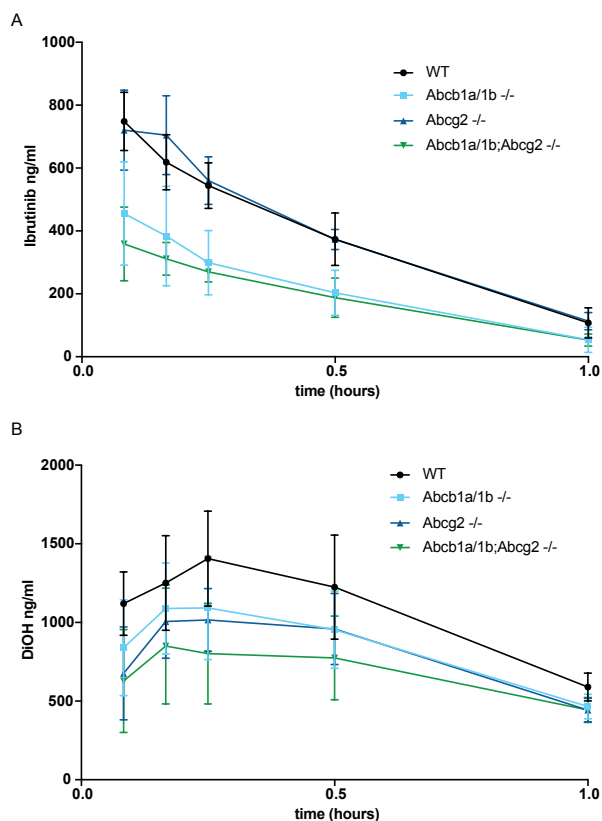


**Figure 2** - Plasma concentration–time curves of ibrutinib (A) and ibrutinib-DiOH (DiOH) (B) in female WT (black circles), Abcb1a/1b<sup>-/-</sup> (blue squares), Abcg2<sup>-/-</sup> (dark blue triangles) and Abcb1a/1b;Abcg2<sup>-/-</sup> (green triangles) mice over 1 h after oral administration of 10 mg/kg ibrutinib. Note the difference in Y-axis scales between the panels. Data are given as mean  $\pm$  SD. n = 5–6 mice per group.

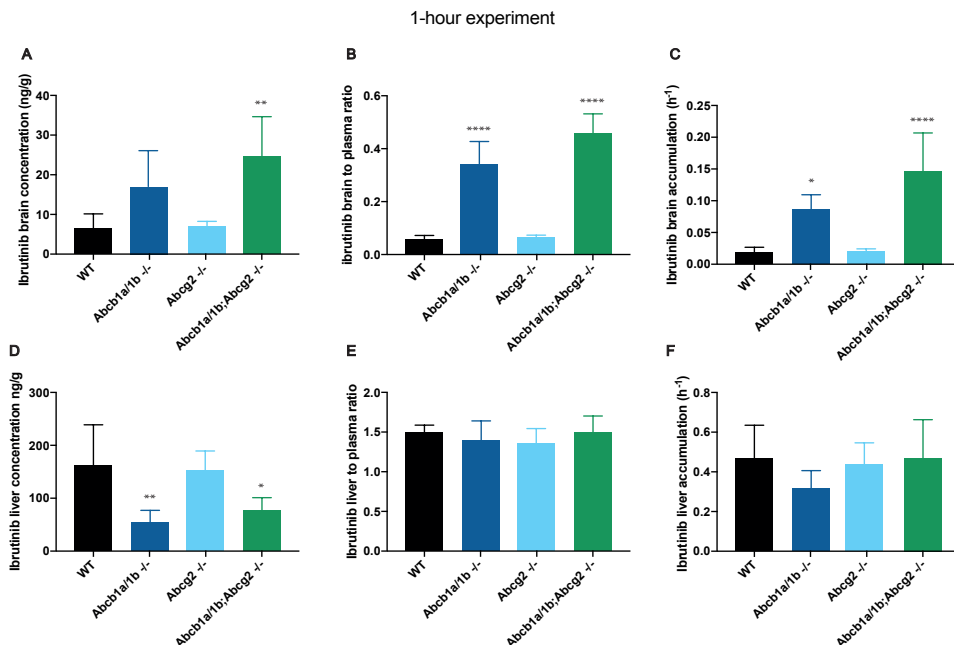


**Figure 3** - Brain and liver concentration (A, D), tissue-to-plasma ratio (B, E) and relative tissue accumulation (C, F) of ibrutinib in female WT, *Abcb1a/1b*<sup>-/-</sup>, *Abcg2*<sup>-/-</sup> and *Abcb1a/1b;Abcg2*<sup>-/-</sup> mice 1 h after oral administration of 10 mg/kg ibrutinib. \*,  $P < 0.05$ ; \*\*,  $P < 0.01$ ; \*\*\*,  $P < 0.001$  compared to WT mice. Data are given as mean  $\pm$  SD.  $n = 5-6$  mice per group.

(Figure 3D-F). Together, these data indicate that *Abcb1a/1b* markedly restricts brain accumulation of ibrutinib. Whether *Abcg2* also contributes to this process is uncertain, as the (modest) differences between the *Abcb1a/1b*<sup>-/-</sup> and *Abcb1a/1b;Abcg2*<sup>-/-</sup> brains were not statistically significant (Figure 3B and C). The intrinsic brain accumulation of ibrutinib was quite low in WT mice, with a brain-to-plasma ratio of 0.081, which however rose to about 0.37 to 0.48 in the *Abcb1a/1b*<sup>-/-</sup> or the combination *Abcb1a/1b;Abcg2*<sup>-/-</sup> strain, respectively (Figure 3B, Table 1). Compared to a liver-to-plasma ratio of 1.4-1.5 at this time point (Figure 3E), this suggests a fairly good brain penetration of this drug, but only when *Abcb1a/1b* is absent.

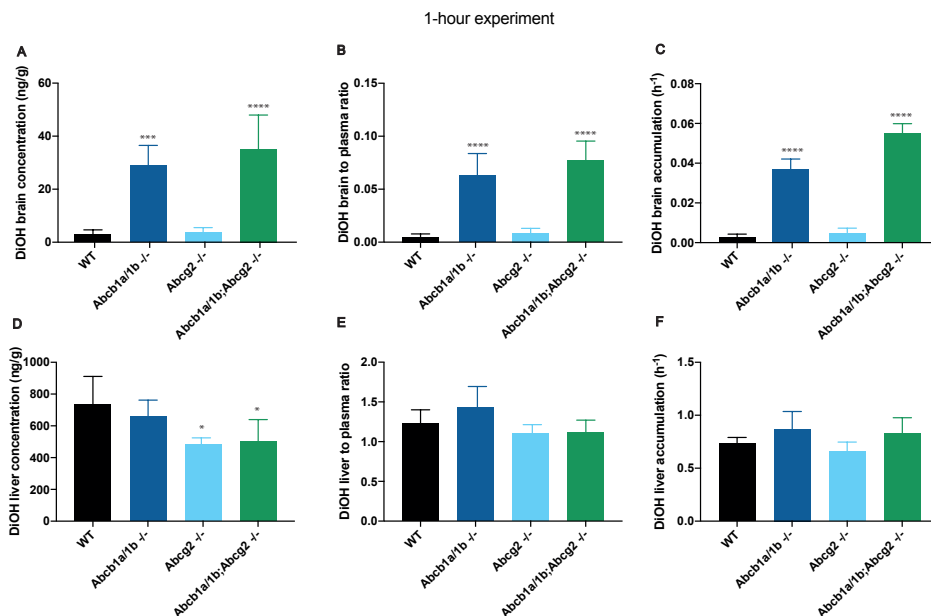


**Figure 4** - Brain and liver concentration (A, D), tissue-to-plasma ratio (B, E) and relative tissue accumulation (C, F) of ibrutinib-DiOH (DiOH) in female WT, *Abcb1a/1b*<sup>-/-</sup>, *Abcg2*<sup>-/-</sup> and *Abcb1a/1b;Abcg2*<sup>-/-</sup> mice 1 h after oral administration of 10 mg/kg ibrutinib. \*,  $P < 0.05$ ; \*\*,  $P < 0.01$ ; \*\*\*,  $P < 0.001$  compared to WT mice. Data are given as mean  $\pm$  SD.  $n = 5-6$  mice per group.

Ibrutinib-DiOH is substantially more polar than the parent ibrutinib, and this is probably reflected in lower brain-to-plasma ratios and brain accumulation than for ibrutinib (Figure 4A-C). However, the impact of the absence of *Abcb1a/1b* on altering brain-to-plasma ratios and brain accumulation of ibrutinib-DiOH was even more pronounced than for ibrutinib, with 12- to 15-fold increases relative to wild-type values (Figure 4A-C, Supplemental Table 1). Like for ibrutinib, any contribution of *Abcg2* to limiting ibrutinib-DiOH brain accumulation was at best small. At the same time, the relative liver accumulation of ibrutinib-DiOH was very similar to that of ibrutinib, and not significantly different between the tested mouse strains (Figure 4D-F). Similar parameters for the distribution of both ibrutinib and ibrutinib-DiOH to kidney and spleen also did not yield pronounced differences between the strains, although there may be some impact of *Abcb1a/1b* deficiency on increasing ibrutinib spleen distribution (Supplemental Figures 5 and 6). Distribution of both ibrutinib and ibrutinib-DiOH to the brain thus appears to be markedly limited by *Abcb1a/1b* activity, but distribution to most of the other tested organs is not. In spite of the marked changes in brain distribution of ibrutinib, we did not see any indications for toxicity of ibrutinib at the dosages used in the *Abcb1a/1b;Abcg2*<sup>-/-</sup> mice.

CYP3A is thought to primarily mediate the oxidation of ibrutinib to ibrutinib-DiOH, and we therefore also investigated the extent and tissue specificity of the impact of CYP3A in WT, *Cyp3a<sup>-/-</sup>*, *Cyp3aXA*, *Cyp3aXV*, and *Cyp3aXAV* mice. *Cyp3a<sup>-/-</sup>* mice lack all mouse *Cyp3a* proteins, whereas the “humanized” *Cyp3aXA*, *Cyp3aXV*, and *Cyp3aXAV* strains express human CYP3A4 in, respectively, the liver (XA), the intestine (XV), or in both liver and intestine (XAV) of the *Cyp3a<sup>-/-</sup>* mice. We first performed a pilot study with oral ibrutinib at 10 mg/kg in WT, *Cyp3a<sup>-/-</sup>*, and *Cyp3aXAV* mice, analyzing the ibrutinib and ibrutinib-DiOH plasma concentrations over 8 h. We found that the absence of *Cyp3a* led to highly increased ibrutinib concentrations in the plasma compared to WT mice, resulting in a 9.7-fold increased  $AUC_{0-8\text{ h}}$ , whereas the  $T_{\text{max}}$  was not substantially altered (Figure 5A, Table 2). Conversely, the formation of ibrutinib-DiOH was dramatically decreased in *Cyp3a<sup>-/-</sup>* mice, resulting in only 6.7% of the ibrutinib-DiOH  $AUC_{0-8\text{ h}}$  in WT mice (Figure 5C, Supplemental Table 2). These data indicate that the mouse *Cyp3a*

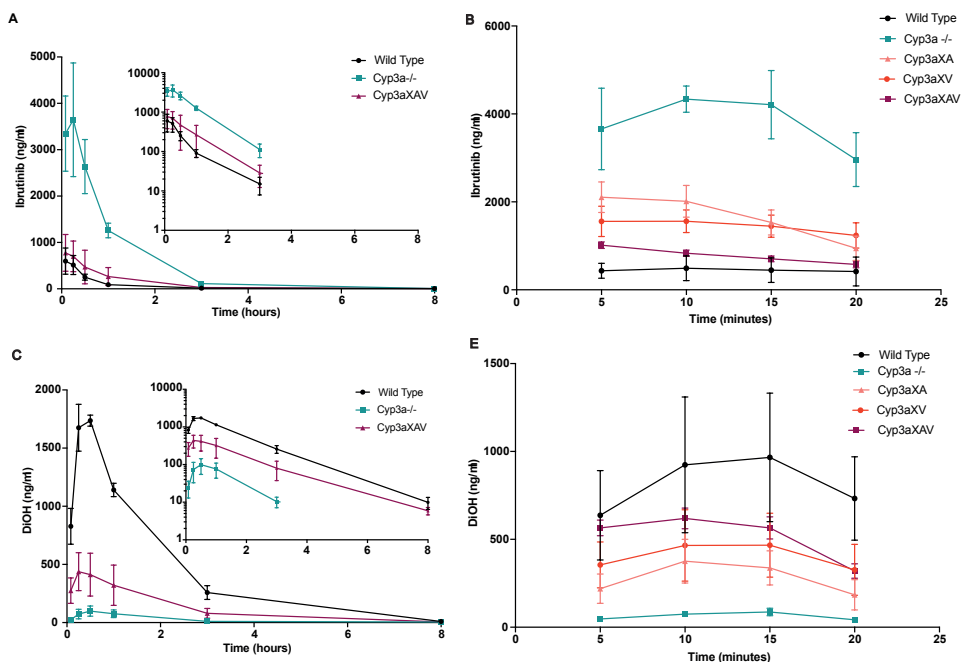


**Figure 5** - Plasma concentration–time curves of ibrutinib (A, B) and ibrutinib-DiOH (DiOH) (C, D) in female WT (black circles), *Cyp3a<sup>-/-</sup>* (blue squares), *Cyp3aXA* (peach triangles), *Cyp3aXV* (red circles) and *Cyp3aXAV* (maroon triangles) mice over 8 h (A & C) or 20 minutes (B & D) after oral administration of 10 mg/kg ibrutinib. Insets: semi-log plots of the data. When the 8 h data were below the lower limit of quantification, data were only plotted up till 3 h. Note the different concentration scales in panels A and C as well as panels B and D. Data are given as mean  $\pm$  SD. n = 5–6 mice per group.

**Table 2** - Pharmacokinetic parameters of ibrutinib at 8 h, 1 h and 20 minutes after oral administration of 10 mg/kg ibrutinib to female WT, Cyp3a<sup>-/-</sup>, Cyp3aXA, Cyp3aXV and Cyp3aXAV mice.

Parameter	Time	Genotype				
		WT	Cyp3a <sup>-/-</sup>	Cyp3aXA	Cyp3aXV	Cyp3aXAV
AUC <sub>0-8</sub> (ng/mLh)	8 h	430.5 ± 96.59	4166 ± 317 *****			832 ± 521 ###
C <sub>max</sub> (ng/ml)		609 ± 276	3865 ± 932			798 ± 404
T <sub>max</sub> (minutes)		7 ± 4	15 ± 8			9 ± 5
AUC <sub>0-1</sub> (ng/mLh)	1 h	341 ± 59	1973 ± 670 *****			
C <sub>max</sub> (ng/ml)		748 ± 93	3305 ± 1425			
T <sub>max</sub> (minutes)		£ 5	13 ± 8			
C <sub>brain</sub> (ng/g)		8.93 ± 4.58	111 ± 34.7 *****			
Brain to plasma ratio		0.081 ± 0.015	0.109 ± 0.021			
Fold change		1	1.3			
C <sub>liver</sub> (ng/g)		162.6 ± 76.4	1415 ± 409 *****			
Liver to plasma ratio		1.493 ± 0.095	1.384 ± 0.221			
Fold change		1	0.9			
Brain to liver ratio		0.054 ± 0.006	0.079 ± 0.010			
Fold change		1	1.4			
AUC <sub>0-33</sub> (ng/mLh)	20 min	113 ± 67	988 ± 139 *****	423 ± 76 *****/###	367 ± 57.53 *****/###	194.5 ± 15.65 ###
C <sub>max</sub> (ng/ml)		590.2 ± 261.0	4544 ± 505.6	2129 ± 360.8	1693 ± 280	1015 ± 73.4
T <sub>max</sub> (minutes)		13 ± 6	11 ± 3	7 ± 3	9 ± 4	£ 5
C <sub>brain</sub> (ng/g)		102 ± 60.5	468 ± 98.3 *****	133 ± 24.9 ####	89 ± 40.4 ####	38 ± 8.8 ###
Brain to plasma ratio		0.256 ± 0.041	0.199 ± 0.027 *	0.190 ± 0.028 **	0.117 ± 0.025 *****/###	0.112 ± 0.011 *****/###
Fold change		1	0.7	0.7	0.5	0.4
C <sub>liver</sub> (ng/g)		2420 ± 1479	8178 ± 1380 *****	2147 ± 551.3 ###	2125 ± 701.3 ###	963.4 ± 207.2 ###
Liver to plasma ratio		5.06 ± 0.96	2.78 ± 0.19 *****	2.36 ± 0.67 *****	1.70 ± 0.34 *****/##	1.66 ± 0.22 *****/##
Fold change		1	0.5	0.5	0.3	0.3
Brain to liver ratio		0.043 ± 0.013	0.057 ± 0.005	0.063 ± 0.009 *	0.040 ± 0.010 #	0.039 ± 0.005 #
Fold change		1	1.3	1.5	0.9	0.9

AUC, area under the plasma concentration-time curve; C<sub>max</sub>, maximum ibrutinib concentration in plasma; T<sub>max</sub>, the time (h) after drug administration needed to reach maximum plasma concentration; C<sub>brain</sub>, brain concentration; C<sub>liver</sub>, liver concentration. \*, P < 0.05; \*\*, P < 0.01; \*\*\*, P < 0.001; \*\*\*\*, P < 0.0001 compared to WT mice and #, P < 0.05; ##, P < 0.01; ###, P < 0.001; ####, P < 0.0001 compared to Cyp3a<sup>-/-</sup> mice. Data are given as mean ± SD

proteins are a major factor in metabolizing ibrutinib to ibrutinib-DiOH. When transgenic human CYP3A4 was expressed in both liver and intestine of Cyp3a<sup>-/-</sup> mice (Cyp3aXAV), the

ibrutinib plasma concentrations decreased again by 5-fold, to less than two-fold the AUC<sub>0-8 h</sub> in WT mice (Figure 5A, Table 2). At the same time, plasma levels of ibrutinib-DiOH in Cyp3aXAV mice increased by 4.2-fold compared to Cyp3a<sup>-/-</sup> mice, to about 28% of the ibrutinib-DiOH AUC<sub>0-8 h</sub> seen in WT mice (Figure 5C, Supplemental Table 2). These data indicate a substantial, albeit not complete reversal of ibrutinib to ibrutinib-DiOH conversion by transgenic human CYP3A4 expression in liver and intestine. Thus, the combined endogenous mouse Cyp3a proteins have a higher overall capacity to metabolize ibrutinib to ibrutinib-DiOH than the exogenously (but orthotopically) expressed human CYP3A4. Accordingly, when we plotted the plasma ibrutinib-DiOH to ibrutinib concentration ratio over the first three hours, the high ratio observed in WT mice (rising well above 5 within 30 min) was very low in Cyp3a<sup>-/-</sup> mice (0.04 around 30 min), but only returned to a ratio of around 1 at 30 min in the Cyp3aXAV mice (Supplemental Figure 7). A small 1-h follow-up experiment in WT and Cyp3a<sup>-/-</sup> mice revealed very similar profiles (Supplemental Figure 8).

To further analyze the separate and combined *in vivo* impact of hepatic and intestinal CYP3A4 on ibrutinib to ibrutinib-DiOH metabolism around or shortly after the T<sub>max</sub> of ibrutinib, we performed a short-term (20 min) oral pharmacokinetic experiment in WT, Cyp3a<sup>-/-</sup>, Cyp3aXA, Cyp3aXV, and Cyp3aXAV mice. As shown in Figure 5B and D, the interindividual variation in plasma levels was high, especially in WT mice, which is not uncommon this shortly after oral drug administration. Nonetheless, absence of Cyp3a led to a highly significant, 8.7-fold increase in ibrutinib plasma levels (AUC<sub>0-0.33 h</sub>), which was partly reversed by either hepatic CYP3A4 expression (2.3-fold reversal), or intestinal CYP3A4 expression (2.7-fold reversal). Combined hepatic and intestinal CYP3A4 expression had an additive effect, resulting in a 5.1-fold reversal of ibrutinib plasma levels (Figure 5B, Table 2). Also over this time period reversal by the transgenic human CYP3A4 was therefore extensive, but not completely back to WT levels. The changes in ibrutinib-DiOH plasma levels between the strains mirrored the changes in levels of ibrutinib metabolism, with absence of Cyp3a resulting in a 12.4-fold decrease in ibrutinib-DiOH levels (AUC<sub>0-0.33 h</sub>), hepatic and intestinal CYP3A4 expression causing a 4.4- and 6.5-fold reversal, respectively, and the combination expression a 7.9-fold reversal (Figure 5D, Supplemental Table 2). Plotting the plasma ibrutinib-DiOH to ibrutinib concentration ratios confirmed these separate and additive effects (Supplemental Figure 9E), including that the reversal even in the Cyp3aXAV strain was far from completely back to the WT levels. Collectively, the data indicate that in these mouse strains hepatic and intestinal CYP3A4 have a more or less comparable impact

on reducing oral ibrutinib plasma levels by metabolizing it to ibrutinib-DiOH. Detailed analysis of changes in the tissue levels of ibrutinib and ibrutinib-DiOH was hampered by the high interindividual variation at this early time point, but the ibrutinib-DiOH to ibrutinib ratios in all tested tissues (liver, kidney, spleen) generally reflected those seen in plasma (Supplemental Figure 9A-E), indicating a relatively rapid equilibration of both compounds between these tissues and plasma.

## DISCUSSION

Our results show that ibrutinib is modestly transported *in vitro* by human ABCB1 and mouse Abcg2, but not detectably by human ABCG2. *In vivo* in mouse models, mAbcb1 and mAbcg2 do not appear to restrict the oral bioavailability of ibrutinib, although under some circumstances mAbcb1 deficiency may indirectly reduce ibrutinib availability (see below). However, the brain distribution of ibrutinib is markedly restricted by mAbcb1 in the BBB, but not substantially by mAbcg2, even in the absence of mAbcb1 activity. The brain distribution of ibrutinib-DiOH, the primary active metabolite of ibrutinib, is also strongly limited by mAbcb1 activity. In contrast, the distribution of ibrutinib and ibrutinib-DiOH to other major tissues such as liver, kidney, and spleen is not markedly affected by mAbcb1 and/or mAbcg2 activity, with the possible exception of a small effect of Abcb1a/1b deficiency in ibrutinib spleen distribution. No ibrutinib toxicity was observed in the Abcb1a/1b;Abcg2-deficient mice. We further found that mouse Cyp3a deficiency caused a profound increase in ibrutinib plasma levels, apparently due to reduced conversion of ibrutinib to ibrutinib-DiOH. Overexpression of human CYP3A4 in either liver or intestine of Cyp3a<sup>-/-</sup> mice markedly reduced ibrutinib oral bioavailability, and to roughly similar extents. The concomitant ibrutinib-DiOH levels observed in these strains qualitatively reflected the predicted changes in conversion of ibrutinib to ibrutinib-DiOH by Cyp3a and CYP3A4.

Our *in vitro* transport data contrast with the FDA and EMA documentation on ibrutinib, stating that *in vitro* studies suggest that ABCB1 and ABCG2 do not transport ibrutinib [6, 29]. Instead, we found clear transport of ibrutinib by hABCB1 and mAbcg2, with efflux ratios (2.33, 1.93) well above the often-used cut-off value of 1.5, and fully inhibitable with specific ABCB1 and ABCG2 inhibitors. We attribute this apparent discrepancy to the relative sensitivity of the transepithelial transport assays applied by us. The *in vivo* significance of these findings is further supported by the marked effect of mAbcb1 deficiency on brain distribution of ibrutinib (Figure 3, Table 1). mAbcg2, instead, did not appear to have a marked impact in restricting brain accumulation of ibrutinib. It is possible that ABCB1 in humans will also limit brain distribution of ibrutinib, which could

affect the therapeutic efficacy of this drug against brain malignancies, either primary lesions or (micro-)metastases, that are positioned in whole or in part behind a functional blood-brain barrier. However, quantitative proteomic research has demonstrated that humans possess an ~4-fold more abundant BBB expression of ABCG2 relative to ABCB1 compared to mice [35]. It can therefore not be excluded that in humans there may still be a role of ABCG2 in limiting ibrutinib brain distribution, even though we did not find a clear impact of Abcg2 in the mouse BBB. Conversely, as the human BBB ABCB1 expression is 2.3-fold lower than that of the mouse BBB Abcb1a, the impact of ABCB1 in human brain penetration of ibrutinib might be somewhat smaller than in mice.

It is worth noting that the intrinsic brain distribution of ibrutinib is not very low, with brain-to-plasma ratios of 8% in WT mice, increasing to 37-48% in the absence of Abcb1 and Abcg2 (Table 1). Even though most of the primary malignancies (lymphomas) for which ibrutinib is currently prescribed do not often occur in, or metastasize to, the brain this does happen now and then. For instance, in Bing Neel syndrome, malignant lymphoplasmacytic cells from Waldenström's macroglobulinemia infiltrate the CNS, mantle cell lymphoma can disseminate to the CNS, and primary CNS lymphoma also occurs [30-34]. Interestingly, ibrutinib is already considered a potential treatment option for all these disorders, as its intrinsic brain penetration is thought to be fair based on CSF drug levels [33]. Moreover, brain metastases are common for a number of malignancies, including non-small cell lung cancer, for which ibrutinib is currently in clinical trials. Considering the broad interest in applying ibrutinib to a range of other cancers as well, this will further increase the likelihood of BBB function interfering with optimal therapeutic efficacy of this drug. Moreover, the observation that hABCB1 can actively extrude ibrutinib opens up the possibility that, when substantially expressed in lymphoma or tumor cells themselves (as is often the case [36, 37]), it can significantly contribute directly to resistance against this drug, which acts against an intracellular target. Given these considerations, it might be worthwhile to consider administering ibrutinib together with a strong ABCB1 inhibitor under some circumstances in order to increase efficacy against brain lesions and malignancies resistant due to ABCB1 overexpression.

From our data ibrutinib-DiOH also appears to be a transported substrate of Abcb1 *in vivo*, which is in line with EMA documentation mentioning *in vitro* transport by hABCB1 [29]. While its brain distribution is strongly restricted by mAbcb1 (Supplemental Figure 5 and Supplemental Table 1), the absolute brain distribution of ibrutinib-DiOH relative to ibrutinib is still very low, even in Abcb1-deficient mice (brain-to-plasma ratio of ~7%). Since ibrutinib-DiOH is also much less (10/15-fold) pharmacodynamically active than ibrutinib, it seems very unlikely that it would substantially contribute to the therapeutic efficacy against CNS lesions.

The oral bioavailability of ibrutinib is clearly not restricted by mAbcb1 and mAbcg2 activity. This contrasts with the clear impact of mAbcb1 on the brain accumulation of ibrutinib. We (and others) have observed this for a range of different drugs: generally, when a drug is only moderately transported *in vitro* by ABCB1 and/or ABCG2, such as ponatinib and regorafenib, we see a more pronounced effect of these transporters in restricting the brain accumulation of these drugs than in reducing their oral availability [38, 39]. Only when drugs are very efficiently transported substrates, such as afatinib, we tend to see a clear role in oral availability [4]. Whereas the exact reason of this apparent discrepancy is unknown, it may be due to the presence of more broad-specificity uptake systems as well as a higher influx capacity in the intestine as compared to the much more restrictive BBB. An obvious translational implication of these findings is that, when inhibiting ABCB1 and/or ABCG2 with a pharmacological ABCB1/ABCG2 inhibitor, the oral availability of a drug will generally be (much) less enhanced than its brain penetration. Especially when there are potential toxic side effects of higher systemic exposure of the drug(s), this might be an advantage.

Our finding that mAbcb1 deficiency unexpectedly decreased ibrutinib oral bioavailability in our new mouse facility, but not in our old facility, may be explained by the concomitant introduction of an entirely new intestinal microflora. For instance, bacterial inducing compounds present in our new microflora, but not the old, might cause upregulation of ibrutinib-metabolizing enzymes. If these inducers are normally kept out of the system by mAbcb1, this would result in higher metabolic clearance, and hence lower plasma levels, of ibrutinib in Abcb1-deficient mice in the new facility. In this context, it is interesting to note that the ibrutinib-DiOH-to-ibrutinib plasma ratios in the old mouse facility were similar between Abcb1a/1b:Abcg2<sup>-/-</sup> and WT mice (Supplemental Figure 3), whereas in the new mouse facility they were about 2-fold higher in both Abcb1a/1b-deficient strains compared to the WT mice (Supplemental Figure 4). This would be in line with a relatively more extensive metabolic conversion of ibrutinib to ibrutinib-DiOH in the new mouse facility in the Abcb1a/1b-deficient strains. Needless to say, given the (mostly uncharted) complexity of intestinal microflora composition, the identity of any intestinal inducing compounds would be difficult to resolve.

Our CYP3A studies show that, like in humans, ibrutinib oral bioavailability is strongly restricted by CYP3A-mediated conversion to ibrutinib-DiOH. This is true for both the mouse Cyp3a family (encompassing some 8 functional Cyp3a genes) and the transgenic human CYP3A4. The observation that the endogenous mouse Cyp3a proteins had an even stronger effect on ibrutinib oral bioavailability than the transgenic human CYP3A4 (Figure 4) may reflect effectively higher expression of one or more of the mouse Cyp3a proteins, and/or higher intrinsic efficacy in metabolizing ibrutinib. This finding is therefore not in itself surprising. In the CYP3A4 transgenic mice, liver and intestinal expression of

CYP3A4 is of the same order as that seen in human liver [40]. Our data on ibrutinib and ibrutinib-DiOH levels in the CYP3A4 transgenic mouse strains therefore suggest that intestinal CYP3A4 is at least as important as hepatic CYP3A4 in limiting ibrutinib oral bioavailability (Table 2 and Supplemental Table 2), most likely through extensive first-pass metabolism. Altogether, it seems likely that the poor oral bioavailability of ibrutinib is in large part due to its extensive first-pass metabolism, primarily by CYP3A. This may well also apply in humans, which show an absolute ibrutinib oral bioavailability of only ~3-8% [6, 29]. Apart from its impact on oral bioavailability, CYP3A activity does not seem to have a substantial effect on the tissue distribution of ibrutinib and ibrutinib-DiOH.

Collectively, our data show that extensive metabolism of ibrutinib by CYP3A in intestine and liver is likely the primary factor in restricting its oral bioavailability, whereas the drug efflux transporters ABCB1 and ABCG2 play very little, if any, role in this process. However, the brain distribution of ibrutinib is clearly limited by ABCB1, whereas the relative distribution of ibrutinib to a range of other tissues is not much affected by either the ABC transporters or CYP3A. Considering that the main types of dose-limiting toxicities of ibrutinib (hemorrhage, opportunistic infections, cytopenia, atrial fibrillation, hypertension) originate outside the CNS, one could consider coadministering ibrutinib with a pharmacological ABCB1 inhibitor in cases where optimal brain penetration of ibrutinib might be therapeutically helpful. However, such treatment modalities would, as always, first have to be very carefully assessed in human patients to judge their practical applicability.

## REFERENCES

1. Schinkel, A.H., et al., *P-glycoprotein in the blood-brain barrier of mice influences the brain penetration and pharmacological activity of many drugs*. J Clin Invest, 1996. 97(11): p. 2517-24.
2. Vlaming, M.L., J.S. Lagas, and A.H. Schinkel, *Physiological and pharmacological roles of ABCG2 (BCRP): recent findings in Abcg2 knockout mice*. Adv Drug Deliv Rev, 2009. 61(1): p. 14-25.
3. Yabuki, N., et al., *Gene amplification and expression in lung cancer cells with acquired paclitaxel resistance*. Cancer Genet Cytogenet, 2007. 173(1): p. 1-9.
4. van Hoppe, S., et al., *Breast cancer resistance protein (BCRP/ABCG2) and P-glycoprotein (P-gp/ABCB1) transport afatinib and restrict its oral availability and brain accumulation*. Pharmacol Res, 2017. 120: p. 43-50.
5. Stuurman, F.E., et al., *Oral anticancer drugs: mechanisms of low bioavailability and strategies for improvement*. Clin Pharmacokinet, 2013. 52(6): p. 399-414.
6. Center for Drug valuation and Research of the U.S., Department of Health and Human Services Food and Drug Administration. . 2017; Available from: [https://www.accessdata.fda.gov/drugsatfda\\_docs/label/2017/205552s017lbl.pdf](https://www.accessdata.fda.gov/drugsatfda_docs/label/2017/205552s017lbl.pdf).
7. Masso-Valles, D., et al., *Ibrutinib exerts potent antifibrotic and antitumor activities in mouse models of pancreatic adenocarcinoma*. Cancer Res, 2015. 75(8): p. 1675-81.
8. Rauf, F., et al., *Ibrutinib inhibition of ERBB4 reduces cell growth in a WNT5A-dependent manner*. Oncogene, 2018.
9. Sagiv-Barfi, I., et al., *Therapeutic antitumor immunity by checkpoint blockade is enhanced by ibrutinib, an inhibitor of both BTK and ITK*. Proc Natl Acad Sci U S A, 2015. 112(9): p. E966-72.
10. Berglof, A., et al., *Targets for Ibrutinib Beyond B Cell Malignancies*. Scand J Immunol, 2015. 82(3): p. 208-17.
11. Busygina, K., et al., *Oral Bruton tyrosine kinase inhibitors selectively block atherosclerotic plaque-triggered thrombus formation*. Blood, 2018.
12. Honigberg, L.A., et al., *The Bruton tyrosine kinase inhibitor PCI-32765 blocks B-cell activation and is efficacious in models of autoimmune disease and B-cell malignancy*. Proc Natl Acad Sci U S A, 2010. 107(29): p. 13075-80.
13. Wang, X., et al., *Bruton's Tyrosine Kinase Inhibitors Prevent Therapeutic Escape in Breast Cancer Cells*. Mol Cancer Ther, 2016. 15(9): p. 2198-208.
14. Zhang, H., et al., *The BTK Inhibitor Ibrutinib (PCI-32765) Overcomes Paclitaxel Resistance in ABCB1- and ABCG2-Overexpressing Cells and Tumors*. Mol Cancer Ther, 2017. 16(6): p. 1021-1030.
15. Scheers, E., et al., *Absorption, metabolism, and excretion of oral (1)(4)C radiolabeled ibrutinib: an open-label, phase I, single-dose study in healthy men*. Drug Metab Dispos, 2015. 43(2): p. 289-97.
16. Center for Drug valuation and Research of the U.S., Department of Health and Human Services Food and Drug Administration, 203469Orig1s000. 2012; Available from: [http://www.accessdata.fda.gov/drugsatfda\\_docs/nda/2012/203469Orig1s000ClinPharmR.pdf](http://www.accessdata.fda.gov/drugsatfda_docs/nda/2012/203469Orig1s000ClinPharmR.pdf).
17. Novartis Pharmaceuticals Corporation, *Gleevec [prescribing information] 2004*; Available from: [https://www.pharma.us.novartis.com/sites/www.pharma.us.novartis.com/files/gleevec\\_tabs.pdf](https://www.pharma.us.novartis.com/sites/www.pharma.us.novartis.com/files/gleevec_tabs.pdf).
18. Novartis Pharmaceuticals, *Tasigna [package insert]*. 2014; Available from: <https://www.pharma.us.novartis.com/product/pi/pdf/tasigna.pdf>.
19. Li, X., et al., *Characterization of dasatinib and its structural analogs as CYP3A4 mechanism-based inactivators and the proposed bioactivation pathways*. Drug Metab Dispos, 2009. 37(6): p. 1242-50.
20. Abbas, R., et al., *Effect of ketoconazole on the pharmacokinetics of oral bosutinib in healthy subjects*. J Clin Pharmacol, 2011. 51(12): p. 1721-7.
21. Rood, J.J., et al., *Liquid chromatography-tandem mass spectrometric assay for the simultaneous determination of the irreversible BTK inhibitor ibrutinib and its dihydrodiol-metabolite in plasma and its application in mouse pharmacokinetic studies*. J Pharm Biomed Anal, 2016. 118: p. 123-31.
22. Durmus, S., et al., *Oral availability and brain penetration of the B-RAFV600E inhibitor vemurafenib can be enhanced by the P-GLYCOprotein (ABCB1) and breast cancer resistance protein (ABCG2) inhibitor elacridar*. Mol Pharm, 2012. 9(11): p. 3236-45.

23. Schinkel, A.H., et al., *Normal viability and altered pharmacokinetics in mice lacking mdr1-type (drug-transporting) P-glycoproteins*. Proc Natl Acad Sci U S A, 1997. 94(8): p. 4028-33.
24. Jonker, J.W., et al., *The breast cancer resistance protein protects against a major chlorophyll-derived dietary phototoxin and protoporphyria*. Proc Natl Acad Sci U S A, 2002. 99(24): p. 15649-54.
25. Jonker, J.W., et al., *The breast cancer resistance protein BCRP (ABCG2) concentrates drugs and carcinogenic xenotoxins into milk*. Nat Med, 2005. 11(2): p. 127-9.
26. van Waterschoot, R.A., et al., *Absence of both cytochrome P450 3A and P-glycoprotein dramatically increases docetaxel oral bioavailability and risk of intestinal toxicity*. Cancer Res, 2009. 69(23): p. 8996-9002.
27. Dai, H., et al., *Distribution of STI-571 to the brain is limited by P-glycoprotein-mediated efflux*. J Pharmacol Exp Ther, 2003. 304(3): p. 1085-92.
28. Goh, L.B., et al., *Endogenous drug transporters in in vitro and in vivo models for the prediction of drug disposition in man*. Biochem Pharmacol, 2002. 64(11): p. 1569-78.
29. *European Medicines Agency*. available from: [http://www.ema.europa.eu/docs/en\\_GB/document\\_library/EPAR\\_-\\_Product\\_Information/human/003791/WC500177775.pdf](http://www.ema.europa.eu/docs/en_GB/document_library/EPAR_-_Product_Information/human/003791/WC500177775.pdf), 2014.
30. Bernard, S., et al., *Activity of ibrutinib in mantle cell lymphoma patients with central nervous system relapse*. Blood, 2015. 126(14): p. 1695-8.
31. Boudin, L., et al., *Efficacy of ibrutinib as first-line treatment of tumoral Bing-Neel syndrome*. Leuk Lymphoma, 2018: p. 1-3.
32. Lionakis, M.S., et al., *Inhibition of B Cell Receptor Signaling by Ibrutinib in Primary CNS Lymphoma*. Cancer Cell, 2017. 31(6): p. 833-843 e5.
33. Mason, C., et al., *Ibrutinib penetrates the blood brain barrier and shows efficacy in the therapy of Bing Neel syndrome*. Br J Haematol, 2017. 179(2): p. 339-341.
34. Hiemcke-Jiwa, L.S., et al., *Efficacy of ibrutinib in a patient with transformed lymphoplasmacytic lymphoma and central nervous system involvement*. Leuk Lymphoma, 2018. 59(5): p. 1256-1259.
35. Uchida, Y., et al., *Quantitative targeted absolute proteomics of human blood-brain barrier transporters and receptors*. J Neurochem, 2011. 117(2): p. 333-45.
36. Drean, A., et al., *ATP binding cassette (ABC) transporters: expression and clinical value in glioblastoma*. J Neurooncol, 2018. 138(3): p. 479-486.
37. Olarte Carrillo, I., et al., *Clinical significance of the ABCB1 and ABCG2 gene expression levels in acute lymphoblastic leukemia*. Hematology, 2017. 22(5): p. 286-291.
38. Kort, A., et al., *Brain and Testis Accumulation of Regorafenib is Restricted by Breast Cancer Resistance Protein (BCRP/ABCG2) and P-glycoprotein (P-GP/ABCB1)*. Pharm Res, 2015. 32(7): p. 2205-16.
39. Kort, A., et al., *Brain Accumulation of Ponatinib and Its Active Metabolite, N-Desmethyl Ponatinib, Is Limited by P-Glycoprotein (P-GP/ABCB1) and Breast Cancer Resistance Protein (BCRP/ABCG2)*. Mol Pharm, 2017. 14(10): p. 3258-3268.
40. van Herwaarden, A.E., et al., *Knockout of cytochrome P450 3A yields new mouse models for understanding xenobiotic metabolism*. J Clin Invest, 2007. 117(11): p. 3583-92.

## SUPPLEMENTAL MATERIAL

**Supplemental Table 1** - Pharmacokinetic parameters of ibrutinib-DiOH at 8 h and 1 h minutes after oral administration of 10 mg/kg ibrutinib to female WT, Abcb1a/1b<sup>-/-</sup>, Abcg2<sup>-/-</sup> and Abcb1a/1b;Abcg2<sup>-/-</sup> mice.

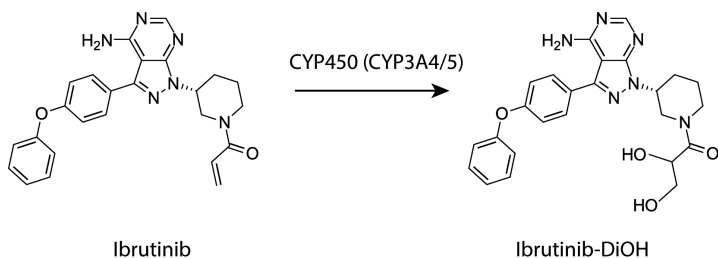
Parameter	Time	Genotype			
		WT	Abcb1a/1b <sup>-/-</sup>	Abcg2 <sup>-/-</sup>	Abcb1a/1b;Abcg2 <sup>-/-</sup>
AUC <sub>0-8</sub> (ng/ml.h)	8 h	3423 ± 213			3427 ± 450
C <sub>max</sub> (ng/ml)		1779 ± 65			2220 ± 146
T <sub>max</sub> (minutes)		21 ± 8			18 ± 7
AUC <sub>0-1</sub> (ng/ml.h)	1 h	992 ± 105	783 ± 86 **	752 ± 73 **	633 ± 92 ****
C <sub>max</sub> (ng/ml)		1422 ± 295	1118 ± 315	1032 ± 205	888 ± 336
T <sub>max</sub> (minutes)		13 ± 3	10 ± 2	12 ± 3	16 ± 8
C <sub>brain</sub> (ng/g)		16.0 ± 4.1	39.7 ± 8.6 **	13.1 ± 2.8 ###	45.1 ± 14.3 ***
Brain to plasma ratio		0.005 ± 0.003	0.063 ± 0.020 ****	0.009 ± 0.004 ****	0.077 ± 0.018 ****
Fold change		1	12.6	1.8	15.4
C <sub>liver</sub> (ng/g)		733 ± 178	660 ± 101	485 ± 40 *	503 ± 137 *
Liver to plasma ratio		1.233 ± 0.168	1.434 ± 0.260	1.106 ± 0.107	1.120 ± 0.150
Fold change		1	1.2	0.9	0.9
Brain to liver ratio		0.022 ± 0.002	0.060 ± 0.011 **** / ###	0.027 ± 0.004 ****	0.089 ± 0.011 ****
Fold change		1	2.7	1.2	4

AUC, area under the plasma concentration-time curve; C<sub>max</sub> maximum ibrutinib-DiOH concentration in plasma; T<sub>max</sub>, the time (min) after drug administration needed to reach maximum plasma concentration; C<sub>brain</sub>, brain concentration; C<sub>liver</sub>, liver concentration. \*, P < 0.05; \*\*, P < 0.01; \*\*\*, P < 0.001; \*\*\*\*, P < 0.0001 compared to WT mice and #, P < 0.05; ##, P < 0.01; ###, P < 0.001 compared to Abcb1a/1b;Abcg2<sup>-/-</sup> mice. Data are given as mean ± SD.

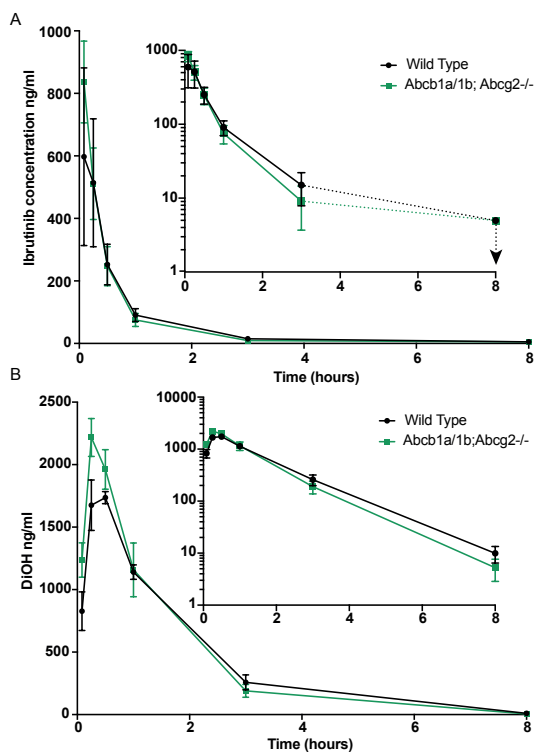
**Supplemental Table 2** - Pharmacokinetic parameters of ibrutinib-DiOH at 8 h, 1 h and 20 minutes after oral administration of 10 mg/kg ibrutinib to female WT, Cyp3a<sup>-/-</sup>, Cyp3aXA, Cyp3aXV and Cyp3aXAV mice.

Parameter	Time	Genotype				
		WT	Cyp3a <sup>-/-</sup>	Cyp3aXA	Cyp3aXV	Cyp3aXAV
AUC <sub>0-8</sub> (ng/ml.h)	8 h	3423 ± 213	229 ± 17 ****			965 ± 436 **** / #
C <sub>max</sub> (ng/ml)		1779 ± 65.2	99.0 ± 44.3			497 ± 160
T <sub>max</sub> (minutes)		21 ± 8	30 ± 0			18 ± 7
AUC <sub>0-1</sub> (ng/ml.h)	1 h	992 ± 105	39.8 ± 7.0 ****			
C <sub>max</sub> (ng/ml)		1422 ± 295	51.8 ± 17.3			
T <sub>max</sub> (minutes)		13 ± 3	38 ± 18			
C <sub>liver</sub> (ng/g)		733 ± 178	68.7 ± 29.6 ****			
Liver to plasma ratio		1.23 ± 0.17	1.63 ± 0.24			
Fold change		1	1.3			
AUC <sub>0-0.33</sub> (ng/ml.h)	20 min	215 ± 81	17.3 ± 2.8 ****	76.4 ± 24.3 ****/####	113 ± 44 ****/####	136 ± 9 ****/####
C <sub>max</sub> (ng/ml)		1086 ± 316	88.8 ± 19.7	379 ± 119	488 ± 189	631 ± 50
T <sub>max</sub> (minutes)		14 ± 3	13 ± 3	11 ± 2	12 ± 3	9 ± 2
C <sub>liver</sub> (ng/g)		5287 ± 2522	244 ± 57 ****	651 ± 235 ****	674 ± 308 ****	729 ± 197 ****
Liver to plasma ratio		4.38 ± 0.65	4.65 ± 0.56	3.05 ± 0.62	2.03 ± 1.48 ***	1.92 ± 0.60 ***
Fold change		1	1.1	0.7	0.5	0.4

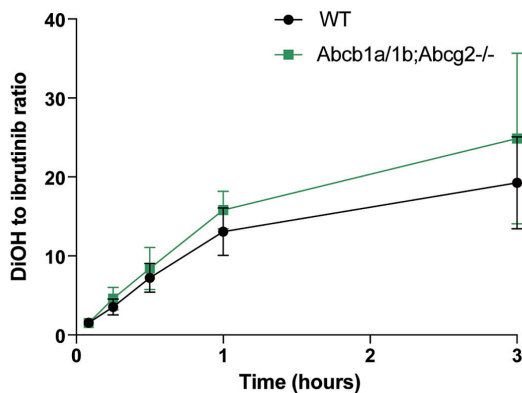
AUC, area under the plasma concentration-time curve; C<sub>max</sub>, maximum DiOH concentration in plasma; T<sub>max</sub>, the time (h) after drug administration needed to reach maximum plasma concentration; C<sub>brain</sub>, brain concentration; C<sub>liver</sub>, liver concentration. \*, P < 0.05; \*\*, P < 0.01; \*\*\*, P < 0.001; \*\*\*\*, P < 0.0001 compared to WT mice and #, P < 0.05; ##, P < 0.01; ###, P < 0.001 compared to Cyp3a<sup>-/-</sup> mice. Data are given as mean ± SD.



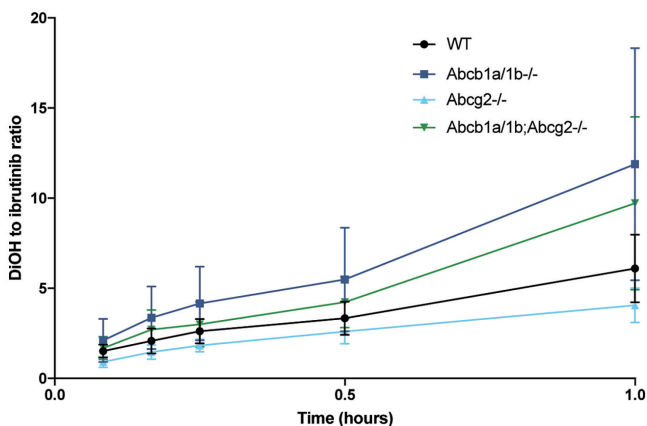
**Supplemental Figure 1** - Schematic representation of the formation of ibrutinib-DiOH from ibrutinib. The main active ibrutinib metabolite, ibrutinib-DiOH (DiOH) is formed by Cytochrome P450 (primarily CYP3A4).



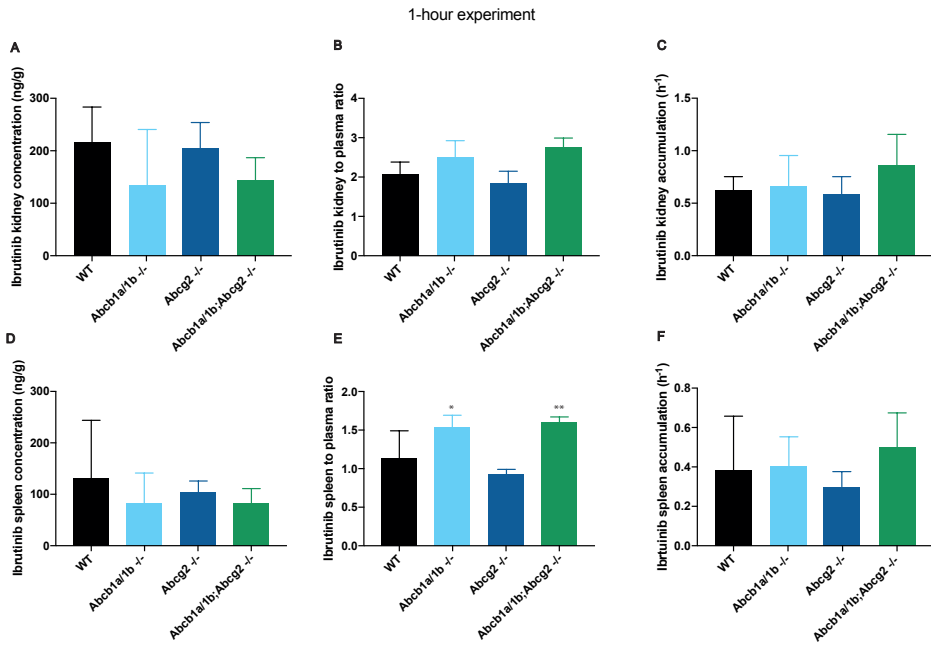
**Supplemental Figure 2** - Plasma concentration–time curves of ibrutinib (A) and ibrutinib-DiOH (DiOH) (B) and in female WT (black circles) and *Abcb1a/1b; Abcg2<sup>-/-</sup>* (green squares) mice over 8 h after oral administration of 10 mg/kg ibrutinib. When the 8 h data were below the lower limit of quantification, data were only plotted up till 3 h. Note the different concentration scales in panels A and B. Data are given as mean  $\pm$  SD. n = 5–6 mice per group.



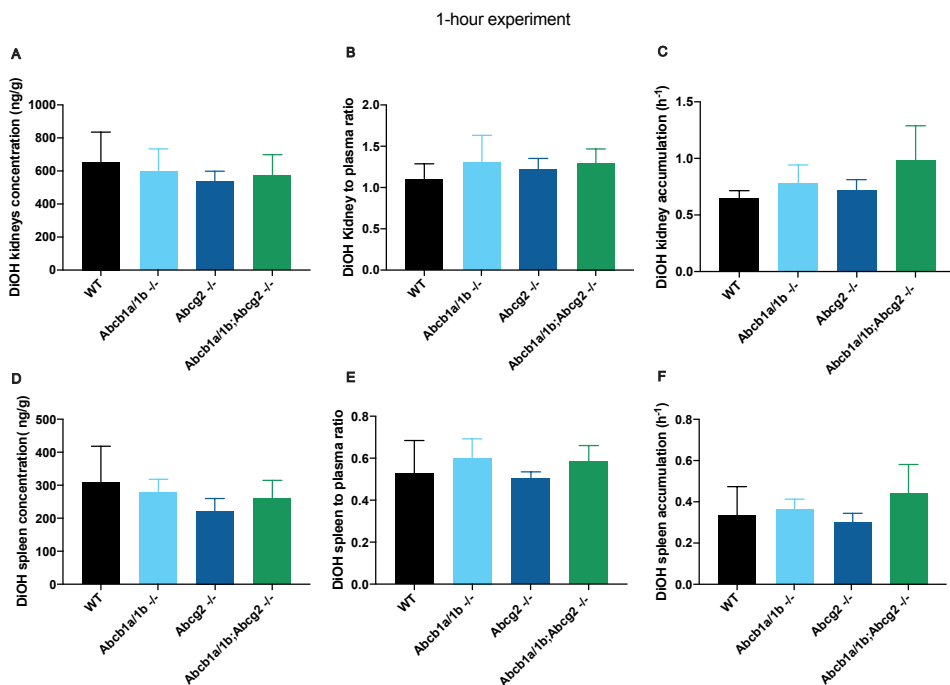
**Supplemental Figure 3** - Ibrutinib-DiOH (DiOH) to ibrutinib concentration ratios in female WT (black circles) and *Abcb1a/1b;Abcg2<sup>-/-</sup>* (green squares) mice over 3 h after oral administration of 10 mg/kg ibrutinib. Data are given as mean  $\pm$  SD. n = 5–6 mice per group.



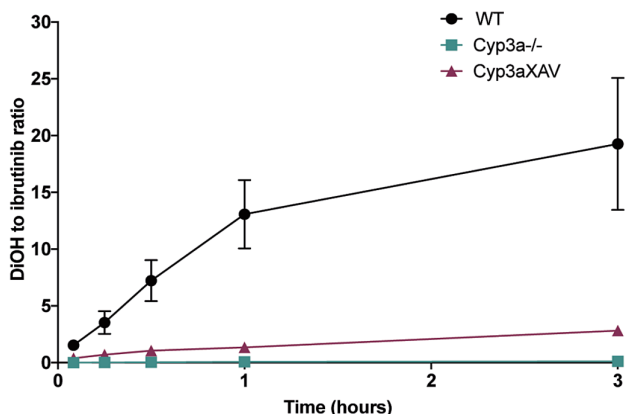
**Supplemental Figure 4** - Ibrutinib-DiOH (DiOH) to ibrutinib concentration ratios in female WT (black circles) and *Abcb1a/1b;Abcg2<sup>-/-</sup>* (green squares) mice over 1 h after oral administration of 10 mg/kg ibrutinib. Data are given as mean  $\pm$  SD. n = 5–6 mice per group.



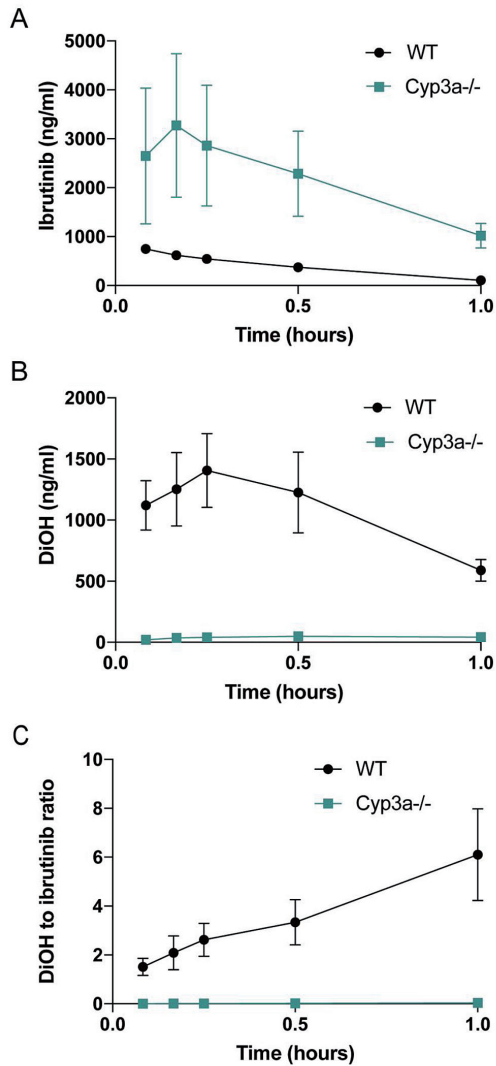
**Supplemental Figure 5** - Kidney and spleen concentration (A, D), tissue-to-plasma ratio (B, E) and relative tissue accumulation (C, F) of ibrutinib in female WT, *Abcb1a/1b*<sup>-/-</sup>, *Abcg2*<sup>-/-</sup> and *Abcb1a/1b;Abcg2*<sup>-/-</sup> mice 1 h after oral administration of 10 mg/kg ibrutinib. \*,  $P < 0.05$ ; \*\*,  $P < 0.01$  compared to WT mice. Data are given as mean  $\pm$  SD.  $n = 5-6$  mice per group.



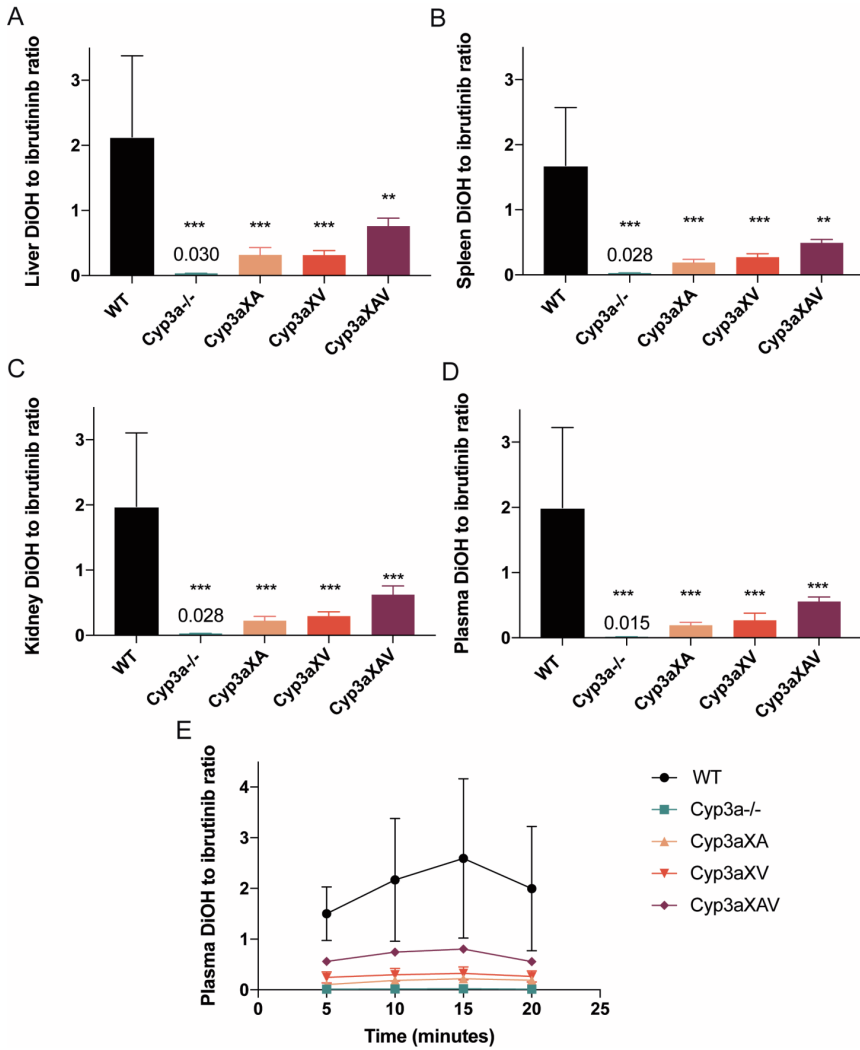
**Supplemental Figure 6** - Kidney and spleen concentration (A, D), tissue-to-plasma ratio (B, E) and relative tissue accumulation (C, F) of ibrutinib-DiOH (DiOH) in female WT, Abcb1a/1b<sup>-/-</sup>, Abcg2<sup>-/-</sup> and Abcb1a/1b;Abcg2<sup>-/-</sup> mice 1 h after oral administration of 10 mg/kg ibrutinib. \*, P < 0.05; \*\*, P < 0.01; \*\*\*, P < 0.001 compared to WT mice. Data are given as mean ± SD. n = 5–6 mice per group.



**Supplemental Figure 7** - Ibrutinib-DiOH (DiOH) to ibrutinib concentration ratio in plasma of female WT (black circles), Cyp3a<sup>-/-</sup> (blue squares) and Cyp3aXAV (purple triangles) mice over 3 h after oral administration of 10 mg/kg ibrutinib. Data are given as mean ± SD. n = 5–6 mice per group.



**Supplemental Figure 8** - Plasma concentration–time curves of ibrutinib (A) and ibrutinib–DiOH (DiOH) (B) and DiOH to ibrutinib concentration ratios (C) in plasma of female WT (black circles) and Cyp3a<sup>-/-</sup> (blue squares) mice over 1 hour after oral administration of 10 mg/kg ibrutinib. Data are given as mean ± SD. n = 5–6 mice per group.



**Supplemental Figure 9** - Ibrutinib-DiOH (DiOH) to ibrutinib concentration ratios in the liver (A), spleen (B), kidney (C) and plasma (D & E) in female WT (black circles), Cyp3a<sup>-/-</sup> (blue squares), Cyp3aXA (peach triangles), Cyp3aXV (red triangles) and Cyp3aXAV (maroon diamonds) mice 20 minutes after oral administration of 10 mg/kg ibrutinib. \*, P < 0.05; \*\*, P < 0.01; \*\*\*, P < 0.001 compared to WT mice. Data are given as mean ± SD. n = 5–6 mice per group.



# 5

---

## Brain accumulation of ponatinib and its active metabolite N-desmethyl ponatinib is limited by P-glycoprotein (P-GP/ABCB1) and breast cancer resistance protein (BCRP/ABCG2)

---

**Stéphanie van Hoppe<sup>a#</sup>, Anita Kort<sup>a,c#</sup>, Rolf W. Sparidans<sup>b</sup>,  
Els Wagenaar<sup>a</sup>, Jos H. Beijnen<sup>b,c,d</sup> and Alfred H. Schinkel<sup>a\*</sup>**

<sup>a</sup> Division of Molecular Oncology, The Netherlands Cancer Institute, Amsterdam

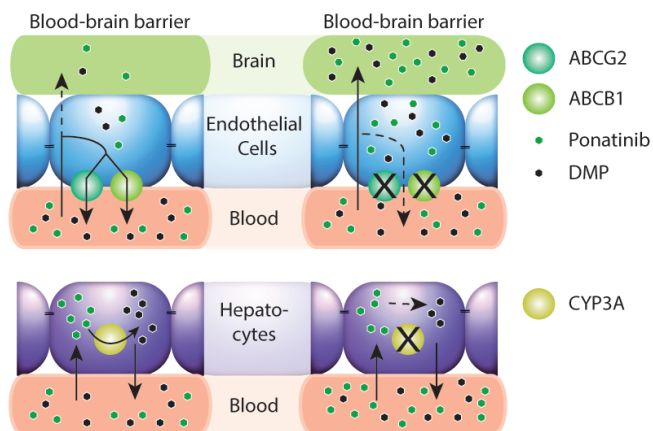
<sup>b</sup> Division of Pharmacoepidemiology & Clinical Pharmacology, Department of Pharmaceutical Sciences, Faculty of Science, Utrecht University, Utrecht,

<sup>c</sup> Department of Pharmacy & Pharmacology, The Netherlands Cancer Institute/  
Slotervaart Hospital, Amsterdam

<sup>d</sup> Department of Clinical Pharmacology, The Netherlands Cancer Institute, Amsterdam

**ABSTRACT**

Ponatinib is an oral BCR-ABL1 inhibitor for treatment of advanced leukemic diseases that carry the Philadelphia chromosome, specifically containing the T315I mutation yielding resistance to previously approved BCR-ABL1 inhibitors. Using *in vitro* transport assays and knockout mouse models, we investigated whether the multidrug efflux transporters ABCB1 and ABCG2 transport ponatinib and whether they, or the drug-metabolizing enzyme CYP3A, affect the oral availability and brain accumulation of ponatinib and its active *N*-desmethyl metabolite (DMP). *In vitro*, mouse *Abcg2* and human *ABCB1* modestly transported ponatinib. In mice, both *Abcb1* and *Abcg2* markedly restricted brain accumulation of ponatinib and DMP, but not ponatinib oral availability. *Abcg2* deficiency increased DMP plasma levels ~3-fold. *Cyp3a* deficiency increased the ponatinib plasma AUC 1.4-fold. Our results suggest that pharmacological inhibition of ABCG2 and ABCB1 during ponatinib therapy might benefit patients with brain (micro-)metastases positioned behind an intact blood-brain barrier, or with substantial expression of these transporters in the malignant cells. CYP3A inhibitors might increase ponatinib oral availability, enhancing efficacy but possibly also toxicity of this drug.



## INTRODUCTION

Ponatinib (Iclusig®, previously AP24524) is a third-generation oral drug for treatment of chronic myeloid leukemia (CML) and Philadelphia chromosome positive (Ph+) acute lymphoblastic leukemia (ALL) [1, 2]. It was initially FDA approved in December 2012 and after a temporary suspension due to life-threatening risks, it was re-approved in December 2013 [3, 4]. Ponatinib is a tyrosine kinase inhibitor (TKI) designed to bind and inhibit BCR-ABL1 and especially its most prominent mutant form, T315I, which confers resistance to other tyrosine kinase inhibitors such as dasatinib, imatinib, nilotinib and bosutinib [5]. Ponatinib also inhibits some other kinases important for the pathogenesis of other malignancies such as vascular endothelial growth factor receptors (VEGFR 1 and 2), platelet-derived growth factor receptor (PDGFR), fibroblast growth factor receptors 1-4 (FGFR1-4), RET, c-KIT, MEKK2, FLT3, RIPK1 and RIPK3 [5-11]. This makes ponatinib a promising and interesting therapeutic drug.

The plasma protein binding of ponatinib is high (99.9%) and its half-life ( $t_{1/2}$ ) is about 24 h in humans [1]. The drug is mainly excreted via feces after phase I and II biotransformation. In humans CYP3A4 is the predominant P450 isoenzyme involved in the microsomal biotransformation of TKIs such as imatinib, nilotinib, bosutinib, dasatinib and also ponatinib [1, 12-15]. The main ponatinib metabolite, however, is the inactive carboxylic acid AP24600, formed by esterase- and/or amidase-mediated hydrolysis [1, 16]. The pharmacodynamically active *N*-desmethyl (DMP, AP24567) and (minor) *N*-oxide (AP24734) metabolites are additionally formed by Cytochrome P450 (mainly CYP3A4)-mediated biotransformation, as schematically shown in Supplementary Figure 1 [1, 17, , 18]. DMP has a 4-fold reduced potency compared to ponatinib [2], and its abundance in patients appears to be modest, with 8.3% of the ponatinib dose retrieved as DMP from feces [18].

Multidrug efflux transporters of the ATP-binding cassette (ABC) protein family affect the disposition of a wide variety of endogenous and exogenous compounds, including numerous anticancer drugs. ABCB1 (P-glycoprotein) and ABCG2 (BCRP) are expressed in the apical membrane of epithelia in a number of organs which are essential for absorption and elimination of drugs like liver, small intestine and kidney. They are also found in luminal membranes of barriers protecting sanctuary tissues like the blood-placenta, blood-testis and blood-brain barriers (BBB). At these barriers ABCB1 and ABCG2 substrates are immediately pumped out of the epithelial or endothelial cells back into the blood. As a consequence, only small amounts of drug can accumulate in, for instance, the brain. This can compromise treatment of (micro-)metastases that are present behind a functionally intact BBB [19-21]. Many anticancer drugs including TKIs are transported substrates of ABCG2 or ABCB1 or both. As a result, these transporters

can significantly modulate the pharmacokinetic behavior, and hence the therapeutic efficacy and toxicity profile of these drugs [22].

Some studies indicated that ponatinib could modestly interact with hABCB1 and more profoundly with hABCG2 *in vitro*, resulting in inhibition of these transporters, and possibly transport by hABCG2 [23]. However, another study found that ponatinib was not noticeably transported by ABCB1 or ABCG2 in CML cells [24]. If these transporters could efficiently transport ponatinib *in vivo*, this might lead to decreased accumulation of ponatinib in transporter-expressing cancer cells, and thus pharmacotherapeutic resistance. Moreover, leukemic cells can spread outside the blood to other parts of the body, including the central nervous system (brain and spinal cord). About 7% of adult ALL patients have central nervous system (CNS) involvement at presentation [25, 26]. Given the high ABCB1 and ABCG2 expression in the BBB, these transporters could potentially limit brain accumulation of ponatinib, which might reduce therapeutic efficiency against CML and ALL CNS metastases.

In this study we investigated whether ponatinib and DMP are transported substrates of ABCB1 and ABCG2 *in vitro* or *in vivo*, and how this might affect their oral plasma pharmacokinetics and brain penetration. Furthermore, ponatinib is substantially metabolized by cytochrome P450 (CYP3A4) [1, 27], indicating that induction or inhibition of this enzyme may influence ponatinib exposure. We therefore also studied the influence of CYP3A on the (oral) systemic availability and tissue exposure of ponatinib and DMP.

## MATERIAL AND METHODS

### Chemicals

Ponatinib and zosuquidar were obtained from Sequoia Research Products (Pangbourne, UK). Ko143 was obtained from Tocris Bioscience (Bristol, UK). Isoflurane was purchased from Pharmachemie BV (Haarlem, The Netherlands), heparin (5000 IU ml<sup>-1</sup>) was from Leo Pharma (Breda, The Netherlands), and Bovine Serum Albumin (BSA) Fraction V from Roche (Mannheim, Germany). Chemicals and reference standards used for the bioanalytical assay of ponatinib and its metabolite DMP were described previously [28]. All other chemicals and reagents were obtained from Sigma-Aldrich (Steinheim, Germany).

### Transport assays

Polarized Madin-Darby Canine Kidney (MDCK-II) cell lines transduced with either human (h)ABCB1, murine (m)Abcg2 or hABCG2 cDNA were cultured in DMEM plus 10% FCS and

100 U/ml penicillin, 100 µg/ml streptomycin (complete medium), and used as described previously [29]. Transepithelial transport assays were performed in complete medium, but without antibiotics, in triplicate on 12-well microporous polycarbonate membrane filters (3.0-µm pore size, Transwell 3402, Corning Inc., Lowell, MA) as previously described [29]. In short, cells were allowed to grow an intact monolayer in 3 days, which was monitored with transepithelial electrical resistance (TEER) measurements. On the third day, cells were pre-incubated with the relevant inhibitors for 1 hour, where 5 µM zosuquidar (ABCB1 inhibitor) and/or 5 µM Ko143 (ABCG2/Abcg2 inhibitor) were added to both apical and basolateral compartments. To inhibit endogenous canine ABCB1 in the MDCK-II Abcg2 and MDCK-II ABCG2 cell lines, we added 5 µM zosuquidar (ABCB1 inhibitor) to the culture medium throughout the experiment. The experiment was initiated by replacing the incubation medium from the donor compartment with freshly prepared medium containing 5 µM ponatinib alone or in combination with the appropriate inhibitors. At 4 and 8 hours, 50 µl samples were collected from the acceptor compartment and stored at -30°C until analysis. TEER was re-checked at the end of the transport experiment to confirm continuing intactness of the monolayer. The amount of transported drug was calculated after correction for volume loss due to sampling at each time point. Active transport was expressed by the transport ratio (*r*), which is defined as the amount of apically directed transport divided by the amount of basolaterally directed transport at a defined time point. Continual testing of transport of a range of other drugs (such as ceritinib and afatinib) and other compounds confirmed proper activity of hABCB1, mAbcg2 and hABCG2 in the MDCKII cell lines used.

## Animals

Female wild-type, Abcb1a/1b<sup>-/-</sup> [30], Abcg2<sup>-/-</sup> [31], Abcb1a/1b;Abcg2<sup>-/-</sup> [32] and Cyp3a<sup>-/-</sup> mice [33], all of a >99% FVB genetic background, were used. Mice between 9 and 14 weeks of age were used in groups of 3-5 mice per strain. The mice were kept in a temperature-controlled environment with a 12 h light/dark cycle and received a standard diet (AM-II, Hope Farms, Woerden, The Netherlands) and acidified water *ad libitum*. Animals were housed and handled according to institutional guidelines in compliance with Dutch and EU legislation.

## Drug solutions

Ponatinib stock solution was prepared in DMSO at 20 mg/ml and stock aliquots were frozen at -80°C. All working solutions were prepared freshly on the day of the experiment by allowing an aliquot to thaw and subsequent dilution of the aliquot 20-fold in 25 mM sodium citrate buffer in water (pH 2.75) resulting in a 1 mg/ml solution. This solution was immediately protected from light and vigorously shaken for 1 minute to obtain a

homogeneous and clear solution. Ponatinib was administered orally at a dose of 10 mg/kg (10  $\mu$ l/g).

### **Plasma and tissue pharmacokinetics of ponatinib**

To minimize variation in absorption, mice were fasted for two hours prior to oral administration of ponatinib, using a blunt-ended needle. Fifty  $\mu$ l blood samples were drawn from the tail vein using heparin-coated capillaries (Sarstedt, Germany). At the last time point mice were anesthetized using isoflurane inhalation and blood was collected via cardiac puncture. For the 24-hour experiment, tail vein sampling took place at 0.5, 1, 2, 4 and 8 h after oral administration. For the 2-hour experiment, tail vein sampling took place at 0.25, 0.5 and 1 h after oral administration. At 24 or 2 h, respectively, mice were sacrificed by cervical dislocation and a set of organs was rapidly removed, weighed and subsequently frozen as whole organ at  $-30^{\circ}\text{C}$ . Prior to analysis, organs were allowed to thaw and homogenized in appropriate volumes of 4% (w/v) BSA in water using a FastPrep<sup>®</sup>-24 device (MP Biomedicals, SA, California, USA). Homogenates were stored at  $-30^{\circ}\text{C}$ . Blood samples were immediately centrifuged at 2,100 g for 6 min at  $4^{\circ}\text{C}$ , and plasma was collected and stored at  $-30^{\circ}\text{C}$  until analysis. Ponatinib concentrations in brain tissue were corrected for the presence of plasma in the vascular space (1.4%) [34].

### **Drug analysis**

Ponatinib and N-desmethyl ponatinib (DMP) concentrations in culture medium, plasma and tissue homogenates were analyzed with a previously reported liquid-chromatography tandem mass spectrometric (LC-MS/MS) assay, using deuterated internal standards [28]. Briefly, plasma and tissue homogenate samples were pre-treated using liquid-liquid extraction with *tert*-butylmethylether, evaporated and reconstituted before separation by reversed-phase liquid chromatography under alkaline conditions. The calibration curves of the linear assay ranged from 5-5,000 ng/ml for ponatinib and 1-1,000 ng/ml for DMP. Culture medium samples were pre-treated using protein precipitation with acetonitrile and diluted before chromatographic injection. Ponatinib was quantified in the range 5-5,000 ng/ml.

### **Statistics and pharmacokinetic calculations**

The unpaired two-tailed Student's t-test was used to determine significance in the transepithelial transport assays. The area under the curve (AUC) of the plasma concentration-time curve was calculated using the trapezoidal rule, without extrapolating to infinity. Individual concentration-time data were used to determine the peak plasma concentration ( $C_{\text{max}}$ ) and the time to reach  $C_{\text{max}}$  ( $T_{\text{max}}$ ). Relative organ accumulation (Porgan) was calculated by dividing organ concentrations (Corgan) at

either  $t = 2$  h or  $t = 24$  h by the area under the plasma concentration-time curve from 0–2 h (AUC<sub>0-2h</sub>) or 0-24 h (AUC<sub>0-24h</sub>), respectively. Ordinary one-way analysis of variance (ANOVA) was used to determine significant differences between groups. Post-hoc Tukey's multiple comparisons were used to compare significant differences between individual groups. When variances were not homogeneously distributed, data were log-transformed before applying statistical tests. Differences were considered statistically significant when  $P < 0.05$ . Data are presented as mean  $\pm$  SD with each experimental group containing 3-5 mice.

## RESULTS

### **Ponatinib is moderately transported by hABCB1 and mAbcg2 in vitro**

We analyzed ponatinib (5  $\mu$ M) transport across polarized monolayers of MDCKII cell lines stably transduced with hABCB1, mAbcg2, or hABCG2 cDNAs. The parental MDCKII cell line did not show apically directed transport (Figure 1A,  $r = 0.8$ ) and addition of the potent ABCB1 inhibitor zosuquidar did not change this result (Figure 1B,  $r = 1.0$ ). This indicates that endogenously present canine ABCB1 did not noticeably transport ponatinib in the parental cells. In the hABCB1 subclone, however, we observed modest apically directed transport of ponatinib (Figure 1C,  $r = 1.8$ ), which was effectively inhibited by addition of zosuquidar (Figure 1D,  $r = 0.9$ ). In MDCKII cells overexpressing mAbcg2 and hABCG2, we performed the transport assay in the presence of zosuquidar to exclude any transport contribution of endogenous canine ABCB1. We observed clear apically directed transport of ponatinib in mAbcg2 cells ( $r = 2.3$ ), which was largely inhibited by the ABCG2 inhibitor Ko143 (Figure 1E and F). This indicates that ponatinib was moderately transported by mAbcg2. In the hABCG2 subclone we did not detect active transport of ponatinib and addition of Ko143 did not alter this profile (respective  $r = 0.9$  and  $1.0$ , Figure 1G and H). However, we note that the MDCKII-hABCG2 cell line consistently yields (much) lower transport rates for many drugs compared to the MDCKII-mAbcg2 line, which may relate to difficulty in expressing a high amount of hABCG2 in these cells [35, 36]. These data demonstrate that ponatinib is moderately transported by hABCB1 and mAbcg2. Therefore, both transporters might play a role in the oral availability and brain penetration of ponatinib.

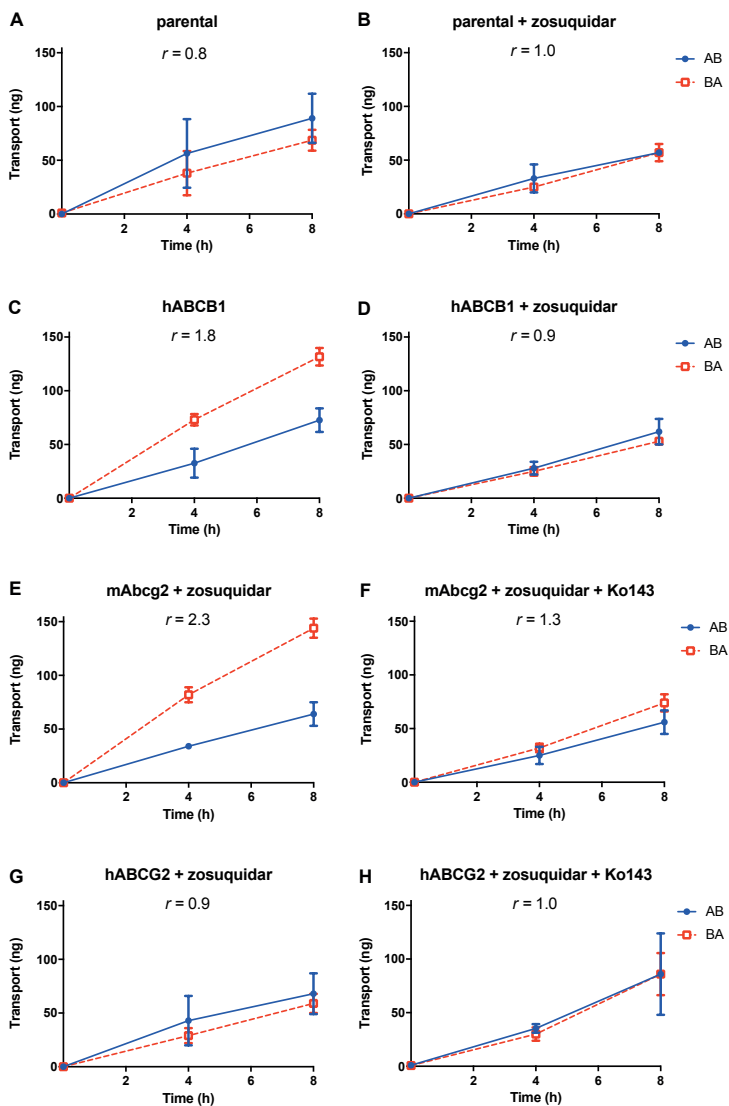


**Figure 1** - *In vitro* transport of ponatinib. Transepithelial transport of ponatinib (5  $\mu$ M) was assessed in MDCK-II cells either non-transduced (A, B) or transduced with hABCB1 (C, D), mAbcg2 (E, F), or hABCG2 (G, H) cDNA. At t = 0 h ponatinib was added to the donor compartment; thereafter at t = 4 and 8 h the concentrations were measured and plotted as total amount (ng) of transport (n = 3). B, D-H: Zosuquidar (5  $\mu$ M) or Ko143 (5  $\mu$ M) were added as indicated to inhibit hABCB1 or hABCG2 and mAbcg2, respectively. r, relative transport ratio. BA (red squares, dashed line) translocation from the basolateral to the apical compartment; AB (blue circles), translocation from the apical to the basolateral compartment. Data are presented as mean  $\pm$  SD. The curves were forced through the origin, assuming 0 transport at t = 0.

## Availability of oral ponatinib is restricted by Cyp3a, but not by mAbcg2 or mAbcb1a/1b

Ponatinib is given orally to patients. We therefore investigated the single and combined effect of mAbcg2 and mAbcb1a/1b deficiency on ponatinib (10 mg/kg) oral availability and tissue disposition over 24 h in wild-type (WT), *Abcg2*<sup>-/-</sup>, *Abcb1a/1b*<sup>-/-</sup> and *Abcb1a/1b;Abcg2*<sup>-/-</sup> mice (Figure 2A). We further investigated the impact of CYP3A-mediated metabolism on ponatinib kinetics using *Cyp3a*<sup>-/-</sup> mice, as the active ponatinib metabolite DMP is primarily formed by CYP3A4 [1, 16]. Neither single nor combined absence of *Abcg2* and/or *Abcb1a/1b* resulted in a significant change in the oral availability of ponatinib during the first 24 h after oral intake (Figure 2A, Table 1). Absence of *Cyp3a*, however, did result in a significant 1.4-fold increase in plasma AUC<sub>0-24</sub> relative to wild-type mice ( $P = 0.0026$ ), and *Abcb1a/1b*<sup>-/-</sup>;*Abcg2*<sup>-/-</sup> mice ( $P = 0.0168$ ) (Figure 2A, Table 1).

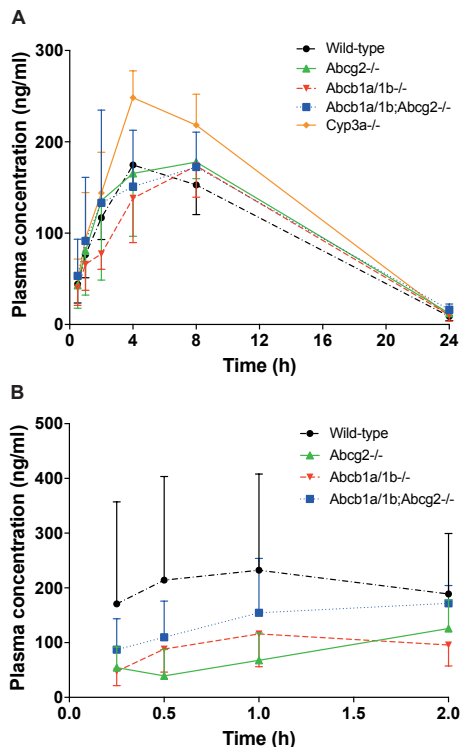


**Figure 2** - Plasma concentration-time curves of ponatinib in female WT (black circles), *Abcg2*<sup>-/-</sup> (green triangles), *Abcb1a/1b*<sup>-/-</sup> (red triangles), *Abcg2;Abcb1a/1b*<sup>-/-</sup> (blue squares) and *Cyp3a*<sup>-/-</sup> mice (yellow diamonds) over 24 hours (A) or 2 hours (B) after oral administration of 10 mg/kg ponatinib. Data are given as mean  $\pm$  SD (SD rendered one-sided for improved clarity).  $n = 4-5$  mice per group.

**Table 1** - Pharmacokinetic parameters of ponatinib and DMP at 24 h after oral administration of 10 mg/kg ponatinib to female wild-type, Abcg2<sup>-/-</sup>, Abcb1a/1b<sup>-/-</sup>, Abcb1a/1b/Abcg2<sup>-/-</sup> and Cyp3a<sup>-/-</sup> mice.

Parameter	Compound	Genotype				
		Wild-type	Abcg2 <sup>-/-</sup>	Abcb1a/1b <sup>-/-</sup>	Abcb1a/1b/Abcg2 <sup>-/-</sup>	Cyp3a <sup>-/-</sup>
Plasma AUC <sub>(0-24)<sup>h</sup></sub> ng/ml	Ponatinib	2378 ± 293	2660 ± 383	2421 ± 395	2602 ± 188	3312 ± 486**
Fold increase AUC <sub>(0-24)</sub>		1.0	1.1	1.0	1.1	1.4
C <sub>max</sub> ng/mL		181 ± 26	201 ± 42	138 ± 49	210 ± 56	251 ± 69
T <sub>max</sub> h		4-8	2-8	4-8	2-8	4-8
C <sub>brain</sub> ng/g		22 ± 8	49 ± 7**	42 ± 19*	558 ± 109***	21 ± 4
Fold increase C <sub>brain</sub>		1.0	2.2	1.9	25.5	1.0
P <sub>brain</sub> (*10 <sup>3</sup> h <sup>-1</sup> )		9.0 ± 2.5	19 ± 2.9**	17 ± 6.6*	215 ± 46***	6.9 ± 1.3
Fold increase P <sub>brain</sub>		1.0	2.2	1.9	24	0.8
Plasma AUC <sub>(0-24)<sup>h</sup></sub> ng/mL	DMP	139 ± 15	445 ± 116***	199 ± 31	544 ± 85***	163 ± 44
Fold increase AUC <sub>(0-24)</sub>		1.0	3.2	1.4	3.9	1.2
C <sub>max</sub> ng/mL		11 ± 1.0	32 ± 7.4	13 ± 5.7	37 ± 6.8	13 ± 5.5
T <sub>max</sub> h		4-8	4-8	4-8	4-8	4-8
C <sub>brain</sub> ng/g		6.1 ± 2.8	13 ± 3.5**	10 ± 2.7	354 ± 26***	6.3 ± 1.6
Fold increase C <sub>brain</sub>		1.0	2.1	1.6	58	1.0
P <sub>brain</sub> (*10 <sup>3</sup> h <sup>-1</sup> )		43 ± 18	29 ± 6.6*	51 ± 10	659 ± 83***	44 ± 5.8
Fold increase P <sub>brain</sub>		1.0	0.7	1.2	15	1.0

AUC, area under the plasma concentration-time curve; C<sub>max</sub>, maximum concentration in plasma; T<sub>max</sub>, the time after drug administration needed to reach maximum plasma concentration; C<sub>brain</sub>, brain concentration; P<sub>brain</sub>, brain accumulation (C<sub>brain</sub> divided by plasma AUC); C<sub>liver</sub>, liver concentration; P<sub>liver</sub>, liver accumulation (C<sub>liver</sub> divided by plasma AUC); \*, P < 0.05; \*\*, P < 0.01; \*\*\*, P < 0.001 compared to WT mice. Data are given as mean ± SD. All groups consisted of n = 4-5 mice.

**Table 2** - Pharmacokinetic parameters of ponatinib and DMP at 2 h after oral administration of 10 mg/kg ponatinib to female wild-type, *Abcg2*<sup>-/-</sup>, *Abcb1a/1b*<sup>-/-</sup>, and *Abcb1a/1b;Abcg2*<sup>-/-</sup> mice.

Parameter	Compound	Genotype			
		Wild-type	<i>Abcg2</i> <sup>-/-</sup>	<i>Abcb1a/1b</i> <sup>-/-</sup>	<i>Abcb1a/1b;Abcg2</i> <sup>-/-</sup>
Plasma AUC <sub>(0-2)'</sub> h.ng/mL	Ponatinib	392 ± 303	142 ± 66	180 ± 85	265 ± 155
Fold increase AUC <sub>(0-2)</sub>		1.0	0.4	0.5	0.7
C <sub>brain</sub> , ng/g		258 ± 195	142 ± 63	247 ± 163	2896 ± 588***
Fold increase C <sub>brain</sub>		1.0	0.5	1.0	11
P <sub>brain</sub> (h <sup>-1</sup> )		0.68 ± 0.01	1.05 ± 0.28	1.28 ± 0.29**	12.3 ± 2.7***
Fold increase P <sub>brain</sub>		1.0	1.5	1.9	18
Plasma AUC <sub>(0-2)'</sub> h.ng/mL	DMP	21 ± 11	13 ± 7	20 ± 11	39 ± 22
Fold increase AUC <sub>(0-2)</sub>		1.0	0.6	0.9	1.9
C <sub>brain</sub> , ng/g		7.2 ± 2.0	2.7 ± 0.5*	5.3 ± 3.3	55 ± 17***
Fold increase C <sub>brain</sub>		1.0	0.4	0.7	7.6
P <sub>brain</sub> (h <sup>-1</sup> )		0.39 ± 0.15	0.23 ± 0.83	0.27 ± 0.58	1.51 ± 0.31***
Fold increase P <sub>brain</sub>		1.0	0.6	0.7	3.9

AUC, area under the plasma concentration-time curve; C<sub>max</sub>, maximum concentration in plasma; T<sub>max</sub>, the time after drug administration needed to reach maximum plasma concentration; C<sub>brain'</sub>, brain concentration; P<sub>brain'</sub>, brain accumulation (C<sub>brain'</sub> divided by plasma AUC); C<sub>liver'</sub>, liver concentration; P<sub>liver'</sub>, liver accumulation (C<sub>liver'</sub> divided by plasma AUC). \*, P < 0.05; \*\*, P < 0.01; \*\*\*, P < 0.001 compared to WT mice. Data are given as mean ± SD. All groups consisted of n = 3-5 mice

For the transporter knockout mice, qualitatively similar results were obtained in an independent experiment where mice were sacrificed 2 h after oral administration of 10 mg/kg ponatinib (Figure 2B, Table 2). There were no significant differences in plasma ponatinib levels between the mouse strains, although it is worth noting that there was high interindividual variation during the first 2 to 4 h after administration in all mouse strains (see also Figure 2A), possibly due to variable rates of stomach emptying for this drug. Collectively, our data indicate that neither *Abcg2* nor *Abcb1a/1b* has a direct impact on the oral availability of ponatinib in mice, but that *Cyp3a* does limit ponatinib oral availability.

### ***Abcg2* and *Abcb1a/1b*, but not *Cyp3a*, limit ponatinib brain accumulation in mice**

To investigate the impact of single and combined knockout of *Abcg2* and *Abcb1a/1b* on ponatinib accumulation in the brain, we isolated mouse brains after termination of the 24-h and 2-h pharmacokinetic experiments. Figure 3A shows that only a low concentration of ponatinib accumulated in the brain of WT mice over 24 h after administration. Single absence of either *Abcg2* or *Abcb1a/1b* resulted in a modestly

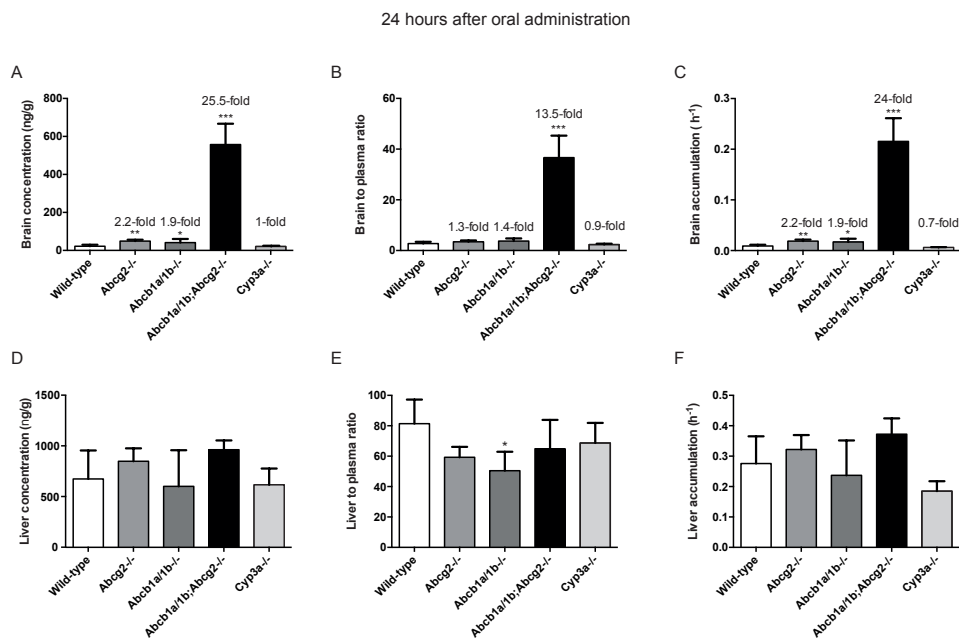


**Figure 3** - Brain and liver concentration (A, D), tissue-to-plasma ratio (B, E) and relative tissue accumulation (C, F) of ponatinib in female WT, *Abcg2*<sup>-/-</sup>, *Abcb1a/1b*<sup>-/-</sup> and *Abcg2*;*Abcb1a/1b*<sup>-/-</sup> mice 24 h after oral administration of 10 mg/kg ponatinib. \*,  $P < 0.05$ ; \*\*,  $P < 0.01$ ; \*\*\*,  $P < 0.001$  compared to WT mice. Data are given as mean  $\pm$  SD.  $n = 4$ -5 mice per group.

increased brain concentration, respectively 2.2-fold ( $P = 0.008$ ) and 1.9-fold ( $P = 0.01$ ) relative to WT mice. However, when both ABC transporters were absent, ponatinib brain concentration was increased by a drastic 25.5-fold compared to WT brain (Figure 3A,  $P < 0.0001$ ). Correcting for differences in plasma concentration, the brain-to-plasma ratio of *Abcb1a/1b*;*Abcg2*<sup>-/-</sup> mice remained markedly higher compared to wild-type mice, while the single ABC transporter knockouts were also still somewhat higher, albeit not significantly (Figure 3B). Correcting for the plasma AUC, the brain accumulation of ponatinib 24 h after oral intake was again clearly and significantly increased by 24-fold in *Abcb1a/1b*<sup>-/-</sup>;*Abcg2*<sup>-/-</sup> mice, and by 2.2- and 1.9-fold in the single *Abcg2*<sup>-/-</sup> and *Abcb1a/1b*<sup>-/-</sup> mice (Figure 3C). These data indicate that ponatinib is kept out of the brain by both *Abcb1a/1b* and *Abcg2*, and that these proteins are able to largely take over each other's transport function at the BBB. Only when both transporters were absent, ponatinib accumulated very substantially in the brain. At the same time, we observed no substantial impact of *Abcg2* and *Abcb1a/1b* on the liver distribution of ponatinib (Figure 3D-F), illustrating the specific function of these transporters in the BBB.

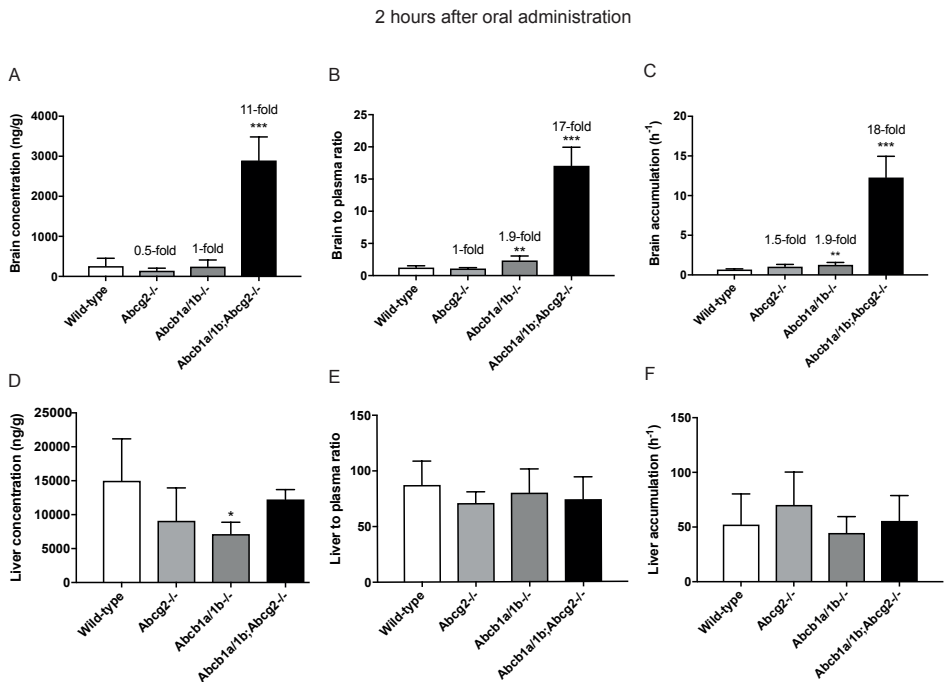


**Figure 4** - Brain and liver concentration (A, D), tissue-to-plasma ratio (B, E) and relative tissue accumulation (C, F) of ponatinib in female WT, *Abcg2*<sup>-/-</sup>, *Abcb1a/1b*<sup>-/-</sup> and *Abcg2*;*Abcb1a/1b*<sup>-/-</sup> mice 2 h after oral administration of 10 mg/kg ponatinib. \*,  $P < 0.05$ ; \*\*,  $P < 0.01$ ; \*\*\*,  $P < 0.001$  compared to WT mice. Data are given as mean  $\pm$  SD.  $n = 3$ -5 mice per group.

Although the *Cyp3a* deficiency resulted in a modest increase in the ponatinib plasma AUC (Figure 2A, Table 1), the plasma concentration at 24 h was not significantly different from that in WT mice. The brain concentration and accumulation were also not significantly altered in *Cyp3a*<sup>-/-</sup> mice (Figure 3A-C). The same applied to the liver concentration and accumulation (Figure 3D-F). Collectively, these data suggest that *Cyp3a* did not impact brain (or liver) accumulation of ponatinib independent of its effect on the plasma concentration.

In general, the impact of transporter proteins on tissue accumulation of drugs is especially relevant when plasma concentrations are high. Mice were therefore also sacrificed 2 h after oral administration of 10 mg/kg ponatinib. Similar to the 24 h experiment, the brain concentration of ponatinib in *Abcb1a/1b*;*Abcg2*<sup>-/-</sup> mice showed a highly significant 11-fold increase ( $P < 0.001$ ) compared to WT mice. No significant differences were found for the single knockout strains compared to WT mice (Figure 4A, Table 2). Correcting the ponatinib brain concentrations for the corresponding plasma AUCs (Figure 4C) showed a more pronounced difference of the single knockout

strains compared to WT mice, especially for *Abcb1a/1b*<sup>-/-</sup> mice with a significant 1.9-fold increase. However, combined transporter deficiency resulted in an 18-fold increase in brain accumulation (Figure 4C). Thus, also at 2 h, both *Abcg2* and *Abcb1a/1b* alone could still quite effectively restrict the brain accumulation of ponatinib, so that only the combination transporter knockout demonstrated a highly increased brain penetration of ponatinib. Similar to the 24 h experiment, we observed no substantial impact of *Abcb1a/1b* and/or *Abcg2* deficiency on the liver distribution of ponatinib (Figure 4D-F). Accordingly, plotting of the brain-to-liver ratios of ponatinib at both 2 and 24 h resulted in qualitatively similar results, indicating a strong effect of the combination knockout on relative brain accumulation of ponatinib (Supplementary Figure 2).

### **The effect of Cyp3a and Abcg2 and Abcb1a/1b on N-desmethyl ponatinib disposition and brain accumulation**

The ponatinib metabolite DMP is pharmacodynamically active, and can thus contribute to ponatinib treatment response. We therefore tested to what extent DMP pharmacokinetics was affected by Cyp3a and/or ABC transporter deficiency in mice. Conversion of ponatinib to DMP in humans is thought to be mediated primarily by CYP3A [1]. Indeed, the plasma AUC of ponatinib was modestly (1.4-fold) increased in *Cyp3a*<sup>-/-</sup> mice (Figure 2A, Table 1), but the plasma concentrations or AUC<sub>0-24</sub> of DMP were not significantly decreased in *Cyp3a*<sup>-/-</sup> mice (Figure 5A, Table 1). However, the plasma DMP/ponatinib ratio was decreased, albeit not significantly, for most time points up to 8 h in *Cyp3a*<sup>-/-</sup> mice (Figure 5B, inset), which is in line with somewhat reduced (Cyp3a-mediated) formation of DMP in these mice. The brain concentration and accumulation of DMP was not significantly affected by Cyp3a deficiency, and the same applies for DMP liver concentration and accumulation (Table 1, Supplementary Figure 2).

Interestingly, in striking contrast to the plasma levels of parental ponatinib, the plasma levels and AUC<sub>0-24</sub> of DMP were increased by about 3- to 4-fold in both *Abcg2*-deficient strains (Figure 5A and Table 1). This suggests that *Abcg2* is involved in the clearance of DMP from plasma. On the other hand, *Abcb1a/1b* deficiency had no marked effect on DMP plasma levels (Figure 5A, Table 1). We further investigated the impact of single and combined *Abcg2* and *Abcb1a/1b* deficiency on DMP brain levels 24 hours after oral intake of ponatinib. While the brain concentrations and accumulations in the single transporter knockout mice were not markedly different from those in WT mice, in the combined *Abcb1a/1b;Abcg2*<sup>-/-</sup> mice they were highly increased (Table 1, Supplementary Figure 3A-C). Incidentally, the comparatively high DMP liver concentrations, liver-to-plasma ratios, and liver accumulations we observed in both the *Abcg2*-deficient strains (Supplementary Figure 3D-F) could reflect diminished elimination of DMP from the liver at this late (24 h) phase, perhaps by reduced hepatobiliary excretion of DMP. When we

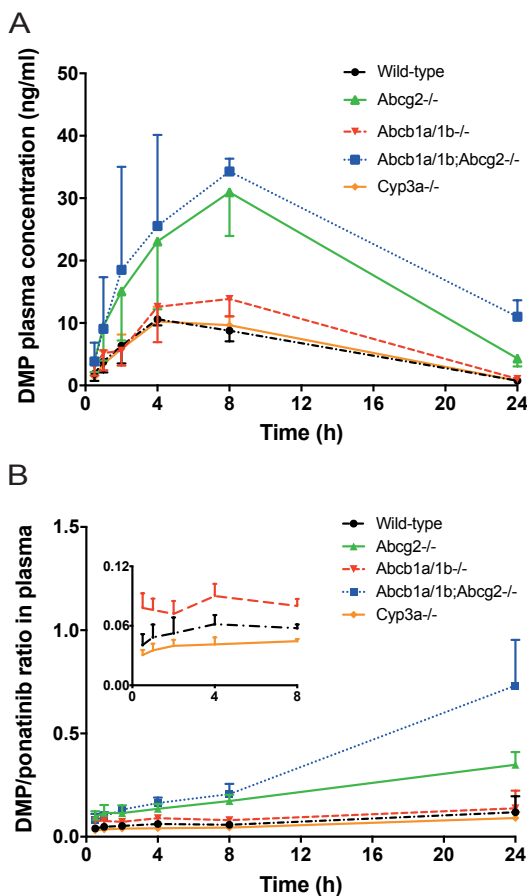


**Figure 5** - Plasma concentration-time curves of DMP in female WT (black circles), Abcg2<sup>-/-</sup> (green triangles), Abcb1a/1b<sup>-/-</sup> (red triangles), and Abcg2;Abcb1a/1b<sup>-/-</sup> mice (blue squares) and Cyp3a<sup>-/-</sup> mice (yellow diamonds) over 24 hours (A) and the DMP:ponatinib plasma concentration ratio (B) after oral administration of 10 mg/kg ponatinib. Data are given as mean  $\pm$  SD (SD rendered one-sided for improved clarity). n = 4-5 mice per group.

looked at brain concentration and accumulation of DMP 2 h after oral administration of ponatinib, we obtained qualitatively similar results as in the 24 h experiment, although the quantitative effects were somewhat less pronounced (Supplementary Figure 4A-C). Overall, these data indicate that both mAbcg2 and mAbcb1a/1b contribute to restricting the brain accumulation of DMP, and can largely take over each other's protective function at the BBB. On the other hand, Abcg2, but not Abcb1a/1b, appears to play a role in the elimination of DMP from plasma.

## DISCUSSION

We found that ponatinib is transported by hABCB1 and mAbcg2 *in vitro*, and that this transport can be inhibited with specific inhibitors. *In vivo*, we did not observe a clear limiting effect of mAbcb1a/1b or Abcg2 on the oral availability of ponatinib in mice. However, the brain accumulation of ponatinib was modestly increased in both single transporter knockout strains, and highly increased in the Abcb1a/1b;Abcg2<sup>-/-</sup> combination knockout strain. No marked differences were observed for ponatinib pharmacokinetics in the liver of the transporter knockout strains. Cyp3a deficiency resulted in a modest (1.4-fold) increase in plasma levels of ponatinib, suggesting increased oral availability of ponatinib. However, no changes were observed in the plasma levels of DMP, one of the active ponatinib metabolites formed by CYP3A in humans. Our data further indicate that DMP is substantially transported *in vivo* by mAbcg2 and mAbcb1a/1b, resulting in markedly (3- to 4-fold) increased plasma levels in both Abcg2-deficient strains, and strongly increased brain accumulation in combination (but not single) transporter knockout mice.

Our *in vitro* transport results are in line with the ATPase experiments of Sen *et al.*, which showed the ability of ponatinib to stimulate hABCG2 and hABCB1 ATPase activity, and indicate that this reflected their ability to transport this drug [23]. Combining all available *in vitro* and *in vivo* data, including from the literature, it seems very likely that mAbcb1a/1b, mAbcg2, hABCB1, and probably also hABCG2, can transport ponatinib. However, it is possible that substantial expression of hABCG2 is needed in order to readily detect ponatinib transport. Expression of ABCG2 and ABCB1 has been associated with resistance to chemotherapy for a range of different drugs in several cancers, including leukemia [37]. Our data suggest that (over)expression of these transporters in cancer cells may also confer ponatinib resistance. This would suggest the possible usefulness of inhibiting these transporters when treating patients with ponatinib in order to reverse such tumor resistance. Moreover, possible drug-drug interactions affecting systemic effects of ABC transporters could also alter treatment efficacy.

Our results for the brain accumulation studies (Figures 3 and 4) clearly show that both mAbcg2 and mAbcb1a/1b can restrict brain accumulation of ponatinib in mice. Whereas single deficiency of Abcg2 or Abcb1a/1b results in only small increases in brain accumulation, the combined deficiency of both transporters causes a disproportionately large rise in brain accumulation. At the same time, ponatinib concentration and accumulation in for instance liver were not markedly altered between the strains (Figures 3 and 4), illustrating the unique behavior of brain in this respect. It appears that the liver primarily reflected the plasma concentration(s) of ponatinib, which suggests relatively easy translocation of this drug across the basolateral (sinusoidal)

membrane of hepatocytes. The disproportionate increase in brain accumulation of ponatinib (and of its metabolite DMP, Supplementary Figures 3 and 4) observed in the *Abcb1a/1b;Abcg2<sup>-/-</sup>* mice compared to single knockout strains was similar to that found for a range of other TKIs (e.g. axitinib, vemurafenib, lapatinib, gefitinib, erlotinib, sunitinib, dasatinib, regorafenib and imatinib [29, 35, 38-43]), and can be explained by relatively straightforward pharmacokinetic models [40, 44]. These models indicate that if two transporters each have a high contribution of efflux transport relative to the background efflux at the BBB in the absence of both transporters, the effect of single transporter ablation on brain accumulation will be far less than the effect of combined ablation. An interesting implication of these models and our findings on ponatinib (and DMP) brain accumulation is that next to *Abcg2* and *Abcb1a/1b*, there can be no other efflux transporters in the BBB that are remotely as efficient in keeping ponatinib and DMP out of the brain.

The increase in treatment options and efficacy for patients with leukemia due to the advent of modern targeted drugs has increased the chance for isolated metastases behind the BBB to emerge, as effective control of peripheral malignancies greatly increases patient survival times. Malignancies in the brain are often hard to reach for drugs because of the presence of ABCB1 and ABCG2 in the continuous physical barrier between blood and brain tissue formed by the BBB. Pharmacological inhibition of these transporters during pharmacotherapy could therefore also improve treatment of metastases positioned in part or in whole behind the BBB. However, it should be noted that studies in mice can only provide qualitative information on the possible impact of these transporters in the blood-brain barrier of patients. In order to better assess the impact of such processes in patients, one can consider appropriate physiologically based pharmacokinetic modeling, or clinical positron-emission tomography (PET) studies with the drug of interest, in combination with highly efficacious ABCB1 and ABCG2 inhibitors, such as for instance elacridar [45-47]. Next to treatment of (metastatic) CML and ALL, a study by Whittle et al. has shown that ponatinib could potentially also be used for neuroblastoma therapy *in vivo* [48]. Also here pharmacological inhibition of the ABC efflux transporters in the BBB might possibly increase the therapeutic efficacy.

Our finding that *Cyp3a* deficiency in mice increases ponatinib oral availability (Figure 2A, Table 1) is in line with a significant role of CYP3A in metabolizing ponatinib. The fact that we did not observe obvious changes in the pharmacokinetics of DMP, one of its CYP3A-generated metabolites, could be explained by the possibility that other mouse enzymes, for instance one or more of the many mouse *Cyp2c* isoforms, might form this metabolite as well [49]. Additionally, it may be possible that CYP3A further metabolizes DMP. In this context it is worth noting that patients receiving ponatinib and the CYP3A inhibitor ketoconazole showed both an increase in plasma ponatinib

levels, and a decrease in DMP levels [27]. The latter effect might indicate that in patients there are no efficient alternative pathways to form DMP from ponatinib, illustrating a difference between mice and man. Nonetheless, all data suggest that altered activity of CYP3A, which commonly occurs in humans, may affect the effective exposure of the body to ponatinib, and thus its therapeutic efficacy and toxicity risks.

Ponatinib is approved for treatment for CML and ALL. However, its use has to be carefully monitored, with revised prescribing information including a black box warning, and the need for risk evaluation and mitigation strategies mainly because of serious cardiovascular risks [50], vascular occlusions and heart failure, but also hepatotoxicity. Ponatinib use therefore remains limited to second-generation drug-resistant and (T3511) mutated patients with Ph+ ALL [51], or as third-line therapy in CML [52]. Since our data indicate that ABC efflux transporters and CYP3A4 could affect the biological availability of ponatinib and its active metabolite DMP at several levels, it will be important to also consider these factors as possible players in unexpected toxicity of ponatinib.

Based on our findings, it is likely that tumors substantially expressing ABCB1 and/or ABCG2 will demonstrate resistance to ponatinib. Thus, inhibiting these transporters with effective dual ABCG2 and ABCB1 inhibitors such as elacridar during ponatinib therapy could potentially improve the tumor response. It may further be possible to increase the ponatinib concentration in the brain of patients with CNS tumors or metastases when ponatinib is coadministered with elacridar. Indeed, a recent case study suggested that ponatinib does not normally effectively enter the CNS [53]. Our results suggest that the oral availability, and hence the risk of toxicity, of ponatinib is not likely to be increased by such an elacridar coadministration treatment. In contrast, the oral availability of ponatinib could potentially be enhanced by coadministration of a CYP3A4 inhibitor, such as ketoconazole. However, caution should be exercised to prevent unexpected toxicity. Collectively, our findings suggest that co-administration of a dual inhibitor of ABCB1 and ABCG2 may increase the exposure to ponatinib and its active metabolite for brain (micro)metastases positioned behind a functionally intact blood-brain barrier, and could thus reduce the chance that patients will ultimately die of such normally poorly tractable lesions.

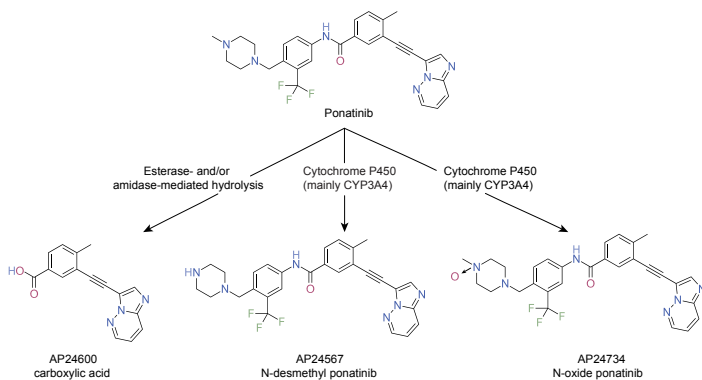
## REFERENCES

1. Center for Drug valuation and Research of the U.S., Department of Health and Human Services Food and Drug Administration, 203469Orig1s000. 2012; Available from: [http://www.accessdata.fda.gov/drugsatfda\\_docs/nda/2012/203469Orig1s000ClinPharmR.pdf](http://www.accessdata.fda.gov/drugsatfda_docs/nda/2012/203469Orig1s000ClinPharmR.pdf).
2. European Medicines Agency, Science Medicines Health, Assessment report Iclusig. 2013; Available from: [http://www.ema.europa.eu/docs/en\\_GB/document\\_library/EPAR\\_-\\_Public\\_assessment\\_report/human/002695/WC500145648.pdf](http://www.ema.europa.eu/docs/en_GB/document_library/EPAR_-_Public_assessment_report/human/002695/WC500145648.pdf).
3. FDA Drug Safety Communication. U.S. Food and Drug Administration, "FDA asks manufacturer of the leukemia drug Iclusig (ponatinib) to suspend marketing and sales". 2013; Available from: <http://www.fda.gov/Drugs/DrugSafety/ucm373040.htm>.
4. FDA Drug Safety Communication. U.S. Food and Drug Administration, "Iclusig (Ponatinib): Drug Safety Communication - Increased Reports Of Serious Blood Clots In Arteries And Veins" 2013; Available from: <http://www.fda.gov/Safety/MedWatch/SafetyInformation/SafetyAlertsforHumanMedicalProducts/ucm370971.htm>.
5. O'Hare, T., et al., AP24534, a pan-BCR-ABL inhibitor for chronic myeloid leukemia, potently inhibits the T315I mutant and overcomes mutation-based resistance. *Cancer Cell*, 2009. 16(5): p. 401-12.
6. Gozgit, J.M., et al., Ponatinib (AP24534), a multitargeted pan-FGFR inhibitor with activity in multiple FGFR-amplified or mutated cancer models. *Mol Cancer Ther*, 2012. 11(3): p. 690-9.
7. Mologni, L., et al., Ponatinib is a potent inhibitor of wild-type and drug-resistant gatekeeper mutant RET kinase. *Mol Cell Endocrinol*, 2013. 377(1-2): p. 1-6.
8. Garner, A.P., et al., Ponatinib inhibits polyclonal drug-resistant KIT oncoproteins and shows therapeutic potential in heavily pretreated gastrointestinal stromal tumor (GIST) patients. *Clin Cancer Res*, 2014. 20(22): p. 5745-55.
9. Ahmad, S., G.L. Johnson, and J.E. Scott, Identification of ponatinib and other known kinase inhibitors with potent MEKK2 inhibitory activity. *Biochem Biophys Res Commun*, 2015. 463(4): p. 888-93.
10. Gozgit, J.M., et al., Potent activity of ponatinib (AP24534) in models of FLT3-driven acute myeloid leukemia and other hematologic malignancies. *Mol Cancer Ther*, 2011. 10(6): p. 1028-35.
11. Fauster, A., et al., A cellular screen identifies ponatinib and pazopanib as inhibitors of necroptosis. *Cell Death Dis*, 2015. 6: p. e1767.
12. Novartis Pharmaceuticals Corporation, Gleevec [prescribing information] 2004; Available from: [https://www.pharma.us.novartis.com/sites/www.pharma.us.novartis.com/files/gleevec\\_tabs.pdf](https://www.pharma.us.novartis.com/sites/www.pharma.us.novartis.com/files/gleevec_tabs.pdf).
13. Novartis Pharmaceuticals, Tasigna [package insert]. 2014; Available from: <https://www.pharma.us.novartis.com/product/pi/pdf/tasigna.pdf>.
14. Li, X., et al., Characterization of dasatinib and its structural analogs as CYP3A4 mechanism-based inactivators and the proposed bioactivation pathways. *Drug Metab Dispos*, 2009. 37(6): p. 1242-50.
15. Abbas, R., et al., Effect of ketoconazole on the pharmacokinetics of oral bosutinib in healthy subjects. *J Clin Pharmacol*, 2011. 51(12): p. 1721-7.
16. Narasimhan, N.I., et al., Evaluation of pharmacokinetics and safety of ponatinib in subjects with chronic hepatic impairment and matched healthy subjects. *Cancer Chemother Pharmacol*, 2014. 74(2): p. 341-8.
17. Adnan A. Kadi, H.W.D., Mohamed W. Attwa, Sawsan M. Amer, Detection and characterization of ponatinib reactive metabolites by liquid chromatography tandem mass spectrometry and elucidation of bioactivation pathways. *RSC advances*, 2016. 6(76).
18. Ye, Y.E., C.N. Woodward, and N.I. Narasimhan, Absorption, metabolism, and excretion of [14C]ponatinib after a single oral dose in humans. *Cancer Chemother Pharmacol*, 2017. 79(3): p. 507-518.
19. Schinkel, A.H., et al., P-glycoprotein in the blood-brain barrier of mice influences the brain penetration and pharmacological activity of many drugs. *J Clin Invest*, 1996. 97(11): p. 2517-24.
20. Vlaming, M.L., J.S. Lagas, and A.H. Schinkel, Physiological and pharmacological roles of ABCG2 (BCRP): recent findings in *Abcg2* knockout mice. *Adv Drug Deliv Rev*, 2009. 61(1): p. 14-25.
21. Yabuki, N., et al., Gene amplification and expression in lung cancer cells with acquired paclitaxel resistance. *Cancer Genet Cytogenet*, 2007. 173(1): p. 1-9.

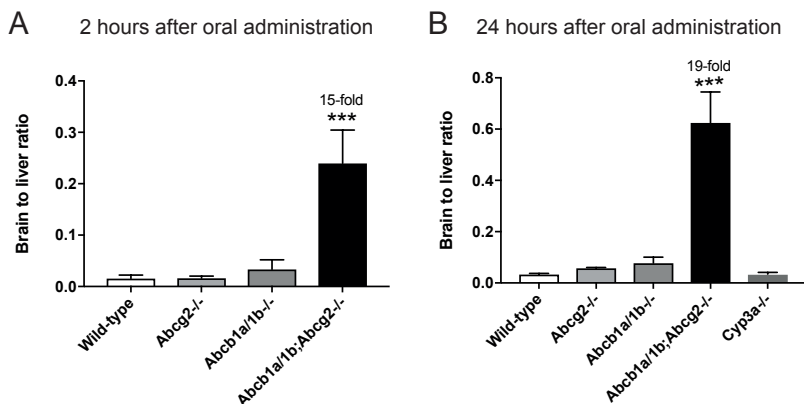
22. Stuurman, F.E., et al., *Oral anticancer drugs: mechanisms of low bioavailability and strategies for improvement*. Clin Pharmacokinet, 2013. 52(6): p. 399-414.
23. Sen, R., et al., *The novel BCR-ABL and FLT3 inhibitor ponatinib is a potent inhibitor of the MDR-associated ATP-binding cassette transporter ABCG2*. Mol Cancer Ther, 2012. 11(9): p. 2033-44.
24. Lu, L., et al., *Ponatinib is not transported by ABCB1, ABCG2 or OCT-1 in CML cells*. Leukemia, 2015. 29(8): p. 1792-4.
25. Fiere, D., et al., *Adult acute lymphoblastic leukemia: a multicentric randomized trial testing bone marrow transplantation as postremission therapy. The French Group on Therapy for Adult Acute Lymphoblastic Leukemia*. J Clin Oncol, 1993. 11(10): p. 1990-2001.
26. Kantarjian, H.M., et al., *Results of treatment with hyper-CVAD, a dose-intensive regimen, in adult acute lymphocytic leukemia*. J Clin Oncol, 2000. 18(3): p. 547-61.
27. Narasimhan, N.I., et al., *Effects of ketoconazole on the pharmacokinetics of ponatinib in healthy subjects*. J Clin Pharmacol, 2013. 53(9): p. 974-81.
28. Sparidans, R.W., et al., *Liquid chromatography-tandem mass spectrometric assay for ponatinib and N-desmethyl ponatinib in mouse plasma*. J Chromatogr B Analyt Technol Biomed Life Sci, 2016. 1023-1024: p. 24-9.
29. Durmus, S., et al., *Oral availability and brain penetration of the B-RAFV600E inhibitor vemurafenib can be enhanced by the P-GLYCOPROTEIN (ABCB1) and breast cancer resistance protein (ABCG2) inhibitor elacridar*. Mol Pharm, 2012. 9(11): p. 3236-45.
30. Schinkel, A.H., et al., *Normal viability and altered pharmacokinetics in mice lacking mdr1-type (drug-transporting) P-glycoproteins*. Proc Natl Acad Sci U S A, 1997. 94(8): p. 4028-33.
31. Jonker, J.W., et al., *The breast cancer resistance protein protects against a major chlorophyll-derived dietary phototoxin and protoporphyria*. Proc Natl Acad Sci U S A, 2002. 99(24): p. 15649-54.
32. Jonker, J.W., et al., *The breast cancer resistance protein BCRP (ABCG2) concentrates drugs and carcinogenic xenotoxins into milk*. Nat Med, 2005. 11(2): p. 127-9.
33. van Waterschoot, R.A., et al., *Absence of both cytochrome P450 3A and P-glycoprotein dramatically increases docetaxel oral bioavailability and risk of intestinal toxicity*. Cancer Res, 2009. 69(23): p. 8996-9002.
34. Dai, H., et al., *Distribution of STI-571 to the brain is limited by P-glycoprotein-mediated efflux*. J Pharmacol Exp Ther, 2003. 304(3): p. 1085-92.
35. Poller, B., et al., *Differential impact of P-glycoprotein (ABCB1) and breast cancer resistance protein (ABCG2) on axitinib brain accumulation and oral plasma pharmacokinetics*. Drug Metab Dispos, 2011. 39(5): p. 729-35.
36. Kort, A., et al., *Brain and Testis Accumulation of Regorafenib is Restricted by Breast Cancer Resistance Protein (BCRP/ABCG2) and P-glycoprotein (P-GP/ABCB1)*. Pharm Res, 2015. 32(7): p. 2205-16.
37. Steinbach, D. and O. Legrand, *ABC transporters and drug resistance in leukemia: was P-gp nothing but the first head of the Hydra?* Leukemia, 2007. 21(6): p. 1172-6.
38. Polli, J.W., et al., *An unexpected synergist role of P-glycoprotein and breast cancer resistance protein on the central nervous system penetration of the tyrosine kinase inhibitor lapatinib (N-{3-chloro-4-[(3-fluorobenzyl)oxy]phenyl}-6-[5-({[2-(methylsulfonyl)ethyl]amino }methyl)-2-furyl]-4-quinazolinamine; GW572016)*. Drug Metab Dispos, 2009. 37(2): p. 439-42.
39. Agarwal, S., et al., *Distribution of gefitinib to the brain is limited by P-glycoprotein (ABCB1) and breast cancer resistance protein (ABCG2)-mediated active efflux*. J Pharmacol Exp Ther, 2010. 334(1): p. 147-55.
40. Kodaira, H., et al., *Kinetic analysis of the cooperation of P-glycoprotein (P-gp/Abcb1) and breast cancer resistance protein (Bcrp/Abcg2) in limiting the brain and testis penetration of erlotinib, flavopiridol, and mitoxantrone*. J Pharmacol Exp Ther, 2010. 333(3): p. 788-96.
41. Tang, S.C., et al., *Brain accumulation of sunitinib is restricted by P-glycoprotein (ABCB1) and breast cancer resistance protein (ABCG2) and can be enhanced by oral elacridar and sunitinib coadministration*. Int J Cancer, 2012. 130(1): p. 223-33.
42. Lagas, J.S., et al., *Brain accumulation of dasatinib is restricted by P-glycoprotein (ABCB1) and breast cancer resistance protein (ABCG2) and can be enhanced by elacridar treatment*. Clin Cancer Res, 2009. 15(7): p. 2344-51.
43. Oostendorp, R.L., et al., *The effect of P-gp (Mdr1a/1b), BCRP (Bcrp1) and P-gp/BCRP inhibitors on the in vivo absorption, distribution, metabolism and excretion of imatinib*. Invest New Drugs, 2009. 27(1): p. 31-40.

44. Kalvass, J.C. and G.M. Pollack, *Kinetic considerations for the quantitative assessment of efflux activity and inhibition: implications for understanding and predicting the effects of efflux inhibition*. Pharm Res, 2007. 24(2): p. 265-76.
45. Bauer, M., et al., *Pilot PET Study to Assess the Functional Interplay Between ABCB1 and ABCG2 at the Human Blood-Brain Barrier*. Clin Pharmacol Ther, 2016. 100(2): p. 131-41.
46. Sjostedt, N., et al., *Challenges of using in vitro data for modeling P-glycoprotein efflux in the blood-brain barrier*. Pharm Res, 2014. 31(1): p. 1-19.
47. Badhan, R.K., M. Chenel, and J.I. Penny, *Development of a physiologically-based pharmacokinetic model of the rat central nervous system*. Pharmaceutics, 2014. 6(1): p. 97-136.
48. Whittle, S.B., et al., *The novel kinase inhibitor ponatinib is an effective anti-angiogenic agent against neuroblastoma*. Invest New Drugs, 2016. 34(6): p. 685-692.
49. van Waterschoot, R.A., et al., *Midazolam metabolism in cytochrome P450 3A knockout mice can be attributed to up-regulated CYP2C enzymes*. Mol Pharmacol, 2008. 73(3): p. 1029-36.
50. Douxfils, J., et al., *Association Between BCR-ABL Tyrosine Kinase Inhibitors for Chronic Myeloid Leukemia and Cardiovascular Events, Major Molecular Response, and Overall Survival: A Systematic Review and Meta-analysis*. JAMA Oncol, 2016.
51. Malagola, M., C. Papayannidis, and M. Bacarani, *Tyrosine kinase inhibitors in Ph+ acute lymphoblastic leukaemia: facts and perspectives*. Ann Hematol, 2016. 95(5): p. 681-93.
52. Yilmaz, M. and E. Jabbour, *Tyrosine Kinase Inhibitors Early in the Disease Course: Lessons From Chronic Myelogenous Leukemia*. Semin Oncol, 2015. 42(6): p. 876-86.
53. Abid, M.B. and S. De Mel, *Does ponatinib cross the blood-brain barrier?* Br J Haematol, 2016.

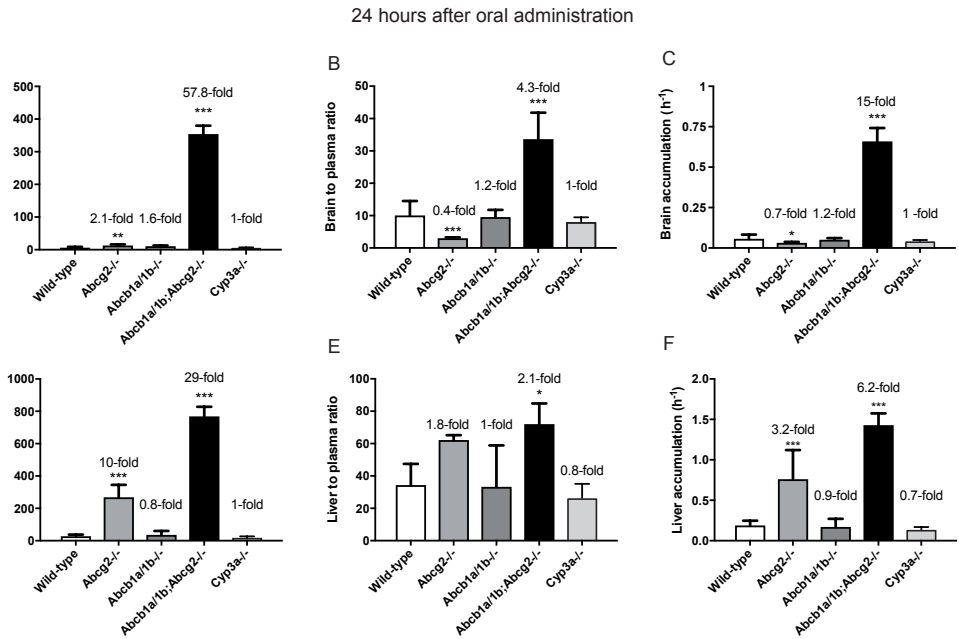
## SUPPLEMENTARY MATERIAL



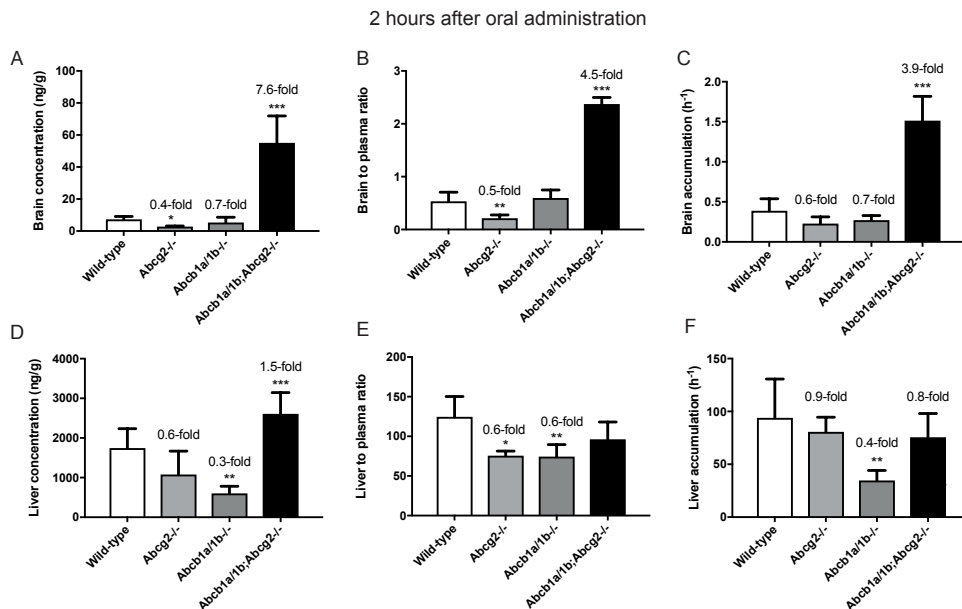
**Supplementary Figure 1** - Schematic representation of the main metabolites formed from ponatinib in humans. The main ponatinib metabolite, carboxylic acid (AP24600), is formed by esterase- and/or amidase-mediated hydrolysis. Two other pharmacodynamically active metabolites formed by Cytochrome P450 (mainly CYP3A4) are N-desmethyl ponatinib (DMP, AP24567) and N-oxide ponatinib (AP24734).



**Supplementary Figure 2** - Brain to liver ratio at 2 h (A) and 24 h (B) in female WT, Abcg2<sup>-/-</sup>, Abcb1a/1b<sup>-/-</sup> and Abcg2;Abcb1a/1b<sup>-/-</sup> mice after oral administration of 10 mg/kg ponatinib. \*, P < 0.05; \*\*, P < 0.01; \*\*\*, P < 0.001 compared to WT mice. Data are given as mean ± SD. N = 3-5 mice per group.



**Supplementary Figure 3** - Brain and liver concentration (A, D), tissue-to-plasma ratio (B, E) and relative tissue accumulation (C, F) of DMP in female WT, *Abcg2*<sup>-/-</sup>, *Abcb1a/1b*<sup>-/-</sup>, *Abcg2;Abcb1a/1b*<sup>-/-</sup> and *Cyp3a*<sup>-/-</sup> mice 24 h after oral administration of 10 mg/kg ponatinib. \*, P < 0.05; \*\*, P < 0.01; \*\*\*, P < 0.001 compared to WT mice. Data are given as mean ± SD. n = 4-5 mice per group.



**Supplementary Figure 4** - Brain and liver concentration (A, D), tissue-to-plasma ratio (B, E) and relative tissue accumulation (C, F) of DMP in female WT, *Abcg2*<sup>-/-</sup>, *Abcb1a/1b*<sup>-/-</sup> and *Abcg2;Abcb1a/1b*<sup>-/-</sup> mice 2 h after oral administration of 10 mg/kg ponatinib. \*,  $P < 0.05$ ; \*\*,  $P < 0.01$ ; \*\*\*,  $P < 0.001$  compared to WT mice. Data are given as mean  $\pm$  SD.  $n = 3-5$  mice per group.





# 6

---

## The impact of Organic Anion-Transporting Polypeptides (OATPs) on disposition and toxicity of antitumor drugs; insights from knockout and humanized mice

---

**Stéphanie van Hoppe<sup>1\*</sup>, Selvi Durmus<sup>2\*</sup>, Alfred H. Schinkel<sup>1</sup>**

<sup>1</sup>The Netherlands Cancer Institute, Division of Molecular Oncology, Amsterdam,

<sup>2</sup>Bilkent University, Department of Molecular Biology and Genetics, Ankara, Turkey

*Drug Resist Updat.* 2016 Jul;27:72-88.

## ABSTRACT

It is now widely accepted that organic anion-transporting polypeptides (OATPs) can have a strong impact on the disposition and elimination of a variety of endogenous molecules and drugs, especially members of the OATP1A/1B family. Owing to their prominent expression in the sinusoidal plasma membrane of hepatocytes, OATP1B1 and OATP1B3 play key roles in the hepatic uptake and plasma clearance of many, structurally diverse anti-cancer and other drugs. Here, we present a critical assessment of the currently available OATP1A and OATP1B knockout and transgenic mouse models as tools to study *in vivo* OATP functions. We discuss recent studies using these models demonstrating the importance of OATPs, primarily in the plasma and hepatic clearance of anticancer drugs such as taxanes, irinotecan/SN-38, methotrexate, doxorubicin, and platinum compounds. We further discuss recent work on OATP-mediated drug-drug interactions in these mouse models, as well as on the role of OATP1A/1B proteins in the phenomenon of hepatocyte hopping, an efficient and flexible way of liver detoxification for both endogenous and exogenous substrates. Interestingly, glucuronide conjugates of both the heme breakdown product bilirubin and the targeted anticancer drug sorafenib are strongly affected by this process. The clinical relevance of variation in OATP1A/1B activity in patients has been previously revealed by the effects of polymorphic variants and drug-drug interactions on drug toxicity. The development of *in vivo* tools to study OATP1A/1B functions has greatly helped in a better mechanistic understanding of their functional relevance in drug pharmacokinetics, and their implications for therapeutic efficacy and toxic side effects of anticancer and other drug treatment.

## 1. INTRODUCTION TO OATP1A/1B TRANSPORTERS AND GENETICALLY MODIFIED MOUSE MODELS TO STUDY THEIR FUNCTIONS

### 1.1. Properties of OATP1A/1B transporters

Organic anion-transporting polypeptide (OATP) uptake transporters can play a major role in the uptake of numerous compounds, including many anticancer drugs, into cells and organs. Positioned in the plasma membrane, these multispansing transmembrane proteins can mediate the uptake of a structurally highly diverse range of substrates into the cell, by as yet incompletely resolved mechanisms. As a consequence, they can have a major impact on the pharmacokinetic disposition of transported drugs, determining their oral availability and plasma clearance, as well as their distribution to liver and other organs, and the main route(s) of elimination (for recent reviews see: Gong and Kim, 2013; König et al., 2013; Niemi et al., 2011; Shitara et al., 2013; Stieger and Hagenbuch, 2014). OATPs can therefore have a strong effect on the therapeutic efficacy, but also the toxic side effects of substrate drugs. Moreover, several OATPs are variably expressed in a range of human cancers. As this may obviously influence the effective intracellular exposure of the cancer cells to OATP substrate anticancer drugs, this can directly affect the therapy susceptibility of these cancers (for recent reviews see: Nakanishi and Tamai, 2014; Obaidat et al., 2012; Sissung et al., 2012; Thakkar et al., 2015). The activity of the human OATPs that are thought to be most important for the general pharmacokinetic behavior of drugs, OATP1A2, OATP1B1, and OATP1B3 (as well as possibly OATP2B1, but see below), can further vary dramatically because of genetic polymorphisms and mutations that affect drug transport, but also because of drug-drug interactions with a variety of coadministered drugs (e.g. Durmus et al., 2015; Franke et al., 2009; Gong and Kim, 2013; König et al., 2013; Niemi et al., 2011; Obaidat et al., 2012; Shitara et al., 2013; Stieger and Hagenbuch, 2014; van de Steeg et al., 2012).

Given their obvious medical importance, it is crucial to obtain clear insight into the *in vivo* pharmacological, toxicological, and physiological functions of the OATP proteins, especially those of the OATP1A/1B family. One way to achieve this goal is to generate and study mouse strains that have the mouse *Oatp1a* and *Oatp1b* genes knocked out, or that have replaced the mouse *Oatp1a/1b* genes with one or more of their human analogues (although the formal gene name for the OATP-encoding genes is *SLCO* (for Solute Carrier of Organic Anions), for simplicity we will mostly use the OATP/*Oatp* nomenclature in this review). These mouse models can then be used to investigate the impact of the genetic modifications on the behavior of, amongst others, anticancer drugs. This review focuses on recent studies on such mouse strains and the insights obtained for a number of anticancer drugs. As some aspects have already been extensively reviewed previously (Iusuf et al., 2012b, c; Sprowl and Sparreboom, 2014;

Tang et al., 2013), we will only briefly touch upon those.

## 1.2. OATP1A/1B knockout and transgenic mouse strains characterized to date

To date, most characterized knockout and transgenic mouse models concern members of the OATP1A and OATP1B subfamilies, as these are thought to be most relevant for overall pharmacokinetics in man. Some initial studies suggested that human OATP1A2 was expressed in the intestinal epithelium, which would potentially indicate an important role in drug absorption (Glaeser et al., 2007). However, many independent later studies could not corroborate these findings, and it is now probably safe to conclude that normally there is no substantial level of OATP1A2 present in the small or large intestine of humans (e.g. Drozdik et al., 2014). On current data, OATP1A2 is substantially expressed in cholangiocytes lining the bile ducts in the liver, in the human blood-brain barrier, in apical membranes of kidney tubules, and in a variety of human tumors (van de Steeg et al., 2013 and references therein). In contrast to OATP1A2, human OATP1B1 and OATP1B3 are highly and primarily expressed in the basolateral (sinusoidal) membrane of human hepatocytes, where they can mediate the hepatic uptake of numerous substrate compounds (e.g. Nakanishi and Tamai, 2012). As these genes are also known to be substantially affected by genetic polymorphisms and mutations in humans (e.g. Niemi et al., 2011; van de Steeg et al., 2012), they have attracted most attention. The functionally related OATP2B1 protein is also a broad-specificity multidrug-uptake transporter, especially at lower pH, and highly expressed in both intestine and the sinusoidal membrane of hepatocytes. It has therefore been suggested that it might also have considerable pharmacokinetic impact (Nakanishi and Tamai, 2012). However, to date no OATP2B1 mouse models have been published, so we will not further cover this transporter here.

A complication in studying mouse models for the OATP1A/1B transporters is that there are no straightforward orthologues between the individual mouse and human *Oatp1a/1b* and OATP1A/1B genes. As indicated in **Figure 1**, there are no less than 4 different *Oatp1a* genes in the mouse, *Oatp1a1*, *Oatp1a4*, *Oatp1a5* and *Oatp1a6*, in addition to 2 *Oatp1a*-like elements that may be pseudo-genes. This compares with the single OATP1A2 gene in humans. On the other hand, the mouse has only one *Oatp1b2* gene, contrasting with the two human OATP1B1 and OATP1B3 genes (**Figure 1**). Although the mouse and human OATP1A proteins are obviously more similar to each other than to the mouse and human OATP1B proteins, and vice versa, the amino acid divergence within each subfamily is still considerable (as low as 67% amino acid identity within the OATP1A subfamily, and 65% within the OATP1B subfamily). Consequently, with these broad-specificity multidrug transporters, no reliable statements can be made

on overlapping substrates just based on amino acid similarity. As the tissue distribution is also not conserved between members of one subfamily (for instance, mouse Oatp1a1 and Oatp1a4 are present in the sinusoidal membrane of hepatocytes, whereas human OATP1A2 is not) it is clear that one cannot use single-gene mouse Oatp1a or Oatp1b knockout strains to make reliable predictions on the *in vivo* behavior of human OATP1A2, OATP1B1, or OATP1B3. This was an important motivation to generate a complete Oatp1a/1b knockout strain, and use it to specifically express human OATP1A2, OATP1B1, and OATP1B3 in this knockout background (van de Steeg et al., 2012; van de Steeg et al., 2013; van de Steeg et al., 2010).

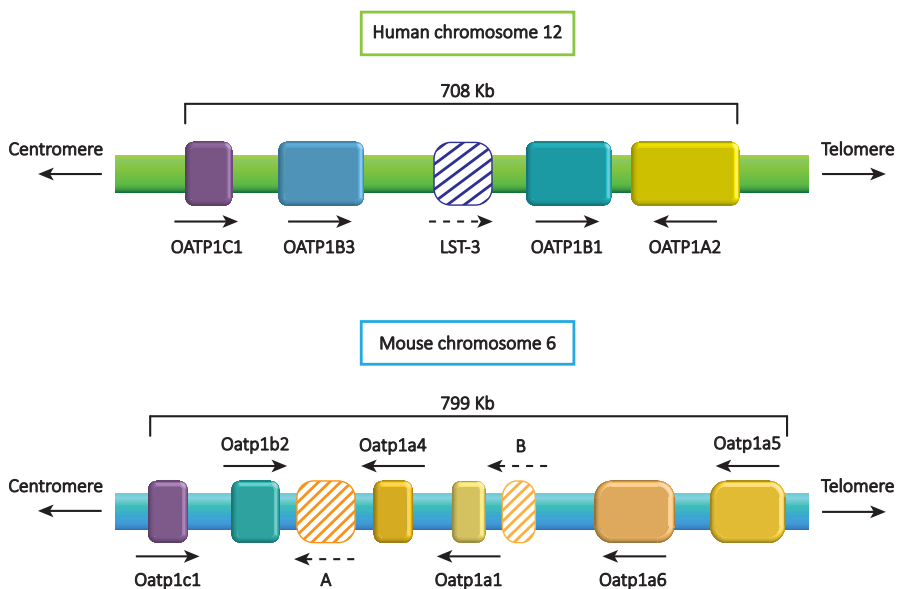


**Figure 1** - Comparison of the human and mouse OATP1A/B/C gene clusters. The human OATP1A/B/C gene cluster is located on chromosome 12p. OATP1C1 is followed by OATP1B3, the OATP1B-like pseudogene LST-3 (OATP1B7 according to Ensembl), OATP1B1, and OATP1A2. OATP1A2 is transcribed from the opposite strand compared to the OATP1B- and OATP1C-type genes in the cluster. The mouse Oatp1a/b/c genes are located on chromosome 6p in a similar order as the human genes, starting with Oatp1c1 followed by Oatp1b2, Oatp1a-like pseudogene A (Ensembl: Gm5724), Oatp1a4, Oatp1a1, Oatp1a-like pseudogene B (Ensembl: Gm6614), Oatp1a6, and Oatp1a5. Analogous to the human gene cluster, all Oatp1a-type genes (and pseudogenes) are oriented in the opposite transcription direction of the Oatp1b- and Oatp1c-type genes. The relative sizes and distances of the genes are depicted roughly to scale, also between the mouse and human chromosome, but without showing exon/intron structures, and arrows indicate the direction of transcription. Pseudogenes and their putative direction of transcription are rendered hatched. Directions of centromeres and telomeres and the approximate size of the human and mouse gene clusters are indicated.

Table 1 lists the various Oatp1a and Oatp1b knockout strains, and OATP1A/1B humanized strains that have been described so far. Oatp1a1 and Oatp1a4 knockout strains were described by Ose et al. (2010) and Gong et al. (2011). These mouse strains, originally made in 129/Ola ES cells by Deltagen, were backcrossed 10 times to a C57BL/6 background, and subsequent characterization of these lines was mainly done in this genetic background. A few independent Oatp1b2 knockout strains were generated. Lu et al. (2008) described the generation and initial characterization of an Oatp1b2 knockout strain generated in 129S1 ES cells, which was backcrossed for 7 generations to a C57BL/6 background. Independently, Zaher et al. (2008) generated Oatp1b2 knockout mice using DBA1/lacJ ES cells, which were further kept and characterized in a DBA1/lacJ genetic background. Combined Oatp1a/1b knockout mice, covering all the mouse Oatp1a and Oatp1b genes, were generated in 129/Ola ES cells. Initial characterization of Oatp1a/1b(-/-) mice was done in a mixed (~50%) 129/Ola and FVB genetic background (van de Steeg et al., 2010), but this strain was subsequently backcrossed for at least 7 generations to an FVB background, in which further characterization took place (van de Steeg et al., 2012). These FVB background Oatp1a/1b(-/-) mice were then used to generate three different humanized mouse strains with predominant expression of human OATP1A2, OATP1B1, or OATP1B3 cDNA, respectively, in the liver parenchyme cells, again all in FVB background (van de Steeg et al., 2012; van de Steeg et al., 2013). Moreover, a combined humanized OATP1B1/OATP1B3 strain was created by crossing the separate transgenic strains (Salphati et al., 2014).

**Table 1** - Oatp1a/b mouse models.

Mouse models	Genetic background	Primary references
Oatp1a1 knockout	C57BL/6N	(Gong et al., 2011)
Oatp1a4 knockout	C57BL/6N	(Gong et al., 2011; Ose et al., 2010)
Oatp1b2 knockout (variant 1)	C57BL/6	(Lu et al., 2008)
Oatp1b2 knockout (variant 2)	DBA1/lacJ	(Zaher et al., 2008)
Oatp1a/1b knockout	FVB	(van de Steeg et al., 2010)
Humanized hepatic OATP1A2 transgenic	FVB	(van de Steeg et al., 2013)
Humanized hepatic OATP1B1 transgenic	FVB	(van de Steeg et al., 2009)
Humanized hepatic OATP1B3 transgenic	FVB	(van de Steeg et al., 2013)
Humanized hepatic OATP1B1 and OATP1B3 transgenic	FVB	(Salphati et al., 2014)

### 1.3. Caveats in using OATP1A/1B genetically modified mouse models

It should be noted that the genetic background strain may at times be important for the extent to which certain phenotypes are detectable in knockout and transgenic mice.

Although this has not been systematically analyzed so far in the various *Oatp* knockout strains, we have observed modest physiological changes in *Oatp1a/1b(-/-)* mice in mixed *Ola/129/FVB* background, that disappeared upon further backcrossing into an *FVB* background (unpublished data).

Also the environmental conditions (e.g., diet, bedding, intestinal microflora) may at times be important factors in the penetrance of certain phenotypes. For instance, we have observed that *FVB* background *Oatp1a/1b(-/-)* mice analyzed in our facility (The Netherlands Cancer Institute, NKI) had a marked induction of carboxylesterase genes relative to wild-type *FVB* mice (Iusuf et al., 2014). However, the very same strain of mice obtained by other groups through a commercial supplier (Taconic) did not show a difference in carboxylesterase expression with wild-type mice (Salphati et al., 2014). Further analysis suggested that this was because the wild-type *FVB* mice obtained from Taconic already had a much higher endogenous hepatic carboxylesterase expression compared to *FVB* mice kept at the NKI, most likely because of environmental differences. The *Oatp1a/1b* knockout from “Taconic” circumstances did not further increase carboxylesterase expression. Interestingly, humanizing the *Oatp1a/1b* knockout mice with the *OATP1B1* transgene did reverse the high carboxylesterase expression in both NKI and Taconic mice (Iusuf et al., 2014; Salphati et al., 2014), indicating that this could apparently overrule any environmental factors causing the different carboxylesterase expression in *FVB* wild-type mice. On the other hand, transgenic *OATP1B3* could fully reverse the carboxylesterase overexpression in the NKI facility, but not elsewhere. This further supports that, whatever the factor(s) pushing up carboxylesterase expression in the *Oatp1a/1b(-/-)* (and *FVB*) mice, they were more prominent in the other facilities than in the NKI facility. It is important to keep such complications in mind when comparing the results in genetically modified mouse strains obtained by different groups. Moreover, as environmental conditions in mouse facilities cannot always be kept under complete control, it is also possible that shifts in phenotypes occur over time even within one facility.

Thirdly, also gender may substantially affect results obtained with *Oatp1a/1b* genetically modified mice. For instance, *Oatp1a1*, *Oatp1a4*, and *Oatp1b2* are all substantially expressed in the basolateral (sinusoidal) membrane of the mouse liver. Judged by RNA level, *Oatp1a1* is more abundant in male than in female liver (about 2-fold), and *Oatp1a4* in female liver (also about 2-fold), whereas *Oatp1b2* is similarly expressed in both genders (Cheng et al., 2005). This can directly affect whether certain pharmacokinetic effects can be detected in knockout strains. For instance, Gong et al. (2011) found that *Oatp1a1* deficiency substantially reduced the clearance of the diagnostic dye dibromosulphophthalein in male mice, but not in female mice.

In some cases, authors have asserted that the knockout of mouse *Oatp1b2*, as the

single mouse representative of the mammalian OATP1B subfamily (**Figure 1**), might be more or less equivalent to the deficiency of OATP1B1 and OATP1B3 in humans (e.g., Zaher et al., 2008). However, for many OATP substrates this assumption clearly does not apply. In humans, OATP1B1 and OATP1B3 are the only members of the OATP1A/1B family that are present in the basolateral membrane of liver parenchyme cells, and thus involved in the uptake of substrates from blood into the liver. Human OATP1A2 is also expressed in the liver, but only found in the cholangiocytes, and therefore irrelevant for the direct uptake of compounds from blood into the liver. In contrast, in the mouse there are two OATP1A proteins that are substantially present in the sinusoidal membrane of liver parenchyme cells, *Oatp1a1* and *Oatp1a4*. This means that for any substrate that is substantially transported by both *Oatp1b2* and either or both of *Oatp1a1* or *Oatp1a4*, results obtained in single *Oatp1b2*<sup>-/-</sup> mice may underestimate the effects of OATP1B1 and OATP1B3 deficiency in humans. A case in point is the role of OATP1B1 and OATP1B3 in the uptake of conjugated bilirubin. Whereas single *Oatp1b2*<sup>-/-</sup> mice showed only a marginal increase in plasma total and conjugated bilirubin levels (Lu et al., 2008; Zaher et al., 2008), in full *Oatp1a/1b*<sup>-/-</sup> mice there was a pronounced increase in plasma bilirubin glucuronide levels (van de Steeg et al., 2010). The latter observation pointed to the prominent role that human OATP1B1 and OATP1B3 play in the reuptake of conjugated bilirubin in human liver, and provided the mechanistic explanation for the human Rotor syndrome caused by full OATP1B1 and OATP1B3 deficiency (van de Steeg et al., 2012). Clearly, the redundant role of *Oatp1a1* and *Oatp1a4* relative to *Oatp1b2* in hepatic uptake of conjugated bilirubin in the mouse obscured the important contribution of the human OATP1B proteins in this process. Great care must therefore be taken when extrapolating from results in *Oatp1b2*<sup>-/-</sup> mice to the functional role of the human OATP1B1 and OATP1B3 proteins in liver. For pharmacokinetic studies, given the very substantial but incomplete and unpredictable overlap in substrate specificity between the various mouse and human OATP1A/1B transporters, every drug should be carefully assessed in its own right, and great caution should be used in extrapolating from results obtained in single knockout strains to the human situation.

Keeping these caveats in mind, in this review we will focus on recent studies performed with these mouse models for a range of anticancer drugs. **Figure 2** provides an overview of the structures of these drugs, also illustrating their structural diversity. The aim of such studies was to obtain basic insight into the handling of the anticancer drugs by OATP1A/1B proteins, in the hope that this knowledge may ultimately be used to improve current anticancer drug treatment regimens, by enhancing therapeutic efficacy of these drugs, reducing toxic side effects, and possibly both.

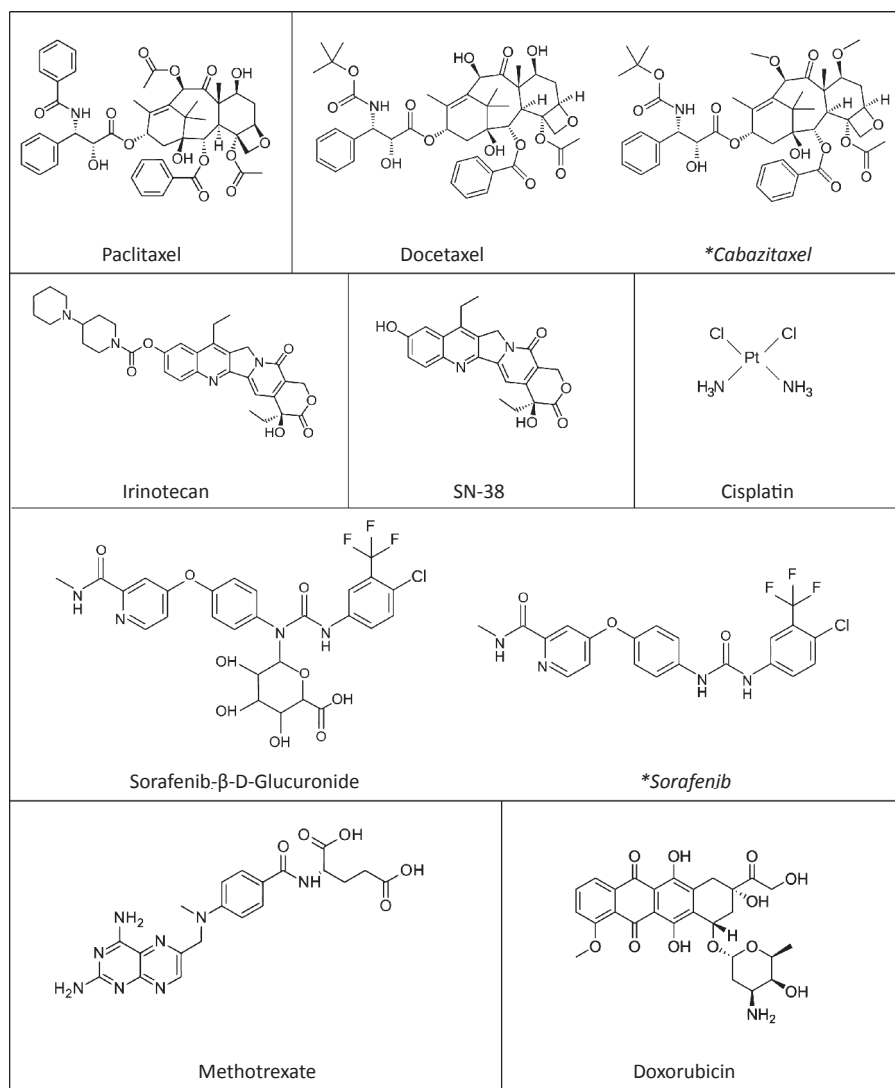


**Figure 2** - Structures of anticancer drugs clearly affected by Oatp1a/1b activity *in vivo*. Drugs that are structurally closely related, but that are not appreciably affected by Oatp1a/1b-mediated transport *in vivo* are named in italics and marked with an asterisk. While paclitaxel and docetaxel are clearly transported, cabazitaxel, which differs in just two methoxy groups from docetaxel, is not appreciably transported by Oatp1a/1b *in vivo*. Oatp1a/1b activity in mice clearly affects disposition of both irinotecan and its active metabolite SN-38. Sorafenib itself is not noticeably transported by Oatp1a/1b *in vivo*, but its glucuronate conjugate sorafenib-β-D-glucuronide is. For cisplatin it should be noted that this drug is highly reactive, and only total Pt levels are measured in *in vivo* experiments. It is therefore possible that structurally different complexes resulting from cisplatin reactions are primarily transported by Oatp1a/1b proteins.

## 2. RECENT PHARMACOLOGICAL AND TOXICITY STUDIES WITH OATP KNOCKOUT AND HUMANIZED MICE

### 2.1. Taxanes

The taxanes paclitaxel and docetaxel are cytotoxic anticancer drugs that bind to microtubules and disrupt their function by stabilizing GDP-bound tubulin, thus interfering with proper cell division. Paclitaxel and docetaxel are currently applied intravenously (i.v.) in the treatment of several types of cancer, such as non-small cell lung cancer, ovarian, breast, gastric, prostate, and head-and-neck cancer (Gligorov and Lotz, 2004; Koolen et al., 2010). Both paclitaxel and docetaxel are quite large, very hydrophobic, uncharged molecules (**Figure 2**). It was therefore thought that they could pass cell membranes primarily by passive diffusion, so it was initially a bit of a surprise that these molecules were substantially taken up into cells by OATP1B1 and OATP1B3 in several (but not all, see also section 4) *in vitro* expression systems (Baker et al., 2009; de Graan et al., 2012; Nieuweboer et al., 2014; Smith et al., 2006; Svoboda et al., 2011). To assess the possible *in vivo* relevance of this uptake transport, a number of studies with paclitaxel and docetaxel were performed in OATP/Oatp knockout and transgenic mice.

#### 2.1.1. Paclitaxel

Van de Steeg et al. (2011) found that the paclitaxel plasma AUC was more than 2-fold increased in Oatp1a/1b(-/-) relative to wild-type mice after i.v. administration at 10 mg/kg. Conversely, the liver AUC was 2-fold lower in the Oatp1a/1b(-/-) mice. Clear differences in plasma and liver paclitaxel concentrations were not yet apparent at 3.5 minutes, but emerged from 7.5 minutes after administration. This suggests that the very early paclitaxel distribution, when plasma concentrations were very high (>20 mg/l), was not much dependent on Oatps. However, with plasma concentrations below 20 mg/l, paclitaxel liver uptake and hence plasma clearance became strongly dependent on Oatp1a/1b transporters. This suggested that at plasma levels above 20 mg/l the sinusoidal Oatp1a/1b proteins were saturated, and other uptake processes, perhaps passive diffusion, dominated the liver uptake of paclitaxel. This was supported by limited paclitaxel distribution studies at a higher dosage (50 mg/kg), which yielded reduced differences between Oatp1a/1b(-/-) and wild-type mice in plasma concentration (1.7-fold) and liver concentration (1.5-fold) 30 minutes after paclitaxel administration compared to the 10 mg/kg dose (1.9-fold and 2.2.-fold, respectively). Overall, the data indicate a substantial role of hepatic sinusoidal Oatp1a/1b proteins in the clearance of paclitaxel from plasma, at plasma concentrations that can also occur in patients. Following high-dose paclitaxel chemotherapy, peak plasma concentrations range from 2 to 11 mg/l (Rowinsky and Donehower, 1995), i.e. well below the saturation

level of the Oatp1a/1b proteins. A later, independent study by Nieuweboer et al. (2014) found quantitatively similar effects of a single Oatp1b2 knockout on the plasma AUC and liver accumulation of i.v. paclitaxel dosed at 5 mg/kg in mice. This could indicate that most of the effects on paclitaxel observed in the Oatp1a/1b(-/-) mice were primarily mediated by Oatp1b2 deficiency, although differences in genetic background strain (DBA/1lacJ vs. FVB), exact paclitaxel formulation used, laboratory and even period of experimentation, may all affect the detailed outcome of such studies (e.g. Nieuweboer et al., 2014; Sparreboom and Mathijssen, 2014).

In a follow-up study, the pharmacokinetics of paclitaxel was analyzed in “humanized” Oatp1a/1b(-/-) mice with transgenic expression of human OATP1B1, OATP1B3, or OATP1A2 in the liver parenchyme cells (van de Steeg et al., 2013). The transgenic promoter/enhancer used was chosen to obtain preferential expression of the human proteins in liver parenchyme cells, which was successful, although minor OATP1B1 and OATP1B3 transgene expression was also found in kidney, but not small intestine. Based on protein immunoblot analysis and protein mass spectrometry, the hepatic level of transgenic OATP1B1 was in the same order as that observed in human liver samples, and that of transgenic OATP1B3 somewhat higher, with estimated humanized/human ratios of 0.5- to 1-fold and ~3-fold for OATP1B1 and OATP1B3, respectively (Higgins et al., 2014; Salphati et al., 2014). Transgenic OATP1A2 expression was much higher than in human liver, but this relates mostly to the fact that OATP1A2 in human liver is only expressed in cholangiocytes, whereas in the transgenic mice it is expressed in the far more abundant liver parenchyme cells. This also means that the OATP1A2 humanized mouse strain does not represent a physiologically correct model of the normal OATP1A2 function in human liver. However, it does allow an assessment of the *in vivo* functioning of OATP1A2 in uptake of drugs and other compounds from plasma. This may, *inter alia*, be relevant as OATP1A2 is substantially expressed in the human blood-brain barrier, in apical membranes of kidney tubules, and in a variety of human tumors (van de Steeg et al., 2013 and references therein). Immunohistochemically, transgenic OATP1B1 was found in the sinusoidal membrane of hepatocytes and expressed throughout the liver lobule, albeit with stronger staining around the portal vein in human liver, whereas this transporter is variously reported to be expressed throughout the liver lobule, or primarily in centrolobular hepatocytes (van de Steeg et al., 2009; van de Steeg et al., 2013). Transgenic OATP1B3 was likewise found in the hepatocyte sinusoidal membrane, showing somewhat dispersed distribution throughout the liver lobules (van de Steeg et al., 2013). In human liver OATP1B3 is preferentially found in the sinusoidal membranes of centrolobular hepatocytes. Although the transgenic OATP1B1 and OATP1B3 therefore do not exactly reflect the lobular subdistribution of OATPs in human liver, subsequent studies revealed good functionality of these proteins (as well as transgenic OATP1A2) in

the liver uptake and plasma clearance of a range of compounds.

Strong support for the functional activity of the hepatic OATP1B1, -1B3 and -1A2 transporters in the humanized strains came from the reversal of the highly increased plasma bilirubin levels found in the *Oatp1a/1b(-/-)* mice relative to wild-type mice (van de Steeg et al., 2013). The increased plasma levels of bilirubin monoglucuronide and diglucuronide were reversed to nearly wild-type levels (>15-fold and >7-fold reduction, respectively) by both OATP1B1 and OATP1B3 expression, whereas OATP1A2 caused a more modest 2-fold reduction. Interestingly, transgenic OATP1A2 was the only transporter that could significantly reduce the 2-fold increased levels of unconjugated bilirubin back to wild-type levels. This suggests that OATP1A2 is a relatively more efficient transporter of unconjugated bilirubin compared to conjugated bilirubin, whereas the inverse is true for OATP1B1 and OATP1B3. What this means for the normal biological function of human OATP1A2 in cholangiocytes is as yet unclear. Perhaps it plays a role in the resorption of highly insoluble unconjugated bilirubin inadvertently formed in bile, thus reducing the chance of formation of bilirubin-containing gallstones, but for the moment this possibility remains speculative.

A limited pharmacokinetic study of paclitaxel in the OATP humanized mice revealed a modest, ~1.6-fold, but highly significant effect of OATP1B3 and OATP1A2 in enhancing the liver uptake of paclitaxel dosed i.v. at 2 mg/kg compared to that in *Oatp1a/1b* knockout mice. A smaller effect was observed at 10 mg/kg i.v. paclitaxel (only significant for OATP1A2). Transgenic OATP1B1 did not elicit significant changes relative to *Oatp1a/1b(-/-)* mice at either dose (van de Steeg et al., 2013). Collectively, these data suggest that OATP1B3 and perhaps OATP1B1 may only have modest effects on paclitaxel liver uptake and clearance in humans. It should be kept in mind, though, that, unlike the situation in single humanized mice, in human liver OATP1B1 and OATP1B3 usually function simultaneously, which could well enhance their overall pharmacokinetic impact by additive effects. Such an additive effect was indeed observed for another drug in recently generated OATP1B1/1B3 double-transgenic mice, where single OATP1B1 or OATP1B3 transgenes did not markedly reduce the AUC of pravastatin after i.v. administration, but the combination reversed the AUC to close to that seen in wild-type mice (Salphati et al., 2014).

### 2.1.2. Docetaxel

Although quantitatively divergent results have been obtained for the impact of *Oatp1b2* and *Oatp1a/1b* knockouts, and of various OATP1A2/1B1/1B3 humanized transgenes on docetaxel pharmacokinetics, all studies to date support a role of these OATP/Oatps in docetaxel clearance. De Graan et al. (2012) reported that after i.v. administration of docetaxel at 10 mg/kg to wild-type and *Oatp1b2(-/-)* mice, the plasma AUC was 26.3-

fold higher in *Oatp1b2(-/-)* mice, indicating a very large effect of *Oatp1b2* removal. As expected, the liver-to-plasma AUC ratio was reduced in *Oatp1b2(-/-)* mice, by 6.2-fold. However, somewhat surprisingly, the liver docetaxel AUC itself was substantially higher (4.3-fold) in *Oatp1b2(-/-)* compared to wild-type mice, rather than lower (or perhaps equal, see below). This result was unexpected in case the liver uptake of docetaxel was strongly reduced in the knockout mice. An analysis of potential compensatory expression changes of functionally related genes in the knockout mice did not yield obvious alternative causes of the changes in docetaxel pharmacokinetics. A simple mechanistic explanation of the observed increased liver AUC of docetaxel in the *Oatp1b2(-/-)* mice is for the moment therefore still lacking.

The potential experimental variability of these docetaxel pharmacokinetic studies was illustrated by the outcome of very similar experiments that were performed a few years later by the same group, in the same mouse strains, under apparently the same conditions (Hu et al., 2014; Sparreboom and Mathijssen, 2014). Instead of a 26-fold higher plasma AUC of docetaxel in the *Oatp1b2(-/-)* mice, only a 1.6-fold increase was observed, which was, however, still statistically significant. The main difference was not a change over time in the plasma AUC of the *Oatp1b2(-/-)* mice (~7400 vs. ~8800 ng x h/ml), but almost entirely attributable to a much higher plasma AUC of docetaxel in the wild-type mice compared to the earlier experiments (4500 vs. 336 ng x h/ml). Despite extensive later analyses by the same group, the cause of these divergent results is still unclear (Sparreboom and Mathijssen, 2014). Although in our experience it is not uncommon to see some variation in absolute drug levels (AUC) measured in pharmacokinetic studies performed a few years apart under otherwise seemingly identical conditions, this usually concerns less than about 2-fold differences. However this may be, collectively, the data still indicate a role for *Oatp1b2* in the clearance of i.v. docetaxel, most likely by mediating uptake of docetaxel from blood into the liver. This was further corroborated by independent studies by two other groups.

Using the same strain of *Oatp1b2(-/-)* mice, Lee et al. (2015) very recently reported a limited, 30 min pharmacokinetic study with i.v. [<sup>3</sup>H]-docetaxel dosed at 1 mg/kg. Measuring plasma and liver radioactivity, they found a 5.5-fold higher plasma AUC of [<sup>3</sup>H]-docetaxel equivalents in *Oatp1b2(-/-)* mice (340 +/- 149 vs 62 +/- 8 ng x h/ml,  $P < 0.05$ ), no significant difference in liver concentrations, but a 3-fold decreased liver-to-plasma ratio ( $P < 0.05$ ). While concerning total radioactivity measurements, which may be complicated by extensive and possibly differential docetaxel metabolism, these results qualitatively support the findings of Hu et al. (2014) and De Graan et al. (2012), indicating a role of *Oatp1b2* in plasma clearance of docetaxel by mediating uptake into the liver.

Iusuf et al. (2015) studied docetaxel pharmacokinetics in *Oatp1a/1b(-/-)* mice of an

FVB genetic background, using a low-polysorbate 80 formulation to minimize possible inhibitory effects on Oatps (de Graan et al., 2012; Nieuweboer et al., 2014). After i.v. administration of docetaxel at 10 mg/kg, the plasma AUC was 2.9-fold higher in the Oatp1a/1b(-/-) mice (609 vs 212  $\mu\text{g} \times \text{min}/\text{ml}$ ,  $P < 0.001$ ). Similar to the findings of Lee et al. (2015), the liver exposure was not substantially altered in the Oatp1a/1b(-/-) mice, but the liver-to-plasma ratio was markedly lower at all except the earliest time points (at least 3-fold or more after 15 min). A limited pharmacokinetic study (15-60 min) of i.v. docetaxel (dosed at 10 mg/kg) in OATP1B1, OATP1B3, and OATP1A2 humanized mice indicated a 4-fold increase in docetaxel plasma AUC in Oatp1a/1b(-/-) compared to wild-type mice, which was largely reversed in both OATP1B1- and OATP1A2-transgenic mice ( $P < 0.001$ ), and more modestly ( $P < 0.01$ ) in OATP1B3-transgenic mice (Iusuf et al., 2015) (**Figure 3A and B**). In accordance with the unaltered liver AUC in the Oatp1a/1b(-/-) mice, the liver AUCs in all the humanized strains were not significantly different from those in the wild-type and Oatp1a/1b(-/-) mice.

These unaltered liver AUC data are readily explained by a physiologically based pharmacokinetic model developed by Watanabe et al. (2009; 2010). This shows that a strong reduction in hepatic uptake of drugs that have little alternative extrahepatic clearance (e.g., renal clearance), will often result in markedly increased plasma levels of the drug, but only very small changes in the liver AUC. Accordingly, liver-to-plasma concentration ratios will decrease, but mainly due to the increased plasma concentrations of the drug. This is exactly the behavior that was observed for docetaxel in the studies of Iusuf et al. (2015) and Lee et al. (2015), but also earlier for rosuvastatin, another OATP substrate (Iusuf et al., 2013). Only the earlier data of De Graan et al. (2012), which appeared to show a >4-fold increase in liver AUC of docetaxel in Oatp1b2(-/-) mice are not yet adequately explained.

Nonetheless, the collective data in Oatp knockout and various OATP1B-humanized strains provide strong support for the concept that mouse Oatp1b2 and human OATP1B1 and OATP1B3 in the sinusoidal membrane of the liver can contribute substantially to the liver uptake of docetaxel, and thus its plasma clearance as shown in **Figure 3A and B**. It is further noteworthy that the contribution to docetaxel clearance of OATP1B1 and OATP1B3 in the human liver will likely be at least additive. It could therefore be that coadministration of docetaxel with strong inhibitors of OATP1B1 and OATP1B3 might result in unwarranted overexposure of patients to docetaxel, which only has a narrow therapeutic window.

### 2.1.3. Cabazitaxel

The taxane cabazitaxel was recently introduced in the clinic as a second-line treatment of hormone-refractory prostate cancer. Amongst others this compound is less affected

by multidrug resistance caused by the MDR1 P-glycoprotein than docetaxel (Figg and Figg, 2010). Interestingly, cabazitaxel has a very similar structure as docetaxel, with the only difference being that two hydroxy groups in docetaxel are replaced by methoxy groups (Figure 2). In spite of this great similarity to docetaxel, however, cabazitaxel appears not to be transported by human OATP1B1 and OATP1B3 or mouse Oatp1b2 in HEK293 cells, or *in vivo* in Oatp1b2 knockout mice (Nieuweboer et al., 2014). This illustrates how apparently minor structural modifications can sometimes have dramatic effects on whether a compound is transported by OATPs. On the plus side, this probably also means that for this drug, variations in OATP1B activity in patients due to genetic polymorphisms, drug-drug interactions or variable expression in tumors, are less likely to affect the therapeutic efficacy or toxicity.

## 2.2. Irinotecan/SN-38

The anticancer drug irinotecan is a topoisomerase I inhibitor widely used in the treatment of colorectal, ovarian and lung cancer. Its therapeutic index is quite low, in part owing to its complex pharmacokinetics involving a variety of metabolic enzymes and drug transporters. Irinotecan, essentially a prodrug, is hydrolyzed to its primary pharmacodynamically active metabolite, SN-38, by various carboxylesterases occurring in liver, intestine, and, in mice, also in plasma (Innocenti et al., 2009; Mathijssen et al., 2002). Severe toxic side effects of irinotecan therapy include diarrhea and neutropenia, and these generally correlate with the systemic exposure to SN-38 (Smith et al., 2006). Low-activity polymorphic variants of OATP1B1, which may lead to impaired hepatic clearance of irinotecan and/or SN-38, are associated with increased systemic exposure to SN-38 and life-threatening toxicity (Han et al., 2008; Takane et al., 2009; Xiang et al., 2006). It was therefore of great interest to improve our understanding of the *in vivo* impact of OATPs on irinotecan/SN-38 pharmacokinetics and toxicity using a panel of Oatp/OATP knockout and transgenic mice. As it turned out, however, this study also revealed a potentially important confounder in studies with these mouse strains for drugs that can be affected by plasma carboxylesterases.

Initial studies of i.v. administered irinotecan (10 mg/kg) in wild-type and Oatp1a/1b(-/-) mice showed consistently higher plasma levels of irinotecan (AUC 1.7-fold higher) and SN-38 (AUC 2.9-fold higher) in the knockout mice, and roughly similar liver concentrations, resulting in clearly decreased liver-to-plasma ratios of both compounds in the knockouts at virtually all time points (Iusuf et al., 2014). This is consistent with reduced uptake of both these compounds from blood into the liver in the absence of Oatp1a/1b transporters, causing higher plasma levels. The amount of plasma SN-38 as a fraction of plasma irinotecan was ~10% in wild-type mice, and ~23% in knockout mice. A medium-term toxicity experiment, with daily i.v. administrations of irinotecan (30 mg/

kg) over 6 days resulted in more extensive weight loss in the Oatp1a/1b(-/-) mice, and a more pronounced reduction in the white blood cell count than in the wild-type mice measured at the end of the experiment (day 7). Assessed at this same day 7, there was some toxic damage observed in the bone marrow, thymus, and small intestine of wild-type mice, but this was much more pronounced in the Oatp1a/1b(-/-) mice (Iusuf et al., 2014). These data were in line with a much higher trough plasma concentration of SN-38 in the Oatp1a/1b(-/-) mice measured 24 hours after the last irinotecan administration, whereas the irinotecan concentrations at this time point were not significantly different from wild-type mice. It seems very likely that the higher exposure to SN-38 in the Oatp1a/1b(-/-) mice was the main cause of the increased toxicity. The most obvious explanation for the higher SN-38 exposure was strongly reduced hepatic clearance of SN-38, and likely also of its precursor irinotecan, by removal of the mouse Oatp1a/1b proteins.

### ***2.2.1. Upregulation of plasma carboxylesterase in Oatp1a/1b(-/-) mice***

Further analyses revealed, however, that the higher SN-38 exposure was not caused only by a decreased clearance of SN-38 directly due to a deficiency of Oatp1a/1b transporters. It turned out that, tested *ex vivo*, plasma of Oatp1a/1b(-/-) mice contained a highly increased level of irinotecan hydrolase activity, which caused a far more rapid formation of SN-38 from spiked irinotecan than observed in wild-type plasma. This difference was most likely the result of the highly increased expression of a number of carboxylesterase (Ces) genes in the liver of Oatp1a/1b(-/-) mice, namely Ces1b, Ces1c, Ces1d and Ces1e. Ces1c, which is relatively abundant, displayed an 80-fold increase in RNA levels (Iusuf et al., 2014). Interestingly, the mouse Ces1c enzyme is known to be mainly secreted from liver into plasma, due to the absence of a C-terminal endoplasmic reticulum retention signal in its amino acid sequence (Holmes et al., 2010). Application of the carboxylesterase inhibitor bis(4-nitrophenyl) phosphate (BNPP) supported that increased plasma carboxylesterase activity was responsible for the hydrolysis of irinotecan in Oatp1a/1b(-/-) plasma. Moreover, various other tested Ces1, Ces2, and Ces3 family genes, and genes for other candidate plasma esterase enzymes like butyrylcholinesterase, Aadamc, and Pon1-3, were not upregulated in the Oatp1a/1b(-/-) liver. Altogether, Ces1c upregulation is thus the most likely cause of the increased hydrolysis of irinotecan in Oatp1a/1b(-/-) mice.

That the increase in Ces1c expression was a direct consequence of the functional Oatp1a/1b deficiency was strongly supported by analysis of Ces gene expression in OATP1B1- and OATP1B3-humanized transgenic derivatives of the Oatp1a/1b(-/-) mice: the highly increased liver expression of Ces1c, but also of Ces1b, Ces1d and Ces1e, were markedly reduced, for Ces1c and Ces1d to even below the level of expression seen

in wild-type mice, by both transgenic OATP1B1 and OATP1B3 (Iusuf et al., 2014). This indicates that the function of the removed *Oatp1a/1b* genes responsible for keeping liver *Ces1* expression low could be taken over by both human OATP1B1 and human OATP1B3. Still, the exact mechanism underlying these *Ces*-regulatory functions of *Oatp/OATP1* proteins is as yet unclear. An obvious possibility seems some detoxifying function of these proteins, normally involved in removing one or more *Ces*-inducing compounds from the body. Such compounds might be of endogenous or exogenous origin (dietary, or metabolites or even primary products formed by the intestinal microflora), or possibly both. Their prolonged retention in the body might increase the overall liver exposure and thus *Ces* induction in the knockout strain. Further support for the involvement of a detoxifying role of the *Oatp1a/1b* proteins in *Ces* gene expression comes from the finding that the knockout of a number of other broad-specificity detoxifying proteins in FVB mice, including the multidrug efflux transporters *Abcb1a/1b* and *Abcg2*, and the multidrug metabolizing *Cyp3a* complex, cause similar levels of upregulation of hepatic *Ces1b*, *Ces1c*, *Ces1d*, and *Ces1e* expression (Lagas et al., 2012; Tang et al., 2015; Tang et al., 2014). Alternatively, a function of the OATPs in liver uptake of *Ces*-repressing compounds is also a possibility. If these compounds then get efficiently cleared through alternative routes, maybe renal or metabolic, the effective liver exposure to these compounds might be reduced in the *Oatp1a/1b* knockout mice. However, for the moment these options remain speculative.

#### ***2.2.2. Irinotecan studies in OATP1B1 and OATP1B3 humanized mice***

Whatever the mechanism of *Ces* upregulation, the increased plasma levels of *Ces1c* in *Oatp1a/1b*(-/-) mice might confound interpretation of the irinotecan and SN-38 disposition and toxicity results in these mice. The increased conversion of irinotecan to SN-38 could reduce plasma irinotecan levels, and increase SN-38 levels independent of direct *Oatp*-mediated transport. For this reason, among others, i.v. irinotecan studies were also performed in the OATP1B1 and OATP1B3 humanized mice, as these have a mostly normalized plasma *Ces1c* activity. The results obtained for irinotecan and SN-38 were strikingly different: the humanized mice showed higher plasma levels of irinotecan compared to wild-type mice, but similar liver concentrations, resulting in markedly reduced liver-to-plasma ratios of irinotecan. As these differences cannot be attributed to *Ces* upregulation, the results suggest that the transgenic OATP1B1 and OATP1B3 are far less efficient (if at all) in taking up irinotecan into the liver than the mouse *Oatp1a/1b* proteins (which are absent from the humanized mice). This also explains the higher plasma levels of irinotecan in the humanized mice compared to wild-type mice.

In contrast, for SN-38 after i.v. irinotecan administration we found that the plasma levels in the transgenic mice were markedly reduced compared to *Oatp1a/1b*(-/-) mice,

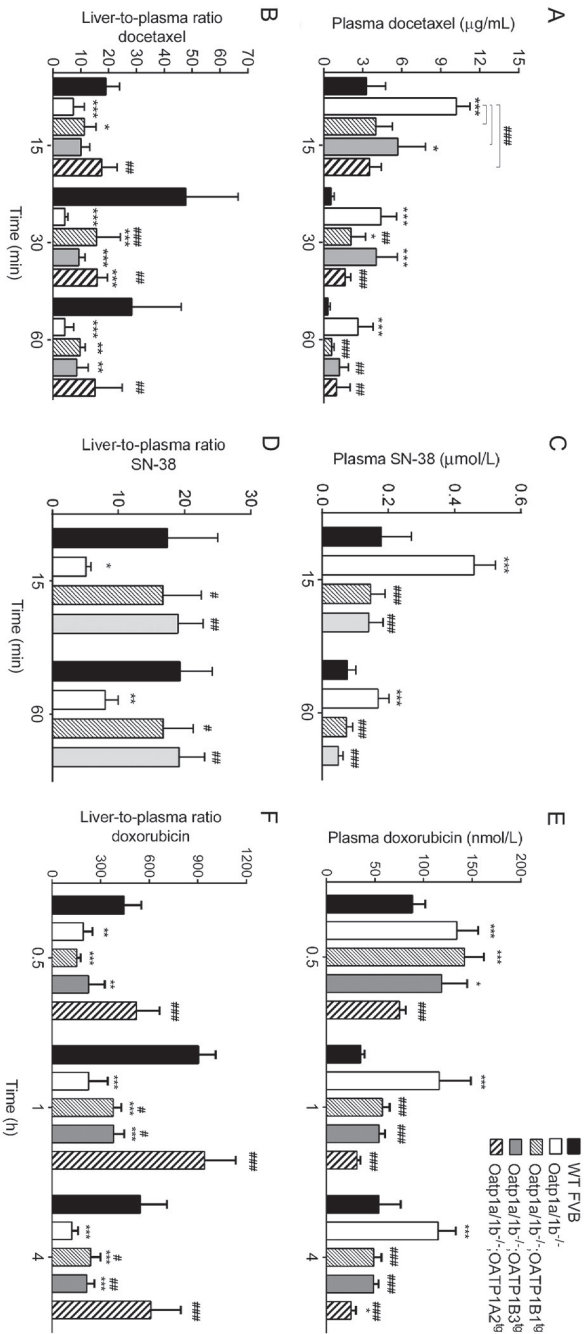


**Figure 3** - Impact of mouse and human OATP1A/1B transporters on the plasma and liver disposition of various anti-cancer drugs. Plasma disposition (A, C, and E) and liver-to-plasma ratios (B, D, and F) of docetaxel, SN-38 and doxorubicin are shown in the figure at various time points after i.v. administration of 10 mg/kg docetaxel, 10 mg/kg irinotecan (pro-drug of SN-38) or 5 mg/kg of doxorubicin, respectively. Drugs were administered to wild-type and Oatp1a/1b(-/-) mice, and to OATP1B1-, OATP1B3-, and OATP1A2-transgenic mice in an Oatp1a/1b(-/-) background. Data are presented as mean ± SD [\* , P < 0.05; \*\* , P < 0.01; \*\*\* , P < 0.001 when compared with wild-type; # , P < 0.05; ## , P < 0.01; ### , P < 0.001 when compared with Oatp1a/1b(-/-) mice]. Note that different units are used to indicate the plasma concentrations of each drug. This figure was modified with permission from previously published experimental data of Iusuf *et al.* (2015; 2014) and Durmus *et al.* (2014).

but similar to those in wild-type mice (**Figure 3C and D**). In theory this could either be caused by the up- and down-regulation of *Ces1c*, or by changes in SN-38 clearance. Interestingly, the liver levels in all tested strains were the same, and the liver-to-plasma ratios of SN-38 were identical between the wild-type and transgenic strains, but markedly higher than in *Oatp1a/1b(-/-)* mice. The latter result strongly suggests that the liver uptake of SN-38 was compromised in the *Oatp1a/1b(-/-)* mice, and mostly restored by OATP1B1 and OATP1B3 in the humanized strains (**Figure 3C and D**).

### 2.2.3. SN-38 disposition in *Oatp1a/1b(-/-)* mice

In an alternative approach to circumvent the complications of *Ces* upregulation in the *Oatp1a/1b(-/-)* mice, SN-38 was directly administered i.v. to these mice, at 1 mg/kg in view of the considerable solubility and formulation limitations of SN-38. This resulted in significantly higher plasma levels of SN-38 shortly after administration, and significantly lower liver concentrations compared to levels in wild-type mice. A reduced short-term liver uptake of SN-38 was further supported by a two-fold decrease in biliary excretion of SN-38 in the *Oatp1a/1b(-/-)* mice (Iusuf et al., 2014).

Collectively, the mouse studies indicate that both irinotecan and SN-38 are cleared from plasma by uptake into the liver through one or more of the mouse hepatic *Oatp1a/1b* transporters. In contrast, the transgenic human OATP1B1 and OATP1B3 can mediate substantial liver uptake and plasma clearance of SN-38, but not of irinotecan. These results fit well with *in vitro* studies, which found that SN-38 is readily transported by human OATP1B and OATP1B3, whereas irinotecan is not (Nozawa et al., 2005; Oostendorp et al., 2009; Yamaguchi et al., 2008). The results indicate species differences in substrate specificity between the mouse and human hepatic OATP1A/1B proteins, as expressed *in vivo* in mouse hepatocytes. The irinotecan/SN-38 toxicity data in the mouse strains are more difficult to interpret in view of the altered *Ces1c* levels and rate of SN-38 formation in *Oatp1a/1b(-/-)* mice. However, extrapolating from the delayed hepatic SN-38 clearance in *Oatp1a/1b(-/-)* mice and its reversal by human OATP1B1 and OATP1B3, it seems very likely that also in humans these proteins are involved in the detoxification of SN-38. This would be in line with the clinical observations that partial deficiencies in OATP1B1 due to genetic polymorphisms correlate with increased irinotecan/SN-38 toxicity (Han et al., 2008; Takane et al., 2009; Xiang et al., 2006). The data of Iusuf et al. (2014) strongly suggest that this has primarily to do with delayed SN-38 clearance in these patients due to the compromised function of OATP1B1.

## 2.3. Methotrexate

Methotrexate is a folate antimetabolite that is used in the treatment of several important cancer types (breast cancer, lung cancer, head- and neck cancer, non-

Hodgkin's lymphoma). It is also used, albeit at usually lower dosage, and mostly orally, to treat other diseases such as rheumatoid arthritis and psoriasis (van Outryve et al., 2002; Wessels et al., 2008). Methotrexate is a bicarboxylic organic anion, that is known to be transported *in vitro* by a number of OATP1A/1B proteins, including human OATP1B1, OATP1B3, and OATP1A2 (Abe et al., 2001; Badagnani et al., 2006; Sasaki et al., 2004). In addition, a genome-wide association study showed that SNPs in *SLCO1B1* associated with reduced transport activity were linked to decreased plasma clearance and decreased gastrointestinal toxicity in children with acute lymphoblastic leukemia (ALL) treated with high-dose i.v. methotrexate infusions (Trevino et al., 2009).

### 2.3.1. Methotrexate pharmacokinetics in *Oatp1a/1b* knockout mice

Initial characterization of i.v. methotrexate pharmacokinetics in *Oatp1a/1b*<sup>-/-</sup> mice revealed dramatic effects on plasma clearance and liver uptake of the drug (van de Steeg et al., 2010). The plasma AUC was increased 5-fold in *Oatp1a/1b*<sup>-/-</sup> mice, and liver concentrations were about 20-fold reduced. Hepatic methotrexate uptake was very rapid, with >50% of the dose accumulating in the wild-type liver within 3.5 min after i.v. dosing, whereas only ~2% accumulated in the *Oatp1a/1b*<sup>-/-</sup> liver. As could be expected from the dramatically reduced liver uptake of methotrexate, the total intestinal content of i.v. methotrexate, which mostly derives from biliary excretion, was about 17-fold reduced in the *Oatp1a/1b*<sup>-/-</sup> mice. Accordingly, the amount of unchanged methotrexate excreted in the feces was reduced from ~20% to ~2% of the dose. In contrast, the urinary excretion rose from ~40% of the dose in wild-type mice to ~100% in *Oatp1a/1b*<sup>-/-</sup> mice, indicating a substantial rerouting from hepatobiliary to renal excretion.

As some *Oatp1a/1b* proteins are also expressed in the mouse small intestine (*Slco1a4*, and to a lower extent *Slco1a5* and *Slco1a6* RNA was detected (Cheng et al., 2005)), an oral methotrexate study was also performed to assess possible changes in oral availability. However, whereas the systemic plasma and liver concentrations of methotrexate followed similar patterns as seen after i.v. administration, short-term hepatic portal vein sampling didn't provide any indication for a reduced rate of intestinal uptake of methotrexate in the *Oatp1a/1b*<sup>-/-</sup> mice. Apparently other intestinal uptake systems are primarily involved in the uptake of this charged compound.

In fact, in broader terms, despite extensive efforts, to our knowledge no one has so far been able to directly demonstrate for any OATP substrate drug that its intestinal uptake is detectably dependent on *Oatp1a/1b* proteins in available mouse models. Directly tested drugs include, in addition to methotrexate, fexofenadine, pravastatin, and rosuvastatin (Iusuf et al., 2012a; Iusuf et al., 2013; van de Steeg et al., 2010), as well as a number of other, as yet unpublished, drugs. This raises the more general question

whether Oatp1a/1b proteins play any significant role in the intestinal uptake of orally administered substrate drugs. However, there can be many causes of negative results in this respect, including the possibility of extensive redundancy with one or more other intestinal uptake transport systems. Further experimentation will be needed to resolve the intriguing question what transport systems are primarily involved in the intestinal uptake of a wide variety of relatively polar or charged drugs.

The Oatp1a/1b(-/-) mice can also be used to assess the efficacy and specificity of OATP-inhibiting drugs, for instance as a cause of drug-drug interactions. For this purpose rifampicin, a known OATP inhibitor, was administered i.v. 3 min before i.v. methotrexate to wild-type and Oatp1a/1b(-/-) mice, and methotrexate plasma and liver concentrations were determined 15 min later (van de Steeg et al., 2010). The methotrexate plasma concentration was increased threefold by rifampicin treatment in wild-type mice, to the same levels as seen in Oatp1a/1b(-/-) mice. In the knockout mice, rifampicin treatment had no effect on the plasma levels of methotrexate. The liver concentration of methotrexate in wild-type mice was 4-fold decreased by rifampicin, to about 9% of the dose. The liver concentration in Oatp1a/1b knockout mice was still lower (~1% of the dose), and not affected by rifampicin treatment. These results indicate that rifampicin could largely, but not completely, inhibit Oatp1a/1b-mediated methotrexate uptake into the liver, and thus its associated plasma clearance. The lack of effect of rifampicin on methotrexate in the Oatp1a/1b(-/-) mice indicates that it did not significantly affect other methotrexate clearance mechanisms, testifying to its specificity under these conditions.

### **2.3.2. Methotrexate pharmacokinetics in OATP-humanized mice**

In a follow-up study, methotrexate pharmacokinetics was analyzed in OATP1B1-, OATP1B3- and OATP1A2-humanized Oatp1a/1b(-/-) mice (van de Steeg et al., 2013). As explained elsewhere in this review (section 2.1.1), these three transgenes are primarily expressed in liver parenchyme cells of these mice, and the proteins are situated in the basolateral (sinusoidal) membrane. For OATP1B1 and OATP1B3 this is the physiologically relevant localization, but for OATP1A2 it is not, as in human liver it is found primarily in cholangiocytes, the epithelial cells lining the bile ducts. Still, inclusion of the latter strain allows analysis of the *in vivo* functioning of OATP1A2 in drug uptake, which can be relevant for assessment of any drug uptake that it may mediate in other tissues and in tumor cells.

Methotrexate was administered i.v. at two different dosages (10 and 2 mg/kg) to wild-type, Oatp1a/1b(-/-), and the three humanized mouse strains, and plasma, liver, and intestine (tissue plus contents) levels of methotrexate were measured 15 minutes after administration (van de Steeg et al., 2013). As observed previously, at 10 mg/kg

in the knockout mice methotrexate plasma levels were increased 5-fold, whereas liver levels were decreased 24-fold, and small intestinal levels 20-fold. Each of the three humanized transgenes partially reversed all of the three measured parameters, albeit not to the levels seen in wild-type mice. Plasma levels of methotrexate were reduced ~2-fold, and liver levels increased by 4- to 9-fold. Small intestinal levels were 2- to 4-fold increased. Qualitatively very similar results were obtained at the 2 mg/kg methotrexate dose. In general, transgenic OATP1B3 and OATP1A2 caused a ~2-fold more effective reversal of liver and small intestinal concentrations than OATP1B1, whereas the plasma reversal effects were similar between the three transgenes. The partial reversal by the humanized OATP1B1 and OATP1B3 proteins compared to wild-type parameters could relate to species differences in substrate preference between mouse and human Oatp/OATP proteins, but also to differences in effective expression level. Also, in human liver OATP1B1 and OATP1B3 would presumably act additively towards methotrexate, and thus may cause larger pharmacokinetic effects than suggested by the effects seen in the single transgenic strains. Regardless, the data clearly show that human OATP1B1 and OATP1B3 can have major effects on the plasma level, hepatic uptake clearance, and subsequent hepatobiliary/intestinal excretion of methotrexate. Moreover, as OATP1B3 is also expressed in various gastrointestinal, hepatocellular, breast, and lung cancers, it may further affect susceptibility of these cancers to OATP1B3 substrate drugs (Abe et al., 2001; Cui et al., 2003; Monks et al., 2007; Muto et al., 2007). The data obtained for human OATP1A2 suggest that this protein could substantially affect methotrexate uptake *in vivo* in other relevant tissues and barriers, such as the blood-brain barrier, kidney tubules, and tumor cells that express OATP1A2 (Gao et al., 2000; Lee et al., 2005).

### ***2.3.3. Impact of rifampicin and telmisartan coadministration on OATP-mediated methotrexate disposition***

The humanized mouse strains were subsequently used to further investigate OATP-dependent drug-drug interactions, starting with the inhibitory effect of rifampicin on *in vivo* methotrexate transport by human OATP1B1 and OATP1B3. Using various human OATP-overexpressing HEK293 cells, Durmus et al. (2015) showed that rifampicin inhibited methotrexate uptake *in vitro*, with  $IC_{50}$  levels ranging from 0.3 to 0.9  $\mu$ M. In the mouse models, rifampicin (20 mg/kg, i.v.) substantially inhibited both mouse and human OATP-mediated hepatic uptake and plasma disposition of methotrexate (10 mg/kg, i.v.) at clinically achievable concentrations for each of the drugs. Liver-to-plasma ratios of methotrexate were decreased 6- to 8-fold by inhibiting the mouse Oatp1a/1b proteins, ~4-fold by inhibiting human OATP1B1 and 11- to 18-fold by inhibiting human OATP1B3. This also led to increased plasma levels of methotrexate by 4- to 5-fold in mouse Oatp1a/1b background and up to 2-fold in humanized OATP1B1 or OATP1B3

background.

Although this specific combination of drugs (methotrexate and rifampicin) would be rare in the clinic, these results still suggest that more than one OATP-substrate or -inhibitor drugs might bring the risk of drug-drug interactions at the systemic and hepatic level. This would be especially important for patients chronically taking OATP-interacting drugs, such as statins and hypertension drugs. More importantly, people who already have activity-reducing polymorphisms in their *OATP* genes (Nakanishi and Tamai, 2012) might be at increased risk for altered drug disposition due to this type of drug-drug interactions, and consequently ineffective treatment and/or increased toxicity.

The possible drug-drug interaction effect of a clinically more common drug combination was investigated using a hypertensive drug, telmisartan, and methotrexate. This also allowed further evaluation of the applicability of knock-out and humanized mouse strains in drug-drug interaction studies. A similar set-up to the rifampicin and methotrexate experiments was chosen, but the dose of telmisartan had to be kept lower (7 mg/kg) due to solubility issues. *In vitro* cellular uptake studies resulted in fairly but not very low  $IC_{50}$  levels for telmisartan inhibiting methotrexate uptake ( $<11 \mu\text{M}$ ), and *in vivo* studies in the mouse models showed that telmisartan pre-treatment did not yield important changes in methotrexate disposition. There was only a weak inhibition of OATP1B1-mediated hepatic uptake of methotrexate by telmisartan, leading to ~2-fold decreased liver-to-plasma ratios of methotrexate. However, comparing the systemic telmisartan levels (40 - 200 nM) in patients (Stangier et al., 2000) with the levels achieved in mouse plasma (7 - 13  $\mu\text{M}$ ) suggests only a very low risk of adverse OATP-mediated drug-drug interactions between telmisartan and methotrexate in the clinic. These findings are helpful for patients who are simultaneously treated with methotrexate and telmisartan. However, additional clinically relevant combinations of drugs that are OATP-substrates and/or -inhibitors should be tested to evaluate the risks of OATP-mediated drug-drug interactions in the clinic, especially for the systemic and hepatic effects on drug concentrations due to the function of OATPs in liver uptake of their substrates. We suggest that the humanized transgenic mouse models with liver-specific OATP expression could be used to obtain a more realistic view of the human situation. However, it should be noted that these mouse models, while very useful to support the development of basic mechanistic insights, should not be used as simple one-to-one models of drug behavior in humans.

#### 2.4. Doxorubicin

Doxorubicin, an important topoisomerase II inhibitor drug used in cancer treatment, was recently shown to be an OATP substrate (Durmus et al., 2014). Doxorubicin is an

anthracycline antibiotic, commonly used in the treatment of several cancers, including Hodgkin's and non-Hodgkin's lymphoma, multiple myeloma, leukemia, sarcoma and breast, ovarian, thyroid, gastric and lung cancers (Cortes-Funes and Coronado, 2007; Gewirtz, 1999). Various mechanisms of action have been described for doxorubicin, of which two major mechanisms are intercalation of DNA that leads to inhibition of the topoisomerase II enzyme, required for smooth DNA transcription and replication, and, perhaps more controversially, generation of free radicals that leads to DNA and cell membrane damage (Gewirtz, 1999). Cardiotoxicity is the major and dose-limiting side effect of doxorubicin both in adult and pediatric cancer patients (Grenier and Lipshultz, 1998). Thus, recent efforts to improve doxorubicin treatment focus on improved anti-tumor efficacy and decreased cardiotoxicity by developing tumor-targeting strategies such as liposomal formulations of doxorubicin or developing new doxorubicin analogs (Cortes-Funes and Coronado, 2007; Minotti et al., 2004). Another strategy for lowering the toxicity and increasing the efficacy of doxorubicin is to understand the factors affecting its tissue disposition, such as its interactions with drug transporters, and utilize these insights to modify the pharmacokinetics, possibly with transporter inhibitors. Although doxorubicin has been used in the clinic for a very long time, information on its interaction with drug uptake transporters has been very limited. Okabe *et al.* (2005) for the first time suggested that doxorubicin might enter cells via organic cation transporter (OCT6)-mediated active transport.

Very recently, it was shown that both mouse and human OATP1A/1B family members can mediate the cellular uptake of doxorubicin (Durmus et al., 2014). This was rather surprising, as its structure, with properties of a weak base, was not considered a typical OATP substrate. In human OATP1A2-overexpressing HEK293 cells, the uptake of doxorubicin was ~2-fold increased compared to control cells, but there was no noticeable transport by human OATP1B1 or OATP1B3 *in vitro*. Mouse Oatp1a/1b proteins transported doxorubicin *in vivo*, as evidenced by up to ~2-fold increased plasma concentrations and up to 4-fold decreased liver-to-plasma ratios in Oatp1a/1b(-/-) mice after i.v. doxorubicin administration (**Figure 3E and F**) (Durmus et al., 2014). Moreover, the doxorubicin levels in the small intestinal content were also reduced in the knockout mice, suggesting a decreased biliary output, probably due to the lower liver levels. Interestingly, addition of one of the human OATP1A or 1B proteins in transgenic mice (on a mouse Oatp1a/1b knockout background) rescued the altered levels seen in the knockout mice to various extents (**Figure 3E and F**). Transgenic liver-specific expression of human OATP1A2 could completely revert the hepatic uptake and intestinal excretion of doxorubicin back to wild-type levels, whereas that of human OATP1B1 or OATP1B3 resulted in partial, but substantial rescue of these phenotypes (Durmus et al., 2014). Only the OATP1B1 or OATP1B3 proteins alone were present in these transgenic

mouse livers, instead of both simultaneously as in humans. The substantial impact of either transporter alone therefore suggests an even stronger impact of OATP1Bs on doxorubicin pharmacokinetics in humans, especially affecting plasma clearance and hepatic uptake characteristics. Obviously, for a drug with a narrow therapeutic index like doxorubicin, this might be critical for its therapeutic efficacy and toxicity in patients. It may therefore also be of interest to investigate possible associations between OATP activity and doxorubicin pharmacokinetics, therapeutic efficacy, and toxicity in patient cohorts.

## 2.5. Platinum chemotherapeutics

Cisplatin and more recent platinum chemotherapeutics such as carboplatin and oxaliplatin are used to treat a wide spectrum of cancers, including testicular, bladder, lung, ovarian, colorectal, cervical, and breast cancers, as well as some lymphomas and sarcomas. In a COMPARE analysis of 60 human tumor cell lines (the well-characterized NCI-60 panel), Lancaster et al. (2013) found that high OATP1B3 expression as judged by Real-time RT-PCR was statistically significantly linked with sensitivity to the cytotoxicity of 9 anticancer drugs, amongst which cisplatin, carboplatin, and a platinum compound structurally related to oxaliplatin. Unlike OATP1B1, which was found to be only expressed in liver and liver tumor tissue, OATP1B3 was found expressed in a range of different tissues and derived tumor tissue samples, suggesting that it might play a role in tumor sensitivity to platinum compounds.

Subsequent *in vitro* studies revealed that human OATP1B3 and OATP1B1 can mediate the cellular uptake of Pt upon exposure to cisplatin, and additionally OATP1B3 can mediate cellular Pt uptake upon exposure to carboplatin and oxaliplatin. *In vivo* studies with cisplatin administered intraperitoneally to wild-type and *Oatp1b2*<sup>-/-</sup> mice showed up to 35% reduced liver levels of Pt in the knockout mice shortly after administration, and 2.5-fold higher urinary excretion of Pt, the latter amounting to more than 60% of the administered dose (Lancaster et al., 2013). The data suggest a rapid and substantial liver uptake of a fraction of Pt being mediated by *Oatp1b2* in wild-type mice. In the *Oatp1b2*<sup>-/-</sup> mice this Pt fraction may instead be excreted primarily into the urine. As a consequence, the plasma levels of Pt are not much different between the two strains. It should be noted, however, that cisplatin is highly reactive, for instance with carbonate, and the *Oatp1b2*-mediated Pt uptake may therefore well represent uptake of various resulting negatively charged Pt complexes instead of cisplatin itself. Cisplatin also binds irreversibly to plasma proteins, further complicating pharmacokinetic analyses. However that may be, *in vivo* *Oatp1b2* function does clearly affect the pharmacokinetics of cisplatin-derived Pt. Extrapolating to human patients, this could mean that variations in OATP1B1 and OATP1B3 expression and activity in liver, in other tissues, and

especially in tumors, might affect the efficacy and toxic side effects of cisplatin-based chemotherapy. It will therefore be of interest to extend preclinical studies of cisplatin to OATP1B1- and OATP1B3-humanized Oatp1a/1b knockout strains, and also include studies of carboplatin and oxaliplatin. It will further be worthwhile to assess whether part of the high interindividual variation in efficacy and toxicity of these drugs seen in patients can in part be attributed to variations in OATP function.

## 2.6. Tyrosine kinase inhibitors

Tyrosine kinase inhibitors (TKIs), with as prime example imatinib (Gleevec), have to an extent revolutionized the treatment of a number of malignancies (Druker et al., 2001). As of 2015, more than 28 TKIs have been FDA-approved (Wu et al., 2015). These rationally designed, targeted anticancer drugs can make use of specific vulnerabilities of the tumor cells, for instance by targeting specific oncogenic mutations in proteins, thus increasing disease-specificity and reducing the risk of toxic side effects. Understandably, there has been significant interest in whether TKIs are transported OATP substrates, as this could affect their accumulation in tumor cells as well as in various important tissues in the body, and control their plasma pharmacokinetics and elimination. Such parameters can be decisive in the overall therapeutic efficacy and tolerability of anticancer and other drugs.

While many TKIs have now been tested for interaction with OATPs, the *in vivo* relevance for transport of the unchanged parent compounds appears to be quite limited. In RNA-injected *Xenopus* oocytes, human OATP1A2 mediates modest imatinib uptake, OATP1B3 a little, and OATP1B1 none (Hu et al., 2008). Initial tests failed to show significant uptake of sorafenib and sunitinib mediated by OATP1A2, OATP1B1, and OATP1B3 in RNA-injected *Xenopus laevis* oocytes (Hu et al., 2008). However, later tests in highly OATP-overexpressing HEK293 cells reported significant uptake transport of crizotinib, nilotinib, pazopanib, and sorafenib by OATP1B1 and OATP1B3; of imatinib, gefitinib, dasatinib, vandetanib, and vemurafenib by OATP1B3 but not by OATP1B1; and of sunitinib by OATP1B1 but not OATP1B3 (Zimmerman et al., 2013). It should be noted, however, that often OATP-mediated relative levels of uptake of TKIs in the various *in vitro* model systems were small compared to those of the anionic OATP control substrates. Modern targeted TKIs are rarely, if at all, designed to be anionic, given the usual requirements of good oral availability (intestinal absorption) and efficient tumor cell penetration of these compounds. A possible further cause of discrepancies between *in vitro* and *in vivo* OATP-mediated transport results for certain drugs is discussed later in this review (section 4).

### 2.6.1. Sorafenib *in vitro* and *in vivo* studies

The TKI sorafenib was further investigated *in vivo* in mouse models because it was readily transported by both OATP1B1 and OATP1B3 *in vitro*. Unlike its conjugate, sorafenib-glucuronide, which will be discussed later, the plasma pharmacokinetics of parent sorafenib, or its relative accumulation in the liver, was not substantially altered in either *Oatp1b2*<sup>-/-</sup> mice (DBA background strain), or in *Oatp1a/1b*<sup>(-/-)</sup> mice (FVB background strain) after administration of 10 mg/kg oral sorafenib (Zimmerman et al., 2013). A partial explanation might be that *in vitro* sorafenib was poorly transported by mouse *Oatp1b2*. However, sorafenib transport by the two other prominent sinusoidal uptake transporters in the mouse liver, *Oatp1a1* and *Oatp1a4*, was not tested *in vitro*, so it remains uncertain whether there is an *in vitro/in vivo* discrepancy here (Zimmerman et al., 2013).

Some TKIs have been further tested for their ability to inhibit human OATP1B1 *in vitro* and *in vivo* (Hu et al., 2014). These studies were triggered by clinical observations that coadministration of several TKIs can increase the systemic exposure to docetaxel in cancer patients. The underlying mechanism was poorly understood, but, as docetaxel clearance may in part depend on OATP function (see section 2.1.2), it might involve inhibition of OATPs by these TKIs (Hu et al., 2014). Nearly all 16 tested TKIs inhibited E2G uptake by human OATP1B1 *in vitro* when applied at 10 microM, and 4 of these (axitinib, nilotinib, pazopanib, and sorafenib) by more than 10-fold. Interestingly, three of these (axitinib, pazopanib, and sorafenib) are known to increase the docetaxel AUC by up to 50% or more when coadministered in patients (clinical data for nilotinib/docetaxel coadministration are not available). Further analysis of sorafenib showed that it inhibited docetaxel uptake by OATP1B1 *in vitro* with an IC<sub>50</sub> below 100 nM, and very extensively when applied at 10 microM. Mouse *Oatp1b2* showed similar inhibition of E2G and docetaxel transport by sorafenib *in vitro*. *In vivo*, however, no significant effect of high-dose (60 mg/kg) oral sorafenib coadministration could be demonstrated on 10 mg/kg i.v. docetaxel plasma C<sub>max</sub> or AUC in wild-type, *Oatp1b2*<sup>(-/-)</sup>, *Oatp1a/1b*<sup>(-/-)</sup>, or OATP1B1-humanized mice. Also multiple sorafenib administrations did not elicit significant effects (Hu et al., 2014). Of note, in these specific experiments (see also section 2.1.2 above), the effects of *Oatp1b2* knockout or OATP1B1 transgenics on docetaxel AUC were relatively modest (about 2-fold). This may have rendered these experiments less sensitive to picking up small pharmacokinetic effects of sorafenib-mediated inhibition. The absence of an obvious pharmacokinetic interaction between sorafenib and docetaxel in the various mouse strains suggests that there may be other factors in mice, perhaps alternative or compensatory mechanisms, that can sufficiently offset any changes in OATP1B-like activity towards docetaxel clearance. Also here we have to consider the possibility that interactions of OATPs with certain drugs may be

dependent on the cellular context in which they are expressed (in this case mouse hepatocytes). However that may be, for the moment it remains uncertain whether the observed clinical pharmacokinetic interaction between sorafenib and docetaxel is mediated through OATP1B1, or rather by some other mechanism(s).

### **3. HEPATOCYTE HOPPING OF A CONJUGATED ANTICANCER DRUG: THE CASE OF SORAFENIB GLUCURONIDE**

In contrast to the nearly absent effect of Oatp1b2 or Oatp1a/1b deficiency on the pharmacokinetics of orally administered sorafenib, in the same experiments a pronounced increase in plasma levels of sorafenib glucuronide was observed, with a 5.5-fold increased AUC in Oatp1b2(-/-) mice, and 29-fold in Oatp1a/1b(-/-) mice – although the bigger relative increase in the latter case mainly arose from a substantially lower AUC of sorafenib glucuronide in wild-type FVB mice than in wild-type DBA mice, with the plasma AUCs in both the knockout strains being similar (Zimmerman et al., 2013). The plasma levels of sorafenib glucuronide in the knockout strains equalled or surpassed those of parental sorafenib itself, indicating the quantitative importance of this process. Subsequent *in vitro* experiments indicated that sorafenib glucuronide was efficiently taken up by mouse Oatp1b2 and human OATP1B1 and OATP1B3 expressed in HEK293 cells. Furthermore, transgenic expression of either human OATP1B1 or OATP1B3 in the liver of “humanized” Oatp1a/1b(-/-) mice resulted in a partial reversal of the increased plasma sorafenib glucuronide levels (Zimmerman et al., 2013). This confirmed a prominent role of the mouse and human sinusoidal OATP proteins in hepatic uptake of sorafenib glucuronide.

An important question was the origin of the sorafenib glucuronide, as it is known that both enterocytes and hepatocytes can have substantial drug glucuronidation capacity, and the oral sorafenib might have undergone rapid glucuronidation in the intestinal wall upon absorption. However, mouse intestinal microsomes showed only marginal sorafenib glucuronidation capacity, compared to mouse liver microsomes (>50-fold difference), suggesting that most sorafenib glucuronide had been formed in the liver (Zimmerman et al., 2013). Taken together, these findings suggested strongly that under normal conditions a substantial part of sorafenib glucuronide formed in the liver is extruded across the sinusoidal membrane into the blood, and then taken up again into the liver by Oatp1b2, OATP1B1, and OATP1B3.

### 3.1. Hepatocyte hopping of bilirubin glucuronide

This process inferred to explain the behavior of sorafenib glucuronide was highly reminiscent of the previously proposed “hepatocyte hopping” process for the endogenous metabolite bilirubin glucuronide (Iusuf et al., 2012c; van de Steeg et al., 2012; van de Steeg et al., 2010). The hydrophobic, very poorly water-soluble, and potentially highly toxic unconjugated bilirubin, the primary breakdown product of heme (from hemoglobin) degradation, is directly transported from the spleen, where red blood cells are mostly degraded, via the splenic and portal veins, to the liver. Extensive binding to plasma albumin prevents precipitation of bilirubin in blood. Bilirubin is then efficiently taken up into the liver, presumably in part by Oatp1a/1b transporters, but also by one or more other, substantial, transport mechanisms, which may or may not include passive diffusion. Inside the hepatocytes bilirubin is efficiently conjugated by UGT1A1 to yield bilirubin glucuronide, which is more water-soluble and generally easier to detoxify by the body. Normally, the bulk of hepatic bilirubin glucuronide is excreted into the bile by the ABCC2 multidrug efflux transporter and then released into the small intestinal lumen to leave the body through the feces. However, analysis with a range of different single and combination transporter knockout and transgenic mouse strains has revealed that also under normal circumstances a substantial fraction of hepatic bilirubin glucuronide (possibly up to half of the total amount formed) is secreted by the multidrug efflux transporter ABCC3 across the basolateral (sinusoidal) membrane of hepatocytes into the blood (van de Steeg et al., 2013; van de Steeg et al., 2010). Most of this bilirubin glucuronide is quickly taken up again into the liver by Oatp1a/1b proteins in the mouse, and by OATP1B1 and OATP1B3 in humans, a cycle resulting in very low overall plasma levels of conjugated bilirubin in the general circulation. In contrast, in mice that lack Oatp1a/1b proteins, or in humans that lack both OATP1B1 and OATP1B3 in the liver, the interruption of this cycle leads to highly increased plasma levels of conjugated bilirubin in the general circulation, and somewhat increased levels of unconjugated bilirubin, causing a disorder known as Rotor syndrome (van de Steeg et al., 2012). The phenotype of this Rotor-type conjugated hyperbilirubinemia is fortunately quite benign, mainly a generally mild jaundice.

The underlying mechanistic process, where bilirubin glucuronide is secreted from a hepatocyte by ABCC3 into the sinusoidal blood, only to be taken up again in a downstream hepatocyte via Oatp1a/1b or OATP1B proteins, has been called “hepatocyte hopping”, as it allows bilirubin glucuronide to readily “hop” from one hepatocyte to the next. It has been speculated that this hepatocyte hopping process might be beneficial under circumstances where the bile canalicular excretion of bilirubin glucuronide through ABCC2 in upstream situated hepatocytes is overloaded or otherwise compromised. The hepatocyte hopping salvage pathway for such trapped bilirubin glucuronide allows it

to be secreted back into the blood, and taken up into a downstream hepatocyte, where it has another chance of being excreted into the bile, and so on, and so forth. This added flexibility in the hepatobiliary excretion process of bilirubin glucuronide might reduce the risk of toxic damage due to glucuronide accumulation in upstream hepatocytes (Iusuf et al., 2012b, c; van de Steeg et al., 2012; van de Steeg et al., 2010).

### 3.2. Hepatocyte hopping of sorafenib glucuronide

It has been theorized that this same hepatocyte hopping process might apply to many drugs that are extensively glucuronidated in the liver as well, as the transporters involved (ABCC2, ABCC3, OATP1B1 and OATP1B3 in human, Abcc2, Abcc3 and Oatp1a/1b proteins in mouse) are all known to have very broad substrate specificities, that include the glucuronide conjugates of many compounds (Iusuf et al., 2012c; van de Steeg et al., 2010). Especially as the glucuronide conjugates of several drugs are thought to be important in yielding reactive intermediates that could cause direct or indirect liver damage and toxicity (Zhou et al., 2005), it would be very important to have a mechanism that can relieve the intracellular exposure level of the hepatocyte to these glucuronides also when canalicular excretion is compromised.

The findings with sorafenib glucuronide described above suggested that sorafenib might present an example of a drug (conjugate) that is strongly affected by hepatocyte hopping, analogous to bilirubin. In order to test this hypothesis, the transport and pharmacokinetics of sorafenib and its conjugate were studied *in vitro* and in a number of single and combination knockout mouse strains, in a collaboration between the groups of S. Baker and A.H. Schinkel (Vasilyeva et al., 2015). *In vitro* transport assays indicated that sorafenib glucuronide is efficiently transported by mouse, rat, and human Abcc2/ABCC2, but also by human ABCC3 and ABCC4. Together with the demonstrated transport by Oatp1a/1b and OATP1B1 and OATP1B3, this means that all transport elements minimally necessary for the hepatocyte hopping process are available for sorafenib glucuronide. *In vivo*, after oral administration of sorafenib to Abcc2 knockout mice, the plasma AUC of parental sorafenib was hardly altered, but the plasma AUC of sorafenib glucuronide surged from practically undetectable in wild-type mice to more than 200-fold higher levels in the Abcc2 knockout. The sorafenib glucuronide AUC was also at least 5-fold higher than that of parental sorafenib. As expected, there was a dramatic decrease in biliary excretion of sorafenib glucuronide, from 26% of the administered sorafenib dose over a limited time span in wild-type mice to less than 2.5% in the Abcc2 knockout mice. Sorafenib glucuronide is thus normally extensively excreted into bile, primarily by Abcc2. Accordingly, liver levels of sorafenib glucuronide were 3- to 8-fold increased in the Abcc2 knockout mice (Vasilyeva et al., 2015).

To assess whether Abcc3 and/or Abcc4 were involved in secretion of sorafenib

glucuronide from the hepatocyte back into blood, sorafenib and sorafenib glucuronide pharmacokinetics were studied in various single and combination Abcc3, Abcc4, Oatp1a/1b, and Abcc2 knockout strains, after oral sorafenib administration. Single Abcc3, Abcc4, or Abcc3/4 combination knockout strains displayed no significant effect on plasma AUCs of sorafenib or sorafenib glucuronide, but both the Abcc3-deficient strains had an about 2-fold higher liver-to-plasma ratio of sorafenib glucuronide than wild-type and Abcc4 knockout mice, suggesting a role of Abcc3 in limiting hepatic accumulation of sorafenib glucuronide. Indeed, when the Abcc3 deficiency was combined with either the Oatp1a/1b deficiency, or a combined Oatp1a/1b;Abcc2 deficiency, this resulted in, respectively, a 1.9-fold reduction or a 29% reduction in plasma AUCs of sorafenib glucuronide. This clearly demonstrated that Abcc3 is substantially involved in the transport of sorafenib glucuronide from the hepatocyte back into blood. Liver-to-plasma ratios of sorafenib glucuronide in these combination knockout strains further supported this interpretation. Collectively, these findings provide strong support for the idea that also sorafenib glucuronide is subject to the process of hepatocyte hopping. The fact that sorafenib glucuronidation capacity in the mouse intestine is very small compared to the hepatic glucuronidation capacity (Zimmerman et al., 2013) further strengthens the interpretation that primarily sorafenib glucuronide formed in hepatocytes is subject to the hepatocyte hopping process. **Figure 4** shows a schematic diagram of the hepatocyte hopping process for sorafenib glucuronide, with the legend providing more detail on the separate steps undergone by sorafenib and sorafenib glucuronide.

It should be noted that, in addition to Abcc3, there must be at least one or more other sinusoidal export processes for sorafenib glucuronide, as the reversal of plasma levels of sorafenib glucuronide was far from complete in the various Abcc3 combination knockout strains. Based on the results in the Abcc4-deficient strains it seems unlikely that Abcc4 makes a significant contribution, so the nature of the alternative sinusoidal sorafenib glucuronide exporter(s) still remains to be elucidated. It could well be that the relative contribution of these alternative export processes increases at the elevated hepatocyte concentrations of sorafenib glucuronide that occur in the Abcc2- and/or Abcc3-deficient mice, for instance due to a high(er)  $K_m$  for transport.

Since the hepatocyte hopping process has now been documented for at least two quite divergent compounds (bilirubin glucuronide and sorafenib glucuronide), it stands to reason that it will also apply to many other compounds that are conjugated in the liver, and that are substrates of ABCC2, ABCC3, and the sinusoidal OATP1 proteins. Given the very broad and often overlapping substrate specificity of all of these transporters, encompassing glucuronide-, glutathione-, and sulfoconjugates of many endobiotic and xenobiotic compounds, including many drugs, it seems likely that a large number

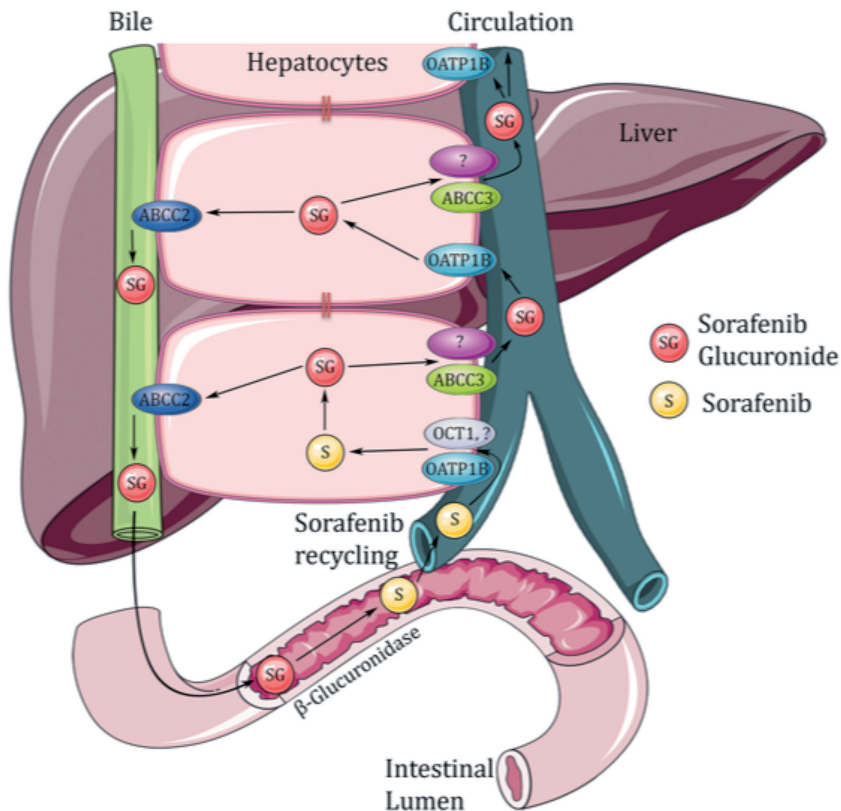


**Figure 4** - Schematic diagram of hepatocyte hopping of sorafenib glucuronide and possible recirculation of sorafenib. This schematic presents the likely situation in human liver, as extrapolated from findings in various knockout and humanized mouse strains. After oral administration and intestinal absorption, sorafenib is taken up into the hepatocytes by incompletely defined mechanisms, possibly including OATP1B-type carriers, OCT1, passive diffusion, and perhaps other transporters. Within the hepatocytes, sorafenib undergoes conjugation by UGT1A9 to form sorafenib glucuronide (SG). SG is secreted into the bile primarily by ABCC2, but under physiological conditions a substantial fraction of intracellular SG can also be secreted back into the blood by sinusoidal ABCC3 and one or more other sinusoidal transport mechanisms. From there SG can be efficiently taken up again by downstream hepatocytes via OATP1B-type carriers (Oatp1a and Oatp1b carriers in mice), resulting in only low SG concentrations reaching the general circulation. This secretion-and-reuptake loop may help to prevent the saturation of ABCC2-mediated biliary SG secretion in hepatocytes positioned upstream within liver lobules. Overall, this can result in efficient biliary elimination and hepatocyte detoxification. Once secreted into the bile, SG enters the intestinal lumen where it can serve as a substrate for bacterial  $\beta$ -glucuronidases that regenerate sorafenib. This sorafenib can then undergo intestinal absorption, thus reentering the circulation. It has been proposed that this ongoing reabsorption of recirculated SG after hydrolysis to sorafenib contributes to the long-lasting sorafenib plasma levels observed in patients (Hilger et al., 2009; Jain et al., 2011; Vasilyeva et al., 2015). This figure was produced using Servier Medical Art ([www.servier.com](http://www.servier.com)).

of drugs and other compounds will be affected by the hepatocyte hopping process to a greater or lesser extent. Moreover, additional broad-specificity canalicular and sinusoidal transporters in the liver, such as ABCG2, possibly ABCB11, ABCC4, and OATP2B1, are likely to further contribute to a wide-ranging impact of the hepatocyte hopping process.

#### **4. SPECIFICITY OF OATP1A/1B-MEDIATED DRUG TRANSPORT MAY DEPEND ON THE CELLULAR CONTEXT**

In the context of this review it is worth noting that in some cases, for unknown reasons, it appears that transport of OATP substrates is strongly dependent on the cellular context (cell type) in which a specific OATP is expressed. For instance, de Graan et al. (2012) found that docetaxel was not appreciably taken up when OATP1B1 was expressed in *Xenopus* oocytes, whereas OATP1B3 in the same system readily mediated docetaxel uptake. In contrast, when OATP1B1 and OATP1B3 were expressed in a human embryonic kidney cell line (HEK293), or in a Chinese Hamster Ovary cell line (CHO), both transporters mediated more or less the same amount of docetaxel uptake. Very similar findings were reported for paclitaxel, which was readily transported by OATP1B1 and OATP1B3 expressed in HEK293 and CHO cells, but not by OATP1B1 expressed in *Xenopus* oocytes, whereas *Xenopus*-expressed OATP1B3 was active (Nieuweboer et al., 2014). Positive control substrates were readily taken up in all these cases. As described above, subsequent studies in humanized mice indicated that OATP1B1 and OATP1B3 can both transport docetaxel *in vivo* when expressed in mouse hepatocytes (Iusuf et al., 2015). Similar observations were further made for doxorubicin by Durmus et al. (2014), who found that *in vitro* in various OATP-transfected HEK293 cells, doxorubicin was not appreciably taken up by human OATP1B1 or OATP1B3, whereas it was taken up by OATP1A2. In contrast, in transgenic humanized mice with overexpression of OATP1B1 or OATP1B3 in the liver, clearly increased liver-to-plasma ratios of doxorubicin were seen, indicating that in mouse hepatocytes these proteins can mediate appreciable doxorubicin uptake. Of note, though, transgenic OATP1A2 was even more effective in mediating doxorubicin uptake into mouse hepatocytes *in vivo* (Durmus et al., 2014). We therefore cannot exclude that the discrepancy with doxorubicin uptake in the cell lines may in part have been a sensitivity issue related to expression levels of the transporters.

However that may be, the mechanistic background of such discrepancies is as yet a mystery. One can speculate that perhaps in some cases a covalent modification of an OATP (like phosphorylation or similar process) must occur in order for a certain substrate to be recognized, and that the capacity to make such modifications differs

strongly between cell types. There may also be substrate-specific competitive or non-competitive inhibition or stimulation of transport of certain substrates by an OATP by some compounds abundant in some cell types, but not in others. In fact, heterotropic or even homotropic cooperativity phenomena are quite common for multidrug-handling proteins like CYP3A (Ekroos and Sjogren, 2006; Harlow and Halpert, 1998) or multispecific ABC transporters like P-glycoprotein (ABCB1) and ABCC2 (Aller et al., 2009; Bakos et al., 2000; Huisman et al., 2002; Kondratov et al., 2001; Shapiro and Ling, 1998; Zelcer et al., 2003), and this might also apply to the multidrug-handling OATPs. Indeed, a number of compounds have been identified that can stimulate OATP-mediated uptake of some, but not all known substrates of OATP1B1 and/or OATP1B3 (e.g. Gui et al., 2008; Ohnishi et al., 2014; Roth et al., 2011). If the presence of such (endogenous) co-stimulatory or inhibitory molecules differs between cell types, they may also affect the apparent substrate specificity of OATPs between cell types. Differential pH-dependent uptake of various substrates by OATPs (e.g. Leuthold et al., 2009; Martinez-Becerra et al., 2011; Oostendorp et al., 2009) can perhaps sometimes play a role, and there may be other mechanisms involved that have not been realized yet. Resolving these aspects will present an interesting area for future research into OATP functioning.

## 5. CONCLUDING REMARKS AND FUTURE PERSPECTIVE

With this review we have aimed to provide a number of illustrations of how the recent use of knockout and transgenic (humanized) *Oatp1a/1b* and OATP1A/1B mouse strains has helped us to gain insight into the *in vivo* functioning of OATP1A/1B transporters, especially with respect to antitumor agents. Apart from their pharmacokinetic and toxicological functions, also a number of physiological functions of OATP1A/1B proteins have been further elucidated, as well as their interaction with several other transporters, although clearly more work needs to be done in this area. We further touched upon possible pitfalls that can occur during the use of these mouse models, such as the up- (and down-)regulation of a number of carboxylesterase genes in the knockout and transgenic mice. Nonetheless, we think we can safely state that, when used judiciously, these mouse models can yield a wealth of information on the *in vivo* functions of OATP1A/1B proteins.

We would like to point out that, while our opinion is that these mouse models are extremely powerful in elucidating principles of *in vivo* OATP1A/1B functions, one should still use the utmost caution in directly extrapolating from findings in the humanized mouse models to the situation in human patients. An important reason for this is that, even while one may have reproduced the right level of expression and activity of a

humanized protein in the right cellular or organ compartment, one still is studying the behavior of this protein in the complex context of a mouse. This context may well differ in some relevant aspects for the parameter studied from the context in a human patient. This caveat should always be borne in mind, and ultimately only careful studies in patients can point out whether the insights and results obtained with the mouse models do also apply fully in humans.

Having said that, we think that there are many additional interesting and promising research lines in cancer and general drug disposition and toxicology, but also in broader physiology, that can be explored with the current set of OATP1A/1B mouse models. Such possibilities can be even further expanded by creating new combinations with existing or newly generated knockout and transgenic mouse lines for other drug transporters and drug-metabolizing enzymes.

### **Acknowledgements**

Part of the work in the Schinkel group reviewed in this paper was funded by grant NKI 2007-3764 of the Dutch Cancer Society to A.H. Schinkel.

## REFERENCES

- T. Abe, M. Unno, T. Onogawa, T. Tokui, T.N. Kondo, R. Nakagomi, H. Adachi, K. Fujiwara, M. Okabe, T. Suzuki, K. Nunoki, E. Sato, M. Kakyo, T. Nishio, J. Sugita, N. Asano, M. Tanemoto, M. Seki, F. Date, K. Ono, Y. Kondo, K. Shiiba, M. Suzuki, H. Ohtani, T. Shimosegawa, K. Iinuma, H. Nagura, S. Ito and S. Matsuno, LST-2, a human liver-specific organic anion transporter, determines methotrexate sensitivity in gastrointestinal cancers, *Gastroenterology* 120 (2001), pp. 1689-1699.
- S.G. Aller, J. Yu, A. Ward, Y. Weng, S. Chittaboina, R. Zhuo, P.M. Harrell, Y.T. Trinh, Q. Zhang, I.L. Urbatsch and G. Chang, Structure of P-glycoprotein reveals a molecular basis for poly-specific drug binding, *Science* 323 (2009), pp. 1718-1722.
- I. Badagnani, R.A. Castro, T.R. Taylor, C.M. Brett, C.C. Huang, D. Stryke, M. Kawamoto, S.J. Johns, T.E. Ferrin, E.J. Carlson, E.G. Burchard and K.M. Giacomini, Interaction of methotrexate with organic-anion transporting polypeptide 1A2 and its genetic variants, *J Pharmacol Exp Ther* 318 (2006), pp. 521-529.
- S.D. Baker, J. Verweij, G.A. Cusatis, R.H. van Schaik, S. Marsh, S.J. Orwick, R.M. Franke, S. Hu, E.G. Schuetz, V. Lamba, W.A. Messersmith, A.C. Wolff, M.A. Carducci and A. Sparreboom, Pharmacogenetic pathway analysis of docetaxel elimination, *Clin Pharmacol Ther* 85 (2009), pp. 155-163.
- E. Bakos, R. Evers, E. Sinko, A. Varadi, P. Borst and B. Sarkadi, Interactions of the human multidrug resistance proteins MRP1 and MRP2 with organic anions, *Mol Pharmacol* 57 (2000), pp. 760-768.
- X. Cheng, J. Maher, C. Chen and C.D. Klaassen, Tissue distribution and ontogeny of mouse organic anion transporting polypeptides (Oatps), *Drug Metab Dispos* 33 (2005), pp. 1062-1073.
- H. Cortes-Funes and C. Coronado, Role of anthracyclines in the era of targeted therapy, *Cardiovasc Toxicol* 7 (2007), pp. 56-60.
- Y. Cui, J. Konig, A.T. Nies, M. Pfannschmidt, M. Hergt, W.W. Franke, W. Alt, R. Moll and D. Keppler, Detection of the human organic anion transporters SLC21A6 (OATP2) and SLC21A8 (OATP8) in liver and hepatocellular carcinoma, *Lab Invest* 83 (2003), pp. 527-538.
- A.J. de Graan, C.S. Lancaster, A. Obaidat, B. Hagenbuch, L. Elens, L.E. Friberg, P. de Buijn, S. Hu, A.A. Gibson, G.H. Bruun, T.J. Corydon, T.S. Mikkelsen, A.L. Walker, G. Du, W.J. Loos, R.H. van Schaik, S.D. Baker, R.H. Mathijssen and A. Sparreboom, Influence of polymorphic OATP1B-type carriers on the disposition of docetaxel, *Clin Cancer Res* 18 (2012), pp. 4433-4440.
- M. Drozdziak, C. Groer, J. Penski, J. Lapczuk, M. Ostrowski, Y. Lai, B. Prasad, J.D. Unadkat, W. Siegmund and S. Oswald, Protein abundance of clinically relevant multidrug transporters along the entire length of the human intestine, *Mol Pharm* 11 (2014), pp. 3547-3555.
- B.J. Druker, M. Talpaz, D.J. Resta, B. Peng, E. Buchdunger, J.M. Ford, N.B. Lydon, H. Kantarjian, R. Capdeville, S. Ohno-Jones and C.L. Sawyers, Efficacy and safety of a specific inhibitor of the BCR-ABL tyrosine kinase in chronic myeloid leukemia, *N Engl J Med* 344 (2001), pp. 1031-1037.
- S. Durmus, G. Lozano-Mena, A. van Esch, E. Wagenaar, O. van Tellingen and A.H. Schinkel, Preclinical Mouse Models To Study Human OATP1B1- and OATP1B3-Mediated Drug-Drug Interactions in Vivo, *Mol Pharm* 12 (2015), pp. 4259-4269.
- S. Durmus, J. Naik, L. Buil, E. Wagenaar, O. van Tellingen and A.H. Schinkel, In vivo disposition of doxorubicin is affected by mouse Oatp1a/1b and human OATP1A/1B transporters, *Int J Cancer* 135 (2014), pp. 1700-1710.
- M. Ekroos and T. Sjogren, Structural basis for ligand promiscuity in cytochrome P450 3A4, *Proc Natl Acad Sci U S A* 103 (2006), pp. 13682-13687.
- W.D. Figg, 2nd and W.D. Figg, Cabazitaxel: filling one of the gaps in the treatment of prostate cancer, *Cancer Biol Ther* 10 (2010), pp. 1233-1234.
- R.M. Franke, L.A. Scherkenbach and A. Sparreboom, Pharmacogenetics of the organic anion transporting polypeptide 1A2, *Pharmacogenomics* 10 (2009), pp. 339-344.
- B. Gao, B. Hagenbuch, G.A. Kullak-Ublick, D. Benke, A. Aguzzi and P.J. Meier, Organic anion-transporting polypeptides mediate transport of opioid peptides across blood-brain barrier, *J Pharmacol Exp Ther* 294 (2000), pp. 73-79.
- D.A. Gewirtz, A critical evaluation of the mechanisms of action proposed for the antitumor effects of the anthracycline antibiotics adriamycin and daunorubicin, *Biochem Pharmacol* 57 (1999), pp. 727-741.

- H. Glaeser, D.G. Bailey, G.K. Dresser, J.C. Gregor, U.I. Schwarz, J.S. McGrath, E. Jolicoeur, W. Lee, B.F. Leake, R.G. Tirona and R.B. Kim, Intestinal drug transporter expression and the impact of grapefruit juice in humans, *Clin Pharmacol Ther* 81 (2007), pp. 362-370.
- J. Gligorov and J.P. Lotz, Pre-clinical pharmacology of the taxanes: implications of the differences, *Oncologist* 9 Suppl 2 (2004), pp. 3-8.
- I.Y. Gong and R.B. Kim, Impact of genetic variation in OATP transporters to drug disposition and response, *Drug Metab Pharmacokinet* 28 (2013), pp. 4-18.
- L. Gong, N. Aranibar, Y.H. Han, Y. Zhang, L. Lecureux, V. Bhaskaran, P. Khandelwal, C.D. Klaassen and L.D. Lehman-McKeeman, Characterization of organic anion-transporting polypeptide (Oatp) 1a1 and 1a4 null mice reveals altered transport function and urinary metabolomic profiles, *Toxicol Sci* 122 (2011), pp. 587-597.
- M.A. Grenier and S.E. Lipshultz, Epidemiology of anthracycline cardiotoxicity in children and adults, *Semin Oncol* 25 (1998), pp. 72-85.
- C. Gui, Y. Miao, L. Thompson, B. Wahlgren, M. Mock, B. Stieger and B. Hagenbuch, Effect of pregnane X receptor ligands on transport mediated by human OATP1B1 and OATP1B3, *Eur J Pharmacol* 584 (2008), pp. 57-65.
- J.Y. Han, H.S. Lim, E.S. Shin, Y.K. Yoo, Y.H. Park, J.E. Lee, H.T. Kim and J.S. Lee, Influence of the organic anion-transporting polypeptide 1B1 (OATP1B1) polymorphisms on irinotecan-pharmacokinetics and clinical outcome of patients with advanced non-small cell lung cancer, *Lung Cancer* 59 (2008), pp. 69-75.
- G.R. Harlow and J.R. Halpert, Analysis of human cytochrome P450 3A4 cooperativity: construction and characterization of a site-directed mutant that displays hyperbolic steroid hydroxylation kinetics, *Proc Natl Acad Sci U S A* 95 (1998), pp. 6636-6641.
- J.W. Higgins, J.Q. Bao, A.B. Ke, J.R. Manro, J.K. Fallon, P.C. Smith and M.J. Zamek-Gliszczynski, Utility of Oatp1a/1b-knockout and OATP1B1/3-humanized mice in the study of OATP-mediated pharmacokinetics and tissue distribution: case studies with pravastatin, atorvastatin, simvastatin, and carboxydichlorofluorescein, *Drug Metab Dispos* 42 (2014), pp. 182-192.
- R.A. Hilger, H. Richly, M. Grubert, S. Kredtke, D. Thyssen, W. Eberhardt, J. Hense, M. Schuler and M.E. Scheulen, Pharmacokinetics of sorafenib in patients with renal impairment undergoing hemodialysis, *Int J Clin Pharmacol Ther* 47 (2009), pp. 61-64.
- R.S. Holmes, M.W. Wright, S.J. Laulerkind, L.A. Cox, M. Hosokawa, T. Imai, S. Ishibashi, R. Lehner, M. Miyazaki, E.J. Perkins, P.M. Potter, M.R. Redinbo, J. Robert, T. Satoh, T. Yamashita, B. Yan, T. Yokoi, R. Zechner and L.J. Maltais, Recommended nomenclature for five mammalian carboxylesterase gene families: human, mouse, and rat genes and proteins, *Mamm Genome* 21 (2010), pp. 427-441.
- S. Hu, R.M. Franke, K.K. Filipksi, C. Hu, S.J. Orwick, E.A. de Bruijn, H. Burger, S.D. Baker and A. Sparreboom, Interaction of imatinib with human organic ion carriers, *Clin Cancer Res* 14 (2008), pp. 3141-3148.
- S. Hu, R.H. Mathijssen, P. de Bruijn, S.D. Baker and A. Sparreboom, Inhibition of OATP1B1 by tyrosine kinase inhibitors: in vitro-in vivo correlations, *Br J Cancer* 110 (2014), pp. 894-898.
- M.T. Huisman, J.W. Smit, K.M. Crommentuyn, N. Zelcer, H.R. Wiltshire, J.H. Beijnen and A.H. Schinkel, Multidrug resistance protein 2 (MRP2) transports HIV protease inhibitors, and transport can be enhanced by other drugs, *AIDS* 16 (2002), pp. 2295-2301.
- F. Innocenti, D.L. Kroetz, E. Schuetz, M.E. Dolan, J. Ramirez, M. Relling, P. Chen, S. Das, G.L. Rosner and M.J. Ratain, Comprehensive pharmacogenetic analysis of irinotecan neutropenia and pharmacokinetics, *J Clin Oncol* 27 (2009), pp. 2604-2614.
- D. Iusuf, J.J. Hendriks, A. van Esch, E. van de Steeg, E. Wagenaar, H. Rosing, J.H. Beijnen and A.H. Schinkel, Human OATP1B1, OATP1B3 and OATP1A2 can mediate the in vivo uptake and clearance of docetaxel, *Int J Cancer* 136 (2015), pp. 225-233.
- D. Iusuf, M. Ludwig, A. Elbatsh, A. van Esch, E. van de Steeg, E. Wagenaar, M. van der Valk, F. Lin, O. van Tellingen and A.H. Schinkel, OATP1A/1B transporters affect irinotecan and SN-38 pharmacokinetics and carboxylesterase expression in knockout and humanized transgenic mice, *Mol Cancer Ther* 13 (2014), pp. 492-503.
- D. Iusuf, R.W. Sparidans, A. van Esch, M. Hobbs, K.E. Kenworthy, E. van de Steeg, E. Wagenaar, J.H. Beijnen and A.H. Schinkel, Organic anion-transporting polypeptides 1a/1b control the hepatic uptake of pravastatin in mice, *Mol Pharm* 9 (2012a), pp. 2497-2504.
- D. Iusuf, E. van de Steeg and A.H. Schinkel, Functions of OATP1A and 1B transporters in vivo: insights from mouse models, *Trends Pharmacol Sci* 33 (2012b), pp. 100-108.

- D. Iusuf, E. van de Steeg and A.H. Schinkel, Hepatocyte hopping of OATP1B substrates contributes to efficient hepatic detoxification, *Clin Pharmacol Ther* 92 (2012c), pp. 559-562.
- D. Iusuf, A. van Esch, M. Hobbs, M. Taylor, K.E. Kenworthy, E. van de Steeg, E. Wagenaar and A.H. Schinkel, Murine Oatp1a/1b uptake transporters control rosuvastatin systemic exposure without affecting its apparent liver exposure, *Mol Pharmacol* 83 (2013), pp. 919-929.
- L. Jain, S. Woo, E.R. Gardner, W.L. Dahut, E.C. Kohn, S. Kummar, D.R. Mould, G. Giaccone, R. Yarchoan, J. Venitz and W.D. Figg, Population pharmacokinetic analysis of sorafenib in patients with solid tumours, *Br J Clin Pharmacol* 72 (2011), pp. 294-305.
- R.V. Kondratov, P.G. Komarov, Y. Becker, A. Ewenson and A.V. Gudkov, Small molecules that dramatically alter multidrug resistance phenotype by modulating the substrate specificity of P-glycoprotein, *Proc Natl Acad Sci U S A* 98 (2001), pp. 14078-14083.
- J. König, F. Müller and M.F. Fromm, Transporters and drug-drug interactions: important determinants of drug disposition and effects, *Pharmacol Rev* 65 (2013), pp. 944-966.
- S.L. Koolen, J.H. Beijnen and J.H. Schellens, Intravenous-to-oral switch in anticancer chemotherapy: a focus on docetaxel and paclitaxel, *Clin Pharmacol Ther* 87 (2010), pp. 126-129.
- J.S. Lagas, C.W. Damen, R.A. van Waterschoot, D. Iusuf, J.H. Beijnen and A.H. Schinkel, P-glycoprotein, multidrug-resistance associated protein 2, Cyp3a, and carboxylesterase affect the oral availability and metabolism of vinorelbine, *Mol Pharmacol* 82 (2012), pp. 636-644.
- C.S. Lancaster, J.A. Sprowl, A.L. Walker, S. Hu, A.A. Gibson and A. Sparreboom, Modulation of OATP1B-type transporter function alters cellular uptake and disposition of platinum chemotherapeutics, *Mol Cancer Ther* 12 (2013), pp. 1537-1544.
- H.H. Lee, B.F. Leake, W. Teft, R.G. Tirona, R.B. Kim and R.H. Ho, Contribution of hepatic organic anion-transporting polypeptides to docetaxel uptake and clearance, *Mol Cancer Ther* 14 (2015), pp. 994-1003.
- W. Lee, H. Glaeser, L.H. Smith, R.L. Roberts, G.W. Moeckel, G. Gervasini, B.F. Leake and R.B. Kim, Polymorphisms in human organic anion-transporting polypeptide 1A2 (OATP1A2): implications for altered drug disposition and central nervous system drug entry, *J Biol Chem* 280 (2005), pp. 9610-9617.
- S. Leuthold, B. Hagenbuch, N. Mohebbi, C.A. Wagner, P.J. Meier and B. Stieger, Mechanisms of pH-gradient driven transport mediated by organic anion polypeptide transporters, *Am J Physiol Cell Physiol* 296 (2009), pp. C570-582.
- H. Lu, S. Choudhuri, K. Ogura, I.L. Csanaky, X. Lei, X. Cheng, P.Z. Song and C.D. Klaassen, Characterization of organic anion transporting polypeptide 1b2-null mice: essential role in hepatic uptake/toxicity of phalloidin and microcystin-LR, *Toxicol Sci* 103 (2008), pp. 35-45.
- P. Martínez-Becerra, O. Briz, M.R. Romero, R.I. Macías, M.J. Pérez, C. Sancho-Mateo, M.P. Lostao, J.M. Fernández-Abalos and J.J. Marin, Further characterization of the electrogenicity and pH sensitivity of the human organic anion-transporting polypeptides OATP1B1 and OATP1B3, *Mol Pharmacol* 79 (2011), pp. 596-607.
- R.H. Mathijssen, W.J. Loos, J. Verweij and A. Sparreboom, Pharmacology of topoisomerase I inhibitors irinotecan (CPT-11) and topotecan, *Curr Cancer Drug Targets* 2 (2002), pp. 103-123.
- G. Minotti, P. Menna, E. Salvatorelli, G. Cairo and L. Gianni, Anthracyclines: molecular advances and pharmacologic developments in antitumor activity and cardiotoxicity, *Pharmacol Rev* 56 (2004), pp. 185-229.
- N.R. Monks, S. Liu, Y. Xu, H. Yu, A.S. Bendelow and J.A. Moscow, Potent cytotoxicity of the phosphatase inhibitor microcystin LR and microcystin analogues in OATP1B1- and OATP1B3-expressing HeLa cells, *Mol Cancer Ther* 6 (2007), pp. 587-598.
- M. Muto, T. Onogawa, T. Suzuki, T. Ishida, T. Rikiyama, Y. Katayose, N. Ohuchi, H. Sasano, T. Abe and M. Unno, Human liver-specific organic anion transporter-2 is a potent prognostic factor for human breast carcinoma, *Cancer Sci* 98 (2007), pp. 1570-1576.
- T. Nakanishi and I. Tamai, Genetic polymorphisms of OATP transporters and their impact on intestinal absorption and hepatic disposition of drugs, *Drug Metab Pharmacokinet* 27 (2012), pp. 106-121.
- T. Nakanishi and I. Tamai, Putative roles of organic anion transporting polypeptides (OATPs) in cell survival and progression of human cancers, *Biopharm Drug Dispos* 35 (2014), pp. 463-484.
- M. Niemi, M.K. Pasanen and P.J. Neuvonen, Organic anion transporting polypeptide 1B1: a genetically polymorphic transporter of major importance for hepatic drug uptake, *Pharmacol Rev* 63 (2011), pp. 157-181.

- A.J. Nieuweboer, S. Hu, C. Gui, B. Hagenbuch, I.M. Ghobadi Moghaddam-Helmantel, A.A. Gibson, P. de Bruijn, R.H. Mathijssen and A. Sparreboom, Influence of drug formulation on OATP1B-mediated transport of paclitaxel, *Cancer Res* 74 (2014), pp. 3137-3145.
- T. Nozawa, H. Minami, S. Sugiura, A. Tsuji and I. Tamai, Role of organic anion transporter OATP1B1 (OATP-C) in hepatic uptake of irinotecan and its active metabolite, 7-ethyl-10-hydroxycamptothecin: in vitro evidence and effect of single nucleotide polymorphisms, *Drug Metab Dispos* 33 (2005), pp. 434-439.
- A. Obaidat, M. Roth and B. Hagenbuch, The expression and function of organic anion transporting polypeptides in normal tissues and in cancer, *Annu Rev Pharmacol Toxicol* 52 (2012), pp. 135-151.
- S. Ohnishi, A. Hays and B. Hagenbuch, Cysteine scanning mutagenesis of transmembrane domain 10 in organic anion transporting polypeptide 1B1, *Biochemistry* 53 (2014), pp. 2261-2270.
- M. Okabe, M. Unno, H. Harigae, M. Kaku, Y. Okitsu, T. Sasaki, T. Mizoi, K. Shiiba, H. Takanaga, T. Terasaki, S. Matsuno, I. Sasaki, S. Ito and T. Abe, Characterization of the organic cation transporter SLC22A16: a doxorubicin importer, *Biochem Biophys Res Commun* 333 (2005), pp. 754-762.
- R.L. Oostendorp, E. van de Steeg, C.M. van der Kruijssen, J.H. Beijnen, K.E. Kenworthy, A.H. Schinkel and J.H. Schellens, Organic anion-transporting polypeptide 1B1 mediates transport of Gimatecan and BNP1350 and can be inhibited by several classic ATP-binding cassette (ABC) B1 and/or ABCG2 inhibitors, *Drug Metab Dispos* 37 (2009), pp. 917-923.
- A. Ose, H. Kusahara, C. Endo, K. Tohyama, M. Miyajima, S. Kitamura and Y. Sugiyama, Functional characterization of mouse organic anion transporting peptide 1a4 in the uptake and efflux of drugs across the blood-brain barrier, *Drug Metab Dispos* 38 (2010), pp. 168-176.
- M. Roth, J.J. Araya, B.N. Timmermann and B. Hagenbuch, Isolation of modulators of the liver-specific organic anion-transporting polypeptides (OATPs) 1B1 and 1B3 from *Rollinia emarginata* Schlecht (Annonaceae), *J Pharmacol Exp Ther* 339 (2011), pp. 624-632.
- E.K. Rowinsky and R.C. Donehower, Paclitaxel (taxol), *N Engl J Med* 332 (1995), pp. 1004-1014.
- L. Salphati, X. Chu, L. Chen, B. Prasad, S. Dallas, R. Evers, D. Mamaril-Fishman, E.G. Geier, J. Kehler, J. Kunta, M. Mezler, L. Laplanche, J. Pang, A. Rode, M.G. Soars, J.D. Unadkat, R.A. van Waterschoot, J. Yabut, A.H. Schinkel and N. Scheer, Evaluation of organic anion transporting polypeptide 1B1 and 1B3 humanized mice as a translational model to study the pharmacokinetics of statins, *Drug Metab Dispos* 42 (2014), pp. 1301-1313.
- M. Sasaki, H. Suzuki, J. Aoki, K. Ito, P.J. Meier and Y. Sugiyama, Prediction of in vivo biliary clearance from the in vitro transcellular transport of organic anions across a double-transfected Madin-Darby canine kidney II monolayer expressing both rat organic anion transporting polypeptide 4 and multidrug resistance associated protein 2, *Mol Pharmacol* 66 (2004), pp. 450-459.
- A.B. Shapiro and V. Ling, The mechanism of ATP-dependent multidrug transport by P-glycoprotein, *Acta Physiol Scand Suppl* 643 (1998), pp. 227-234.
- Y. Shitara, K. Maeda, K. Ikejiri, K. Yoshida, T. Horie and Y. Sugiyama, Clinical significance of organic anion transporting polypeptides (OATPs) in drug disposition: their roles in hepatic clearance and intestinal absorption, *Biopharm Drug Dispos* 34 (2013), pp. 45-78.
- T.M. Sissung, K.M. Reece, S. Spencer and W.D. Figg, Contribution of the OATP1B subfamily to cancer biology and treatment, *Clin Pharmacol Ther* 92 (2012), pp. 658-660.
- N.F. Smith, W.D. Figg and A. Sparreboom, Pharmacogenetics of irinotecan metabolism and transport: an update, *Toxicol In Vitro* 20 (2006), pp. 163-175.
- A. Sparreboom and R.H. Mathijssen, Hepatic uptake transporters and docetaxel disposition in mice—letter, *Clin Cancer Res* 20 (2014), p. 4167.
- J.A. Sprowl and A. Sparreboom, Uptake carriers and oncology drug safety, *Drug Metab Dispos* 42 (2014), pp. 611-622.
- J. Stangier, C.A. Su and W. Roth, Pharmacokinetics of orally and intravenously administered telmisartan in healthy young and elderly volunteers and in hypertensive patients, *J Int Med Res* 28 (2000), pp. 149-167.
- B. Stieger and B. Hagenbuch, Organic anion-transporting polypeptides, *Curr Top Membr* 73 (2014), pp. 205-232.
- M. Svoboda, K. Wlcek, B. Taferner, S. Hering, B. Stieger, D. Tong, R. Zeillinger, T. Thalhammer and W. Jager, Expression of organic anion-transporting polypeptides 1B1 and 1B3 in ovarian cancer cells: relevance for paclitaxel transport, *Biomed Pharmacother* 65 (2011), pp. 417-426.

- H. Takane, K. Kawamoto, T. Sasaki, K. Moriki, K. Moriki, H. Kitano, S. Higuchi, K. Otsubo and I. Ieiri, Life-threatening toxicities in a patient with UGT1A1\*6/\*28 and SLCO1B1\*15/\*15 genotypes after irinotecan-based chemotherapy, *Cancer Chemother Pharmacol* 63 (2009), pp. 1165-1169.
- S.C. Tang, J.J. Hendrikk, J.H. Beijnen and A.H. Schinkel, Genetically modified mouse models for oral drug absorption and disposition, *Curr Opin Pharmacol* 13 (2013), pp. 853-858.
- S.C. Tang, A. Kort, K.L. Cheung, H. Rosing, T. Fukami, S. Durmus, E. Wagenaar, J.J. Hendrikk, M. Nakajima, B.J. van Vlijmen, J.H. Beijnen and A.H. Schinkel, P-glycoprotein, CYP3A, and Plasma Carboxylesterase Determine Brain Disposition and Oral Availability of the Novel Taxane Cabazitaxel (Jevtana) in Mice, *Mol Pharm* 12 (2015), pp. 3714-3723.
- S.C. Tang, R.W. Sparidans, K.L. Cheung, T. Fukami, S. Durmus, E. Wagenaar, T. Yokoi, B.J. van Vlijmen, J.H. Beijnen and A.H. Schinkel, P-glycoprotein, CYP3A, and plasma carboxylesterase determine brain and blood disposition of the mTOR Inhibitor everolimus (Afinitor) in mice, *Clin Cancer Res* 20 (2014), pp. 3133-3145.
- N. Thakkar, A.C. Lockhart and W. Lee, Role of Organic Anion-Transporting Polypeptides (OATPs) in Cancer Therapy, *AAPS J* 17 (2015), pp. 535-545.
- L.R. Trevino, N. Shimasaki, W. Yang, J.C. Panetta, C. Cheng, D. Pei, D. Chan, A. Sparreboom, K.M. Giacomini, C.H. Pui, W.E. Evans and M.V. Relling, Germline genetic variation in an organic anion transporter polypeptide associated with methotrexate pharmacokinetics and clinical effects, *J Clin Oncol* 27 (2009), pp. 5972-5978.
- E. van de Steeg, V. Stranecky, H. Hartmannova, L. Noskova, M. Hrebicek, E. Wagenaar, A. van Esch, D.R. de Waart, R.P. Oude Elferink, K.E. Kenworthy, E. Sticova, M. al-Edreesi, A.S. Knisely, S. Kmoch, M. Jirsa and A.H. Schinkel, Complete OATP1B1 and OATP1B3 deficiency causes human Rotor syndrome by interrupting conjugated bilirubin reuptake into the liver, *J Clin Invest* 122 (2012), pp. 519-528.
- E. van de Steeg, C.M. van der Kruijssen, E. Wagenaar, J.E. Burggraaff, E. Mesman, K.E. Kenworthy and A.H. Schinkel, Methotrexate pharmacokinetics in transgenic mice with liver-specific expression of human organic anion-transporting polypeptide 1B1 (SLCO1B1), *Drug Metab Dispos* 37 (2009), pp. 277-281.
- E. van de Steeg, A. van Esch, E. Wagenaar, K.E. Kenworthy and A.H. Schinkel, Influence of human OATP1B1, OATP1B3, and OATP1A2 on the pharmacokinetics of methotrexate and paclitaxel in humanized transgenic mice, *Clin Cancer Res* 19 (2013), pp. 821-832.
- E. van de Steeg, A. van Esch, E. Wagenaar, C.M. van der Kruijssen, O. van Tellingen, K.E. Kenworthy and A.H. Schinkel, High impact of Oatp1a/1b transporters on in vivo disposition of the hydrophobic anticancer drug paclitaxel, *Clin Cancer Res* 17 (2011), pp. 294-301.
- E. van de Steeg, E. Wagenaar, C.M. van der Kruijssen, J.E. Burggraaff, D.R. de Waart, R.P. Elferink, K.E. Kenworthy and A.H. Schinkel, Organic anion transporting polypeptide 1a/1b-knockout mice provide insights into hepatic handling of bilirubin, bile acids, and drugs, *J Clin Invest* 120 (2010), pp. 2942-2952.
- S. van Outryve, D. Schrijvers, J. van den Brande, P. Wilmes, J. Bogers, E. van Marck and J.B. Vermorken, Methotrexate-associated liver toxicity in a patient with breast cancer: case report and literature review, *Neth J Med* 60 (2002), pp. 216-222.
- A. Vasilyeva, S. Durmus, L. Li, E. Wagenaar, S. Hu, A.A. Gibson, J.C. Panetta, S. Mani, A. Sparreboom, S.D. Baker and A.H. Schinkel, Hepatocellular Shuttling and Recirculation of Sorafenib-Glucuronide Is Dependent on Abcc2, Abcc3, and Oatp1a/1b, *Cancer Res* 75 (2015), pp. 2729-2736.
- T. Watanabe, H. Kusuvara, K. Maeda, Y. Shitara and Y. Sugiyama, Physiologically based pharmacokinetic modeling to predict transporter-mediated clearance and distribution of pravastatin in humans, *J Pharmacol Exp Ther* 328 (2009), pp. 652-662.
- T. Watanabe, H. Kusuvara and Y. Sugiyama, Application of physiologically based pharmacokinetic modeling and clearance concept to drugs showing transporter-mediated distribution and clearance in humans, *J Pharmacokinetic Pharmacodyn* 37 (2010), pp. 575-590.
- J.A. Wessels, T.W. Huizinga and H.J. Guchelaar, Recent insights in the pharmacological actions of methotrexate in the treatment of rheumatoid arthritis, *Rheumatology (Oxford)* 47 (2008), pp. 249-255.
- P. Wu, T.E. Nielsen and M.H. Clausen, FDA-approved small-molecule kinase inhibitors, *Trends Pharmacol Sci* 36 (2015), pp. 422-439.
- X. Xiang, S.R. Jada, H.H. Li, L. Fan, L.S. Tham, C.I. Wong, S.C. Lee, R. Lim, Q.Y. Zhou, B.C. Goh, E.H. Tan and B. Chowbay, Pharmacogenetics of SLCO1B1 gene and the impact of \*1b and \*15 haplotypes on irinotecan disposition in Asian cancer patients, *Pharmacogenet Genomics* 16 (2006), pp. 683-691.

- H. Yamaguchi, M. Kobayashi, M. Okada, T. Takeuchi, M. Unno, T. Abe, J. Goto, T. Hishinuma and N. Mano, Rapid screening of antineoplastic candidates for the human organic anion transporter OATP1B3 substrates using fluorescent probes, *Cancer Lett* 260 (2008), pp. 163-169.
- H. Zaher, H.E. Meyer zu Schwabedissen, R.G. Tirona, M.L. Cox, L.A. Obert, N. Agrawal, J. Palandra, J.L. Stock, R.B. Kim and J.A. Ware, Targeted disruption of murine organic anion-transporting polypeptide 1b2 (Oatp1b2/Slco1b2) significantly alters disposition of prototypical drug substrates pravastatin and rifampin, *Mol Pharmacol* 74 (2008), pp. 320-329.
- N. Zelcer, M.T. Huisman, G. Reid, P. Wielinga, P. Breedveld, A. Kuil, P. Knipscheer, J.H. Schellens, A.H. Schinkel and P. Borst, Evidence for two interacting ligand binding sites in human multidrug resistance protein 2 (ATP binding cassette C2), *J Biol Chem* 278 (2003), pp. 23538-23544.
- S. Zhou, E. Chan, W. Duan, M. Huang and Y.Z. Chen, Drug bioactivation, covalent binding to target proteins and toxicity relevance, *Drug Metab Rev* 37 (2005), pp. 41-213.
- E.I. Zimmerman, S. Hu, J.L. Roberts, A.A. Gibson, S.J. Orwick, L. Li, A. Sparreboom and S.D. Baker, Contribution of OATP1B1 and OATP1B3 to the disposition of sorafenib and sorafenib-glucuronide, *Clin Cancer Res* 19 (2013), pp. 1458-1466.





# 7

---

## Conclusions and future perspectives

---



In this thesis we investigated the pharmacological functions of ABC efflux transporters *in vitro*, by using transwell transport assays and *in vivo*, by using the single and combination knockout mouse models of ABCB1 and ABCG2. We demonstrated the usefulness of these mouse models to study the impact of ABCB1 and ABCG2 on oral availability of several transported targeted anticancer drugs and their organ exposure – especially for the brain. We have shown that dual deficiency of ABCB1 and ABCG2 most effectively increases the brain penetration of the studied tyrosine kinase inhibitors (TKIs) and, when applicable, their active metabolite(s). We further used CYP3A knockout and humanized transgenic mouse models to assess the *in vivo* impact of this multispecific drug-metabolizing complex on the study drugs.

The findings in this thesis suggest that tumors expressing ABCB1 and/or ABCG2 may demonstrate resistance to afatinib-, osimertinib-, ibrutinib- and ponatinib-based cancer therapy. Inhibiting both these ABC transporters during therapy might therefore be beneficial for the response of these tumors. It may further be possible to increase the levels of the afore-mentioned TKIs in the brain of patients with CNS involvement for better treatment efficacy by co-administration of an efficacious dual inhibitor of ABCB1 and ABCG2 such as elacridar. From our studies it appears that this sort of co-administration might perhaps also increase the oral availability and consequently overall tissue levels of afatinib, which should be taken into account for possible dose adjustment, to avoid increased toxicity.

The oral availability of osimertinib, ibrutinib or osimertinib, however, does not seem to be noticeably affected by the activity of ABCB1 or ABCG2. While afatinib is barely metabolized, osimertinib, ibrutinib and ponatinib are all metabolized into a subset of active and inactive metabolites. Their metabolism by CYP3A and possibly other CYPs in the intestines and liver is more likely the primary factor in restricting the oral bioavailability of these TKIs. Therefore, the oral availability of these TKIs could potentially be enhanced by co-administration of a CYP3A4 inhibitor, such as ketoconazole or ritonavir. However, caution should be exercised in such approaches to prevent unexpected toxicity.

Our results suggest that co-administration of ABCG2 and ABCB1 inhibitors may be considered to increase exposure of afatinib, osimertinib, ibrutinib and ponatinib in patients, especially in the brain, thus providing an option to better treat, amongst others, NSCLC and its metastases positioned in part or in whole behind a functionally intact blood-brain barrier. However, we feel that the best option for patients with brain (micro-) metastases would be if it were possible to treat them with drugs that are not substantially transported by these transporters. As few of such drugs are as yet available, it can still be considered for the current generation of TKIs to try and carefully inhibit ABCB1 and ABCG2 with a coadministered inhibitor, as this may give these patients a better chance of survival. However, the considerable risk of completely inhibiting ABCB1 and ABCG2 in

the blood-brain barrier of patients in a chronic setting, as would be required for clinical treatment with most targeted anticancer drugs, should be carefully assessed. Based on our experience with knockout mouse models, unpredictable (CNS) toxicity of drugs, pesticides and even some food components to which such patients will inevitably be exposed might emerge. Even in cases where we did not see any toxicity in mice, this cannot always be simply translated to humans. Therefore, whether this inhibition option could be effective and plausible in the clinic remains to be further investigated. As suggested before, we think it would be better if pharmaceutical companies would give additional weight to developing targeted anticancer drugs that are hardly or preferably not at all transported by ABCB1 and ABCG2. As illustrated (amongst others) in this thesis, the tools to help achieving that goal are in principle available.







# 8

---

## Summary

---



Membrane transporters are key players in the regulation of homeostasis, cell integrity and metabolism in organisms. The ATP-binding cassette (ABC) efflux transporters and Organic Anion-transporting Polypeptide (OATP) influx transporters are two main superfamilies that are expressed in pharmacologically important organs such as the liver, small intestine, kidney and the blood-brain barrier (BBB). These transporters can transport endogenous and exogenous molecules and thereby are important in the absorption, disposition, elimination and toxicity of many drugs. In this thesis we delved deeper into the pharmacological functions of ABCB1 and ABCG2 *in vitro* and *in vivo* for several anti-cancer drugs using specialized cell lines and various knockout and transgenic mouse models. We additionally looked into the pharmacological impact of CYP3A proteins which form one of the main metabolic enzyme complexes. We used various knockout and humanized mouse models to study its effects on a subset of anti-cancer drugs.

In **chapter 1** of this thesis we provide a brief introduction to the ABC transporters and their tissue localization and their pharmacologic role in the distribution of their substrates. We also introduced the Cytochrome P450 enzymes and the tyrosine kinase inhibitors (TKIs). We gave further insight at the end of the chapter into what we believe would be a more desirable approach for the future, *i.e.* the development of TKIs that are not substantially transported by ABC transporters.

**Chapter 2** focusses on the role ABCB1 and ABCG2 play in the distribution of the irreversible TKI afatinib. We have shown that ABCB1 and ABCG2 transport afatinib *in vitro*, and that *in vivo* they limit the oral bioavailability and brain accumulation of afatinib. We additionally showed that the liver distribution is not affected heavily by these ABC transporters. In **chapter 3** we demonstrated the importance of these ABC transporters, especially ABCB1, for brain accumulation of the irreversible TKI osimertinib and its main active metabolite AZ5104. However, the bioavailability or liver distribution of these compounds was not noticeably affected by these ABC transporters.

In **chapter 4** we investigated the roles ABCB1 and ABCG2, as well as CYP3A, play in the disposition of the irreversible TKI ibrutinib and its main metabolite, ibrutinib-DiOH. We found that ABCB1 and ABCG2 do not play a significant role in the oral bioavailability of ibrutinib. On the other hand, we showed that CYP3A does restrict the bioavailability of ibrutinib. The brain distribution of ibrutinib as well as ibrutinib-DiOH was clearly limited by ABCB1 activity, whereas the relative distribution to a range of other tissues did not seem to be much affected by either the ABC transporters or CYP3A.

**Chapter 5** describes the effects of the ABC transporters and CYP3A on the distribution of ponatinib and its main metabolite, DMP. We demonstrated that ABCB1 and ABCG2 both transport ponatinib *in vitro*, and that together they affect its brain disposition, but

not its oral bioavailability or liver distribution. We further found that CYP3A does affect the oral bioavailability of ponatinib *in vivo*.

**Chapter 6** reviews the impact of the OATP1A/1B family on the disposition and toxicity of anti-cancer drugs and how the recent use of knockout and humanized OATP1A/1B mouse models has helped us gain insight into the *in vivo* role of these OATP1A/1B transporters. We especially focused on their functional role in drug pharmacokinetics and their implications for therapeutic efficacy and toxic side effects of anti-cancer and other drug treatments.

In summary, the studies presented in this thesis contribute to our current knowledge on ABC efflux transporters and CYP3A metabolizing enzymes. We demonstrated the role ABCB1 and ABCG2 play in restricting brain accumulation of the TKIs afatinib, osimertinib, ibrutinib and ponatinib by means of *in vitro* and *in vivo* experiments. We also found that while these two ABC transporters impact the oral bioavailability of afatinib, that this is not the case for the other three TKIs, whose oral bioavailability is restricted mainly due to the metabolizing Cytochrome P450 enzymes. Our studies illustrate the continued importance of using mouse models to study the transport proteins *in vivo*, thereby enhancing our understanding of their functions. Taking everything together, we believe there is still much to be discovered in the field of transporter proteins as well as the metabolizing enzymes, in terms of their pharmacological, but also their physiological functions.





# Appendices

---

Nederlandse samenvatting

Résumé en français

Curriculum vitae

List of publications

Acknowledgements

---



## NEDERLANDSE SAMENVATTING

Membraan transporteurs zijn belangrijke spelers in de regulatie van homeostase, cel integriteit en metabolisme in organismes. De ATP-binding cassette (ABC) efflux transporteurs en Organic Anion-Transporting Polypeptide (OATP) influx transporteurs zijn twee belangrijke superfamilies die onder andere tot expressie komen in farmacologisch belangrijke organen zoals de lever, dunne darm, nier en bloedsheerbarrière (BBB). Deze transporteurs kunnen endogene en exogene moleculen transporteren en zijn daardoor belangrijk in de absorptie, dispositie, eliminatie en toxiciteit van vele geneesmiddelen. In dit proefschrift duiken we dieper in de farmacologische functies van ABCB1 en ABCG2 *in vitro* en *in vivo* voor verschillende anti-kanker geneesmiddelen, gebruikmakend van speciale cellijnen en verscheidene knock-out en transgene muismodellen om de effecten van deze transporteurs op een subset van anti-kanker geneesmiddelen te bestuderen.

In **hoofdstuk 1** van dit proefschrift geven we een korte introductie van de ABC transporteurs, hun weefsel lokalisatie en hun farmacologische rol in de verdeling van hun substraten. We introduceren ook de Cytochroom P450 enzymen en de Tyrosine Kinase Inhibitors (TKI's). Aan het eind van dit hoofdstuk geven we verder inzicht in wat wij denken dat een betere benadering voor de toekomst is, nl. de ontwikkeling van TKI's die niet substantieel getransporteerd worden door ABC transporteurs.

**Hoofdstuk 2** focust op de rol die ABCB1 en ABCG2 spelen bij de verdeling van de irreversibel bindende TKI afatinib. We laten zien dat ABCB1 en ABCG2 afatinib *in vitro* transporteren, en dat ze *in vivo* de orale biologische beschikbaarheid en hersenaccumulatie van afatinib beperken. We tonen bovendien aan dat de leverdistributie niet sterk beïnvloed wordt door deze ABC transporteurs.

In **hoofdstuk 3** laten we het belang van deze ABC transporteurs zien, vooral ABCB1, bij de hersenaccumulatie van de irreversibel bindende TKI osimertinib en zijn meest actieve metaboliet AZ5104. De biologische beschikbaarheid en leverdistributie van zowel osimertinib als AZ5104 was niet merkbaar beïnvloed door deze ABC transporteurs.

In **hoofdstuk 4** onderzoeken we de rollen die ABCB1 en ABCG2, alsook CYP3A, spelen bij de dispositie van de irreversibel bindende TKI ibrutinib en zijn belangrijkste metaboliet, ibrutinib-DiOH. We laten zien dat ABCB1 en ABCG2 geen significante rol spelen bij de orale biologische beschikbaarheid van ibrutinib. Aan de andere kant zien we dat CYP3A de biologische beschikbaarheid van ibrutinib beperkt. De verdeling van ibrutinib alsook ibrutinib-DiOH in de hersenen is duidelijk beperkt door ABCB1 activiteit, terwijl de relatieve verdeling in een reeks andere weefsels niet aanmerkelijk beïnvloed wordt door hetzij de ABC transporteurs of CYP3A.

**Hoofdstuk 5** beschrijft de effecten van de ABC transporteurs en CYP3A op de verdeling van ponatinib en zijn belangrijkste metaboliet DMP. We laten zien dat zowel ABCB1 als ABCG2 ponatinib *in vitro* transporteren en dat ze samen de dispositie in de hersenen beïnvloeden, maar niet de orale biologische beschikbaarheid of leverdistributie. Daarnaast zien we dat CYP3A wel de orale biologische beschikbaarheid van ponatinib *in vivo* beïnvloedt.

**Hoofdstuk 6** bespreekt de impact van de OATP1A/1B familie op de dispositie en toxiciteit van anti-kanker geneesmiddelen en hoe het recente gebruik van knock-out en gehumaniseerde OATP1A/1B muis modellen ons geholpen heeft om het inzicht in de *in vivo* rol van deze OATP1A/1B transporteurs te vergroten. Wij richten ons vooral op hun functionele rol in de geneesmiddel farmacokinetiek en de implicaties bij therapeutische en toxische bijwerkingen van anti-kanker en andere medicamenteuze behandelingen.

Samengevat dragen de in dit proefschrift gepresenteerde studies bij tot onze kennis van ABC efflux transporteurs en de CYP3A metaboliserende enzymen. We demonstreren de rol die ABCB1 en ABCG2 spelen in het beperken van de hersenaccumulatie van de TKI's afatinib, osimertinib, ibrutinib en ponatinib door middel van *in vitro* en *in vivo* experimenten. We zien daarbij dat terwijl deze twee ABC transporteurs de orale biologische beschikbaarheid van afatinib beïnvloeden, dit niet het geval is bij de andere drie TKI's, waarvan de orale biologische beschikbaarheid voornamelijk beperkt wordt door de metaboliserende Cytochroom P450 enzymen. Onze studies illustreren het blijvende belang van het gebruik van muismodellen om de transporteiwitten *in vivo* te bestuderen, en zodoende ons begrip van hun functies te verbeteren. Alles samennemend, geloven we dat er nog veel te ontdekken valt op het gebied van transporteiwitten alsmede de metaboliserende enzymen, in termen van hun farmacologische en ook fysiologische functies.

## RÉSUMÉ EN FRANÇAIS

Les transporteurs à membrane sont les acteurs clés dans la régulation des homéostasies, intégrité cellulaire et métabolisme dans les organismes. Les ATP-Binding Cassette (ABC) transporteurs d'efflux et Organic Anion-Transporting Polypeptide (OATP) transporteurs d'influx sont deux supères familles principales qui sont exprimés dans les organes pharmacologiquement importants tout comme le foie, l'intestin grêle, le rein et la barrière hémato-encéphalique (BBB). Ces transporteurs peuvent transporter des molécules endogènes et exogène et ainsi sont importants dans l'absorption, la disposition, l'élimination et la toxicité de beaucoup de médicaments. Dans cette thèse nous avons plongé au plus profond dans les fonctions pharmacologiques de ABCB1 et ABCG2 *en vitro* et *en vivo* pour plusieurs médicaments anti-cancer utilisant des lignées cellulaires spécialisées et divers knock-out et des modèles de souris transgéniques pour étudier leurs effets sur un sous-ensemble de médicaments anti-cancer.

Dans le **chapitre 1** de cette thèse nous fournissons une brève introduction des transporteurs ABC, leur localisation tissulaire ainsi que leur rôle pharmacologique dans la distribution de leurs substrats. Nous introduisons également les enzymes Cytochrome P450 et la Tyrosine Kinase Inhibitors (les TKIs). Nous donnons un aperçu supplémentaire à la fin du chapitre dans ce que nous croyons serait une approche plus souhaitable dans le futur, à savoir le développement des TKIs qui ne sont pas transportés d'une manière substantielle par les transporteurs ABC.

**Chapitre 2** on se concentre sur le rôle de ABCB1 et ABCG2 joue dans la distribution du TKI afatinib qui se lie irréversiblement. Nous montrons que ABCB1 et ABCG2 transportent afatinib *en vitro*, et qu'*en vivo* ils limitent la biodisponibilité orale et l'accumulation cérébrale de afatinib. Nous montrons en plus que la distribution du foie n'est pas lourdement influencé par ces transporteurs ABC.

Dans le **chapitre 3** nous montrons l'importance de ces transporteurs ABC, spécialement ABCB1, pour l'accumulation du TKI osimertinib, qui se lie irréversiblement, et son plus actif métabolite AZ5204. La biodisponibilité et la distribution de osimertinib ainsi que AZ5104 dans le foie n'étaient pas visiblement affectée par ces transporteurs ABC.

Dans le **chapitre 4** nous enquêtons sur les rôles ABCB1 et ABCG2, ainsi que CYP3A, jouent dans la disposition du TKI ibrutinib, qui se lie irréversiblement, et son principale métabolite ibrutinib-DiOH. Nous voyons que ABCB1 et ABCG3 ne jouent pas un rôle significatif dans la biodisponibilité orale de ibrutinib. D'autre part nous voyons que CYP3A restreint la biodisponibilité de ibrutinib. La distribution de ibrutinib ainsi que ibrutinib-DiOH dans le cerveau est clairement limité par l'activité de ABCB1, tandis que

la distribution relative à une gamme d'autres tissus n'est pas très affectée par aussi bien des transporteurs ABC que CYP3A.

**Chapitre 5** décrit les effets des transporteurs ABC et CYP3A sur la distribution du ponatinib et son principal métabolite DMP. Nous démontrons qu' aussi bien ABCB1 tout comme ABCG2 transportent ponatinib *en vitro et* qu'ensemble ils influencent la disposition dans le cerveau, mais pas la biodisponibilité orale ou la distribution hépatique. En plus nous voyons que CYP3A influence la biodisponibilité orale de ponatinib *en vivo*.

**Chapitre 6** discute l'impacte de la famille de OATP1A/1B sur la disposition et la toxicité des médicaments anti-cancer et comment l'utilisation récente du knock-out et les modèles de souris humanisés OATP1A/1B nous a aidé à agrandir la perspicacité du rôle *en vivo* de ces transporteurs OATP1A/1B. Nous nous concentrons surtout sur leur rôle fonctionnel dans la pharmacocinétique des médicaments et les implications sur les réactions thérapeutiques et toxiques des médicaments anti-cancer et d'autres traitements médicamenteux.

En résumé les études présentées dans cette thèse contribues à nos connaissances actuelles sur les transporteurs efflux ABC et CYP3A enzymes métabolisantes. Nous démontrons le rôle que joue ABCB1 et ABCG2 dans la restriction de l'accumulation cérébrale des TKIs afatinib, osimertinib, ibrutinib et ponatinib par des moyens d'expérimentation *en vitro et en vivo*. Nous voyons en plus que pendant que ces deux transporteurs ABC ont un impacte sur la biodisponibilité orale de afatinib, que ça n'est pas le cas pour les autres trois TKIs dont la biodisponibilité orale se trouve réduit principalement par les enzymes métabolisants Cytochrome P450. Nos études illustrent l'importance continuelle d'utiliser des modèles de souris pour étudier le transport des protéines *en vivo* améliorant ainsi notre compréantion dans leurs fonctions. Tout y compris, nous croyons qu'il y a encore beaucoup à découvrir dans le champs du transporteur des protéines tout comme les enzymes métabolisants, dans les termes de leurs fonctions pharmacologiques et physiologiques.

## CURRICULUM VITAE

Stéphanie Sigrid van Hoppe was born on April 7th 1986 in Bonaire (the Netherlands Antilles). After graduating high school at Radulphus College in Curaçao (the Netherlands Antilles), she chose to study Molecular Life Sciences at the University of Maastricht (the Netherlands). She received her B.Sc. degree in 2010. During the last year of her bachelors she enrolled in the Topmaster program Oncology at the Free University (VU) in Amsterdam (the Netherlands) where she completed two internships. During her first internship in the laboratory of Prof. Dr. Tom Würdinger at the Cancer Center of Amsterdam (CCA), she researched the development of a multiplex bioluminescent reporter system *in vitro* and *in vivo* under the supervision of Dr. Sjoerd van Rijn. She completed her second internship in the lab of Prof. Dr. Bakhos Tannous at Massachusetts General Hospital (MGS) & Harvard Medical School (HMS) (the United States of America), where she researched novel anti-cancer treatments *in vitro* and *in vivo* under the supervision of Dr. Christian E. Badr, which led to a second author publication. End of 2013 Stéphanie received her M.Sc. degree and subsequently in 2014, she started her PhD program in the lab of Dr. Alfred H. Schinkel at the Netherlands Cancer Institute (the Netherlands). During her PhD, she studied the pharmacological functions of ABC efflux and OATP uptake transporters in the disposition of (anti-cancer) drugs *in vitro* and *in vivo*. These projects were conducted in collaboration with the research laboratory of Prof. Dr. Jos H. Beijnen at the Netherlands Cancer institute/ Slotervaart Hospital and Utrecht University (the Netherlands). The results obtained during her PhD are described in this thesis.

## LIST OF PUBLICATIONS

- Badr CE, **Van Hoppe S**, Dumbuya H, Tjon-Kon-Fat LA, Tannous BA. Targeting cancer cells with the natural compound obtusaquinone, *J Natl Cancer Inst*, 9 (2013) 643-653. 10.1093/jnci/djt037
- **van Hoppe S\***, Durmus S\*, Schinkel AH. The impact of Organic Anion-Transporting Polypeptides (OATPs) on disposition and toxicity of antitumor drugs: Insights from knockout and humanized mice, *Drug Resist Updat*, (2016) 72-88. 10.1016/j.drug.2016.06.005
- Sparidans RW, **van Hoppe S**, Rood JJH, Schinkel AH, Schellens JH, Beijnen JH. Liquid chromatography-tandem mass spectrometric assay for the tyrosine kinase inhibitor afatinib in mouse plasma using salting-out liquid-liquid extraction, *J Chromatogr B Analyt Technol Biomed Life Sci*, (2016) 118-123. 10.1016/j.jchromb.2016.01.025
- Rood JJM, **van Hoppe S**, Schinkel AH, Schellens JHM, Beijnen JH, Sparidans RW. Liquid chromatography-tandem mass spectrometric assay for the simultaneous determination of the irreversible BTK inhibitor ibrutinib and its dihydrodiol-metabolite in plasma and its application in mouse pharmacokinetic studies, *J Pharm Biomed Anal*, (2016) 123-131. 10.1016/j.jpba.2015.10.033
- **van Hoppe S**, Sparidans RW, Wagenaar E, Beijnen JH, Schinkel AH. Breast cancer resistance protein (BCRP/ABCG2) and P-glycoprotein (P-gp/ABCB1) transport afatinib and restrict its oral availability and brain accumulation, *Pharmacol Res*, (2017) 43-50. 10.1016/j.phrs.2017.01.035
- **van Hoppe S**, Schinkel AH. What next? Preferably development of drugs that are no longer transported by the ABCB1 and ABCG2 efflux transporters, *Pharmacol Res*, (2017) 144. 10.1016/j.phrs.2017.05.015
- **van Hoppe S\***, Kort A\*, Sparidans RW, Wagenaar E, Beijnen JH, Schinkel AH. Brain Accumulation of Ponatinib and Its Active Metabolite, N-Desmethyl Ponatinib, Is Limited by P-Glycoprotein (P-GP/ABCB1) and Breast Cancer Resistance Protein (BCRP/ABCG2), *Mol Pharm*, 10 (2017) 3258-3268. 10.1021/acs.molpharmaceut.7b00257

\* Contributed equally

- Slijepcevic D, Roscam Abbing RLP, Katafuchi T, Blank A, Donkers JM, **van Hoppe S**, de Waart DR, Tolenaars D, van der Meer JHM, Wildenberg M, Beuers U, Oude Elferink RPJ, Schinkel AH, van de Graaf SFJ. Hepatic uptake of conjugated bile acids is mediated by both sodium taurocholate cotransporting polypeptide and organic anion transporting polypeptides and modulated by intestinal sensing of plasma bile acid levels in mice, *Hepatology*, 5 (2017) 1631-1643. 10.1002/hep.29251
- **van Hoppe S**, Rood JJM, Buil L, Wagenaar E, Sparidans RW, Beijnen JH, Schinkel AH. P-Glycoprotein (MDR1/ABCB1) Restricts Brain Penetration of the Bruton's Tyrosine Kinase Inhibitor Ibrutinib, While Cytochrome P450-3A (CYP3A) Limits Its Oral Bioavailability, *Mol Pharm*, 11 (2018) 5124-5134. 10.1021/acs.molpharmaceut.8b00702
- Wang J, Gan C, Sparidans RW, Wagenaar E, **van Hoppe S**, Beijnen JH, Schinkel AH. P-glycoprotein (MDR1/ABCB1) and Breast Cancer Resistance Protein (BCRP/ABCG2) affect brain accumulation and intestinal disposition of encorafenib in mice, *Pharmacol Res*, (2018) 414-423. 10.1016/j.phrs.2017.11.006
- **Van Hoppe S**, Jamalpoor A, Rood JJM, Wagenaar E, Sparidans RW, Beijnen JH, Schinkel AH. Brain accumulation of osimertinib and its active metabolite AZ5104 is restricted by ABCB1 (P-glycoprotein) and ABCG2 (Breast Cancer Resistance Protein), *Pharmacol Res*. 2019 Aug;146:104297.
- Martínez-Chávez A, **van Hoppe S**, Rosing H, Lebre CM, Tibben M, Beijnen JH, Schinkel AH. P-glycoprotein limits ribociclib brain exposure and CYP3A4 restricts its oral bioavailability, *Mol Pharm*. 2019; *in press*
- Rood JJM, Jamalpoor A, **van Hoppe S**, van Haren MJ, Wasmann RE, Janssen MJ, Schinkel AH, Masereeuw R, Schellens JHM, Beijnen JH, Sparidans RW. Extrahepatic metabolism of the targeted covalent inhibitor ibrutinib through the glutathione cycle. *In preparation*

## ACKNOWLEDGEMENTS

You've now reached the most popular section of a PhD thesis - and rightfully so. We don't perform scientific research alone and therefore, everyone who has affected this thesis, and my time as a PhD student one way or another is hereby acknowledged and thanked. I hope I won't forget anyone, but unfortunately I most likely will, so to anyone I do forget – I'm sorry and I'll try to make it up to you!

First of all I would like to thank **Alfred Schinkel** for hiring me as a PhD student in your lab. Thank you for your guidance and teaching me how to be an overall better scientist. You taught me how to be more critical, efficient in my work and less impulsive. I appreciate the freedom you gave me for my experiments and projects. It goes without saying that without your input, this thesis would not be what it is. I am also very grateful to my promotor, **Jos Beijnen**, for your guidance and your positivity throughout my time at the NKI. Your support and encouragement are greatly appreciated. Furthermore I would like to acknowledge the members of my PhD committee: **Daniel Peeper**, **Wilbert Zwart**, **Olaf van Tellingen** and for a smaller period in time, **Sjaak Neefjes**, for keeping an eye on my progress and your support during these years. A special thank you goes to **Olaf** for our collaborations together on the OATP projects, even though these did not end up in this thesis, it does not take away that I am grateful for your efforts. Thank you for your generosity and allowing me to measure those hundreds of samples in your lab.

**Rolf Sparidans**, you have been such an efficient collaborator. Thank you for measuring so many of my samples and for being super-fast with responding, whether it was answering a question or commentating on a manuscript. It was quite an honor that you came to the NKI from Utrecht to attend our presentations. Thank you for all your efforts.

To my awesome paranymphs, **Zeliha Yalcin** and **Alejandra Martinez Chavez** I'm glad we were able to make the small getaway to Spain together and have that as a nice memory to look back on! **Zeliha**, thank you so much for your support and the coffee/hot chocolate/tea breaks we had to keep the positivity up. I'm so happy I could always count on you for anything and everything. I'm glad we both ended up in the party committee of H5 during my first year which ended up in a great friendship! I admire your hard working mentality and persistency and I know you'll have a great career ahead of you. And **Alejandra**, I was so happy when you started your journey in our lab with your positive attitude and kindheartedness. It was great sharing the office with you. Thank you for your support and friendship and I'm sure you'll do great in your scientific career with your accurate mentality and willingness to collaborate. I'm so lucky to have both of you standing with me at my upcoming defense!

A big thank you to all the people I collaborated with, or who've helped me out in my research: **Piet Borst, Gert-Jan Rood, Levi Buil, Sjoerd Klarenbeek, Sovann Kaing, Krijn Dijkstra, Dirk de Waart, Desiree Verwoerd, Dick Plum, the animal caretakers at G5 and T1 and T2, Leo Ennen, Maaïke van der Meulen, Anne Marie Rhebergen, Roel Sneepers, Filip Mulkens and the intervention unit.** Thank you **Piet** for the fruitful discussions and your advice concerning my projects. I highly admire your knowledge and critique on all the various scientific projects. **Gert-Jan**, thank you for your collaboration on the ibrutinib and the osimertinib projects. I've enjoyed working with you and discussion our results together. Also a big thank you for your willingness to give some guidance to my student while he was measuring samples there in Utrecht. I look forward to seeing your thesis! **Levi**, thank you for helping me out during my busy *in vivo* experiments! I enjoyed working with you as it was a perfect balance of hard work and having fun! I admire that you always remained very calm and collected no matter what happened. Masha masha danki! **Sjoerd**, thank you for all the nice discussions we've had about the OATP project. Unfortunately this did not end up in this thesis, but I wanted to acknowledge your efforts either way. I am grateful that you were so approachable for any questions I had. **Sovann**, thank you for teaching me all about culturing organoids and for being so helpful! Also a thank you to **Krijn** for handing me all those organoids for staining. This project did not make it here, but I remain very thankful for efforts! It was also nice sharing the office with you on H5 for a short period in the 'old' H5, as well as being in the party committee together. **Rudy**, thank you for measuring my bile acid samples, even though these did not make it to this thesis, your efforts won't go unnoticed of course! **Desiree**, thank you for your help in the RNC for both the *in vitro* and *in vivo* experiments along with the nice conversations we've had! The results of these studies are not in this thesis, but I hope these will be published in the near future. **Dick**, thank you for helping me measure with the HPLC in the RNC so I could continue setting up my experiment. And to all **the animal caretakers** in the old and new building, thank you all so much for your help with the mice and the nice atmosphere. A special thanks goes to **Desiree de Wilt** for the nice conversations we've had and for being so helpful. And thank you **Maaïke** for all your help concerning the DECs and the WPs that needed to be adapted. You were always ready to help out. And to **Roel, Filip** and **Anne Marie**, thank you for helping me out with the *in vivo* techniques and always being very friendly and helpful whenever I had any questions. Also thank you to **Niels de Wit** and **Natalie Proost** for all your help during my radioactive *in vivo* experiment at T1.

To all the former and current members of the Schinkel lab: **Selvi Durmus, Anita Kort, Els Wagenaar, Seng Chuan Tang, Yaogeng Wang, Jing Wang, Chanpei Gan, Xiaozhe Qi, Cristina Mesquita Lebre, Wenlong Li** and **Margarida Martins**, thank you all for contributing to my research and coloring my life one way or another. **Selvi**, you've left

the lab too soon! We made such a great team with the *in vivo* (crazy) work and we've had so many great scientific discussions. Thank you for being there for me whenever I had questions or wanted to discuss an idea or two. **Els**, thank you for introducing me to the lab and helping me out with all the mice! Also thank you for keeping us all healthy and happy with fresh fruits and stroopwafels you regularly handed out to us. **Seng**, you joined the lab again for a short time, but I was grateful that you wanted to help out on my radioactive *in vivo* experiment! Even though this study didn't make it in this thesis, your help was of course greatly appreciated! **Yoageng**, it was nice sharing the office with you and hearing about all your traveling stories! **Cristina**, thank you for all your discussions and advice you've given me. It was great to know that I could always ask you for help if I needed any. Also thanks for all the Portuguese treats you've spoiled us with! **Wenlong**, it was also nice sharing the office with you and I hope you'll remain the kind person you were when you sat next to me. **Margarida**, it was great getting to know you in the lab and I'm sure you'll do great! Thanks for the good times we've had together with Alejandra and Cristina during our girls' nights out! And to my student **Amer Jamalpoor**, thank you for working with me on the osimertinib project. I'm sure you're doing great as a PhD student in Utrecht.

A thank you to all the other people I've shared the office with: **Marijn van Jagersveld**, **Koen de Wetering** and **Brigitte Wevers** for the nice atmosphere. **Koen**, even though we shared the office for a short amount of time, I was very glad to be able to have fruitful discussions with you. Thank you for being so easygoing and generous.

I wish to thank all the members of the 'old' H5 for the nice atmosphere: **Vera Boersma**, **Marco Simonetta**, **Judit Serrat**, **Aurora Cerutti**, **Inge de Krijger**, **Nathalie Moatti**, **Jacqueline Jacobs**, **Chelsea McLean**, **Salo Ooft**, **Fleur Weeber**, **Julia Houthuijzen**, **Julia Boshuizen**, **Xinyao Huang**, **Xiangjun Kong**, **Oscar Krijgsman**, **Pierre Levy**, **Maarten Ligtenberg**, **David Vredevoogd**, **Nils Visser**, **Sedef Iskit**, **Joanna Kaplon**, **Judith Muller**, **Juliana Kenski**, **Kristel Kemper**, **Patricia Possik**, **Sunny Mahakena**, **Robert Janssen**, **Marco Barazas**, **Ewa Gogola**, **Guotai Xu**, **Sven Rottenberg**, **Henri van Leunen**, **Tom de Knegt**, **Marij Degen** and everyone else during my time over there. **Vera**, it was great getting to know you when I started and I am so glad that we became friends! I'm so happy to have become colleagues with you once more during my short stay at Cergentis! **Tom**, thank you so much for all your help at H5! And also for getting me to join the party committee. **Marij**, even though you weren't of H5, you helped out a lot during the time we did not have an office manager. Thank you for sending all those packages with samples to Utrecht for me!

After H5 we moved to an entirely different department at H3 and to everyone there, a big thank you for the nice atmosphere and discussions we've had. **Mark de Gooijer**, **Ceren Çitirikkaya**, **Hilal Çolakoğlu**, **Paul Slangen**, **Mark van Bussel**, **Jill Geenen**,

**Kimberley Heinhuis, Hans te Poele, Thea Eggenhuizen, Jan Schellens, Sven de Krou, Onno Bleijerveld, Liesbeth Hoekman, Maarten Altelaar, Evelien van Kampen, Aurelia de Vries Schultink, Hedvig Arnamo, Marit Vermunt, Ignace Roseboom, Jonathan Knikman, Jorn Mulder, Julie Janssen, Karen de Jong, Laura Molenaar - Kuijsten, Lisa van der Heijden, Luka Verrest, Maaike Bruin, Maarten van Eijk, Nikki Ijzerman, Paniz Heydari, Rene Boosman, Roel van Gijn, Sanne Huijberts, Semra Palic, Thomas Dorlo, Merel van Nuland, Steffie Groenland, Linda Henricks, Willeke Ros, Lotte van Andel. Mark (dG), thank you nice discussions and conversations we've had. It's always nice to discuss science with you! Mark (vB) thank you for the discussions concerning the osimertinib project. Onno, you're always filled with joy and I enjoyed our conversations during my time at H3. Liesbeth, it was nice having so many conversations with you. Time flew by way faster than it was supposed to those times!**

A big thank you to all the other colleagues from the NKI that I had good conversations and/or discussions with. There are so many of you but I will try to thank you all: **Elma Mons, Jeroen Hendriks, Koen Flach, Christ Leemans, Ewald van Dyk, Peter Remeijer, Andrea Murachelli, Patti Lagerweij, Tom de Wit, Marijne Schijns, Antonio Sanchez, Joao Neto, Fernando Polo and Behzad Mombeini.** Elma, thank you for all the nice discussions and your great insight into the world of chemistry, which is still quite foreign to me. I enjoyed the times together and look forward to your thesis! Peter, I am grateful for your advice you gave me concerning my PhD and career. This has helped me a lot! Jeroen, it was always great to talk to you about career aspects what to include in a thesis and science overall.

A huge thank you to all my friends outside of academia or the NKI, who were so understanding every time I was either late or had to cancel an appointment because of an experiment or deadline. Thank you all for your support and for listening to me talk about science. I'm super lucky to have friends like you! I wish to especially thank **Jasmin Hettich, Sarah van Leeuwen, Valeria Bella, Barbara van der Hoeven, Emiel Ordelmans, Mindy Au, Marloes Vogel, Sheila Clement, Nicole Boëtius, Melle Holwerda and Ioana Niculescu** for your support!

And a thank you to **Gülsüm Yalcin**, who was able to translate my idea for the cover so well! Thank you for making me so happy with my cover!

To my former colleagues at Cergentis: **Jan Dekker, Max van Min, Erik Splinter, Harma Feitsma, Judith Bergboer, Martijn Kelder, Allan La, Petra Klous, Mehmet Yilmaz, Irina Sergeeva, Elaine Wong, Melinda Aprelia, Joost Swennenhuis, Agata Rakszewska, Cheryl Dambrot and Wietske Stevens:** thank you for your understanding and support during the final phase of writing this thesis while I was working there. It meant the world to me and I had a great time working with you all!

And last but not least, thank you to my parents for all your support and listening to me talk about the complicated academic world and doing your best to understand what my research is about! And to get me to take a bit of vacation to visit you guys in Spain! Thank you for contributing to this thesis with the Dutch and French translations. Now there's also a piece of you in this thesis!

Thank you all!



